THE ALTERATION PETROLOGY OF THE CHEVIOT GRANITE

A thesis submitted for the degree
of Doctor of Philosophy at
the University of Newcastle upon Tyne

Nabeel M. Al-HAFDH

Geology Department
February 1985

University of Newcastle upon Tyne
Newcastle upon Tyne NE1 7RU

PAGE

NUMBERING

AS ORIGINAL

ACKNOWLEDGEMENTS

Now this thesis is complete, a word of gratitude and acknowledgement is due to the people who have helped me during the different phases of writing.

First, I would like to extend my thanks and gratitude to my supervisor, Professor J. R. Cann, for his invaluable help in determining the content of this thesis. In completing this thesis I am greatly indebted to his guidance and supervision and it is only through his help that this thesis became a reality.

I am also greately indebted to Mr. P. J. Oakley for his assistance during the last four years; he has been most helpful, patient and supportive during the time he spent supervising my work in the laboratory.

My thanks go to Mr. Len Rhodes for providing all the facilities needed for my work, to Ann Thwaites and Liz Walton, our secretarial staff, and to Ann Meldrum. I would also like to thank Eric Reed for making my thin sections.

With regard to the computing side of my work I would like to express my gratitude to Dr. Tim Pharaoh, and to the duty advisors of the Computing Department at Newcastle University for their dedication and help. My thanks also go to Mr. Kevin Goodger, my colleague, for his assistance in photographing some of my thin sections. I would also like to give my thanks and gratitude to all the members of the Geology Department in Newcastle University for the help and assistance they gave me during my stay. I am also grateful to Mrs D. Cooper for helping me with some of the diagrams and the maps related to this work.

My special respect and thanks go to Liz for her invaluable help and support both moral and practical.

The kind hospitality of people in the Cheviot District, particularly the Oliver family of Hartside Farm is much appreciated.

Last but not least, my special thanks go to the Department of Geology of Mosul for entrusting me with this study and for providing the funds and facilities needed for my work.

ABSTRACT

The Cheviot Granite complex is a high-level pluton made up of six intrusive phases intruded into a pile of andesites of very similar composition to the bulk of the plutonics. The whole represents the eroded remnant of a lower Devonian volcano, erupted immediately after the continental collision that destroyed the Iapetus Ocean.

The igneous history comprises two igneous cycles, both starting with basic granodiorite and including a late porphyritic ring dyke. The two cycles can be distinguished geochemically using Zr and K contents. Fractionation during each cycle involved precipitation of a biotite diorite cumulate. The second cycle ends with a highly evolved leucocratic microgranite. The geochemistry shows a rather shoshonitic chemistry to the series, and trace elements are consistent with an immediately post-collisional origin.

Hydrothermal alteration occurs in two phases, one associated in space and time with the porphyritic granodiorite of the first igneous cycle, and the other with that of the second cycle. In both systems both potassic and sericitic alteration assemblages are found, and there is a wide development of propylitic alteration around these higher temperature

zones. The two hydrothermal phases can be distinguished by the abundance of tourmaline in sericitic and propylitic rocks of the second cycle, and the abundance of calcium (mostly as calcite) in the sericitic rocks of the first phase.

Geochemical flux calculations show that silica has been widely introduced to the granite during the alteration (in amounts up to 10%) and Ca and Sr removed. Other element fluxes are more complex, and may be coupled together.

Comparison with other granites of N England and S Scotland shows that the Loch Doon complex and the Shap granite are very similar to Cheviot, that the Criffell Dalbeattie granite has a very similar early phase but diverges later, and that the Skiddaw, Weardale and Cairnsmore of Fleet granites are very different from Cheviot, being essentially granitic rather than granodioritic.

CONTENTS

TABLES

FIGURES

PLATES

CHAPTER ONE

INTRODUCTION AND PREVIOUS WORK

CHAPTER ONE

INTRODUCTION AND PREVIOUS WORK

1.1 INTRODUCTION

The Cheviot Granite lies at the centre of a large area of andesitic to rhyolitic volcanics in the Cheviot Hills on the border between England and Scotland. The volcanics represent the remnants of one of the Lower Devonian calc-alkaline volcanoes that post-date the final Caledonide orogeny in this area, and the granite has intruded upwards into the volcanics to a high structural level. Erosion has exposed the upper part of the granite and its aureole. Later faulting has sliced through the granite.

The Cheviot Hills are remote, grass-covered, rounded hills, inhabited by sheep and curlews, with the occasional shepherd and his dog. Exposure is variable. In places the granite forms tors or is exposed continuously in and near streams. In other places a thin cover of glacial drift mantles the outcrop and over several square kilometers no in-situ material can be seen.

Earlier studies of the granite (Teall, 1885; Kynaston, 1899; Carruthers et al., 1932; Jhingran, 1942) showed it to be variable as an intrusive, and to be, at least in parts, extensively altered by hydrothermal activity.

The aims of the work reported in this thesis are first to establish the extent of primary variation in the granite by field mapping and geochemical analysis and second, to study the alteration petrology and geochemistry of the granite, in order to establish the nature of the patterns of alteration there, and to advance the knowledge of alteration petrology of granites in general. It is interesting that the most studies of granite alteration have been related to mineralized granites, rather than barren granites. My work found no evidence of mineralization in the Cheviot, and can act as a useful comparison with the extensive work on ore-bearing granites.

1.2 ALTERATION PATTERNS IN GRANITES

Since the alteration petrology of the Cheviot Granite is a major component of this thesis, it is important at this stage to introduce ideas of alteration patterns in granites.

1.2.1 ALTERATION ASSOCIATED WITH PORPHYRY COPPER DEDOSITS

The term porphyry Cu or Cu-Mo deposit is used for a zoned deposit of disseminated copper and or molybdenum sulphides, with associated hydrothermally altered host rocks. The relatively homogenous and roughly equidimensional deposits are generally on a scale of several hundreds of meters and are usually associated with a complex, passively emplaced stock of intermediate composition. The stock is

intruded at shallow depths, and is made up of a number of different intrusive units including some that are characteristically porphyritic. As early as 1927, Emmons underlined the association between the porphyritic intrusions and disseminated copper mineralization. The earliest thorough descriptions of alteration and the most detailed consideration of the mechanism have been made of wall rock around veins of variable width in granitic rocks (McKinstry and Noble, 1932; Exley, 1957; Brimhall, 1969). With close fracture spacing, alteration selvages of adjacent veins overlap and the vein-veinlet alteration merges to alter the rock totally (Meyer and Hemley, 1967).

At a very early stage all the authors (Buttler and Vanderwilt, 1933; Schwartz, 1955; Creasey, 1959; Meyer, 1965; Charles, Park and Macdiarmid, 1970) recognized the tendancy of the alteration-mineralization system to a zonal arrangement, and that recognizably different mineral assemblages were present with in individual deposits (Schwartz, 1947; Stringham, 1953; Anderson, 1950).

As data accumulated it became apparent that certain alteration mineral assemblages consistently occurred in many deposits of the porphyry copper type (Creasey 1959, 1966; Burnham, 1962; Meyer and Hemley, 1967; Einaudi, 1981; Rose, 1970; Lowell and Guilbert, 1970; Hollister, 1978). At this stage it is worthwhile to say that it was Creasey (1959) who first pointed out the utility of classifying

hydrothermally altered aluminosilicates in terms of mineral assemblages.

This approach has been followed to a large degree by all succeeding workers on porphyry copper deposits and similar ores associated with aluminosilicates. Although there are similarities in hydrothermal studies, a review of these studies reveals many dissimilarities in relation to, among other things, the simultaneous growth of several alteration fronts described by, Sales and Meyer (1948, 1950), and the independent stages of hydrothermal alteration described by Lovering (1949) which he considered to be separated from each other by appreciable time intervals. Studies of alteration of porphyry copper deposits at various levels of detail throughout the world have documented numerous localities which do not correspond with the zoning proposed by Lowell and Guilbert, 1970 (e.g. Titley, 1975; Hollister, 1978; Cheney and Trammell, 1975). Guilbert and Lowell (1974), showed that some of these variations could be attributable to geological factors which include wall rock, fluid and intrusion compositions, level of exposure, and structural controls on intrusion and minerlization. A major deparature from this, the San Manuel-Kalamazoo model (Lowell and Guilbert, 1970) occurs when the ore-related intrusions are of quartz dioritic rather than quartz monzonitic compositions. Table 1.1, summarises some of the varying conclusions on porphyry copper deposits reached by these and other workers.

Table 1.1 A summary of some of the varying conclusions on porphyry copper deposit / cont.

Author	rock type	Zones of alteration and its mineral assemblages				Ore deposits and its occurrence	Area	Comment
		Core	Intermediate zones		periphery			
Lowell and Guilbert (1970)	Laramide dacite porphyry	potassic zone (secopdary biotite, K. feldspar quartz and sericite)	phyllic zone (quartz, sericite chlorite and pyrite)	argillic zone montmorillonite and Kaolinite	propylitic zone chlorite carbonate, epidote ± sericite	overlap the potassic and phyllic zone	San Manuel Kalamazo	both vertical and horizontal zoning
Sillitoe (1973)	Tonalite stock	potassium silicate zone (mineral assemblage same as above)	phyllic zone Feldspar destructive (as above)		propylitic zone chlorite, epidote, calcite and pyrite		Los Pelambres, Chile	
Phillips et al. (1974)	1. Diabase	biotite clay zone	Rarely sericitic and K feldspar		chlorite and epidote zone	Ore appears to favour the Granite Mountain and quartzoss pre-cambrian rocks	Ray Deposit	He noted that the alteration zoning are affected by the host rock
	2. Quartzose	K feldspar biotite, zone	sericitic zone, overlap the K feld. zone		propylitic zone			
Hollister et al.,(1974)	Quartz monzonite	potassic zone (microcline) + or in place of orthoclase + epidote + chlorite	phyllic zone is reduced in size				Appalachian Orogen	Comparison of the Appalachian Qtz monzonite host rocks with the Lowell and Guilbert model, 1970 was made by this paper
Rice and Sharp (1976)	Late Cambrian intrusives	no evidence of pottassic zone	phyllic zone		propylitic zone	Sulphides, Cu and Mo formed the inner zone with pyritic halo	Coed-y- Brenin North Wales	
Armbrust et al (1977)			quartz-sericite-pyrite with minor biotite (phyllic zone)		propylitic zone (calcite, chlorite, epidote and sericite)	phyllic zone coincide with the ore body	Rio Blanco	Silicification and tourmalinization are important in the upper levels of the mine

Table 1.1 A summary of some of the varying conclusions on porphyry copper deposit/cont.

Author	rock type	Zones of alteration and its mineral assemblages				Ore deposits and its occurrence	Area	Comment
		Core	Intermediate zones		periphery			
Olade (1977)	porphyritic granodiorite		intense quartz -sericite and K feldspar veining in the centre	intense pervasive argillic (sericite kaolinite) with later phases of quartz veining		Ore is intimately associated with quartz sericite zone	High Land Valley, Canada	Quartz veining of late origin is superimposed on the argillic zone
Lanier et al, (1978)	equigranular monzonite	quartz orthoclasse phlogopite zone (potassium zone)			Actinolite -chlorite and epidote zone (propylitic zone)		Bingham Mining District	
Watmuff (1978)	Low K tholeiitic Calc-alkaline porphyry	broad area of biotite alteration		Argillic as a late stage	epidote -chlorite zone		Yanderal Papua, New Guinea	Argillic zone symmetrically disposed about an elongate central core of sulfide-barren quartz veining overprint the secondary biotite and epidote -chlorite zone
Scott (1978)	Dacite		Intensely sericitized zone represent the core		as intermediate zone a. chlorite, calcite zone b. epidote calcite zone		Copper Hill New South Wales, Australia	with a peripheral zone of epidote, remnant occasional hornblende phenocrysts disseminated
Wolfe et al, (1978)	Hornblende diorite to trondhjemite	biotite and weaker spotty orthoclase	strong pyritization representing this zone		propylitic zone with (epidote, calcite, chlorite and pyrite)	Ore coincide with the potassic zone	Taysan Philippines	
K'osaka and Wakita (1978)	potash rich adamellite	strong silicification with biotite development	Quartz sericite alteration with veins			Ore is localized both in the intrusion and the wall rocks	Mamut phorphy Cu deposit/ Saba Malaysia	

Table 1.1 A summary of some of the varying conclusions on porphyry copper deposit.

Author	rock type	Zones of alteration and its mineral assemblages				Ore deposites and its	Area	Comment
		Core	Intermediate zones		periphery			
Chivas (1978)	porphyritic intrusion of tonalite composition	two of the four hydrothermal episodes are 1. Sulfide free core 2. potassic zone	potassic sericite-chlorite zone	clay mineral (which over-prints potassic zone)	propylitic zone	coincide with the potassic zone	Koloula igneous complex-Solomon Islands	four distinct episodes of hydrothermal alteration occurred within the sequence of igneous events
Horton (1978)	post orogenic deposits of paleozoic and mesozoic age	weekly developed potassic zone	wide spread phyllic zone	weakly developed or lacking	wide spread propylitic		Queensland Australia	Alteration - mineralization system is fracture controlled
Ambler (1979)	Granodiorite	potassic zone	phyllic zone		propylitic zone	Sericite-chlorite epidote assemblages is most commonly associated with Cu-sulfides	Yeoval, New South Wales Australia	
Bailey et al. (1979)	Alkalic felsic intrusion	Abundant orthoclase + biotite	epidote-garnet + zeolite (intermediate zone)		Albite, calcite + epidote		Cariboo Bell British Coloumbia	Porphyry Cu-Au deposit
Taylor and Fryer (1980)	Granodiorite porphyry	potassic zone with predominant biotite	phyllic zone		propylitic (biotite/ amphibole and epidote)		Turkey	
Taylor (1981)	Bakircay Granodiorite						North Turkey	Alteration, Mineralization and intrusion are clearly spatially related

1.2.2 ALTERATION TYPES

The terms potassic, phyllic, argillic, and propylitic have been adapted or adopted from the literature (Burnham, 1962; Creasey, 1966; Meyer and Hemley, 1967)

1. K Silicate (Creasey 1959, 1966; Meyer and Hemley, 1967) or potassic alteration (Lowell and Guilbert, 1970) is centrally located in or near the porphyry intrusion centres as indicated by Lowell and Guilbert (1970), Rose, (1970) and Sillitoe, (1973). The characteristic alteration minerals are orthoclase, biotite, and quartz accompained by accessory but non-essential albite, sericite, anhydrite, and apatite.
2. Phyllic (Lowell and Guilbert, 1970) or sericitic alteration (Meyer and Hemley, 1967; Rose, 1970) can reflect wholesale replacement of rock-forming silicates by sericite and quartz, and generally results in the destruction of the original texture.
3. Argillic alteration is characterized by the formation of new clay minerals in silicate rocks. Early studies of the porphyry copper deposits which were carried out near the surface described pervasive argillic alteration of silicate rocks (the term pervasive is defined as that which results in wholesale conversion of one rock type to another) associated with mineralisation. On the other hand, deeper development has shown pervasive argillization to be largely of supergene origin at many deposits (Gustafson and Hunt, 1975; Langton, 1973; Graybeal, 1981). The phyllic and intermediate argillic assemblages,

however, are circumferentially arranged at increasingly greater lateral distances from the potassic core.

4. Propylitic alteration is essentially equivalent to greenschist facies metamorphism. The essential minerals chlorite, epidote, and calcite form by alteration of mafic minerals and the anorthitic component of plagioclase leaving albite as the main feldspar. Accessory apatite, anhydrite and hematite accompany the alteration. Propylitic alteration occurs as a broad aureole at the outer limits of hydrothermal effects.

Two additional alteration types consisting of quartz-sericite-chlorite-orthoclase and chlorite-sericite-epidote-magnetite have been considered as deep level equivalents of the potassic and propylitic assemblages respectively by Lowell and Guilbert (1970).

1.2.3 THE FORMATION OF PORPHYRY COPPER DEPOSITS

Much has been written about nature and origin of porphyry Cu-Mo deposits (Lowell and Guilbert, 1970; Mitchell and Garson, 1972; Sillitoe, 1973). Although no two deposits are exactly alike a few geological characteristics are shared by nearly all of them. Particularly important research was carried out by Gustafson and Hunt (1975) at the El Salvador Mine in Chile. This research contained the first detailed examination of the space-time relationships of alteration. It also gave descriptions of the complex and essentially evolutionary character of mineralization in the deposit. During the

early stage of mineralization, K silicate alteration took place, whereas the late stage of mineralization was accompanied by sericitic alteration. Finally, during secondary enrichment, the argillic alteration assemblage was produced. At El Salvador the propylitic alteration zone lay outside the area of investigation. Nevertheless, available paragenetic data for many porphyry copper deposits indicate that phyllic alteration is almost invariably developed after the potassic and propylitic types (Titley, 1975; Gustafson, 1978; Gustafson and Hunt, 1975; Beane, 1981). Relative ages of the potassic and propylitic assemblages are less certain. The potassic and propylitic alteration zones generally developed in the intrusion and enclosing wall rocks, respectively. The fracturing with which later phyllic alteration is associated is localized on or near the contact between these two rock types. One of the reasons for the difficulty in discerning age relations between potassic and propylitic alteration type is that younger, texturally destructive phyllic alteration is superimposed across the boundary between them, obliterating much of the evidence.

Descriptions of porphyry copper deposits indicate that they are the products of large intrusion-related hydrothermal systems (Burnham, 1962) and that alteration-mineralisation although spatially and genetically related to the intrusion, clearly post-dates emplacement (Taylor, 1981). Common features of porphyry copper deposits have been described in almost all the literature and were best summarised by Gustafson (1978). The porphyritic rocks are

characterised by a multiplicity of intrusive events with different textures of the intrusive units, and similar textural patterns in the deposits despite the variation of host rocks (as shown in Table 1.1). Based on this, Gustafson (1978) concluded that most factors of magma genesis are probably not critical in porphyry copper formation. The distinct presence of different suites in a porphyry copper has led him to the belief that mineralisation is thought to coincide with a late low K suite, which in turn explains his conclusions that the mineralization is integrally related to the magmatic evolution of the intrusive rocks. Finally a description of the geological factors responsible for the wide variations of patterns in these deposits was also made by Gustafson (1978); these generally include:

1. structure and its effect in giving concentric alteration - mineralisation zoning as at San Manuel-Kalamazoo, or assymmetric zoning as at Panguna , which is due to the shifting location of intrusive centres and major zones of fracture permeability during hydrothermal activity.
2. Depth, size and timing of intrusion of which large, deep and closely related intrusions cool more slowly than small, shallow and widely timed intrusions.

1.2.4 PORPHYRY COPPER DEPOSITS AND TECTONICS

Most known porphyry copper deposits are interpreted as having formed along destructive plate margins above zones of subduction of oceanic crust. The post Palaeozoic Andean orogen provides the most complete and best-exposed example of metallogeny at a convergent

plate margin. The central Andes is a volcano-plutonic orogen constructed along a convergent, or consuming, plate margin between the overriding continental edge of Americas plate and the subducting, suboceanic Nazca Plate (Sillitoe, 1976). The deposits are related to the thrusting of oceanic crust beneath continents, where it melts at depth, giving rise to metal-and water-rich calc-alkaline magmas. Magmas so derived rise to the shallow crustal environment, where they crystallise and become the igneous progenitors to porphyry copper systems. Once emplaced at shallow levels and fractured, plutons interact extensively with their host rocks through hydrothermal processes. Garson, and Mitchell (1977) postulated that within the continental margin magmatic belts there is a tendancy for an increase in alkalinity from the margin inwards, from tonalite-granodiorite to mica-granite and alkaline granite, and finally, locally to undersaturated rocks, including nepheline-syenite and associated carbonatite, e.g. in Bolivia. The metals of porphyry copper deposits are believed to have originated principally at ridges and to have been transported within both oceanic crust and a thin skin of ocean bottom sediments towards plate edges as a result of spreading. Some were largely derived from the mantle at the ocean rise system and carried to the margin of ocean basin as components of layers 1,2 and 3 of the oceanic crust (Sillitoe, 1972).

Although metals may have their source in the porphyry magmas, attempts to establish such an origin have not been convincing. The only direct record of tectonic processes at the time of formation of

the deposits may be the fracture patterns presented by the intrusive dykes and veins as investigated by Titley and Heidrick (1978). The youthful age of many of the deposits and the rapid erosion within many of the porphyry systems offers the possibility of close examination of tectonic setting of the deposit and make it possible that deposits may be discovered still in process of formation (Gustafson, 1978).

1.2.5 TOURMALINIZATION

The following aspects represent the main areas of previous work on the occurrence of tourmaline in altered granites:

1. NATURE, OCCURRENCE AND FORM OF TOURMALINE:

The occurrence of minute crystals of black tourmaline in veins along with quartz, sericite and sulphides were recognized as early as 1923 (Knopf 1923, 1924). This has been reported by most of the succeeding workers in this field such as Schwartz (1955), who described the minute tourmaline crystals found in sericitized porphyry copper bearing rocks at Cananea, North America. The distribution of tourmaline appears to be closely associated in time with the transitional stage of mineralization (Heatwhole, 1973; Lister, 1978a) as found by Fletcher (1977) who introduced a tourmaline zone as a subzone of the propylitic zone. Three different types of tourmaline have been recorded at El Salvador, Chile (Gustafson and Hunt, 1975) as well as in the Cornubian batholith in Cornwall (Charoy, 1981) and in a quartz monzonite

stock at the Ilkwang mine, Republic of Korea (Fletcher, 1977). The earliest type of tourmaline at El Salvador is as tourmaline in veins cutting plagioclase (oligoclase) as well as K feldspar with no alteration, is associated with chalcopyrite and bornite without pyrite and commonly cuts the earlier (A) quartz veins (which are associated with the earlier mineralization). The second type is also in the form of veins, which contain pyrite without chalcopyrite and are bordered by conspicuous sericite-pyrite alteration haloes. The third type is disseminated tourmaline with or without associated sericite, the relative age of which is not known. Its abundance generally correlates with abundance of tourmaline veining. These three types spatially correspond with the rossette tourmaline, the small interlocking tourmaline crystals and the fine grained massive tourmaline with narrow veinlets described by Fletcher (1977).

The tourmaline of El Salvador in Chile is associated with the porphyry copper deposit and its alteration haloes. However, many tourmaline veins appear to have neither sulphide nor alteration haloes (Gustafson and Hunt, 1975; Fieremans, 1982). It has been considered that post magmatic tourmalinization in the St. Austell granite followed closely on the fissuring of the outer parts of the granite and filled the joints with quartz-tourmaline veins seldom penetrating the wall rock (Exley, 1957). In contrast studies of tourmalinites from Belgium, composed mainly of quartz

and tourmaline in variable proportions, show that they have been subjected to pervasive brecciation as a result of the passage of hydrothermal solutions, which substantially obscure the texture and primary mineralogical composition of the rocks (Fieremans, 1982). Finally tourmaline breccias are described at El Salvador as an early pebble breccias with rounded fragments whose matrix has been cemented with tourmaline and quartz. They contain more or less pyrite with sericitic alteration, and are low in copper with no molybdenite.

2. ORIGIN OF TOURMALINE:

There are several different points of view concerning the origin of tourmaline. Some authors suggest that biotite is necessary for the generation of tourmaline, as was found by Brammall and Harwood (1925) in SW-England. They believed that biotite is necessary to form tourmaline nodules, particularly in basic segregations at a fairly early stage in crystallization, and that these later develop into more extensive tourmalinization. This was supported by the observation that biotite and tourmaline do not coexist in the Tregonning Granite in Cornwall (Stone, 1963; Lister, 1979), and the deduction from this that the assemblage biotite + tourmaline might be unstable. However the occurrence of tourmaline + biotite has been more recently recorded by (Stone, 1975) at Priests Cove, near St. Just.

Other authors suggest that, feldspar (including both alkali feldspar and plagioclase) is necessary for tourmaline generation. Kingsley (1945) through his contribution to the study of luxullianite found that the feldspar, which constitutes one of the three essential components with tourmaline and quartz, is necessary for the production of new tourmaline around yellow primary tourmaline, which acts as nuclei about which radiation occurs with apatite, zircon and a little topaz as accessories. Growth of tourmaline within the feldspar (perhaps associated with K feldspathisation of Na bearing feldspar) has been considered as a possible origin (Lister, 1978b). This was confirmed by Lister (1978a) as well who noted that new generations of tourmaline occurred around margins and along cleavage planes of alkali feldspar and plagioclase. The reddening of the transitional rock at the St. Austell Granite, Cornwall, is found to be associated with the veins of tourmaline and quartz that cut through it (Lister, 1978a), and is especially due to the alteration of feldspar (plagioclase in particular). Alderton (1979) suggests a link between the growth of K feldspar and tourmalinization, as had previously been indicated by Meyer and Hemley (1967), instancing the tourmaline rich assemblages of SW England which are surrounded by veins containing abundant orthoclase, albite and muscovite. Finally growth of tourmaline crystals of El Salvador, Chile is associated with destruction of K feldspar, plagioclase and biotite in alteration haloes (Gustafson and Hunt,1975) confirming the two aspects mentioned above.

3. GEOCHEMICAL STUDIES:

Numerous workers have made great efforts to distinguish primary from hydrothermal tourmaline. It had been suggested by Power (1968) that hydrothermal tourmaline has a distinctive chemical composition, being higher in Mg, Ca, Sr, and Sn and lower in Fe, Mn, and F and also tending to have a higher Cr, V, Ni and Sc content. Such differences were considered with great attention by Charoy (1982) who found that hydrothermal tourmalines are less rich in Fe, F and richer in Mg, Ca and Sn than primary ones.

Studies examining the whole rock chemistry of tourmalinized samples were described by Exley and Stone (1964) who noted that replacement in granitic rock of SW-England of minerals by tourmaline, whether before or after consolidation of the granite, involves considerable chemical changes. Most important among these is release of K, especially where feldspar is involved. This studies have indicated that there is a spatial correspondence of tourmalinization and replacement of plagioclase by K feldspar (Alderton, 1979; Meyer and Hemley, 1967; Lister, 1978a). Many workers on tourmalinization considered that the original magma had to be anomalously boron, fluorine and lithium rich (Charoy,1982). Finally Wilson (1972) found several hundred ppm of boron in granitic biotites from Cornwall. Such high levels, he argued, might be caused by the presence in the biotite of minute crystals of tourmaline or might explain the later

formation of tourmaline from biotite.

1.3 PREVIOUS WORK ON THE CHEVIOT GRANITE

There are three major fields of previous geologic interest in the Cheviot Granite:

1. FIELD OBSERVATION AND PETROLOGY:

The Cheviot Granite occupies the centre of the range of hills lying on the borders of England and Scotland. The granite is almost completely confined to the English side and covers an area of approximately 20 square miles. It is roughly circular in shape with a two-mile long narrow northerly extension. The whole group is named after The Cheviot which is the highest hill (2676 ft above sea level). The Cheviot is separated only by a narrow valley from other hills such as Comb Fell (2132 ft), Hedgehope (2348 ft), Dunmoor (1860 ft), Shielcleugh Edge (1760 ft) and finally Standrop (1751 ft).

The Cheviot Hills have attracted naturalists and geologists for a very long time but the amount of literature available is limited. Winch (1817) first noted the occurrence of "porphyritic syenite and granitic syenite" and that "hornblende is by no means uncommon among these hills". He also pointed out that Housey Crags (958218), near Langleeford and the valley between Hedgehope and The Cheviot, is composed of a coarse grained variety of this rock. A description of the Cheviot igneous rocks in a little more detail was given by Tate (1867) who considered the granite

as a syenite composed of red orthoclase and black hornblende with variable quantity of quartz. The first thorough study was made by Clough (1882) who noted that the granite occupies an area of 24 square miles, that it varies much in texture, is generally not conspicuously rich in quartz, and often contains hornblende as well as mica. Finally he postulated that porphyrite and granite, alternately intrusive one in another, belong both to the same epoch, the Lower Old Red Sandstone.

The first account of petrology of the Cheviot Granite was given by Teall (1885), who noted the occurrence of granular texture and the invariable presence of different constituents. He described the granite that he collected during a day's traverse across the district (from Linhope Burn to Linhope Spout, Standrop Rigg, Comb Fell and Hedgehope) as an augite- biotite granite. A Geological Survey map of the hills as one inch and six inches old series-sheet, No. 108 N.E., was issued in 1888, together with a memoir entitled "The Geology Of The Cheviot Hills, English side" by Clough (1888). This was followed by a petrological study by Kynaston (1899) who noted the occurrence of augite and confirmed the presence of rhombic pyroxene in the neighbourhood of Linhope, Standrop Rigg, and Dunmoor Hill, as had been indicated by previous workers. Kynaston also realized that both plagioclase and orthoclase were present in approximately equal proportions and recorded the chief features of the rock together with the genetic relations between the lavas, the

granite and the dykes. Finally he reported the occurrence of tourmaline as small veins near the margin of the main mass. The Cheviot Hills then remained more or less untouched until 1931, when the Geological Survey produced a revision of the mapping as new series-sheets nos. 3 and 5 along with a new memoir, "The Geology of the Cheviot Hills" Carruthers et al., (1932) with petrological notes by H. H. Thomas. They described the augite-biotite granite (the so called normal granite) as pinkish, fairly coarse, and built up of irregularly bounded crystals of microperthite with subordinate quartz, biotite and a little magnetite, whereas the peripheral regions were described as fine-grained, dark-grey and rich in ferromagnesian minerals, and other more subsidiary types of granite were identified. As a result, they postulated the presence of more than one intrusion. They also recorded that tourmalinization was especially prevalent towards the west, which made them suggest that the centre (or centres) of eruption may have been in that direction. Finally they realized that due to the intrusion of the granite into the lavas of Old Red Sandstone age, patches of the lavas are still preserved within the granite area as remnants of its cover.

Jhingran (1942) redescribed the petrology of the Cheviot Granite and divided it into three different types, the marginal variety, the granophyric variety and the Standrop variety. He described the marginal variety as fine-grained, rather dark and occupying the margin of the granite. He was unable to

distinguish the different varieties of the granite clearly in the field and hence he could not find any evidence of an age relationship. He also referred to two types of inclusions within the granite, first to the large masses of metamorphosed lavas observed by previous workers (Carruthers et al., 1932) and, second, to the presence of more basic inclusions, which he describes as small in size and mostly enclosed by the marginal variety of the granite and to a lesser extent by the standrop type. A reconnaissance study of the district by Tomkeieff (1965) shows the lack of exposure in some places and gives an account of the contact between the granite and hornfelsed lavas and its excellent exposure in Newburn and Hawsen Burn (about half a mile N. of Langleeford (954224) and (955225) respectively). He described the contacts in these burns as "rather complex, with xenoliths of lava in the granite and tongues of granite penetrating the hornfelsed lavas". Crush-zones are also present, and crush breccia at the head of Newburn contains long needles of tourmaline. He confirms the presence of inclusions of andesite lava in granite in Long Crags to the SE of Langleeford observed by other workers. Finally he postulates a large granite off-shoot separated from the main body of granite in the bed of the river Breamish SW of linhope, on the southern margin of the complex.

"A Guide to the Geology of the Cheviot Hills" was produced by Robson (1976) in which he summarised the literature on the

Cheviot Granite. He reported that the junction between granite and lava is seldom straight, except in the Breamish valley above Low Blakehope where the granite may be faulted against unmetamorphosed lava. In the Common Burn above the Common Burn House, at the head of Bizzle, and in the Breamish (964163) above Linhope, the complex relationships between metamorphosed lava and granite may be clearly examined. Robson (1977) stated that "Relief of NW to SE stress at the end of Silurian times" led to intensive volcanism, followed by major and minor intrusive activity in the Cheviot region during the Lower Old Red Sandstone period, while during the Upper Old Red period uplift and erosion took place to such a degree that by the beginning of Carboniferous times, the roof of the granite stock was already exposed.

In a general survey of Caledonian granites, Brown (1979) considers that most British Caledonian granites which were emplaced during the period of 600-390 Ma are characterised by temporal progression towards low K/Rb ratios, low total Sr, low initial 87Sr/86Sr ratios and high U contents coupled with increasingly large negative Bouger gravity anomalies and sometimes large magnetic anomalies. He also reported that early granites from S-Britain and late granites from both the north and south provinces have geochemical characteristics of mantle derived parental magmas capable of metamorphosing the lower crust to a high grade and ascennding to become voluminous high level

and possibly subvolcanic intrusions. Thirlwall(1981) surveyed Lower Old Red Sandstone magmatism in Scotland and England. He suggested that Old Red Sandstone volcanics and all related Newer Granites are voluminous and do not appear to be preceded by any significant calc-alkaline magmatism, despite the long history of northward subduction suggested by many workers. Instead, they appear to be followed by a second calc-alkaline magmatic episode, comprising the Cheviot volcanics and plutons south of the Southern Uplands Faults. This made him to believe that subduction was active during deposition of Scottish Lower Old Red Sandstone.

2. GEOPHYSICAL INVESTIGATION:

Mitchell (1972) applied the K-Ar technique to the Cheviot Granite and dated it at 390 M.Y., which is similar to that of many of the younger members of the British late Caledonian Granites. Thorning(1974) noted that the palaeopoles calculated for the metamorphosed andesites and the Cheviot Granite supported the existence of lower Devonian group of palaeomagnetic northpoles in the region of New Guinea. He also added that the data from both the andesite and the granite were not sufficient and that the calculated poles should be considered as supplementary ones and not to be quoted as accepted lower Devonian poles. Robson and Green (1980) constructed a total field intensity map of the Cheviot Granite and its aureole from a ground level proton magnetometer. Using the granite classification of Jhingran (1942), they demonstrate that

andesitic lava of the aureole and the marginal variety of the Granite have high susceptibilities, whereas the unmetamorphosed andesite and rhyolites, and the granophyric and Standrop varieties have lower susceptibilities. They considered that the junction between the metamorphosed andesites and the underlying marginal granite forms a dome like surface. In addition they concluded that some vertical movement on the Breamish Fault and horizontal movement along the Harthope Fault must have occurred. Finally they confirmed the presence of many xenoliths of metamorphosed andesite within the granite, and they interpreted the small negative anomaly over the Breamish fault to indicate a thin occurrence of the marginal granite in that area.

3. GEOCHEMICAL STUDIES:

Haslam (1975) studied the geochemistry of stream waters and stream sediments from the Cheviot area. He noted that conductivity of water from streams draining the granite is generally between 40 and 120 mhos. The distribution of elements in samples from streams draining the granite and other rocks were discussed. He reported that samples from streams draining granite, relative to the volcanic rocks in the area, are usually higher in U, Cu, Pb, Be, Sn. Samples from streams draining the granite at Linhope Burn are slightly richer in iron, manganese, tin, vanadium, and zirconium than those from streams draining the rest of the granite, which was thought to be due to the concentration of iron oxide, zircon and tourmaline in the stream bed. Haslam also used the enrichment of the granite in B, Be, Sn

and U to investigate the area of poor exposure between Common Burn and Broadstruther Burn and concluded that it is probably, but not certainly, underlain by granite. Leake and Haslam (1978) collected and analysed panned concentrates from stream sites in the Cheviot Hills. They found some samples to be enriched relative to background in elements such as Ti and Zr in parts of the granite area, which led them to suggest that the granite complex may contain units of dioritic rocks. Anomalous values of Cu, Zn, Ba, and Pb were generally related to small-scale vein mineralization and it was evident that baryte and base metal occurrences are frequent in the area.

CHAPTER TWO

FIELD OBSERVATION AND MAPPING

CHAPTER TWO

FIELD OBSERVATION AND MAPPING

2.1 INTRODUCTION

Field work on the Cheviot Granite and associated rocks over three field seasons was undertaken in three stages:

1. Rapid reconnaisance mapping of 40 square km, encompassing the south part of the granite, using as a base previous interpretations (one inch geological sheets 3 and 5; Carruthers et al., 1932).
2. Sampling of representative and anomalous material for petrographical and geochemical investigation.
3. Detailed outcrop mapping of the plutons concentrating on the southern area, which had already been the subject of the previous work, but including a short season on the north area. The results of this mapping are presented on a scale of 1:25.000 on plate 1 in the folder at the rear of the thesis. This map also includes information on dykes drawn from the mapping by the Geological Survey (Clough, 1882; Carruthers, et al. 1932).

A simplified outline geological map of the area on a smaller scale is given in Figure 2.1. Dykes and other small features are omitted from this map. Detailed petrographic and geochemical results for 122 key samples are recorded in subsequent chapters. National grid

references for these samples, all in 100 km square NT, are given in Appendix C.

Exposure is about 10% overall, but is better in a number of areas where detailed mapping is possible, allowing extrapolation to less well-exposed parts of the complex. Rock is often mantled by a thin layer of drift on hillsides, but summits and plateaux are often covered with extensive developments of peat, such as on the summit of The Cheviot. Outcrops occur in crag features, in iron-stained scree associated with breaks of slopes and in some stream sections. An outcrop map of the district has been completed on a scale of 1:10000 and will be deposited in the Department of Geology at Newcastle.

The granite contacts can be defined within 10-20 m where exposure is good as on the Dunmoor hill (968176) in the southern part of the complex , and in Linhope Burn in the southeastern part of the complex, where the coarse brown Linhope Granodiorite can be seen chilled against the coarse grey Standrop Granodiorite (947172). Elsewhere contacts are less clearly defined, but may be inferred, usually from breaks of slopes such as in the area around High Bleakhope (925158). Many such contacts may be fault related which is best exemplified in the SW part of the complex in the High and Low Bleakhope area (921161).

The recognition of different types of granite alteration in this area is mainly based on field observation supplemented by

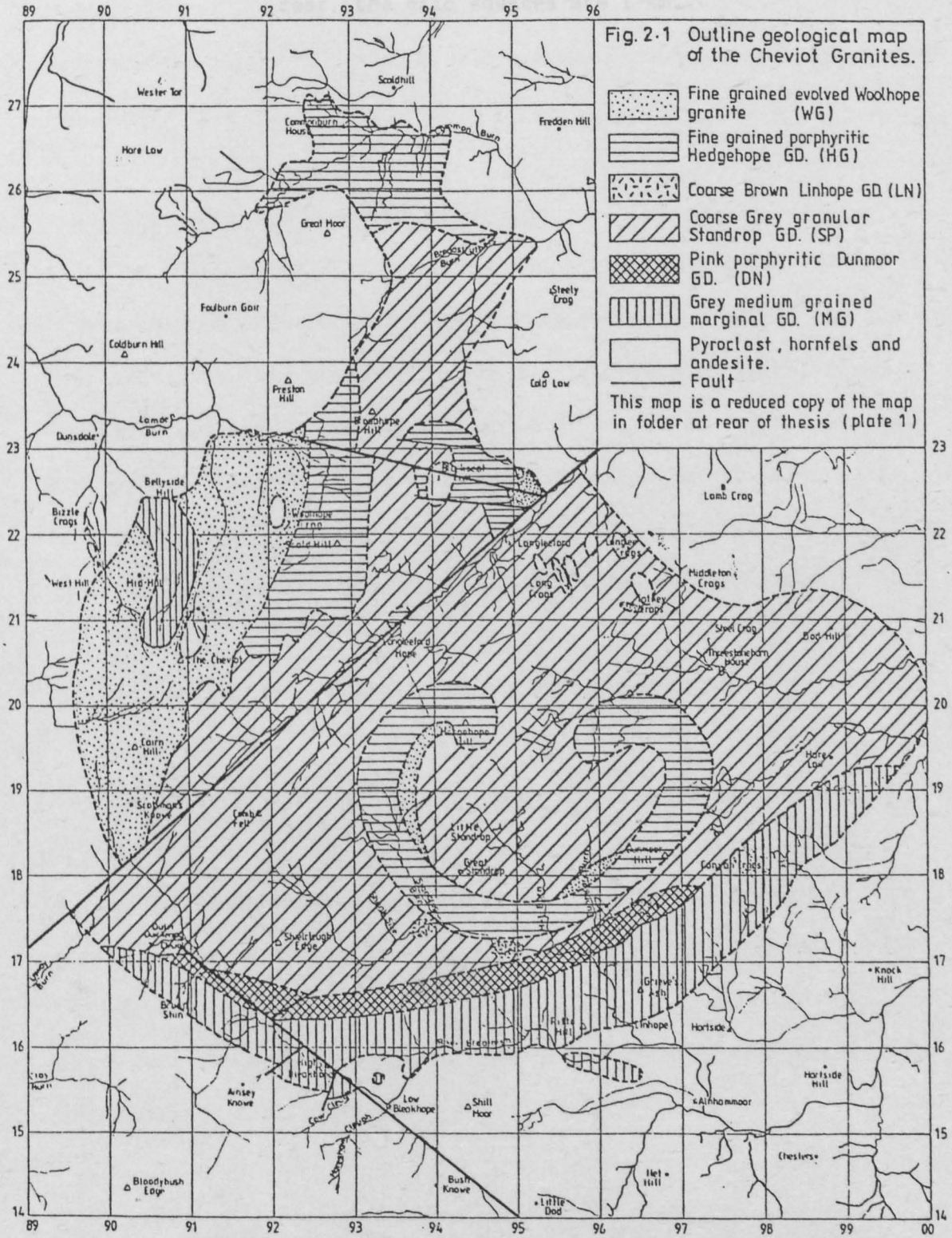
Fig. 2·1 Outline geological map of the Cheviot Granites.
Fine grained evolved Woolhope granite (WG)
Fine grained porphyritic Hedgehope GD. (HG)
Coarse Brown Linhope GD. (LN)
Coarse Grey granular Standrop GD. (SP)
Pink porphyritic Dunmoor GD. (DN)
Grey medium grained marginal GD. (MG)
Pyroclast, hornfels and andesite.
Fault
This map is a reduced copy of the map in folder at rear of thesis (plate 1)
Scaldhill
Wester Tor
Fredden Hill
Hare Law
Great Hoor
Steely Crag
Faulburn Gair
Coldburn Hill
Preston Hill
Cold Law
Dunsdale
Bellyside Hill
Bizzle Crags
West Hill
Mid Hill
The Cheviot
Lamb Crag
Langlee Crags
Middleton Crags
Long Crags
Steel Crag
Dod Hill
Cairn Hill
Scotsman's Knowe
Hedgehope Hill
Little Standrop
Great Standrop
Hare Law
Sheilbrough Edge
Grieve's Ash
Knock Hill
Linhope
Horiside
Bloodybush Edge
Ansley Knowe
Low Blackhope
Shill Moor
Alnhammoor
Horiside Hill
Chesters
Bush Knowe
Little Dod
Hut Hill

Plate 1 Geological map of the Cheviot Granite on 1:25 000, see folder at rear, the grid squares are 1 km.

petrographical and geochemical observations. Field observations were supplemented by surveys with a multi channel gamma ray scintillometer (section 2.4).

2.2 GRANITIC AND GRANODIORITIC INTRUSIONS

The Cheviot Granite is a large complex intrusion containing six different intrusive phases that can be distinguished in the field. The different intrusions are, in order of intrusion (with brackets giving localities where each intrusive phase is particularly well developed):

1. Grey medium grained Marginal Granodiorite, (Cunyan Crags, 979180).
2. Pink porphyritic Dunmoor Granodiorite, (Long Crags - Dunmoor Hill, 967176).
3. Coarse grey granular Standrop Granodiorite, (Great Standrop, 943180).
4. Coarse brown Linhope Granodiorite, (Linhope Burn, 948172).
5. Fine-grained porphyritic Hedgehope Granodiorite, (Hedgehope Hill, 944198).
6. Fine-grained, Leucocratic, chemically evolved, Woolhope Granite, (Woolhope Crag, 925223).

In addition there are numerous dykes and irregular veins which cut through the different units. The granodiorites and granites can be distinguished in the field by their weathered surfaces. Thus the

Marginal Granodiorite , which corresponds closely but not exactly to the marginal granite of Jhingran(1942), is mostly grey and even grained and apparently more melanic than the other intrusions (Plate 2.1). The porphyritic Dunmoor Granodiorite is fleshy in colour, with plagioclase phenocrysts and distinctive large biotite phenocrysts up to 5mm across distributed in a coarse granular groundmass (Plate 2.2). The Standrop Granodiorite is grey, granular and coarse grained (Plate 2.3) with occasional rounded basic xenoliths. In my field mapping (especially at an early stage), the presence of these spots helped as a marker feature to recognise this type of granodiorite, especially the north part of the Cheviot complex north of the Harthope Fault, where highly weathered and crumbly outcrops hinder its recognition. It is very difficult to distinguish between the weathering surface of Standrop Granodiorite and that of Linhope Granodiorite in the field but fortunately they occur next to each other and the chilling relation between them simplifies their field recognition. The Linhope Granodiorite is brown, granular and coarse grained (Plate 2.4). The Hedgehope Granodiorite is the easiest one to recognize in the field as it consists of frequent large white plagioclase phenocrysts which are exremely distinctive especially if the rock is wet, set in a fine-grained khaki coloured groundmass. The Hedgehope Granodiorite almost always contains narrow discontinuous veinlets of tourmaline (up to 3 mm thick), which help with its recognition (Plate 2.5). Finally the very fine-grained saccharoidal, Woolhope Granite has a fleshy colour, and some samples contain plagioclase phenocrysts with accessory tourmaline (Plate 2.6).

Plate 2.1

Grey and even grained Marginal Granodiorite.

Plate 2.2

Porphyritic Dunmoor Granodiorite with plagioclase and biotite phenocrysts.


2CM

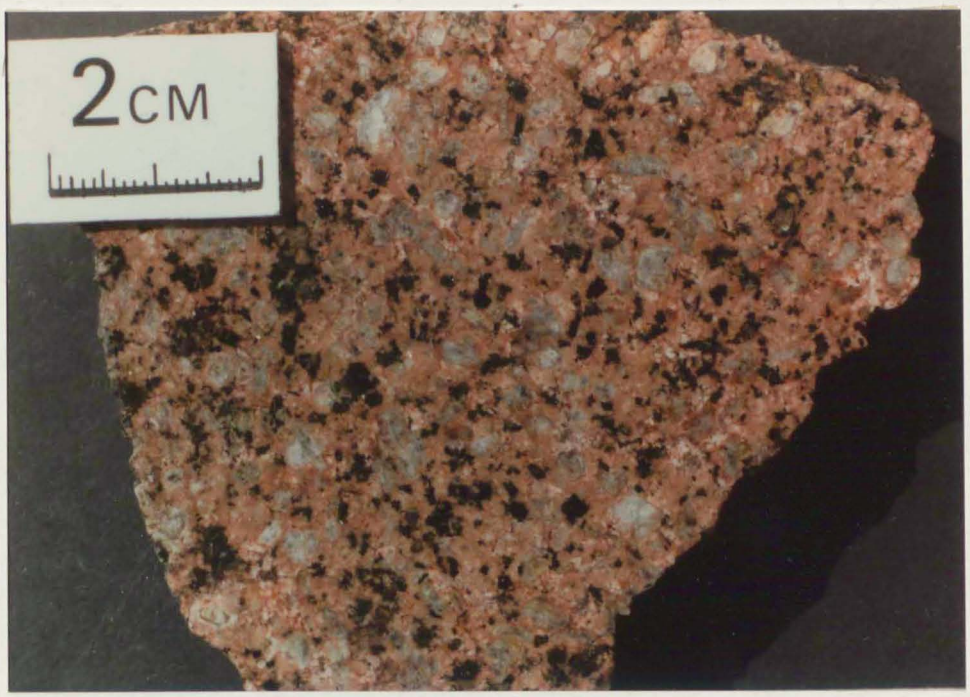
2CM

Plate 2.3

Coarse grey granular Standrop Granodiorite.

Plate 2.4

Coarse brown Linhope Granodiorite.

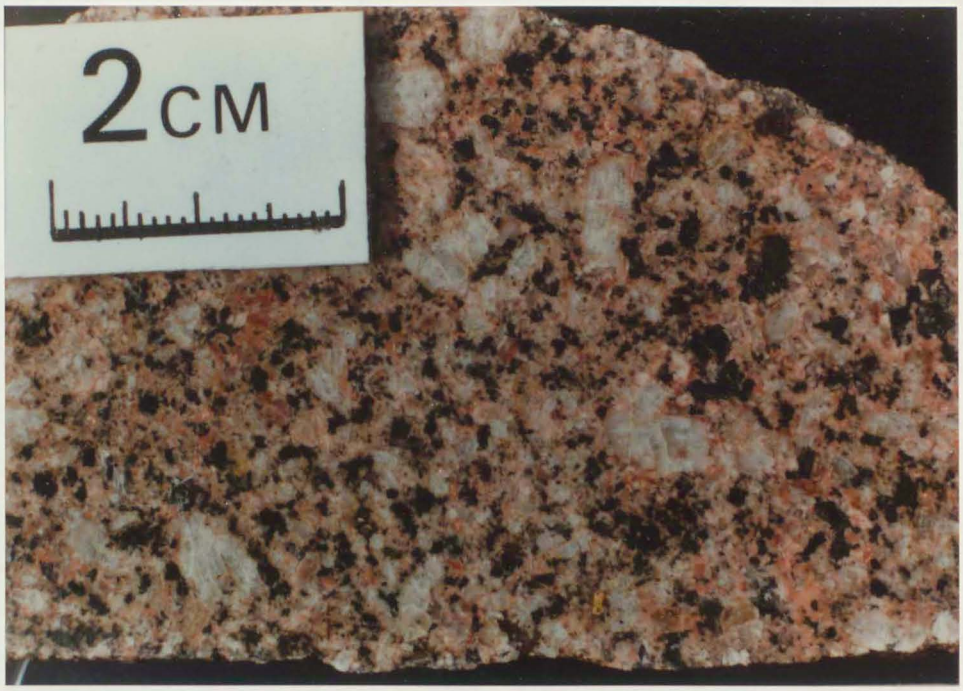
2CM

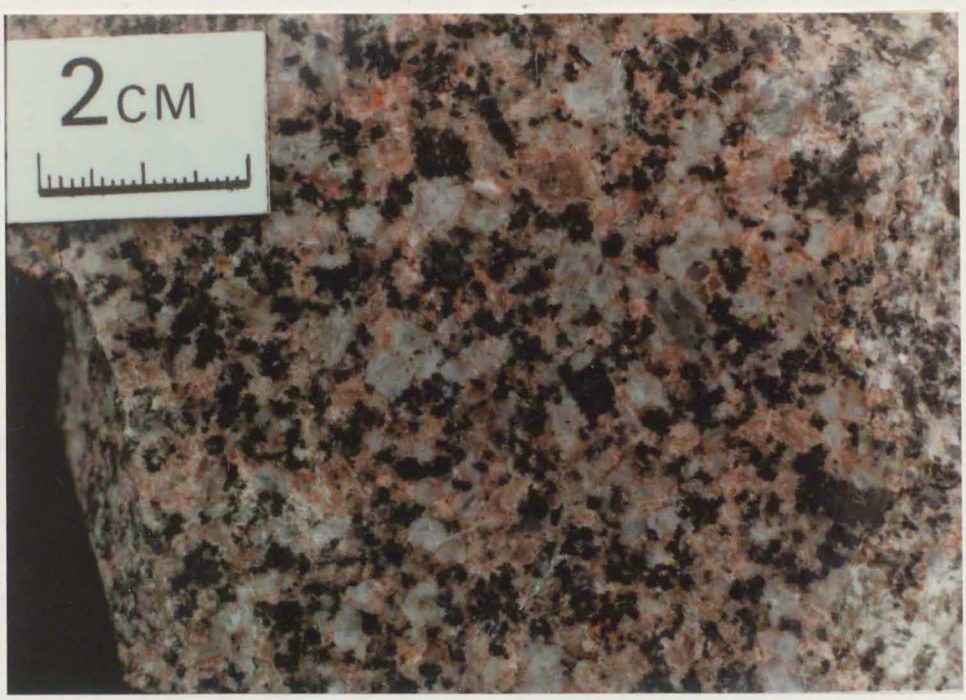
2CM

Plate 2.5

Fine grained porphyritic Hedgehope Granodiorite.

Plate 2.6

Fine grained saccharoidal Woolhope Granite.

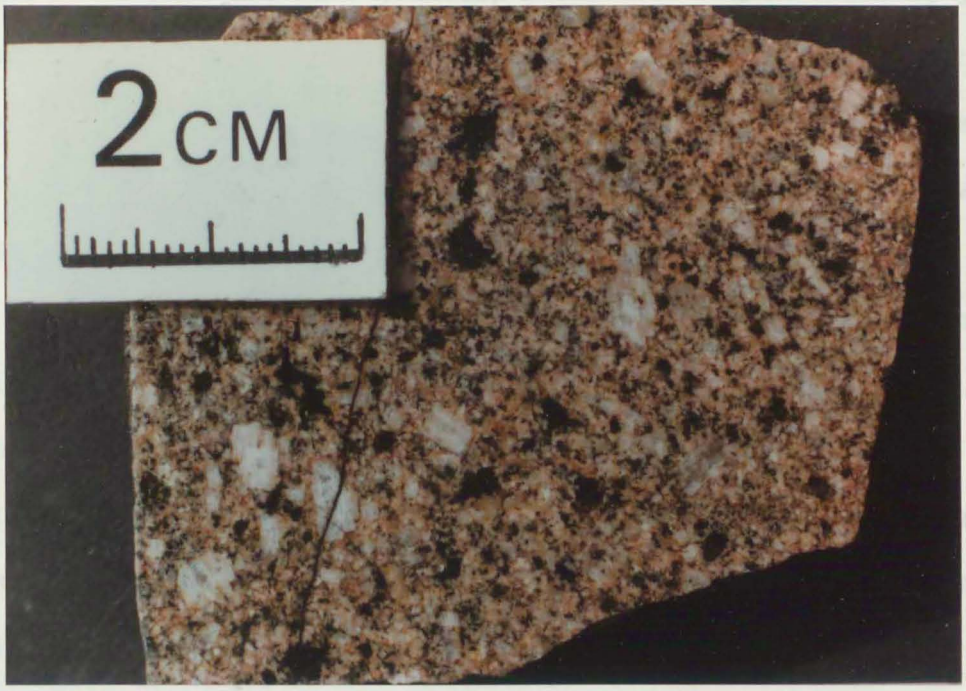
2CM

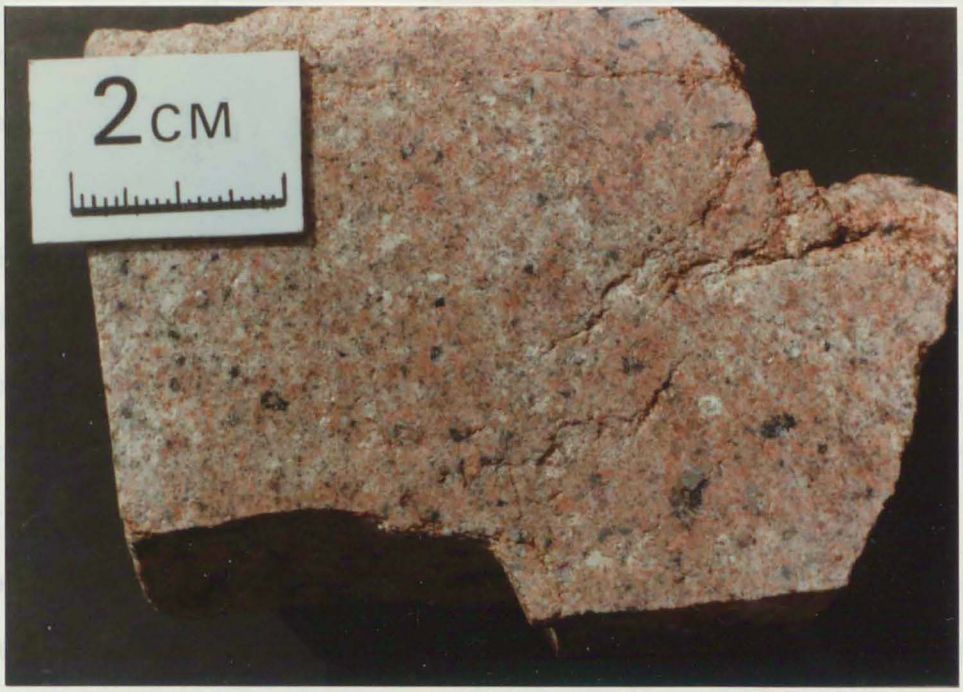
2CM

The intrusions are well jointed, often with veins veneering joint planes and fractures. The field relations show that the Cheviot complex was formed by two major cycles of igneous activity. The intrusives of cycle 1 comprise the Marginal Granodiorite and the Porphyritic Dunmoor granodiorite, in addition to the dykes that are sent off by the Porphyritic Dunmoor Granodiorite and cut through the Marginal Granodiorite and the andesite. Cycle 2 began with the intrusion of the Standrop Granodiorite, which was followed by a minor ring dyke of Linhope Granodiorite and a major ring dyke of Hedgehope Granodiorite, and finally by the intrusion of a narrow partial ring dyke of the fine-grained Woolhope Granite.

The age relationships of the intrusives can be seen at a number of localities. The Marginal Granodiorite forms the outer part of much of the pluton and is seen chilled against the surrounding hornfelsed andesites at Cunyan Crags (984180), but it is never seen to be chilled against any other intrusive body. The Dunmoor Granodiorite is seen chilled against the Marginal Granodiorite at Dunmoor Hill (970178), Dunmoor Burn (959171) and at High Cantle (926164). The second cycle began with the intrusion of the Standrop Granodiorite, which is chilled against Porphyritic Dunmoor Granodiorite at (938167) where the Standrop Granodiorite cuts through the Dunmoor Granodiorite, whereas Linhope Granodiorite is seen chilled against Standrop Granodiorite at 947172 in Linhope Burn. The Hedgehope Granodiorite is seen chilling against Standrop Granodiorite NE of Hedgehope hill (945203). The fine-grained Woolhope Granite has not

been seen chilled against other phases, but is considered to be the last intrusive because of its outcrop pattern, its evolved chemistry and its fine grain size.

2.2.1 FORMS, STRUCTURAL ASPECTS AND MODE OF INTRUSIONS

Though the map shows a complex outcrop pattern, field observations demonstrate that the Cheviot Granite is a comparatively simple type of ring structure in which the two major cycles of magmatic activity can readily be distinguished. The complex is divided into two parts by the NE-SW trending Harthope Fault, and it seems clear that two different levels of erosion are represented on either side of the fault.

To the south-east, the outer contact of the granite appears to dip at a moderate angle outwards, as shown by the inclusions of large xenoliths of hornfels (perhaps roof pendants) in the area east of Langleeford (9521 and 9621), and by the rather complex and irregular southern contact between Linhope and Low Bleakhope. The southward bend in the contact as it descends into the valley of the Breamish near 937157 is particularly clear evidence of an outward dip to the contact. This conclusion agrees with that of Robson and Green (1980) based on magnetic data. However the internal contacts between the different phases of the intrusion appear much steeper. They can be mapped to follow broadly sweeping curves across the ground, regardless of topography. This relation is particularly well seen

where the contact between the Dunmoor Granodiorite and the Marginal Granodiorite runs for about 1 km down from Dunmoor Hill to Linhope Spout (9617). The contact here can be traced very closely on the ground, and it is clearly scarcely deflected over a large change in height. In this part of the complex, then, the different phases apparently form arcuate ring dykes of the classic shape.

To the north-west of the Harthope Fault the same granite and granodioritic units can be recognised as to the south-east, but the disposition of the units is very different. The outer contact with the hornfels is clearly variable in dip. On the north-west margin, on the far side of The Cheviot, it passes across variable topography with little deflection, and is clearly dipping rather steeply, but further north, around Broadstruthers Burn and Common Burn, the contact relations are very different. There the contact tends to contour around hills and up valleys, and where the contact is well seen, as in Common Burn between 942267 and 930269, the granite and hornfels show a complex interfingering relationship, shown in detail in Figure 7 of Robson (1976). These observation suggest stongly that the contact in this area is nearly horizontal. Three large masses of andesites , roughly oval in plan, occur in the northern area, all at or near the summits of hills. These seem too large to be xenoliths, and most probably represent roof pendants. All of this evidence is consistent with the view that over the northern area the level of exposure is very close to the roof of the granite pluton.

The relationships between the different intrusive phases are also different from those in the southern area. Contacts between different phases tend to contour around hills, as is well seen in the area to the north-west of The Cheviot, where the strikingly different Woolhope Granite and Marginal Granodiorite are in contact. The contact between the Hedgehope Granodiorite and the Standrop Granodiorite E of The Cheviot, near 920206, has a similar horizontal, complex interfingering relationship to that seen at the contact with the hornfels further N. These relationships suggest that both the Hedgehope Granodiorite and the Woolhope Granite form thin undulating sheets in this area, both of them discontinuous, but with the Woolhope Granite at a structurally higher level than the Hedgehope Granodiorite where both are present. No contacts are seen between the Standrop Granodiorite and earlier phases, so no information is avaliable about the form of this or earlier phases in the complex in this area.

This demonstrates that the SE part of the complex represents a lower structural level than the NW part, elevated during later movements on the Harthope Fault. Thus the ring dykes in the SE part seem to feed the NW part with horizontal sheets. This relationship is illustrated in Figure 2.2 which represents a cross section along Hartside- Langleeford and Common Burn. Moreover two schematic diagrams (Figures 2.3 and 2.4) are presented to show how repeated subsidence and intrusion has led to the progressive obliteration of the initial stages during the multi-component ring dyke evolution,

resulting in the rocks concerned (the Marginal, the Dunmoor, and the Standrop Granodiorites), being preserved as remnants.

Two major faults are found within the Cheviot Granite, the NE-SW Harthope Fault and the NW-SE Breamish Fault. Supplementary minor fractures occur both in the southern and in the northern parts. They seem to have been initiated shortly after the consolidation of the granite. The Breamish Fault represents a less important fracture plane than the Harthope Fault and occurs along the Breamish river between Low Bleakhope and outer Quickening Cleugh. It contains veins of calcite and silica. This crush is readily traced south-east ward up the valley SE of Low Bleakhope, through the exposure NW of Shank House which has been noted by previous workers (Clough, 1888; Carruthers, et al., 1932). Previous workers (Carruthers, et al., 1932; Robson, 1975, 1980) suggested the presence of another fault plane, which is placed parallel to the Breamish fault running NNW (Robson, 1980), but my field work show no evidence of such a fault. Minor fracture planes occur in the SW part of the Cheviot Granite , in the neighbourhood of the Breamish Fault, together with resulting brecciation and slickensides (Between 928156 and 913168) with a more or less NE-SW trend. The direction of the horizontal movement on these minor fracture planes is shown by the slickensides. In addition there are a few fracture planes north of the Harthope Fault at Hawsen Burn (946230) and in Newburn (950224) which run nearly WNW and along which intense crushing and brecciation occurs. Clough(1888) reported these fracture planes as extensive crush lines

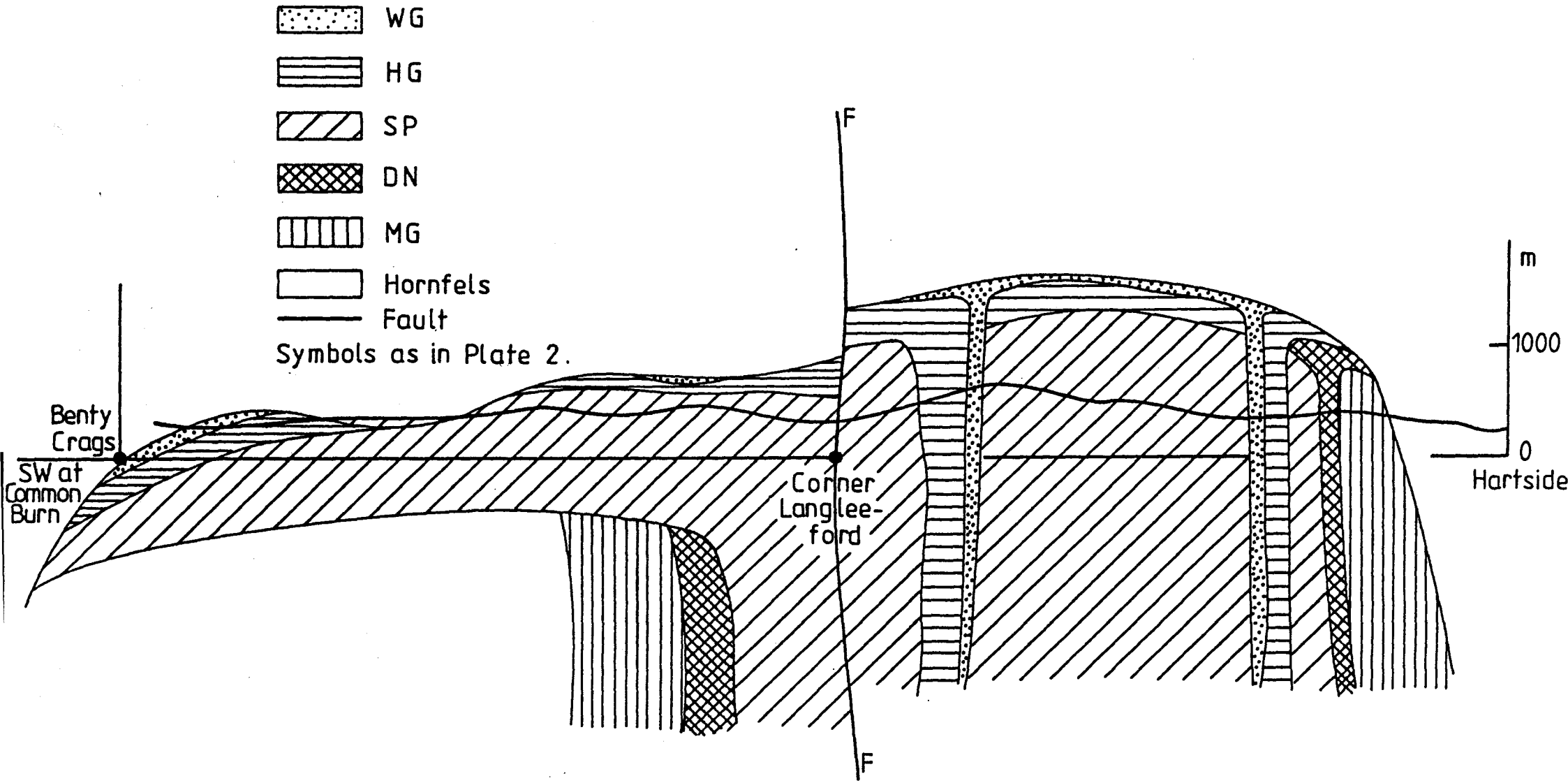

Fig. 2·2 Cross section along Hartside–Langleeford and Common Burn showing the geological history of the Granites intrusion.

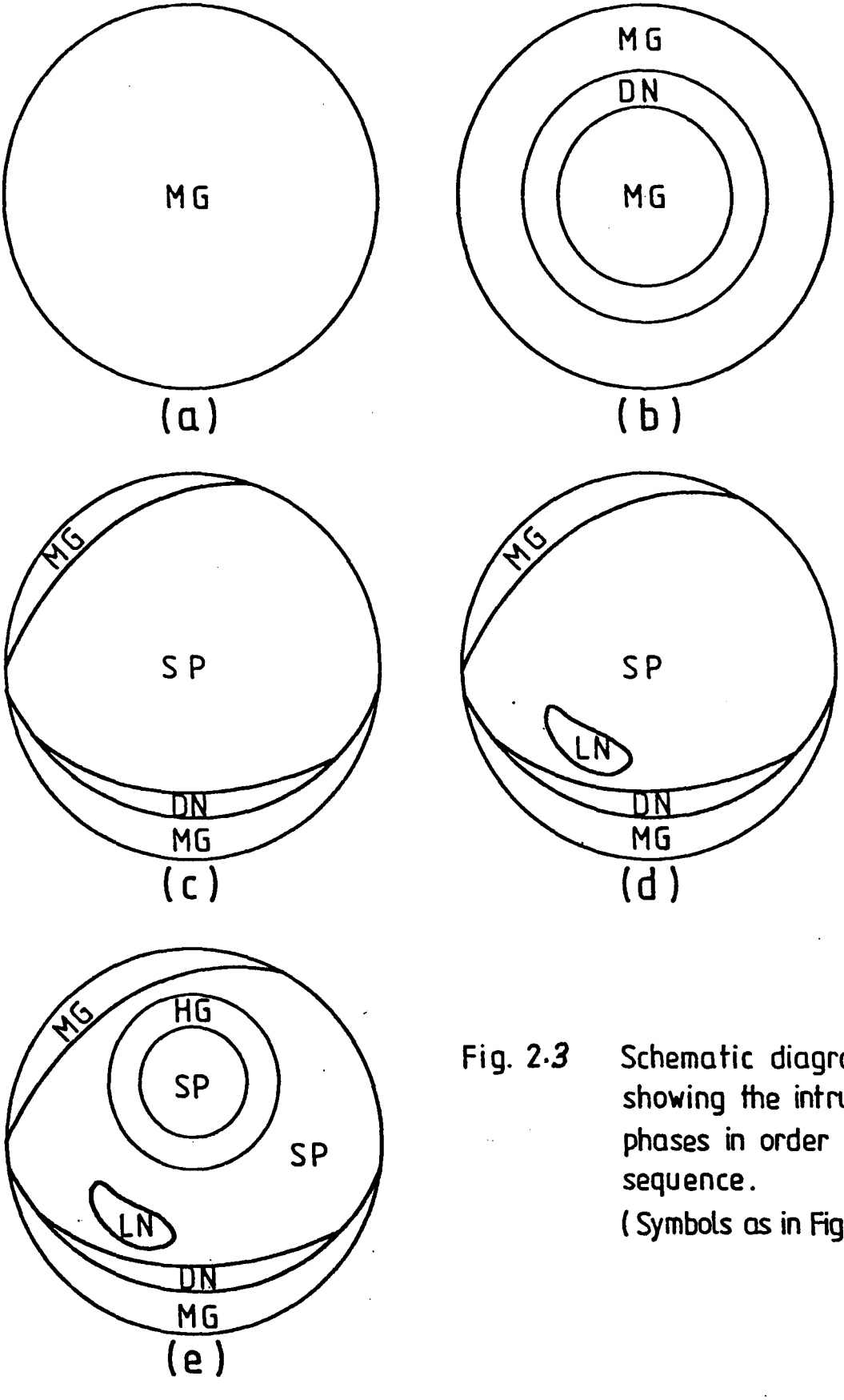

Fig. 2.3 Schematic diagrams showing the intrusive phases in order of sequence.
(Symbols as in Fig. 2.1).

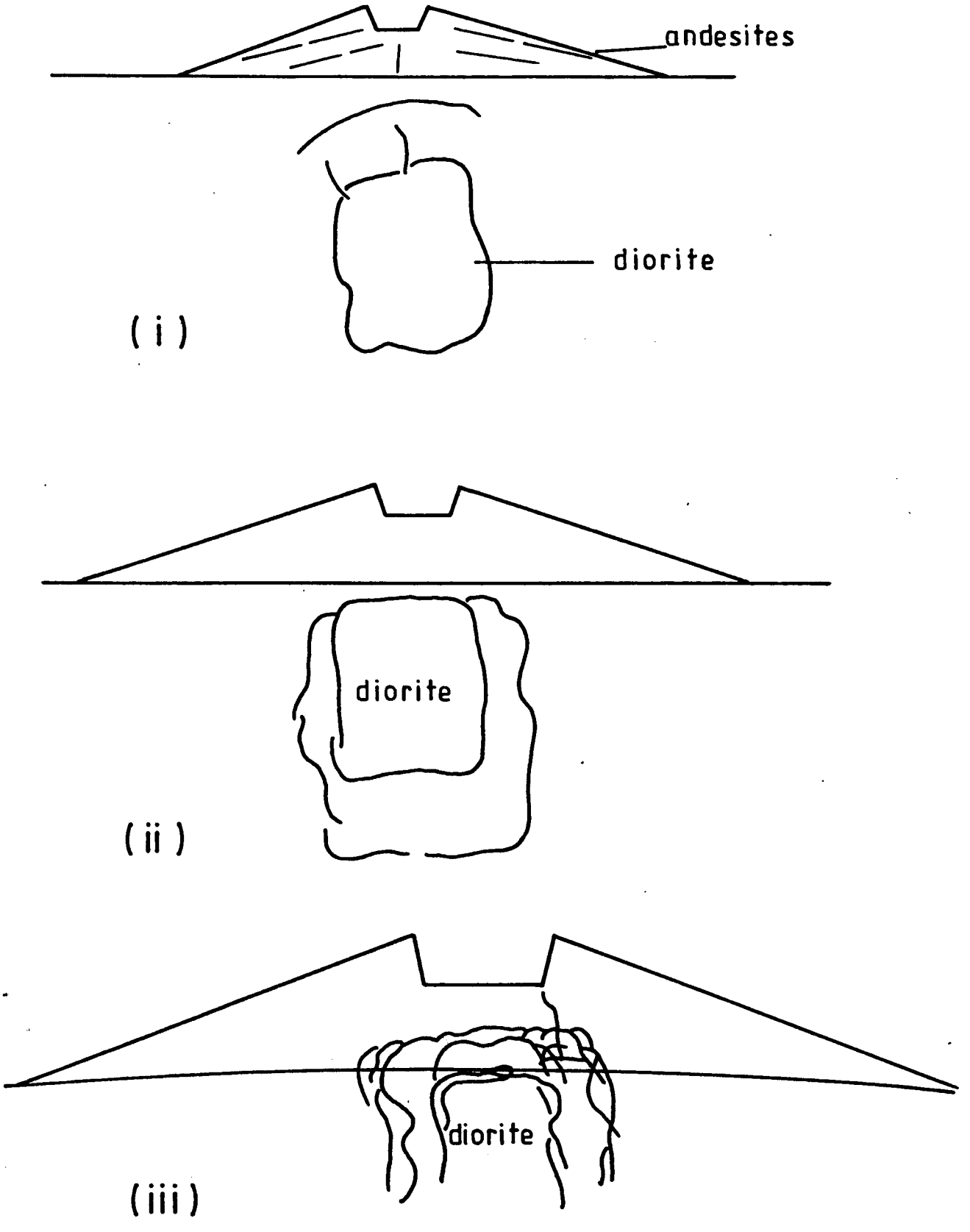

Fig. 2·4 Schematic diagrams showing the mechanism of concentric arrangement produced by a continued operation of gradual subsidence.

in which massive blocks of silica occur.

2.3 ALTERATION TYPE, THEIR DISTRIBUTION AND OCCURRENCE

Several varieties of alteration have affected the aforementioned rocks. The fresh, or slightly altered, rocks are widely distributed in the area. However the primary igneous fabric is shown even by the most intensely altered samples. This in turn plays a very important role in the recognition of the different igneous suites that have undergone different intensities of alteration through the various alteration types. As far as it can be ascertained some primary rock units are transgressed by a distinct alteration type which has a slight effect on the earlier type. Two major areas of hydrothermal alteration (The A and B systems) are spatially centred on the porphyritic Dunmoor Granodiorite and the porphyritic Hedgehope Granodiorite, respectively. The A system alteration postdates the igneous cycle 1 and predates the intrusion of the Standrop Granodiorites of cycle 2, whereas the B system alteration postdates the intrusion of the porphyritic Hedgehope Granodiorite. The spatial distribution of the different alteration systems and their different assemblages is shown on Figure 3.1. The petrology of the A and B alteration systems will be discussed in detail in Chapter 3.

1. The A SYSTEM:

This is the characteristic alteration association of the area between High Bleakhope (928155), Inner Quickening Cleugh (908167) and the Breamish River area-north of Shillmoor (930160 - 964160)

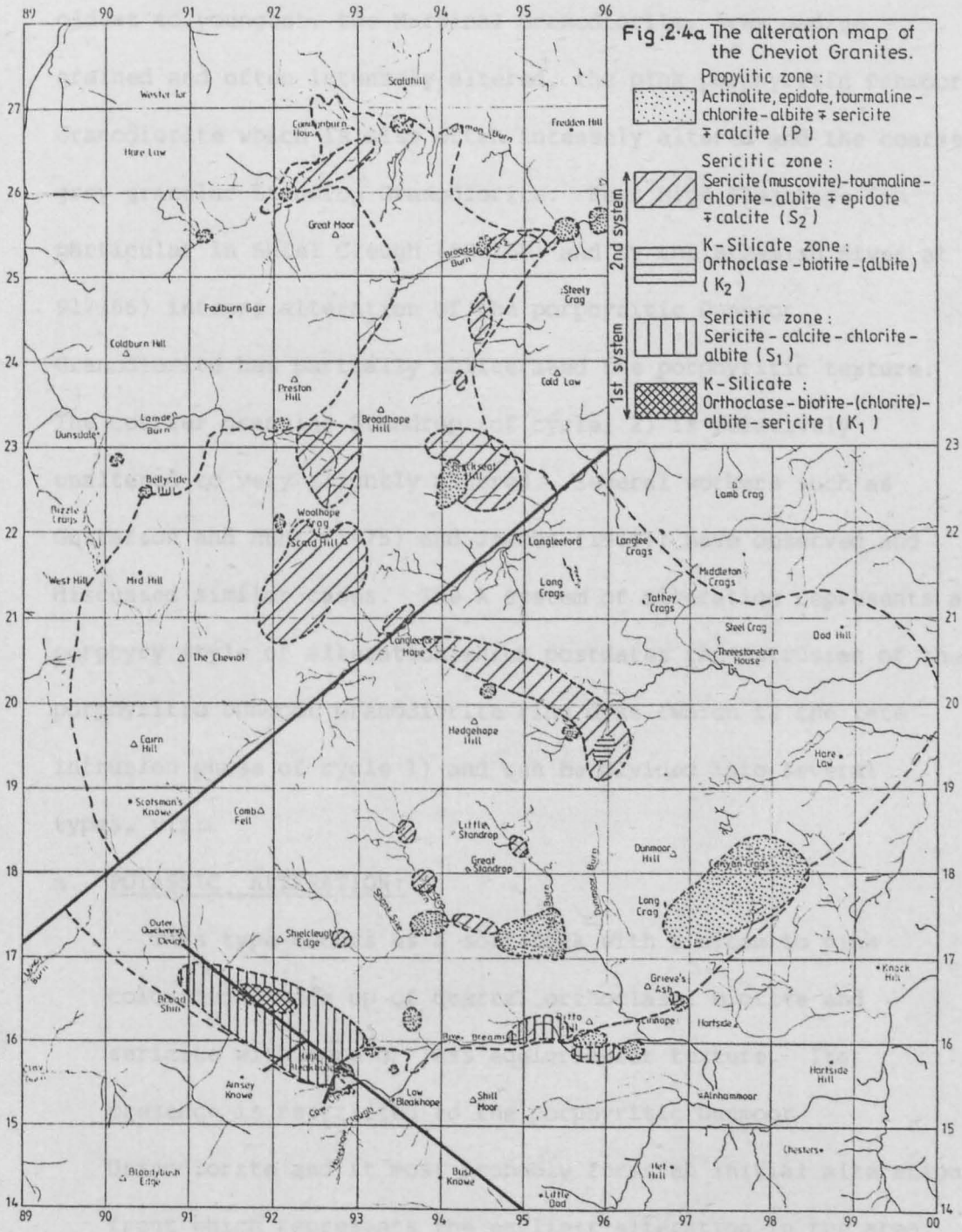
Fig.2·4a The alteration map of the Cheviot Granites.
Propylitic zone : Actinolite, epidote, tourmaline - chlorite - albite ∓ sericite ∓ calcite (P)
Sericitic zone : Sericite (muscovite)-tourmaline - chlorite - albite ∓ epidote ∓ calcite (S_2)
K - Silicate zone : Orthoclase - biotite - (albite) (K_2)
Sericitic zone : Sericite - calcite - chlorite - albite (S_1)
K - Silicate : Orthoclase - biotite - (chlorite) - albite - sericite (K_1)
2nd system
1st system
The Cheviot
Hedgehope Hill
Langleeford
Langlee Crags
Middleton Crags
Lamb Crag
Steel Crag
Dod Hill
Threestoneburn House
Hare Law
Dunmoor Hill
Carlyon Crags
Long Crag
Grieve's Ash
Hartside
Hartside Hill
Alnhammoor
Knock Hill
Chesters
Hut Hill
Little Dod
Bush Knowe
Shill Moor
Low Bleakhope
Ansley Knowe
Bloodybush Edge
Broad Shiel
Outer Queensberry
Shielcleugh Edge
Scotsman's Knowe
Comb Fell
Cairn Hill
Little Standrop
Great Standrop
Dunmoor Burn
Langlee Hope
Tathey Crags
Long Crags
Mid Hill
West Hill
Puzzle Crags
Bellyside
Dunsdale
Lamey Burn
Woolhope Knag
Scald Hill
Preston Hill
Broadhope Hill
Cold Law
Steely Crag
Broadstruther Burn
Foulburn Gair
Coldburn Hill
Great Moor
Hare Law
Scaldhill
Freeden Hill
Cansamburn House
Lyman Burn
Wester Ter

(Figure 3.1). The main lithologic units of this area are, from oldest to youngest, the Marginal Granodiorite, grey medium grained and often intensely altered, the pink porphyritic Dunmoor Granodiorite which is also often intensely altered and the coarse grey granular Standrop Granodiorite. Near High Bleakhope (in particular in Shiel Cleugh (923165) and by the Breamish River at 917166) intense alteration of the porphyritic Dunmoor Granodiorite has partially obliterated the porphyritic texture. The coarser granular Standrop (of cycle, 2) is relatively unaltered to very slightly altered. Several workers such as Gustafson and Hunt (1975) and Jacobs (1979); have observed and discussed similar cases. The A system of alteration represents a porphyry style of alteration which postdates the intrusion of the porphyritic Dunmoor Granodiorite ring dyke (which is the late intrusion phase of cycle 1) and can be divided into several types, viz:

a. POTASSIC ALTERATION:

This type occurs as a soft rock with a cream to pink coloration, made up of quartz, orthoclase, biotite and sericite with more or less equigranular texture. Its presence is restricted to the porphyritic Dunmoor Granodiorite and it most probably forms an initial alteration front which represents the earliest alteration in the area. No mineralization has been found either in the altered rock or in the quartz veins, unlike in other areas of similar alteration assemblage.

b. SERICITIC ALTERATION:

This encompasses rocks affected by alteration processes which produce secondary white mica (sericite). The altered rocks generally are characterised by destruction of their original texture and by their fleshy coloration. The alteration types of cycle 1 are entirely or largely associated with veins which are different in mineralogy from the rocks themselves. Veins of quartz and chlorite or calcite seem to favour the sericitic altered rocks in this area (e.g. in Breamish River, 951161; and at Cat Cleugh, 927156).

c. PROPYLITIC ALTERATION:

This typically makes up the outer zone and is characterised in the field by a more or less red weathering surface and the occurrence of epidote, chlorite, and occasional fibrous amphibole veins which cut through the altered samples.

The A and B systems alteration are both porphyry style in nature, but the similarity of both related propylitic zones makes it difficult to separate one from another. Consequently it is suggested that rocks mapped as belonging to this zone may be the alteration product of either of the two hydrothermal systems mentioned above.

2. THE B SYSTEM:

This is spatially centred on the porphyritic Hedgehope

Granodiorite ring dyke as the alteration postdates its intrusion and mostly takes place during the late stages of its cooling giving rise to different zones of alteration.

a. POTASSIC ALTERATION:

The porphyritic Hedgehope Granodiorite is the sole rock showing this type, which is characterised by cream to pink coloration and more or less equigranular texture. The rocks of this type are mainly composed of quartz, orthoclase, and biotite. However the space-time relationship has led to the interpretation of its earliest formation in system B when this zone was partly overprinted by sericitic zone resulting in the rocks concerned being affected by two types of alteration. This phase of potassic alteration is restricted to one small area of the complex (Threestone Burn 960194).

b. TOURMALINIZATION AND ITS ALTERATION ASSOCIATION:

This is typically associated with the porphyritic Hedgehope Granodiorite ring dyke and always occurs with medium to high temperature alteration assemblages. It was immediately preceded by the above phase of potassic activity and is extremely widespread in the central part of the Cheviot Granite area. Heavily tourmalinized bands several inches wide are not uncommon. Tourmaline has been known to be often associated with sericitisation since the work of Schwartz (1955). Such an association is clearly seen in parts of the system B alteration, especially in the Threestone Burn (959197). Staining of samples from this

locality shows that they contain quartz and albite with varying amounts of orthoclase. Tourmaline is developed extensively in these rocks and is especially associated with areas of most intense sericitization, when the samples are texturally destroyed and posses a fleshy colour which serves to distinguish them in the field.

Tourmaline is also associated with propylitic alteration in system B. Reddening of samples as a result of propylitic alteration occur more or less at the contacts of the porphyritic Hedgehope Granodiorite with other phases (e.g. in Threestone Burn, 956197), and is distributed beyond as an outermost zone, acting as a good control to ascertain the position of contacts. Tourmaline is even found in some propylitic samples (in particular in the Linhope Granodiorite) where it is mostly disseminated in habit.

2.4 GAMMA RAY SCINTILLOMETER

The multi channel gamma ray scintillometer was used to supplement the field observation and to aid in the recognition of the different alteration types. It has a great capability of detecting the gamma rays emitted by the rocks because of the presence of trace amounts of radioactive elements. Among the most intense radiations are those of potassium 40 , bismuth 214 , and thallium 208. The radiation from potassium 40 is useful for geological surveys in as much as potassium distribution is indicative of a variety of rock types. On the other

hand, bismuth 214 and thallium 208 are the radioactive decay products of uranium 238, and thorium 232 respectively and as such are highly diagnostic of the presence of the parent radioactive elements. For simplicity in geologic surveys, the gamma ray energies emitted by bismuth 214 and thallium 208 and potassium 40 are referred to as uranium (U), thorium (Th), and potassium (K); the FUNCTION switch marking on GR-310 reflects this simplification. The instrument reading of K, U and TH , should be recorded at each point and converted into per cent or ppm by the following equations:

$$K\% = 0.96(R\ K - 1.32\ R\ U - 0.1R\ TH) \quad (1)$$

$$U\ PPM = 13.0(R\ U - 0.83R\ TH) \quad (2)$$

$$TH\ PPM = 28.0(R\ TH - 0.089\ U) \quad (3)$$

where R=Reading of the scintllometer.

The first area investigated was the area of intense system A alteration in the region of High and Low Bleakhope. Here both potassic and sericitic alteration is abundant, and the distribution of the most intense alteration could be mapped with the scintillometer. 82 measurements were made for K, U and Th in the area and the values of K are contoured on Figure 2.5 (Those for U and Th showed no coherent pattern). The distribution of anomalies shows the patchy development of the alteration even in this highly altered area, and the scale of individual spots of intense alteration. The second area investigated was in the valley of the Linhope Burn below its junction with the Linhope Burn (near 940174) where a survey of 37 points was made. Again U and Th values showed no pattern, but the K

values brought out very clearly the patches of system B sericitic alteration with associated tourmaline so characteristic of the Standrop and Hedgehope Granodiorites (Figure 2.6). Though alteration is fairly general throughout the area, it is clear that intense alteration is not very widespread.

2.5 SUMMARY

The main features of both the igneous and hydrothermal activity in the Cheviot area may be summarized as follows:

1. The Cheviot Complex was formed by two major cycles of igneous activity. Intrusions of cycle 1 comprise the Marginal, and Dunmoor Granodiorites in that order. On the other hand cycle 2 was formed by intrusion of Standrop, Linhope (both coarse granular) and Porphyritic Hedgehope Granodiorites and was accomplished by the emplacement of the Woolhope Granite.
2. Two major areas of hydrothermal alteration (the A and B systems) are spatially centred on the Porphyritic Dunmoor Granodiorite and the Porphyritic Hedgehope Granodiorite respectively. Both systems are porphry style in nature with the characteristic zonal assemblage (i.e. a core of potassic zone surrounded by an intermediate sericite zone and an outermost propylitic zone)
3. Two episodes associated with tourmalinization are recognized. The earlier stage follows the B system potassic phase, and is associated with sericitisation, while the later stage, characterised by disseminated tourmaline, is associated with

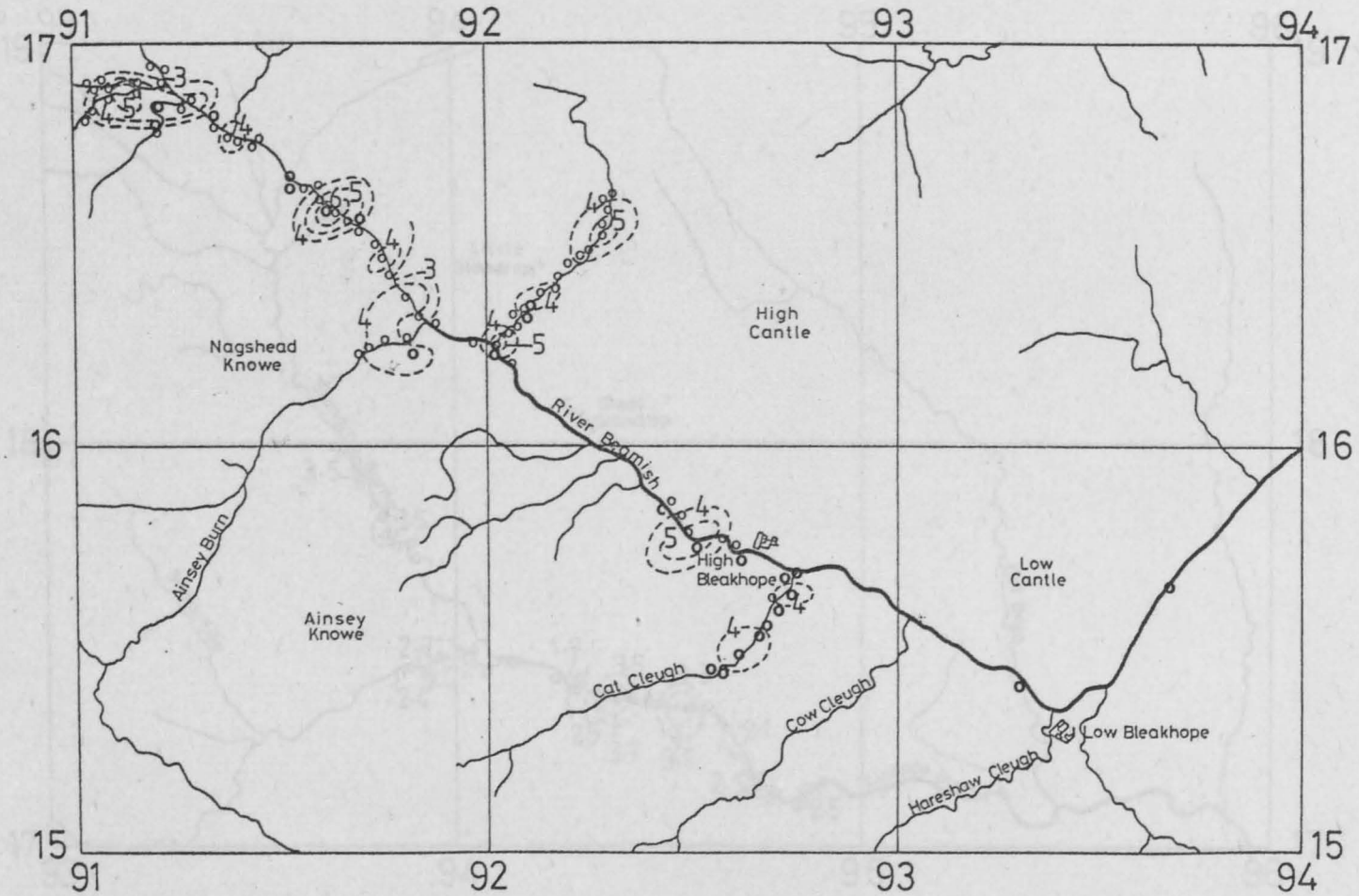

Fig. 2·5 K% anomaly map based on traverse using a Multi Channel X-ray Scintillometer for Dunmoor and Marginal Granodiorites being affected by K-silicate (1) and sericitic (1) alterations (of which a concentration of ≃ 3% K is given by its fresh types).

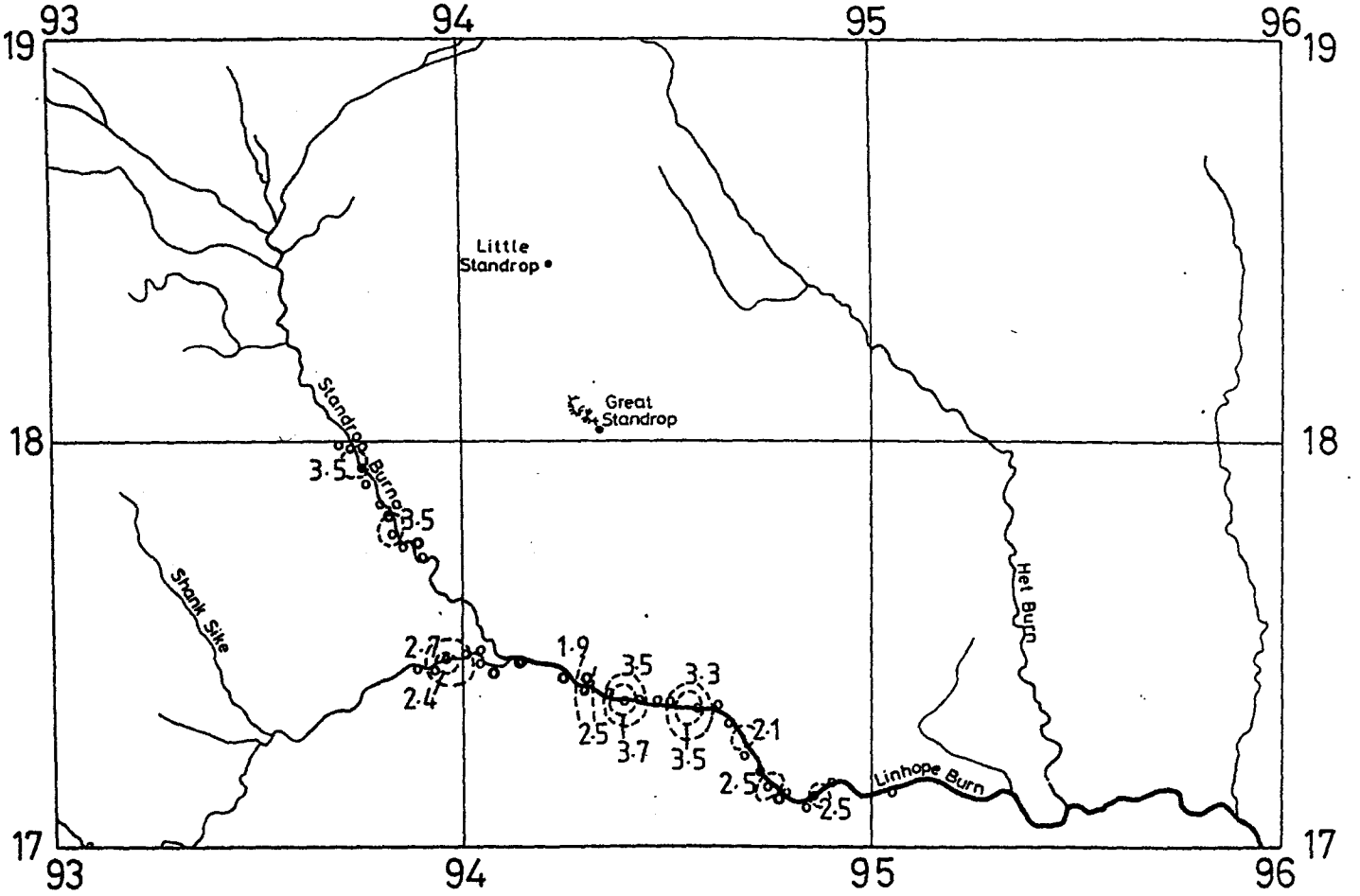

Fig. 2·6 K% anomaly map based on a traverse using a Multi Channel X-ray Scintillometer for Hedgehope and Linhope Granodiorites being affected by sericitic (2) and propylitic alterations.

propylitic alteration.

CHAPTER THREE

PETROGRAPHY OF THE CHEVIOT PLUTON, DYKES AND HORNFELSES

3.1 INTRODUCTION

In this chapter are summarised the petrographic characteristics of the different plutonic units of The Cheviot complex, as well as the dykes that cut these plutons and the hornfelses metamorphosed by the complex.

This summary is based on a collection of over 800 samples from the complex. These were subjected to detailed hand specimen study. Of these 463 were selected for preparation of thin section. On the basis of preliminary petrographic descriptions, 122 rocks were selected for detailed examination (Table 3.1). For all of these samples, detailed petrographic descriptions were prepared, powders were crushed for analysis and major and trace elements were determined. A representative sub-sample of 32 polished sections was prepared for reflected light petrographic investigation and electron micro-probe analysis (Chapter 4). Appendix C lists all of the samples collected, with localities, concise petrogrphic notes and the treatment given to each sample. Table 3.2 summarises this information. The petrographic description of the different intrusive phases, dykes, veins and hornfelses (primary petrography) and the alteration petrography are discussed in turn.

Table 3.1

ROCK TYPES	number of samples
1.Medium grained, altered and unaltered Marginal Granodiorite	25;
2.Porphyritic, altered and unaltered Dunmoor Granodiorite	20;
3.Coarse granular, altered and unaltered Standrop Granodiorite	23;
4.Coarse granular, altered and unaltered Linhope Granodiorite	9;
5.Porphyritic, altered and unaltered Hedgehope Granodiorite	17;
6.Fine grained, chemically evolved Woolhope Granite	5;
7.Dykes	12;
8.Veins	7;
9.Hornfels and andesite	4;
Total	122;

Table 3.2

STAGES IN DETAILED ROCK SAMPLE INVESTIGATION

FIELD SAMPLES(810)

(Grid reference; description of locality and geological occurrence)

HAND SPECIMENS	THIN SECTIONS	POWDERS	POLISHED
(810) as in Appendix C.	(463) samples description of phases & texture with some photo-micrographs.	(122) for major & trace element analyses. (20) of them for REE analyses.	SECTIONS (32) for EDS analyses.

where EDS= Energy Dispersive Analyser System.
REE= Rare Earth Element.

3.2 PRIMARY PETROGRAPHY

3.2.1 MARGINAL GRANODIORITE

The following description is for a typical Marginal Granodiorite sample (B12) from Cunyan Crags which has been analysed for major and trace elements, including REE. This rock is described in detail and then only significant variations in other rocks are mentioned.

B12 is medium grained (2 mm average), allotriomorphic, and slightly more basic in its mineral assemblage than the other granodiorites. It consists of 50% andesine plagioclase crystals, quartz, orthoclase, pyroxene (both augite and hypersthene), and biotite. In addition the accessory minerals zircon, apatite, magnetite and ilmenite are present.

Andesine crystals are subhedral and range from 0.8 mm to 2.5 mm in length. The symmetrical extinction angles indicate a composition of 40-42% An. The plagioclase shows some oscillatory zoning, but this is poorly developed.

Quartz occurs as small and medium sized (up to 1 mm), allotriomorphic crystals. Many of the crystals show undulose extinction.

Orthoclase occurs as medium-sized, allotriomorphic crystals up to 2 mm across. Sometimes twinned on the Carlsbad Law. The orthoclase occurs as microperthite in which the exsolution bodies are about 0.3 mm in size.

Pyroxene crystals (both augite and hypersthene) range up to 1 mm

in length. They are allotriomorphic, and often poikilitically enclose magnetite, apatite and ilmenite grains. The basic inclusions mentioned by Jhingran (1942) which he described as having a special association with this unit are found to be aggregations of interlocked pyroxene crystals and magnetite crystals and appear as dark spots in hand specimen ranging up to 1.5 cm in size. The texture of the intergrown aggregates suggested an origin not as xenoliths, as Jhingran suggested, but perhaps replacing earlier-formed hornblende. Biotite crystals range up to 1.5 mm in length; they are idiomorphic, pleochroic from pale brown to dark brown and often poikilitically enclose magnetite, zircon and apatite crystals. The small euhedral zircon crystals are chiefly associated with biotite.

Small grains of magnetite and ilmehite are often associated with mafic minerals such as pyroxene crystals and biotite.

Many of the apatites are unusual for granodiorites in that they have a large crystal size. This is characteristic of all the different intrusive units.

At the outer margin of the Marginal Granodiorite a change to a finer grained rock (average less than 1 mm) occurs as a result of its chilling gainst the hornfels. This produces poorly developed micrographic intergrowth in the rock (e.g. at Cunyan Crags). Other examples such as samples from Linhope Spout water fall and those from Ritto Hill appear in hand specimen to be slightly coarser than some of the Cunyan Crags samples (i.e. sample B12) but thin sections reveal a very similar petrography. Plates 3.1 and 3.2 are

photomicrographs of the Marginal Granodiorite sample B12 in plane polarised light and in crossed nicols respectively.

3.2.2 DUNMOOR GRANODIORITE

The characteristic feature of this type of granodiorite is its porphyritic texture. Phenocrysts of andesine plagioclase, biotite in the form of characteristic large thin plates, and pyroxene are set in a medium grained groundmass.

A description of one rock, typical of this group, is given below. Sample E177 is from 953169 and has been analysed for major and trace elements including REE.

This sample is characterised by a porphyritic texture with phenocrysts of, (a). idiomorphic, white plagioclase, up to 6 mm in length and slightly more sodic than the plagioclase of the Marginal Granodiorite (An37), (b). characteristic large thin euhedral plates of biotite (up to 5 mm in length), poikilitically enclosing magnetite, apatite and zircon and pleochroic from pale to dark brown, and (C). finally pyroxene (both augite and hypersthene, up to 2 mm across) with stumpy rectangular forms which poikilitically enclose magnetite, ilmenite and apatite. These phenocrysts are surrounded by a medium grained groundmass (varies in grain size between 0.8-1 mm) which is usually composed of a granophyric intergrowth of quartz and potash feldspar. In these intergrowths the quartz is cuneiform, resembling runic inscriptions, set in a background of microperthite feldspar. The granophyrically intergrown groundmass is particularly

Plate 3.1

Photomicrograph of the Marginal Granodiorite, x 13 plane polarised light.

scale |____| 1 mm

Plate 3.2

Photomicrograph of the Marginal Granodiorite, x 13 crossed nicols.

scale |____| 1 mm

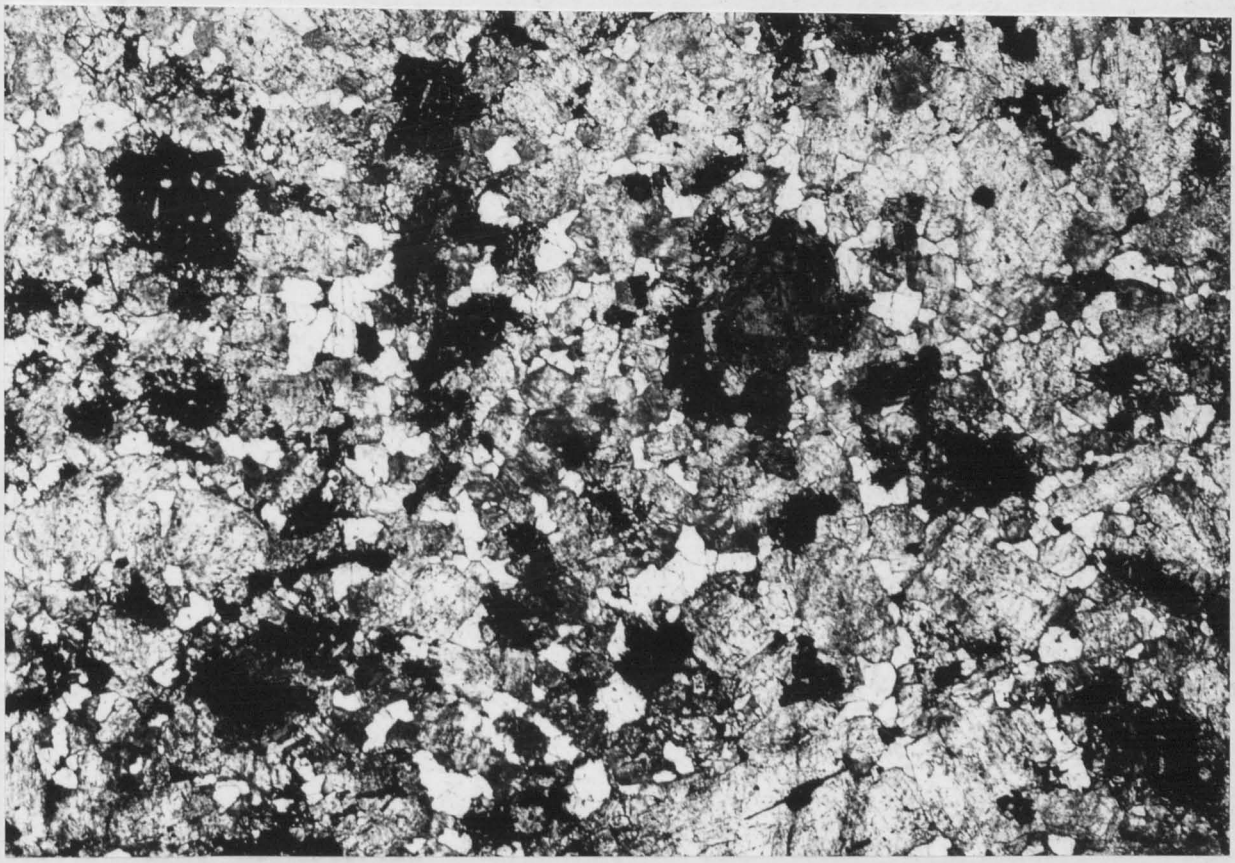

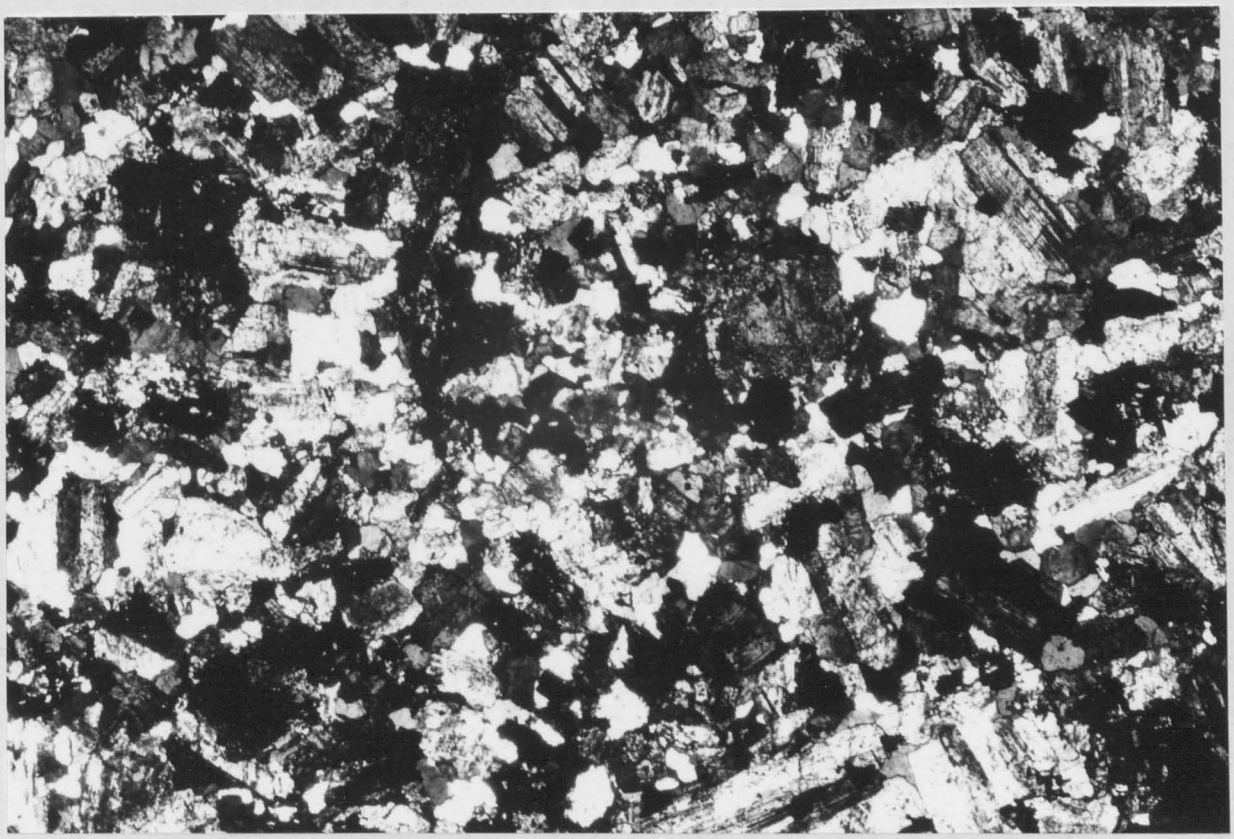

well developed near the outer contact of the Dunmoor Granodiorite, where it is chilled against the Marginal Granodiorite. Clearly in these places the magma cooled relatively fast and as it did so, the residual liquid crystallised both quartz and potash feldspar simultaneously to give this texture. In addition the groundmass also contains biotite, augite, hypersthene and andesine plagioclase. Accessory minerals are zircon, magnetite, ilmenite and apatite which have similar a mineralogical association to that in sample B12 above. Plates 3.3 and 3.4 are photomicrographs of this unit in plane polarised light and in crossed nicols respectively.

3.2.3 STANDROP GRANODIORITE

This is a coarse grained hypidiomorphic granular rock consisting of around 50 per cent andesine plagioclase of composition (An39), pyroxene (both augite and hypersthene), biotite, microperthite and quartz. The accessory minerals are apatite, zircon, ilmenite and magnetite. A description of sample A11, typical of this group from Linhope Burn (947172) is given below and is followed by a discussion of the variations in other specimens of this rock type.

This sample is a coarse grained (4 mm averages) black and white relatively leucocratic rock. There is a tendency for the plagioclase crystals to form as sparse phenocrysts (up to 8 mm in length). The plagioclase is andesine, and occurs as subhedral, poorly zoned crystals which reach 50% per cent of the rock, and are usually fresh.

Quartz (forming up to 21 per cent of the rock) is common and occurs

Plate 3.3

Photomicrograph of the Dunmoor Granodiorite, x 13 plane polarised light.

scale |____| 1 mm

Plate 3.4

Photomicrograph of the Dunmoor Granodiorite, x 13 crossed nicols.

scale |____| 1 mm

occurs as both large and small allotriomorphic crystals.

Augite and hypersthene crystals have stumpy, rectangular forms and often poikilitically enclose magnetite, apatite and ilmenite.

Biotite is present (up to 12 per cent of the rock) in the form of subhedral crystals (up to 3 mm in length) and is pleochroic from pale brown to dark brown. Zircon and its associated pleochroic haloes, and magnetite are associated with the biotite.

Potash feldspar occurs as subhedral microperthitic grains in which the exsolution bodies are about 0.2 mm in size.

The most characteristic and distinguishable feature of this type of granodiorite (which does not occur in sample A11) is its content of fine grained xenoliths (of average grain size 0.1 mm) which consist of plagioclase, augite, hypersthene, quartz, orthoclase and biotite. These are found from the geochemical studies reported later in this thesis to be as basic as the Marginal Granodiorite and appear similar in composition to the andesitic hornfelses. Plates 3.5 and 3.6 are photomicrographs of sample A11 in plane polarised light and in crossed nicols respectively.

3.2.4 LINHOPE GRANODIORITE

This granodiorite is very similar to the Standrop Granodiorite, indeed the only important difference is the brown coloration of its hand specimen and the absence of the xenoliths characteristic of the Standrop type. Generally there is less biotite and andesine than in the Standrop Granodiorite. A description follows of sample A12,

Plate 3.5

Photomicrograph of the Standrop Granodiorite, x 13
plane polarised light.

scale |_____|
1 mm

Plate 3.6

Photomicrograph of the Standrop Granodiorite, x 13
crossed nicols.

scale |_____|
1 mm

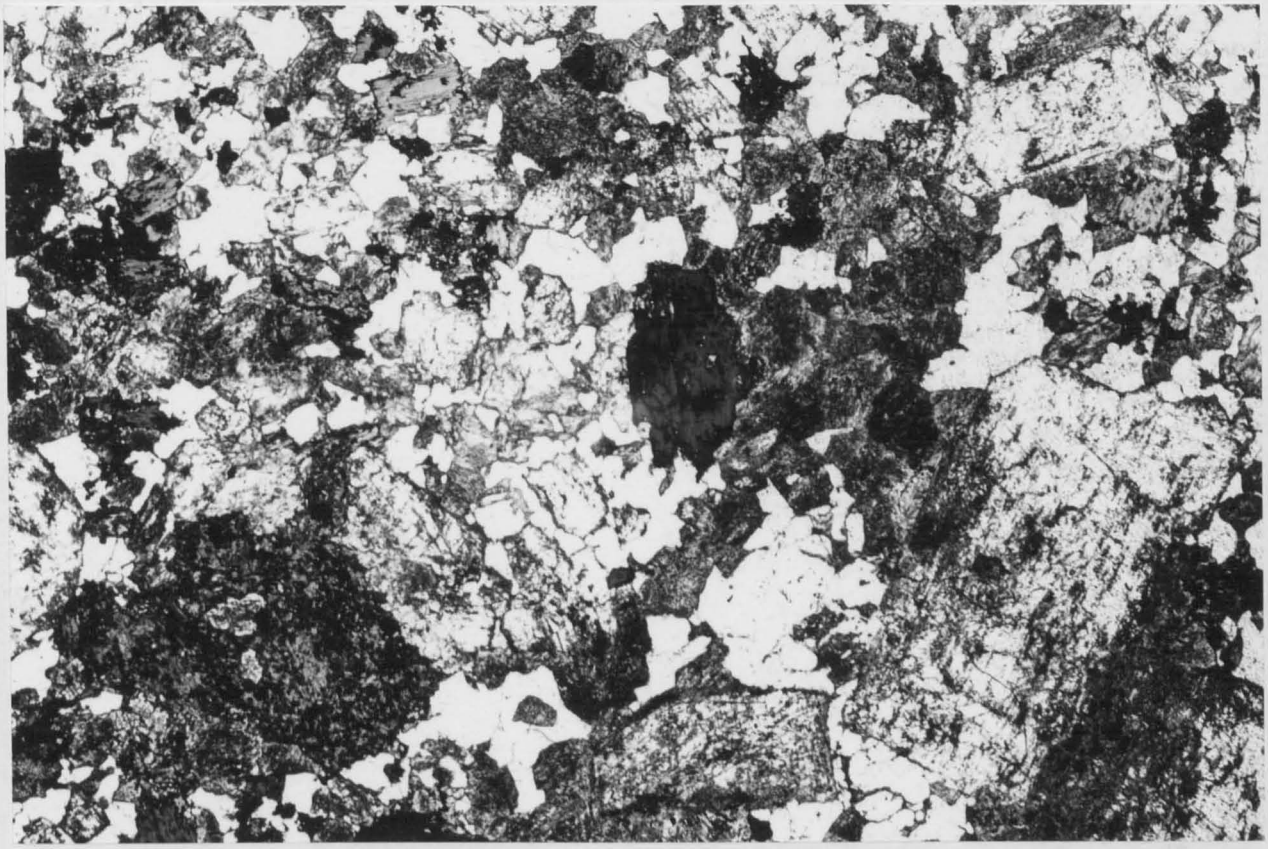

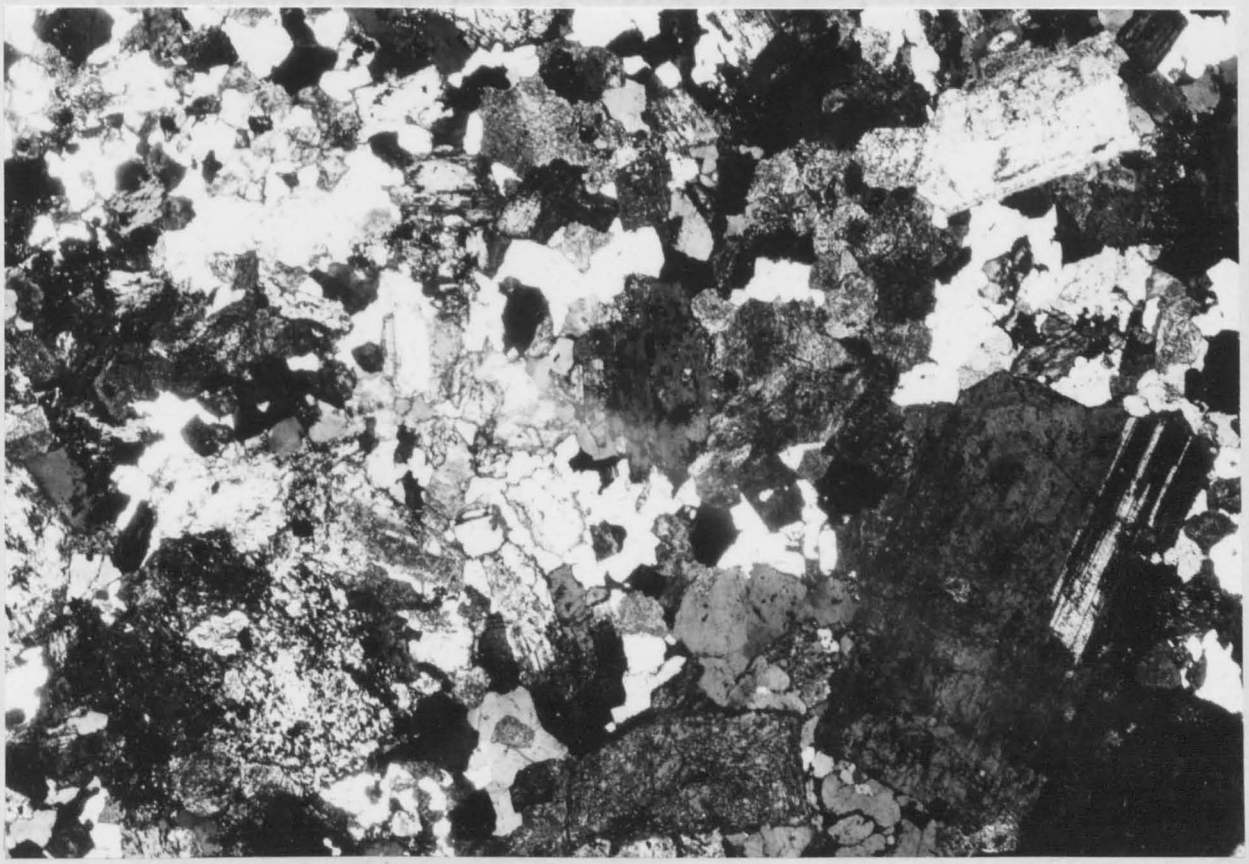

typical of this group from Linhope Burn (947172) which has been analysed for major and trace elements, including REE. The rock is coarse grained and hypidiomorphic granular, with grain size ranging between 3 and 4 mm. It is composed essentially of zoned andesine (An38), forming up to 49 per cent of the rock, stumpy augite and hypersthene which enclose poikilitically magnetite, ilmenite and apatite, biotite and its associated minerals such as zircon, magnetite, and apatite, microperthite and interstitial quartz. Plates 3.7 and 3.8 are photomicrographs of this unit in plane polarised light and in crossed nicols respectively.

3.2.5 HEDGEHOPE GRANODIORITE

This rock type is similar in petrography to the porphyritic Dunmoor Granodiorite but it is fine grained and porphyritic plagioclase is frequent.

Rock E156: This is typical of the Hedgehope Granodiorite. It is porphyritic with phenocrysts (5 mm across) mainly of zoned subhedral andesine plagioclase of composition An37 together with stumpy augite (up to 4 mm across) and hypersthene (up to 4 mm across) which enclose magnetite, ilmenite and apatite poikilitically.

These phenocrysts are surounded by a fine grained groundmass (0.2-0.4 mm average grain size) composed mainly of zoned andesine plagioclase, microperthite, biotite and quartz. The potash feldspar is greater in amount than in the non porphyritic granodiorites. Micrographic texture is also found in this unit and is best developed

Plate 3.7

Photomicrograph of the Linhope Granodiorite, x 13
plane polarised light.

scale |____|
1 mm

Plate 3.8

Photomicrograph of the Linhope Granodiorite, x 13
crossed nicols.

scale |____|
1 mm

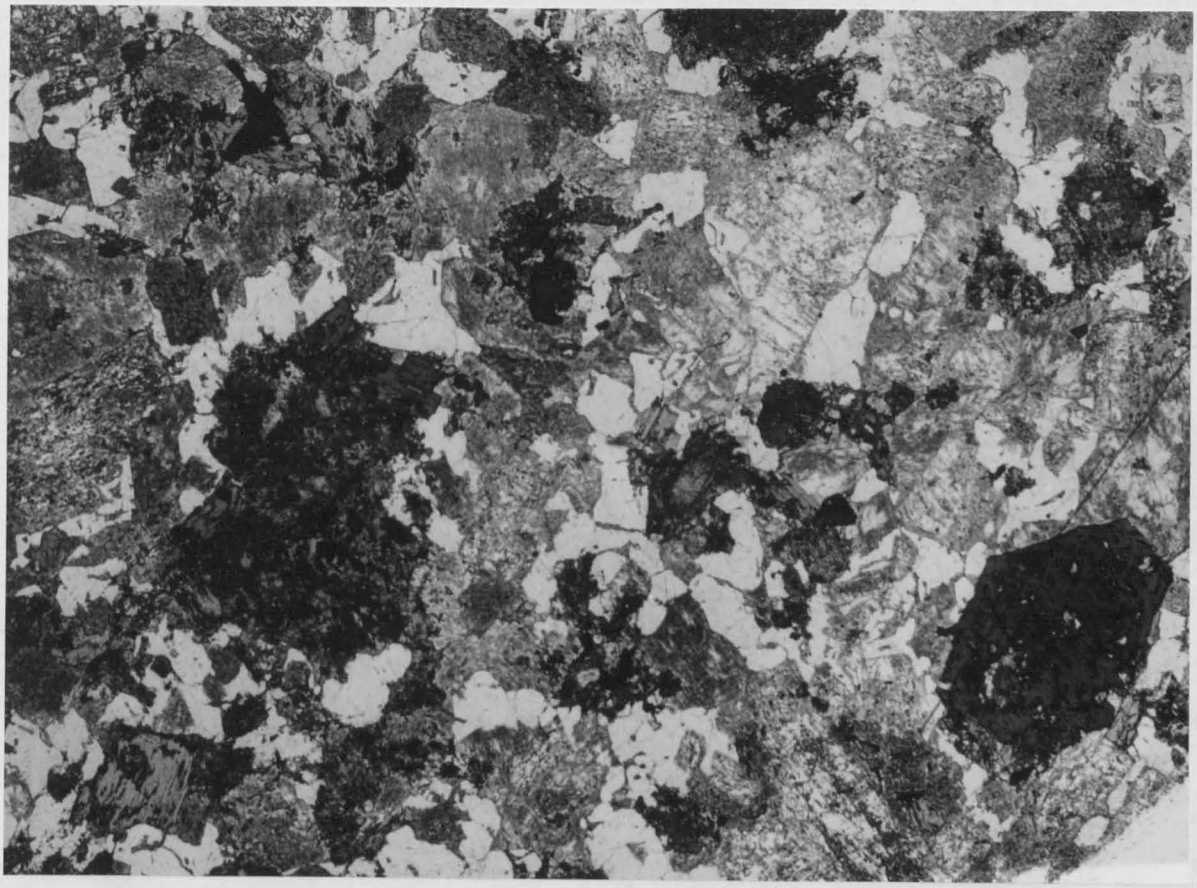

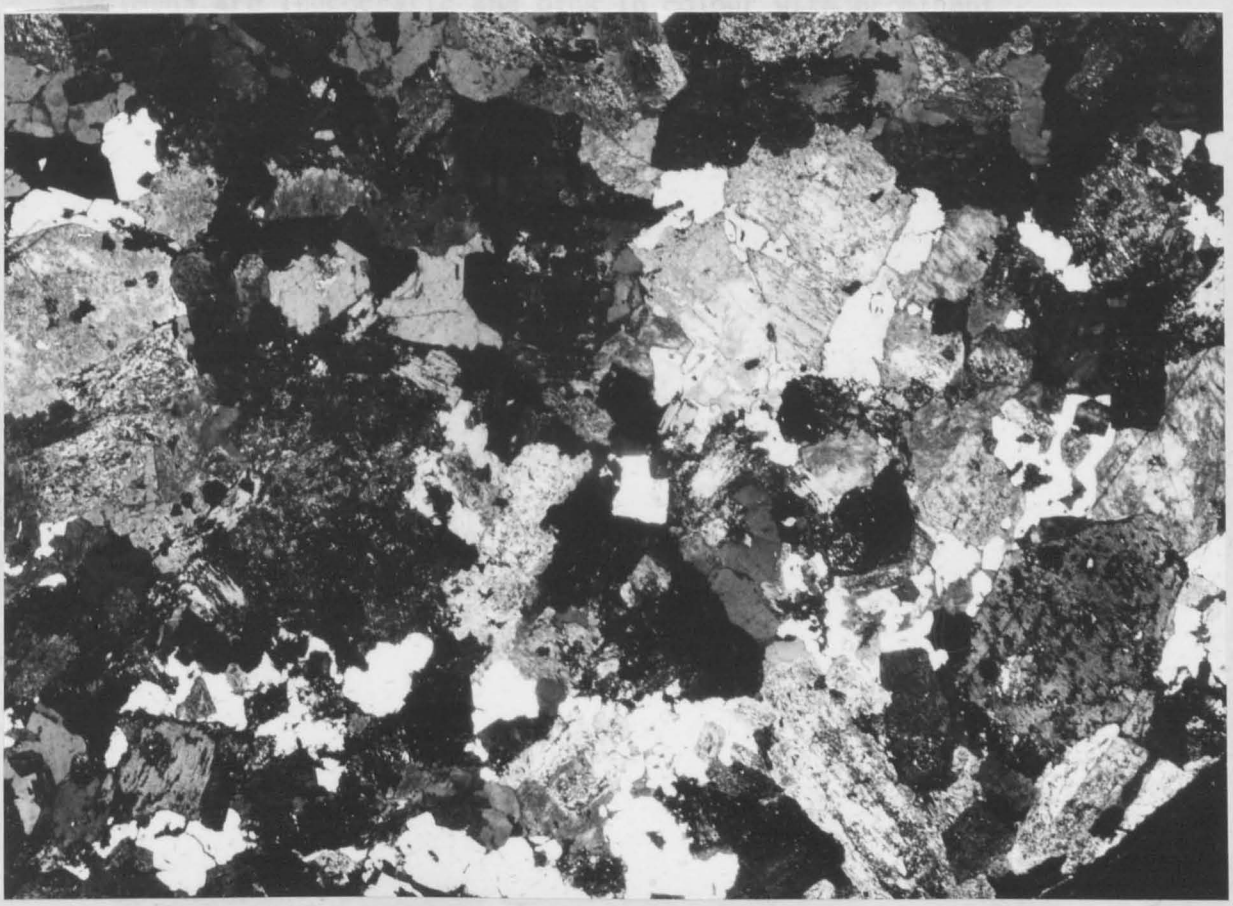

in Newburn (945226) near the contact of the granodiorite with the andesite. This is caused by the rapid cooling and simultaneous crystallisation discussed above. Plates 3.9 and 3.10 are photomicrographs of this unit in plane polarised light and in crossed nicols respectively.

3.2.6 WOOLHOPE GRANITE

This rock type is granitic in mineral composition and texture and is considered to be the last intrusive unit in The Cheviot pluton (see later).

Rock E150: This is typical of the fine grained granite. It shows an equigranular fine grained (0.3-0.5 mm) saccharoidal texture. Hand specimens are leucocratic and pink in colour with prominent phenocrysts of biotite.

Quartz is allotriomorphic, shows undulose extinction. it amounts to 40 per cent of the rock.

Orthoclase is subhedral and amounts up to 20 per cent of the rock.

Plagioclase (mostly albite, up to 20 per cent of the rock) occurs as discrete grains or rarely as phenocrysts.

Biotite (ranging between 10 to 13 per cent of the rock) forms very thin cleavage flakes about 0.5 mm long and 0.2 mm thick, and shows pale to dark brown pleochroism. It encloses magnetite, zircon, apatite and ilmenite as accessory minerals.

Quartz and feldspar are present in higher quantities than in the

Plate 3.9

Photomicrograph of the Hedgehope Granodiorite, x 13 plane polarised light.

scale |_____| 1 mm

Plate 3.10

Photomicrograph of the Hedgehope Granodiorite, x 13 crossed nicols.

scale |_____| 1 mm

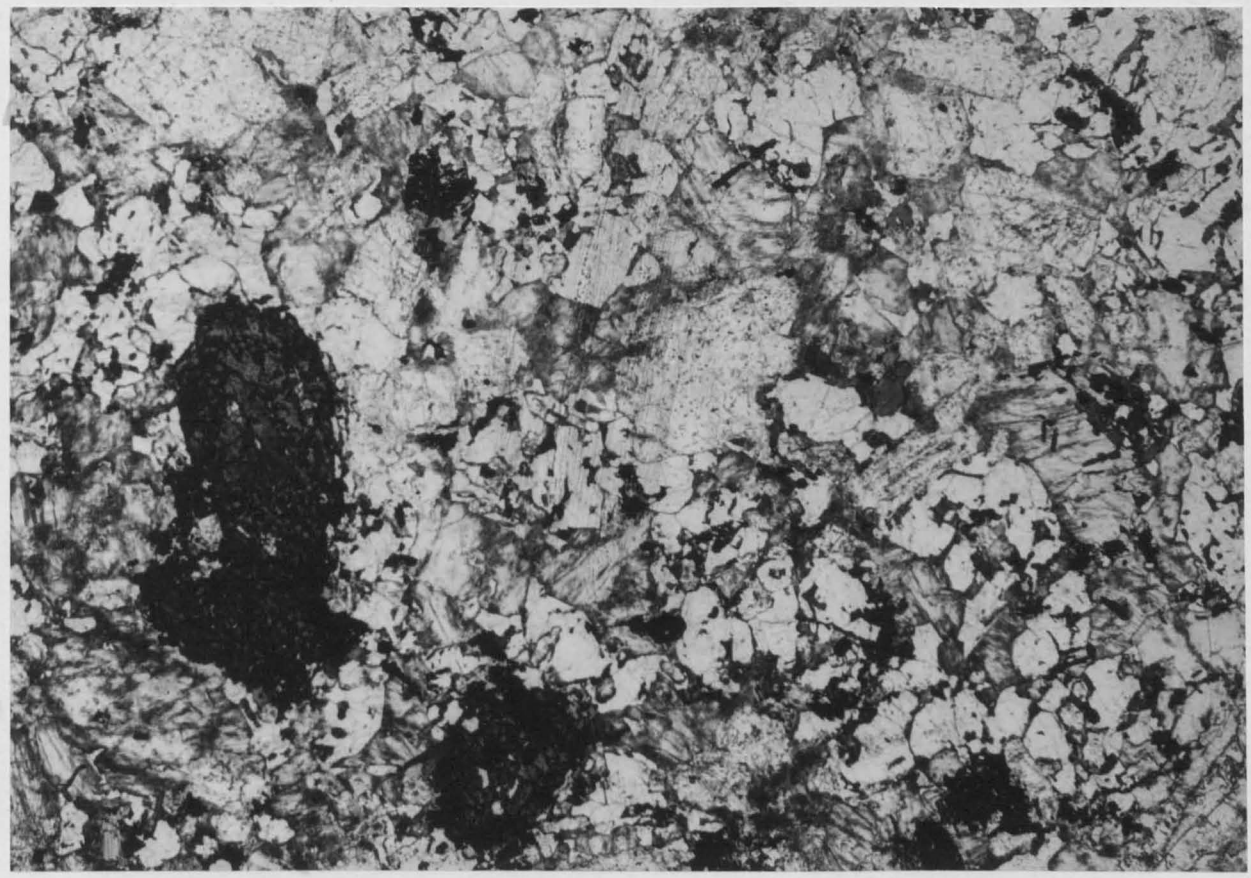

previous rock types and there is tendency for quartz and orthoclase to increase at the expense of plagioclase.

Apatite, zircon, magnetite, ilmenite are present as accessory minerals. This granite type, over the extent of its outcrop, shows considerable variation in its content of biotite. Plates 3.11 and 3.12 are photomicrographs in plane polarised light and in crossed nicols respectively.

3.2.7 Veins

A small number of these veins have been studied and the following is a typical example.

Sample D110: This is a pink fine grained (0.3-0.5 mm) equigranular or saccharoidal textured rock.

Megascopically, biotite is the main ferromagnesian mineral.

Microscopically, this rock is mainly composed of quartz, orthoclase, plagioclase and biotite with accessory minerals zircon, apatite, magnetite and ilmenite.

The similarities of the veins and the Woolhope Granite are sufficiently marked to suggest that the source of these veins may have been related to the Woolhope Granite (see later; Chapter 5).

Plate 3.11

Photomicrograph of the Woolhope Granite, x 13
plane polarised light.

scale |_____|
1 mm

Plate 3.12

Photomicrograph of the Woolhope Granite, x 13
crossed nicols.

scale |_____|
1 mm

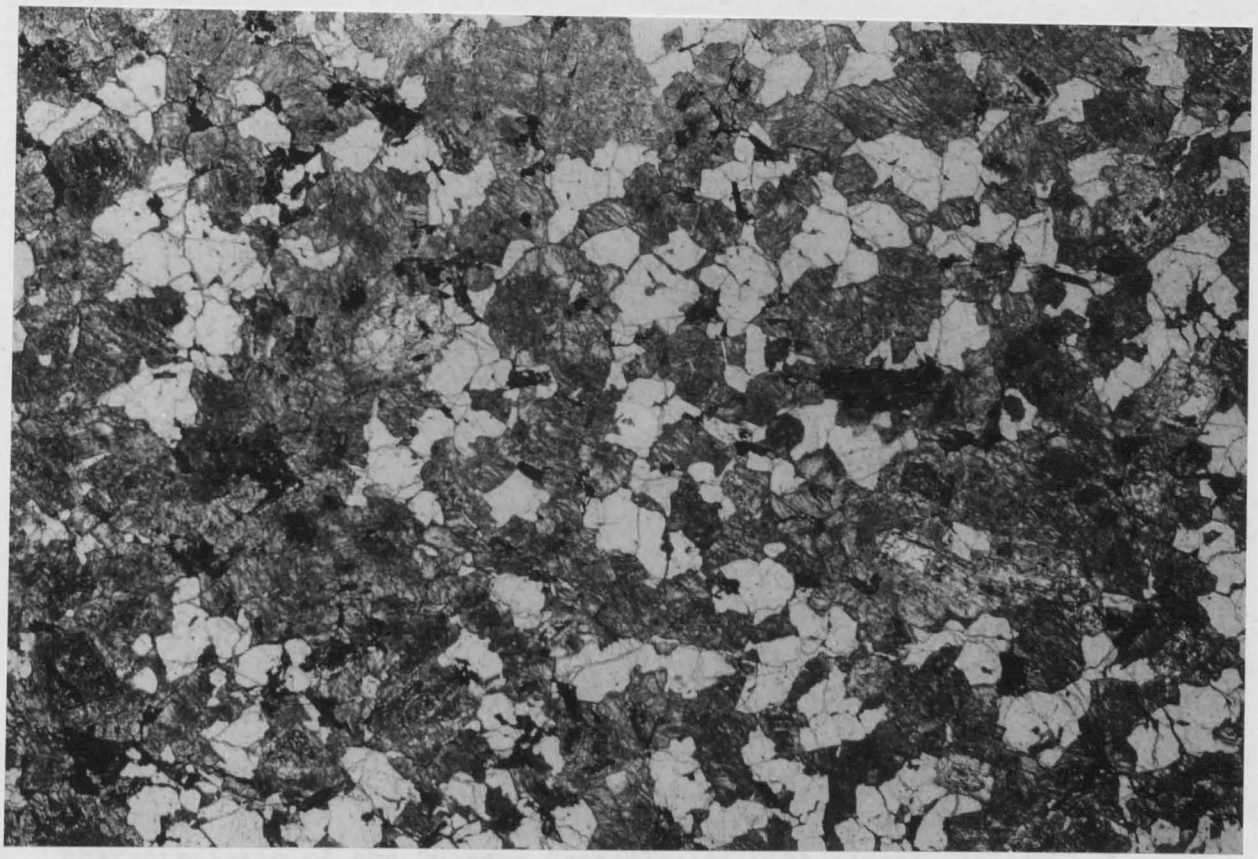

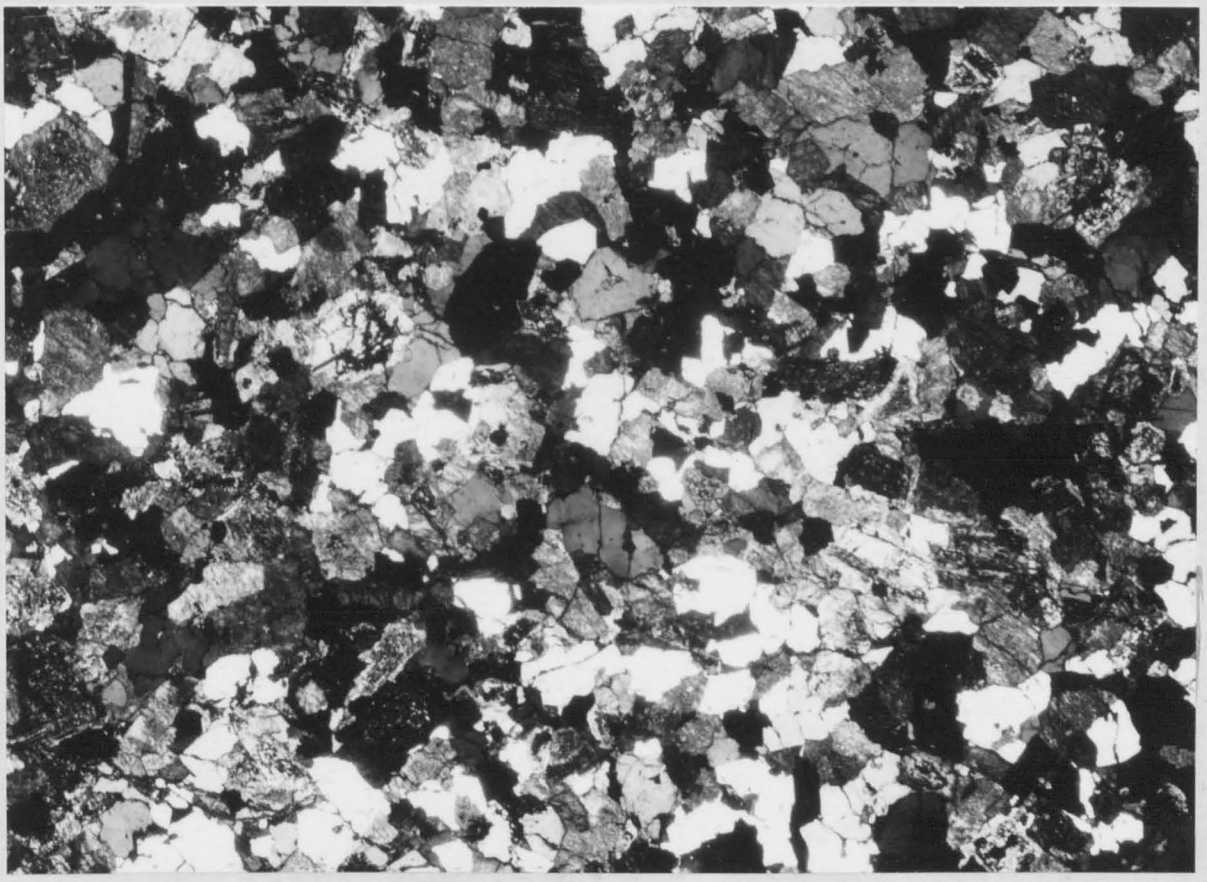

3.2.8 DYKES

Numerous dykes cut through the earlier granodiorite phases of the intrusion (at least up to the Standrop Granodiorite), as well as the surrounding hornfelses. These dykes show a strong resemblance either to the Dunmoor or to the Hedgehope Granodiorite, both in their phenocryst assemblage and in their chemistry. Two examples are described here.

Sample E196: This dyke comes from Low Bleakhope where it cuts the Marginal Granodiorite. The specimen is similar to the Dunmoor Granodiorite. The thin section shows the presence of phenocrysts characteristic of the Dunmoor Granodiorite with almost similar proportions. These are idiomorphic white plagioclase, the characteristic large thin euhedral plates of biotite (up to 5 mm in length), poikilitically enclosing magnetite, apatite and zircon and the stumpy crystals of augite and hypersthene. The chemical analysis of this rock is given in Appendix D, and compares very closely with the mean for the Dunmoor Granodiorite (see Chapter 5).

Sample E376: This dyke cuts the Standrop Granodiorite in Het Burn (949183). The study of this sample under the microscope shows a close resemblance between this sample and the Hedgehope Granodiorite especially in their phenocrysts. The characteristic idiomorphic abundant plagioclae crystals together with their stumpy augite and hypersthene which enclose magnetite, ilmenite and apatite poikilitically are essentially the same in both rock types. Again the chemical analysis of this rock is reported in Appendix D, and is

very close, allowing for the well-developed S2 alteration, to the composition of the Hedgehope Granodiorite (see Chapter 5).

Detailed petrographic study shows that most of these dyke are extremely altered. The type of alteration affecting these dykes is found to be mainly sericitic (both S1 and S2) which are discussed later in Chapter 6.

3.2.9 HORNFELS

Thermal metamorphism of the andesite by the Cheviot Granite produced rocks belonging to the pyroxene hornfels facies which are mainly composed, of very fine grained (less than 0.1 mm) constituents of pyroxene, andesine plagioclase, biotite and quartz with accessory mineral such as magnetite, ilmenite and apatite. In many of the samples this mineral assemblage is overprinted with greenschist facies mineralogy, so that chlorite and albite are extensively developed at the expense of pyroxene and plagioclase. This effect is almost certainly the result of hydrothermal alteration associated with the systems developed in the granite.

3.3 ALTERATION PETROGRAPHY

3.3.1 INTRODUCTION

Petrographical study of the altered rocks in The Cheviot area emphasises the general conclusions about the wide-spread and successive alteration patterns which exist and which are strongly related to the magmatic evolution. All the granodiorite rocks described above have been subjected to at least one type, if not more, of alteration. The superimposition of different alteration phases in the same rocks gives a clear demonstration of the time-space distribution.

3.3.2 DETAILED ALTERATION STUDY

Two major hydrothemal systems were postulated on the basis of field observations, each of them producing a porphyry style of alteration. Detailed petrographic studies of the 463 thin sections were made and on that basis an outline alteration map was compiled (Figure 3.1). Some alteration postdates the intrusion of the porphyritic Dunmoor Granodiorite ring dyke and predates Standrop Granodiorite intrusion. This is described in Chapter (2.3) as hydrothermal system A and is spatially centred on the porphyritic Dunmoor Granodiorite, whereas other alteration in the area is found to postdate the intrusion of the porphyritic Hedgehope Granodiorite

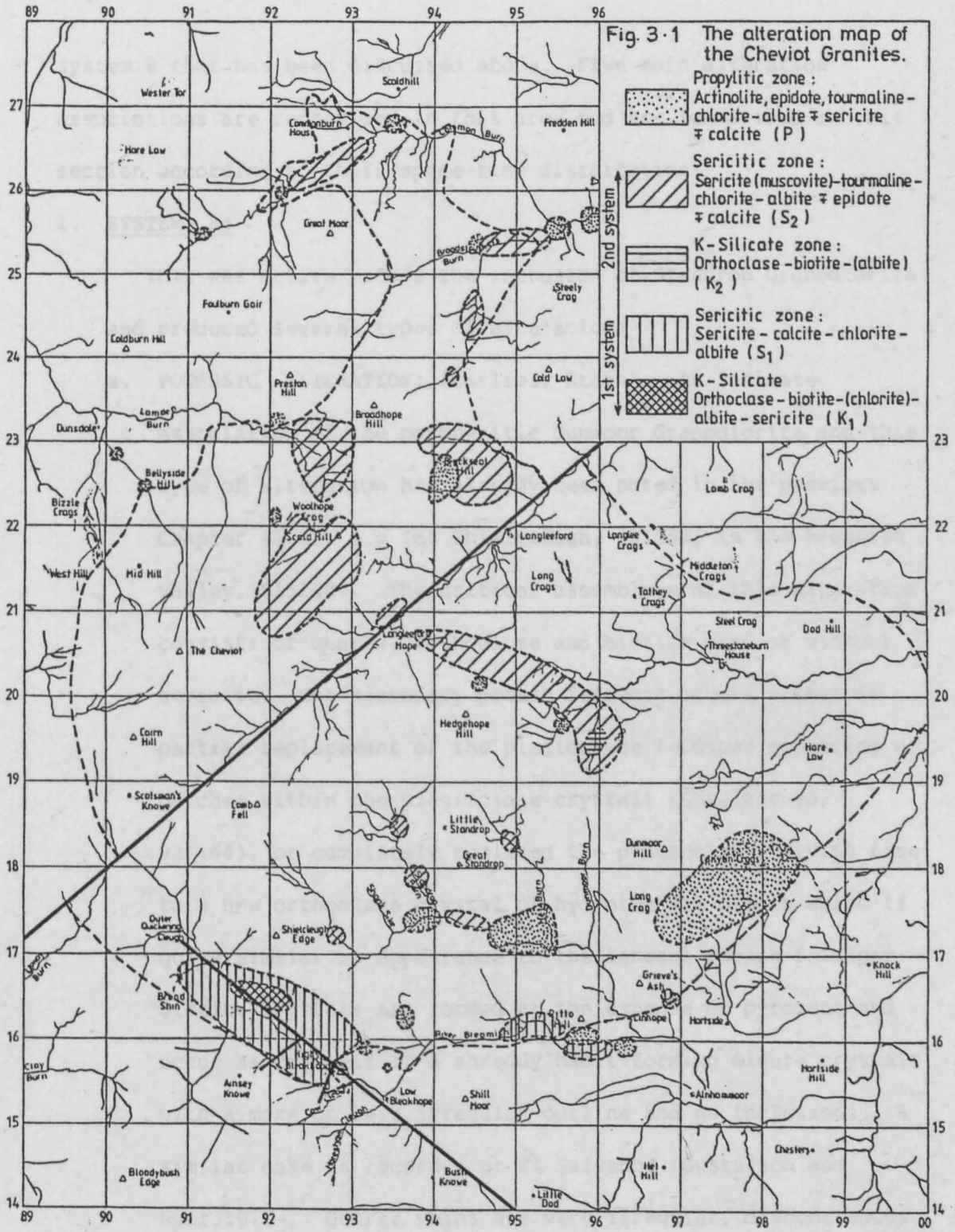
Fig. 3·1 The alteration map of the Cheviot Granites.
Propylitic zone : Actinolite, epidote, tourmaline - chlorite - albite ∓ sericite ∓ calcite (P)
Sericitic zone : Sericite (muscovite) - tourmaline - chlorite - albite ∓ epidote ∓ calcite (S_2)
K-Silicate zone : Orthoclase - biotite - (albite) (K_2)
Sericitic zone : Sericite - calcite - chlorite - albite (S_1)
K-Silicate Orthoclase - biotite - (chlorite) - albite - sericite (K_1)
2nd system
1st system
Wester Tor
Scaldhill
Fredden Hill
Hare Law
Great Moor
Steely Crag
Faulburn Gair
Coldburn Hill
Cold Law
Preston Hill
Broadhope Hill
Dunsdale
Bellyside Hill
Bizzle Crags
Woolhope Crag
Scald Hill
Langleeford
Lamb Crag
Langlee Crags
Middleton Crags
West Hill
Mid Hill
Long Crags
Tathey Crags
The Cheviot
Steel Crag
Dod Hill
Threestoneburn House
Hedgehope Hill
Cairn Hill
Hare Law
Scotsman's Knowe
Comb Fell
Little Standrop
Great Standrop
Dunmoor Hill
Dunmoor Burn
Long Crag
Outer Quickerning Cleugh
Shieldeugh Edge
Knock Hill
Grieve's Ash
Bread Shin
Hartside
Ainsey Knowe
Low Bleakhope
Shill Moor
Ainhamsmoor
Hartside Hill
Bloodybush Edge
Bush Knowe
Little Dod
Hel Hill
Chesters

system B that has been discussed above. Five main alteration associations are recognized in this area and are summarised in this section according to their space-time distribution:

1. SYSTEM A:

This was active before the intrusion of Standrop Granodiorite and produced several types of alteration:

a. POTASSIC ALTERATION: (Earliest Stage). An intimate association of the porphyritic Dunmoor Granodiorite and this type of alteration has already been noted in the previous Chapter (2.3), e.g (at Shielcleugh, 921164; in the Breamish valley, 915168). The critical assemblage of this alteration consists of quartz, orthoclase and biotite with or without sericite. The secondary potash feldspar occurs either as partial replacement of the plagioclase feldspar appearing as patches within the plagioclase crystals (Shielcleugh, 921164), or completely replaced the plagioclase, giving rise to a new orthoclase crystal of hydrothermal origin which is quite similar in appearance to the igneous potash feldspar. Biotite crystals are formed at the expense of pyroxene and occur as crystals of a shreddy habit forming minute crystals with a more or less irregular outline and no inclusions. A similar case is recorded at El Salvador (Gustafson and Hunt,1975). Quartz veins are very irregular, discontinuous and never seen with parallel walls. These are quite similar to the so called A veins which have been described by Gustafson and Hunt (1975) and the formation of which is most

probably the cause of the initiation of this alteration zone.

b. SERICITIC ZONE: This type of alteration is associated with the Dunmoor and Marginal Granodiorites together with their dykes (mostly sent off by the porphyritic Dunmoor Granodiorite ring dyke). The potassic zone described above is seen to be somewhat transgressed by this zone as shown by some samples at Shielcleugh (923165) which show secondary orthoclase and biotite in addition to the mineral assemblages characteristic of this alteration type. Petrographic studies of the different rock types subjected to this type of alteration show similarities in mineral assemblage over a wide area. Rock affected by this alteration either surrounds the previous zone such as in the area between 910170 - 929155, or occur as isolated areas of intense alteration within the Marginal Granodiorite and its related dykes such as in the area south of Ritto Hill (950160). The mineral assemblage characteristic of this zone comprise alteration products of both felsic minerals (plagioclase in particular) and mafic minerals (the pyroxenes and biotite). These alteration assemblages are sericite, albite (both are alteration product of plagioclase feldspar), chlorite and calcite (as an alteration product of the pyroxenes and biotite). All the samples belong to this zone are characterised by intense alteration (intense sericitization in particular). The kind of quartz veins (with calcite and chlorite veins in association) associated with this type of

alteration are continuous and thick with parallel walls (Cat Cleugh, 927156) and they are similar to the so called B veins which were recorded at El Salvador (Gustafson and Hunt, 1975).

Propylitic alteration occurs outside the zones of sericitic alteration, and is generally rather widely in the complex. It is difficult to assign to either system A or system B, and will be described at the end of the next section.

2. SYSTEM B:

This postdates the porphyritic Hedgehope Granodiorite ring dyke as has been already noted. Three types of alteration are recorded associated with this system of which one is referred to in the previous section (i.e propylitic alteration), and they are as follows:

a. POTASSIC ALTERATION: This forms an initial alteration front prior to the succeeding zone of tourmalinization. It is only found associated with the porphyritic Hedgehope Granodiorite and its characteristic alteration assemblages are quartz, orthoclase, biotite and albite. The andesine plagioclase characteristic of the Hedgehope Granodiorite is unstable during this stage, and breaks down to generate orthoclase crystals with or without associated albite. The mafic minerals (in particular mostly the pyroxenes) break down to shreddy biotite with no inclusions and with a mostly irregular

outline (e.g. East/ Threestone Burn, 959195).

b. TOURMALINIZATION AND ITS ALTERATION ASSOCIATION: This is one of the most characteristic feature of the porphyritic Hedgehope Granodiorite. It is preceded by potassic alteration and surrounds it in places (between 938208-959193). Its distribution is generally determined by the Hedgehope Granodiorite ring dyke, though it occasionally affects the Standrop Granodiorite. It has been already noted that during the earliest episode of tourmalinization, sericitic alteration is predominant as exemplified by East/ Threestone Burn, 959198. The majority of tourmalinized samples are associated with intense sericitization and are widely distributed. This type of alteration (the sericitic alteration) constitutes the most important alteration type, associated with tourmalinization, and is best exemplified in the northern part of the complex (north of Harthope Fault). The alteration assemblages of this type are sericite (or muscovite), tourmaline, albite, quartz with patchy occurrence of alkali feldspar (from plagioclase) and chlorite with or without epidote and calcite. The plagioclase feldspar breaks down to sericite and locally to albite, whereas mafic minerals (such as the pyroxenes and biotite grains) produce chlorite with or without calcite.

c. PROPYLITIC ALTERATION ZONE: This is typically exhibited in both systems of alteration where the hydrothermal activity has been weak and it makes up the outer zone of almost a

zoned alteration pattern in the area. This zone is the consequence of both hydrothermal systems A (earlier) and B. The mineral assemblages characteristic of this zone are chlorite, epidote, albite and apatite with or without actinolite, calcite , tourmaline and sericite. Biotite is altered to chlorite and both feldspar types (but especially plagioclase) are mildly sericitized, whereas plagioclase feldspar often develops abandant epidote (e.g. of some epidotized samples; South Ritto, 958159, Threestone Burn, 956197 and at Common Burn, 935268) and albite. The fibrous amphibole and calcite represented an alteration product of the pyroxenes (both clinopyroxene and orthopyroxene) and finally the tourmaline which is mostly disseminated in habit, represents alteration product of biotite, (e.g Dunmoor Hill, 968183, South Ritto Hill, 964159 and Carey Burn, 956255) or feldspar (both alkali and plagioclase feldspars) such as in the Marginal Granodiorite at Low Bleakhope,934157.

CHAPTER FOUR

MINERALOGY AND MINERAL CHEMISTRY

CHAPTER FOUR

MINERALOGY AND MINERAL CHEMISTRY

4.1 INTRODUCTION

Since most of the Cheviot Granite complex is made up of granodiorite, more or less altered by porphyry-style hydrothermal circulation, the mineralogy is in general relatively simple. The fresh granodiorites are composed of major plagioclase, quartz, potash feldspar, biotite, augite and orthopyroxene, as described in Chapter 3, with minor apatite, zircon, ilmenite and magnetite. Alteration minerals include orthoclase, biotite, sericite, tourmaline, albite, chlorite, actinolite and epidote.

Each phase was examined optically and also by electron microprobe analysis (an Energy Dispersive X-ray analysis system that has been interfaced to a scanning electron microscope) carried out on a small number of specimens during five short sessions at the Department of Metallurgy, University of Newcastle-upon-Tyne.

4.2 PRIMARY MINERALOGY

4.2.1 ORTHOPYROXENE

Orthopyroxene is a primary mineral in all five units of granodiorite, whether porphyritic or non-porphyritic. In the porphyritic units, the Dunmoor and Hedgehope Granodiorites, orthopyroxene occurs both as phenocrysts and in the groundmass. It forms as colourless subhedral prismatic grains usually slightly altered to fibrous actinolite or chlorite around crystal edges or adjacent to internal cracks. Grain size varies between 0.1-0.3 mm. Orthopyroxene commonly contains inclusions of other phases, especially euhedral magnetite grains or needles of apatite.

Three grains of orthopyroxene were analysed by electron microprobe from two samples of Marginal and Hedgehope Granodiorites. They are shown in Table 4.1 in order of increasing Fe2+/Mg ratio, together with their structural formulae calculated on the basis of 6 oxygens. All three analyses give a composition corresponding to hypersthene, close to En60, rather more magnesian than might be expected from pyroxene in a granodiorite, but consistent with the Mg/Mg+Fe ratio in the other mafic minerals. The Al content of the pyroxenes is low, as is the content of Ti, consistent with the low pressure of formation envisaged for these rocks. The wollastonite content, at about 3%, is consistent with that of other orthopyroxenes of similar composition reported from andesites, such as the analyses quoted in Deer, Howie

and Zussman (1962) (vol. 2, Table 2, Nos 11, 13 and 15) and those shown graphically by Thirlwall (1981), derived from the Old Red Sandstone volcanics of Straiton, Ayrshire.

The analyses are plotted in Figure 4.1.

4.2.2 CLINOPYROXENE

Clinopyroxene (augite) crystals are even more widespread in the granodiorites than the orthopyroxenes, since during most styles of alteration the orthopyroxene is replaced first, and the clinopyroxenes may survive until alteration is well-advanced. Clinopyroxene crystals are commonly euhedral to subhedral, and are a very pale green colour, sometimes becoming faintly brownish. Simple twinning is common, and the crystals, when euhedral, form stumpy prisms, much less elongated than those of the orthopyroxene. Grain size is in the range 0.1-0.3 mm, and inclusions of euhedral magnetite are common.

Eight clinopyroxene crystals were analysed by electron microprobe, from three samples of Marginal, Standrop and Dunmoor Granodiorites. Table 4.1 presents the analyses and structural formulae calculated to 6 oxygens, and the analyses are plotted in the Ca-Mg-(Fe+Mn) triangular plot of Figure 4.1. The clinopyroxenes all fall within the field of augite, close to the composition Wo46 En39 Fs14. The pyroxenes are all Al poor, consistent with the low pressure envisaged

for their origin, and are also markedly Ti-poor. The wollastonite content of the augite is markedly higher than the values of about Wo40 or less obtained from the Straiton andesites by Thirlwall (1981), and also by comparison with similar augites analyses quoted in Deer, Howie and Zussman (1962). This indicates a much lower temperature of final equilibration for these pyroxenes from the Cheviot granodiorites than for the equivalent pyroxenes from andesites, as would be expected from the plutonic as opposed to volcanic mode of igneous activity.

4.2.3 BIOTITE

Biotite forms the most conspicuous ferromagnesian mineral in most of the granodiorite samples. Most of the biotite observed is clearly primary. Secondary biotite is seen only in the small potassic alteration zones of hydrothermal cycles A and B. The primary biotites tend to be euhedral and tabular in habit, about 0.1-0.3 mm in size. In the Dunmoor Granodiorite, however, biotite is found as large, thin platy phenocrysts, hexagonal in shape and up to 5 mm across. The biotite is uniformly pleochroic from straw yellow to dark, slightly reddish brown. The primary biotite contains abundant inclusions of magnetite, apatite and zircon, a feature that helps to distinguish it from the secondary biotite.

Twelve grains of biotite were analysed by electron microprobe of which one was of a secondary biotite (Table 4.3). The primary

biotites came from five different samples of Marginal, Dunmoor, Linhope, Standrop, Hedgehope Granodioites and from a sample of Woolhope Granite.

The biotites were plotted on the Mg/Fe/Al diagram of Deer, Howie and Zussman (1962) (vol.3, p.57) which separates the different endmembers of the biotite family. On this plot, the analyses fall very close together (Figure 4.4), as aluminium-poor magnesio-annites close to the field boundary separating the annites from the phlogopites. The structural formulae for the biotites, calculated on the basis of 22 oxygens, shows that almost all of the aluminium is present in the Z group, with only very small amounts in Y.

The Ti contents of the primary biotites are unusually high, except for one grain from the Marginal Granodiorite sample B12. The TiO2 contents range from 4.7% to 6.4%, reaching higher levels than the highest recorded in Deer, Howie and Zussman (1962) for granites or granodiorites, and higher than the highest value analysed from the Ben Nevis granite complex (4.65%) (Haslam, 1968, p.96). Such very high values are clearly unusual. If the mean TiO2 content of the granodiorites (0.7%) is taken as the composition of the liquid from which biotite crystallised, then the solid-liquid distribution coefficient for Ti between biotite and liquid is approximately 8. The high levels of TiO2 in the biotites here might reflect a rather high level of TiO2 in the granodiorite magma, or, more probably, and increased distribution coefficient in these Al-poor, Mg-rich

biotites.

The high Mg/Mg+Fe of these biotites is particularly striking by comparison with biotites from granodiorites and granites quoted in Deer, Howie and Zussman (1962) (vol.3, Tables 10 and 12). Mg/Mg+Fe ranges from 0.65 to 0.75, and corresponds closely with the values from orthopyroxene (0.60) and the clinopyroxene (0.72). Such Mg-rich silicates are unexpected in granodiorites, and presumably reflect a stage of Fe-depletion earlier in the magmatic history of the rocks, perhaps involving precipitation of magnetite.

Among the biotites, Mg/Mg+Fe shows the greatest variation, and this is well seen on the scatter plot of Ti against Mg/Mg+Fe (Figure, 4.5). The high-Ti primary biotites form compact group on the diagram, but there is one outlier, the biotite from the Marginal granodiorite B12. This appears primary, though the rock has suffered mild propylitic alteration, but is much lower in Ti and richer in Fe than the other biotites. It may represent the product of local extreme crystal fractionation.

4.2.4 PLAGIOCLASE

Plagioclase occurs both as a primary and secondary mineral. Primary plagioclase occurs as subhedral tablets, about 1 mm long when in the groundmass, or in non-porphyritic granodiorites, but ranging up to 4 mm in length in the phenocryst generation in the Dunmoor

Granodiorite. The plagioclase grains show well-developed oscillatory zoning surrounding cores of a relatively uniform composition. Optical determination of plagioclase composition gave very consistent values of about An38 for the cores, with more variable, more sodic values developed at the extreme margins of the crystals. Commonly plagioclase grains are lightly flecked with small hydrothermal sericite grains. In some sections, plagioclase is mantled by an inclusion-riddled, colourless phase of low relief and low birefringence at the edge of which Carlsbad and albite twins terminate. Sodium cobaltinitrite staining has shown this to be late K feldspar.

Qualitative electron microprobe analysis (summerised in Table 4.5) agrees with the compositions obtained optically, which are preferred because of the analytical difficulties exprienced using the GEOL instrument, particularly with respect to sodium. Five of the analyses are of albites produced during alteration. Two are of primary plagioclase with a composition close to Ab69 An29 Or2, which is andesine, agreeing reasonably well with the optical determinations mentioned above. The final analysis, from E177, is of a sodium-rich exsolution bleb in an orthoclase microperthite crystal. The composition (Ab80 An2 Or18) corresponds closely to the limit of solid solution in orthoclase microperthites recorded by Deer, Howie and Zussman (1963, vol.4, p.18).

4.2.5 POTASH FELDSPAR

Potash feldspar occurs both as a primary and as a secondary mineral. The primary potash feldspar is an orthoclase microperthite, forming subhedral to interstitial grains. The sodium phase exsolved from the orthoclase shows clear lamellar twinning and has a composition close to Ab80 An2 Or18 as shown by the electron probe analysis reported in the preceding section. Three analyses of the potassic host phase are reported in Table 4.6, together with structural formulae calculated on the basis of 8 oxygens. The analyses are from samples B12 and E177, and give a composition close to Or85 (see Figure 4.8). This corresponds well with the potassium-rich limit of solid solution in orthoclase microperthite as reported by Deer, Howie and Zussman (1963, v01.4, p.18). The sodium phase makes up about 20% by volume of the microperthite crystals, giving an overall composition of the microperthite of Or70-75. This corresponds closely to the composition of microperthite phenocrysts in the chemically similar Shap Granite (Deer, Howie and Zussman, 1963, vol.4, Table 4, No 12).

4.2.6 MAGNETITE, ILMENITE AND APATITE

Magnetite represents one of the earliest minerals to solidify from magmas, associated in time with ilmenite, apatite and zircon, and often occurs as inclusions within pyroxenes and biotite crystals.

Ilmenite occurs as large rounded single crystal grains and can easily be distinguised from magnetite in polished thin section. In this section magnetite is greyish in plane polarised light, and isotropic in crossed polars, though it may be weakly anisotropic, whereas ilmenite is pinkish-grey to pinkish brown in colour with strong greenish-brown grey anisotropic colours.

Apatite crystals in all of the granodiorite units are present as relatively large, euhedral prismatic crystals.

One grain of magnetite was analysed by electron microprobe from a fresh Hedgehope Granodiorite (E156). It is shown in Table 4.8 with their structural formulae calculated on the basis of 4 oxygens.

Three grains of ilmenite were analysed by electron microprobe from different samples of Hedgehope and Standrop granodiorites. They are shown in Table 4.8 with thier structural formulae calculated on the basis of 3 oxygens. All three analyses correspond closely to pure ilmenite, except for their content of MnO, present at levels of 2-5%.

Finally the analyses of two grains of apatite by electron microprobe from two samples (E419 and E177 described above) with the structural formulae calculated on the basis of 25 oxygens are shown in Table 4.8. These correspond closely to the ideal apatite composition. One analysis shows a small content of Cl.

4.3 SECONDARY MINERALOGY

4.3.1 GREEN AMPHIBOLE

Green amphibole is a secondary mineral associated with propylitised rocks in all five units of granodiorite, whether porphyritic or non-porphyritic. It tends to be fibrous and commonly developed marginally to the coexisting augite and hypersthene grains. The process of development of fibrous green amphibole from pyroxenes (clinopyroxene in particular), known as uralitization, is usually thought to be associated with late stage crystallisation from hydrothermal solutions (Deer, et al. 1966) at low temperatures associated with high level emplacement of plutons (Leake, 1971). But here it is more likely to be a result of the hydrothermal circulation. Some green amphiboles are in turn replaced or mantled by chlorite or pseudomorphed by chlorite with or without carbonate. Optically there is no difference between the green amphibole replacing orthopyroxene and that replacing clinopyroxene. The study of fibrous amphibole by thin section indicate its actinolitic nature with its characteristic faint pleochroism (colourless-pale green) and symmetrical extinction.

Eight grains of actinolite were analysed by electron microprobe from three different samples of Dunmoor, Standrop and Linhope Granodiorites. They are shown in Table 4.2 with their structural formulae calculated on the basis of 23 oxygens.

All eight analyses give a composition corresponding to actinolite (Figure 4.2), close to (Mg/Mg+Fe2+)7.78 and Si7.7 using the international mineralogical association classification scheme for calcic amphiboles (Leake, 1978, figure 3).

Plotting of these data in an FeO-MgO-Al2O3 triangular diagram (Figure 4.3) supports the view of Nockolds and Mitchell (1948, p.559) in their survey of hornblendes in Caledonian granodiorites, concerning the nature of secondary amphiboles. Out of the eight analyses five are from the Standrop Granodiorite and they show rather more magnesium and total iron than the other three analyses. This might be because they originate from hypersthene, rather than augite, since hypersthene is characterised by higher magnesium and iron than augite. These five analyses plot outside the field of secondary amphiboles towards high magnesian region of Figure 4.3, and are rather more magnesian than might be expected from amphibole in a granodiorite. However their Mg/Mg+Fe ratio is consistent with that of the primary pyroxenes (Figure 4.1). The Al content of the amphibole is low, and so is the content of Ti, consistent with their parentage from augite and hypersthene (Table 4.1).

4.3.2 TOURMALINE

Tourmaline occurs as a secondary mineral. Secondary tourmaline occurs as euhedral to subhedral crystals about 1-2.5 mm in length with pleochroism from yellow to dark blue or bluish green. These are

often zoned and are typically found in highly altered rocks as euhedral to prismatic crystals with a radiating texture. The texture gives clear evidence that the tourmaline has formed by late-stage replacement of biotite and feldspar (both plagioclase and microperthite). There are differences in size and colour of this type of tourmaline from sample to sample which are not controlled by the nature of the minerals they replace but could be related to the variation in chemistry of the tourmaline.

Fourteen grains of tourmaline were analysed by electron microprobe from four different samples of Linhope, and Hedgehope Granodiorites and Woolhope Granite. They are shown in Table 4.4 with their structural formulae on the basis of 49 oxygens. A chemical scan was made through an individual selected zoned grain in sample E416 (altered by potassic alteration 2 (K2) surrounded and partly overprinted by the S2 sericitic alteration zone in which tourmaline is the most characteristic mineral) starting from the core towards the periphery. This revealed considerable chemical variation according to the position of the point analysis within the grain. The variation is well shown by a variation diagram of CaO against MgO which demonstrates the overall compositional trend from a magnesian core (also rich in calcium and to some extent titanium) to a rim with a low magnesium content and lower levels of calcium and to some extent titanium (Figure 4.6).

A triangular diagram of TiO2-MgO-FeO+MnO (Manning, 1982) has been found useful to clarify the relationship between the different varieties and to correlate it with the chemical scan made on the individual grain in sample (E416) (Figure 4.7). The variation in the chemical composition of a single crystal probably reflects the changing chemical composition of the fluids associated with the S2 alteration while the alteration proceded.

The other electron probe analyses of tourmalines (from E127, a linhope Granodiorite affected by propylitic alteration; E418, a Hedgehope Granodiorite affected by S2 alteration and E150, a mildly altered sample of Woolhope Granite) are all very similar in composition, falling near the composition of the high Ca, high Mg central part of the zoned crystal analysed in detail. The reported variation in Na2O may be merely analytical error on the electron probe. The presence of tourmaline of this composition in a propylitic rock may indcate that propylitic alteration was proceding at the same time as at least the later part of the S2 episode, while the development of this tourmaline in the Woolhope Granite suggests the continuing of S2 circulation after the intrusion of this ring dyke.

4.3.3 PLAGIOCLASE

Secondary plagioclase occurs as an essential constituent within the propylitic rocks (p), and may also accompany sericitic alteration 1 (S1) and sericitic alteration 2 (S2) as an accessory but non essential constituent. The fact that samples from potassic alteration 1 and 2 (K1 and K2 respectively) are surrounded and partly overprinted by the S1 and S2 respectively could explain the presence of secondary plagioclase within samples from these zones. Secondary plagioclase occurs as subhedral tablets of similar size to that of primary origin, but differing from that in the absence of zoning. Optical determination of plagioclase composition gave a very consistent value of An10-13 (Albite) from its characteristic albite twinning.

Qualitative electron microprobe analyses for secondary plagioclase are also presented in Table 4.5 which shows that five of the analyses are of albites (Figure 4.8), agreeing reasonably well with the optical determinations, produced during the propylitic (P) and sericitic 1 and 2 (S1 and S2 respectively) hydrothermal episodes. These albites were analysed from five different samples. One sample (E127) is Linhope Granodiorite affected by propylitic alteration, sample (E527) is Marginal Granodiorite affected by S1, sample (E239A) is Dunmoor Granodiorite affected by K1 and overprinted partly by S1, sample (E419) is Standrop Granodiorite affected by S2 and sample (E418) which is Hedgehope Granodiorite affected by S2.

4.3.4 ORTHOCLASE

Secondary potash feldspar can frequently be seen rimming plagioclase grains or replacing plagioclase in scattered patches. Both of these effects are the result of secondary overgrowing and replacement as a result of hydrothermal activity in the area. Optically the secondary potash feldspar (is orthoclase) occurring as subhedral grains about 1 mm long with characteristic carlsbad twinning.

Nine of the analyses in Table 4.6 are of orthoclase produced by potassic alteration. These are plotted in Figure 4.8. Three analyses, from samples E416, E419 and E527 are of composition Or99. Two analyses are from samples (E416 and E419 with a composition of Or95). Four analyses are from samples (E419, E239A and E527) with composition of Or89. These compositions are significantly more potassic than the potassic phases of the primary microperthite (see above), as would be expected from potash feldspar formed at a lower temperature by hydrothermal activity. Of these samples, E416 is a Hedgehope Granodiorite affected by K2 and overprinted partly by S2, sample E419 is Standrop Granodiorite affected by S2 alteration and overprinted by P alteration, sample E527 is Marginal Granodiorite affected by S1 alteration and finally sample E239A is Dunmoor Granodiorite affected by K1 alteration and overprinted by S1.

4.3.5 EPIDOTE

Epidote is a secondary mineral observed in propylitized rocks in all five units of granodiorite. In thin section, it is easily discerned by its pleochroism (colourless to pale yellow) and first order birefringence colours. It is a characteristic mineral of the propylitic zone and mostly replaces plagioclase feldspar and to some extent ferromagnesian minerals. Veins may occur mainly composed of epidote within the propylitized rocks.

Table 4.7 shows the electron microprobe analyses of the epidote together with the structural formulae calculated on the basis of 22 oxygens. The two analyses (of sample E419, described above) agree reasonably well with the analyses quoted in Deer, Howie and Zussman (1962) (vol.1, Table 33, Nos. 8 and 10).

4.3.6 CHLORITE

In hand specimen chlorite is dark green, almost black in colour, brittle and flaky in texture. In thin section it is colourless to pale-green, but gives anomalous (dark blue), low birefringence colours with distinct radial extinction. It is usually found associated with calcite lining and filling cracks where they cut through the rocks to form veins. A good example, is the veins cutting through the Marginal Granodiorite in the Breamish River (950161).

Chorite occurs as a secondary mineral associated with, but constituting a very important phase in, propylitized rocks in all five units of granodiorite. It also occurs as minor phase in the other alteration assemblages, especially in the sericitic zones (S1 and S2).

Five grains of chlorite were analysed by electron microprobe from three different samples of Dunmoor, Standrop and Hedgehope Granodiorites. They are shown in Table 4.7 with their structural formulae calculated on the basis of 23 oxygens.

The first four analyses give a composition corresponding to pycnochlorite using the nomenclature of chlorites and oxidized chlorites (Hey, 1954). These grains come from samples E419 (which is sericitically altered, S2 described above) and E239A (which is potassically altered, K1, and partly overprinted by sericitic alteration, S1) and are present as a minor phase in these alteration types.

The final analysis comes from E156 (fresh Hedgehope Granodiorite). The analysis is of chlorite replacing primary biotite. It calculates as a very silica-rich chlorite, but the high K2O content indicates that it is probably a mixed analysis, overlapping a more normal chlorite and relict biotite.

Table 4.1

Compositions, cation contents of probed orthopyroxene and clinopyroxene

SAMPLE NUMBERS	orthopyroxene			clinopyroxene							
	B12	E156	E156	B12	B12	B12	B12	A11	A11	E177	E177
SiO2	52.93	53.36	52.98	54.00	54.04	54.24	54.18	54.24	53.80	53.78	53.99
TiO2	0.49	n.d.	n.d.	n.d.	0.43	0.13	0.17	0.26	0.34	0.23	0.20
Al2O3	0.78	0.79	2.04	0.23	0.51	0.39	n.d.	0.78	1.95	1.17	0.77
FeO	22.57	23.73	23.00	9.39	9.14	9.96	9.10	8.60	8.83	8.35	7.63
MnO	0.56	0.48	0.60	0.21	0.38	0.26	0.28	0.16	0.27	0.41	0.35
MgO	21.26	20.44	19.98	13.35	13.30	13.52	13.26	13.86	13.30	14.51	14.72
CaO	1.80	0.92	1.58	23.48	23.20	21.50	23.70	22.00	22.30	21.76	21.23
TOTAL	100.4	99.7	100.2	100.7	101.0	100.0	100.2	99.9	100.8	100.2	98.9
Formulae of the analysed grains on the basis of 6 Oxygens.											
*	1.98	2.00	2.00	2.00	2.00	2.00	2.00	2.00	2.00	2.00	2.00
Si	1.95	1.97	1.96	1.99	1.99	2.00	2.00	2.00	1.98	1.98	1.99
Al IV	0.03	0.03	0.04	0.01	0.01	0.00	0.00	0.00	0.02	0.02	0.01
*	1.99	1.92	1.95	1.97	1.97	1.95	1.97	1.96	1.97	1.97	1.93
Al VI	0.00	0.00	0.05	0.00	0.01	0.02	——	0.03	0.06	0.03	0.02
Ti	0.03	——	——	——	0.02	0.01	0.01	0.02	0.02	0.01	0.01
Fe	0.70	0.74	0.72	0.29	0.28	0.31	0.28	0.27	0.27	0.26	0.24
Mg	1.17	1.13	1.10	0.74	0.73	0.75	0.73	0.76	0.73	0.80	0.81
Mn	0.02	0.01	0.02	0.01	0.01	0.01	0.01	0.01	0.01	0.01	0.01
Ca	0.07	0.04	0.06	0.93	0.92	0.85	0.94	0.87	0.88	0.86	0.84
Where * = Sum of cations.											
Fe2+/Mg	0.60	0.65	0.65	0.39	0.38	0.41	0.38	0.36	0.37	0.33	0.30
M/M+F+N	0.62	0.60	0.60	0.71	0.72	0.70	0.72	0.73	0.72	0.75	0.76
C/C+F+M+N	0.04	0.02	0.03	0.47	0.47	0.44	0.48	0.46	0.47	0.45	0.44
M/C+F+M+N	0.60	0.59	0.58	0.38	0.38	0.39	0.37	0.40	0.39	0.41	0.43
F/C+F+M+N	0.36	0.39	0.38	0.15	0.14	0.16	0.14	0.14	0.14	0.13	0.13
Where C=Ca, F=Fe, M=Mg, N=Mn. n.d. = not detected.											

Table 4.2

Compositions, cation contents of probed amphiboles

SAMPLE NUMBERS		E419	E419	E419	A11	A11	E177	E177	A12
SiO2		54.70	53.80	56.32	55.80	56.45	55.24	55.84	55.79
TiO2		0.17	0.47	0.17	0.24	0.25	n.d.	n.d.	0.15
Al2O3		1.66	2.52	1.22	1.22	0.98	2.53	0.94	0.70
FeO		11.65	11.26	13.33	11.36	11.39	14.91	14.86	15.46
MnO		0.57	0.35	0.57	0.68	0.73	0.55	0.40	0.74
MgO		15.98	16.41	16.08	18.00	17.32	14.66	13.85	13.87
CaO		12.62	11.55	12.19	12.96	12.71	12.31	12.77	12.04
Na2O		n.d.	n.d.	n.d.	n.d.	n.d.	n.d.	n.d.	0.19
K2O		n.d.	0.26	0.13	n.d.	n.d.	n.d.	n.d.	0.13
P2O5		0.43	0.39	0.14	0.25	0.45	0.25	0.26	0.40
TOTAL		97.8	97.0	100.2	100.5	100.3	100.5	99.0	99.5
Formulae of the analysed grains on the basis of 23 Oxygens.									
	T	8.00	8.00	8.00	8.00	8.00	8.02	8.00	8.0
Si		7.73	7.61	7.96	7.89	7.98	7.81	7.89	7.90
Al IV		0.27	0.39	0.04	0.11	0.02	0.19	0.11	0.10
	C	5.00	5.00	5.00	5.00	5.00	5.00	4.96	5.00
Al VI		0.02	0.05	0.17	0.10	0.15	0.25	0.05	0.02
Ti		0.02	0.05	0.02	0.03	0.03	----	----	0.02
Fe		1.43	1.38	1.63	1.39	1.40	1.83	1.82	1.89
Mn		0.07	0.04	0.07	0.08	0.08	0.06	0.05	0.08
Mg		3.46	3.48	3.11	3.40	3.34	2.85	3.03	2.99
	B	2.04	1.94	2.34	2.59	2.46	2.30	2.01	2.0
Mg		0.05	0.12	0.42	0.55	0.46	0.37	----	0.05
Ca		1.99	1.82	1.92	2.04	2.00	1.93	2.01	1.90
Na		----	----	----	----	----	----	----	0.05
	A	----	----	----	----	----	----	----	0.09
Na		----	----	----	----	----	----	----	0.05
K		----	0.05	0.03	----	----	----	----	0.04
Sum of Cations		15.04	14.94	15.34	15.59	15.46	15.32	14.97	15.09
Mg/ Mg+Fe2+		0.71	0.72	0.68	0.73	0.73	0.63	0.62	0.62
Where n.d. = not detected.									

Table 4.3

Compositions, cation contents of probed biotite

SAMPLE NUMBERS		B12	E177	E177	A12	A11	A11	E156	E156	E156	E150	E150	E419
SiO2		41.30	40.00	39.98	41.67	40.05	41.40	41.01	41.00	40.22	41.70	40.50	40.20
TiO2		2.50	6.37	6.25	6.0	5.60	5.50	4.84	5.01	5.5	4.70	4.90	4.21
Al2O3		12.70	13.76	13.94	13.43	13.60	14.00	13.63	13.00	13.40	13.70	14.70	13.76
FeO		18.80	10.97	10.28	11.34	11.30	11.10	14.00	14.10	15.30	11.30	12.00	16.54
MnO		0.20	0.10	0.12	-----	-----	0.30	0.04	0.15	-----	0.10	0.20	0.27
MgO		13.70	16.50	17.20	16.40	18.20	17.40	16.00	14.70	14.90	17.90	16.90	14.23
K2O		9.10	9.23	9.29	9.55	9.80	9.90	9.50	9.30	9.50	9.50	9.14	8.24
TOTAL		98.3	97.1	97.4	98.5	98.6	99.5	99.3	97.5	99.2	99.9	99.9	97.7
Formulae of the analysed grains on the basis of 22 Oxygens.													
	Z	8.00	8.00	8.00	8.00	8.00	8.00	7.96	8.00	8.00	8.00	8.00	8.00
Si		5.87	5.70	5.70	5.86	5.70	5.80	5.82	5.90	5.80	5.80	5.76	5.72
Al IV		2.13	2.30	2.30	2.14	2.30	2.20	2.18	2.10	2.20	2.20	2.30	2.28
	Y	5.61	5.59	5.58	5.53	5.84	5.66	5.77	5.56	5.72	5.57	5.67	6.06
Al VI		0.02	0.03	0.06	0.13	-----	0.11	0.14	0.10	0.10	-----	0.19	0.05
Ti		0.28	0.69	0.67	0.64	0.60	0.60	0.52	0.54	0.59	0.50	0.52	0.49
Fe		2.34	1.30	1.20	1.33	1.34	1.30	1.70	1.70	1.83	1.32	1.41	2.16
Mg		2.94	3.56	3.64	3.43	3.90	3.62	3.40	3.20	3.20	3.74	3.53	3.32
Mn		0.03	0.01	0.014	-----	-----	0.03	0.01	0.02	-----	0.01	0.02	0.04
	X	1.73	1.71	1.66	1.72	1.80	1.76	1.71	1.71	1.73	1.70	1.64	1.65
K		1.73	1.71	1.68	1.72	1.80	1.76	1.71	1.71	1.73	1.70	1.64	1.65
		56	73	75	72	74	74	67	65	64	74	71	61
100 Mg/Mg+Fe													

Table 4.4

Compositions, cation contents of probed tourmaline.

SAMPLE NUMBERS	E127	E127	E127	E127	E150	E150	C E416	1/2 way to P (M) E416	3/4 way to P (M) E416	7/8 way to P (M) E416	E416	E418	E418	E418	E418
SiO2	37.40	37.80	36.60	36.30	38.40	37.40	36.20	37.40	37.40	35.00	38.10	36.60	36.60	37.00	38.00
TiO2	0.14	0.00	0.00	0.01	0.51	0.13	0.97	0.32	0.20	0.64	0.19	0.57	0.57	1.10	0.20
Al2O3	28.50	30.30	28.80	24.50	27.20	27.70	26.50	25.60	28.00	37.50	31.50	28.50	28.50	28.00	28.40
FeO	11.80	13.00	10.80	17.80	14.60	14.70	11.30	15.00	14.30	12.30	11.70	10.90	10.90	11.80	15.20
MnO	0.00	0.02	0.00	0.12	0.06	0.23	0.00	0.11	6.00	0.45	0.04	0.00	0.00	0.00	0.12
MGO	7.10	7.20	7.30	6.80	7.30	7.10	8.50	5.70	0.002	0.36	5.60	6.95	7.00	6.80	6.30
CaO	1.30	1.60	1.40	1.90	1.50	1.80	2.60	1.90	1.50	1.20	0.82	1.74	1.70	2.04	1.31
Na_2O	0.95	3.40	1.80	0.90	----	----	0.60	2.20	0.60	0.16	1.92	1.93	1.93	2.08	2.50
TOTAL	87.2	93.2	86.5	88.2	89.6	89.5	88.5	89.9	88.7	87.8	91.8	89.1	89.1	90.9	94.6
Si	12.30	11.90	12.20	12.40	12.50	12.30	12.30	12.40	12.40	11.40	12.20	12.13	12.10	12.10	12.20
Al	11.04	11.20	11.30	9.8	10.40	10.70	10.30	10.20	11.00	14.40	11.86	11.12	11.10	10.80	10.80
Ti	0.03	0.00	0.00	0.003	0.12	0.03	0.24	0.08	0.05	0.16	0.05	0.14	0.14	0.26	0.05
Fe	3.30	3.40	3.00	5.10	4.00	4.01	3.10	4.20	3.97	3.40	3.13	3.02	3.02	3.20	4.10
Mg	3.50	3.40	3.60	3.50	3.50	3.50	4.20	2.90	2.97	0.20	2.67	3.43	3.40	3.30	3.00
Mn	0.00	0.01	0.00	0.03	0.02	0.07	0.00	0.03	0.001	0.12	0.01	0.00	0.00	0.00	0.03
Ca	0.45	0.53	0.49	0.70	0.52	0.63	0.91	0.70	0.52	0.40	0.28	0.62	0.62	0.72	0.45
Na	0.60	2.10	1.20	0.60	----	----	0.40	1.50	0.38	0.10	1.19	1.24	1.24	1.32	1.53

Where C=core ; P=periphery ; M= in between C & P. Where structural formulae calculated on the basis of 49 Oxygens.

Table 4.5

Compositions, cation contents of probed plagioclase.

SAMPLE NUMBERS	E127	E156	E156	E239A	E527	E419	E418	E177
SiO2	69.87	66.10	64.03	68.51	68.51	68.40	68.28	67.92
TiO2	n.d.	n.d.	n.d.	n.d.	n.d.	n.d.	n.d.	0.14
Al2O3	20.00	22.98	22.40	20.66	20.24	19.68	20.30	19.81
FeO	n.d.	n.d.	0.23	n.d.	0.28	0.19	n.d.	0.30
MnO	n.d.	n.d.	n.d.	n.d.	n.d.	n.d.	n.d.	0.12
MgO	0.19	0.11	n.d.	0.17	0.12	0.29	0.30	n.d.
CaO	0.26	3.99	5.93	0.06	0.79	0.67	n.d.	0.35
Na2O	10.11	6.30	7.40	9.54	9.51	8.66	11.80	8.80
K2O	n.d.	0.34	0.32	0.20	0.65	0.12	----	2.86
P2O5	0.46	0.60	0.54	0.30	0.29	0.47	0.17	0.36
TOTAL	100.9	100.4	100.9	99.4	100.4	98.6	101.0	100.7
	Structural formulae calculated on the basis o f 8 Oxygens.							
Si	3.00	2.90	2.75	3.01	2.97	2.97	2.97	2.96
Al	1.01	1.20	1.17	1.04	1.02	1.00	1.03	1.00
Ti	----	----	----	----	----	----	----	0.01
Fe	----	----	0.01	----	0.01	0.007	----	0.01
Mg	0.01	0.01	----	0.01	0.01	0.02	0.02	----
Mn	----	----	----	----	----	----	----	0.01
Ca	0.01	0.19	0.27	0.03	0.04	0.03	----	0.02
Na	0.84	0.53	0.62	0.81	0.80	0.78	0.95	0.75
K	----	0.02	0.02	0.01	0.04	0.01	----	0.16
P	0.02	0.02	0.02	0.01	0.01	0.02	0.01	0.01
Sum of cations	4.89	4.87	4.86	4.92	4.90	4.84	4.98	4.93

Where n.d.= not detected

Table 4.6

Compositions, cation contents of probed K feldspar

SAMPLE NUMBERS	B12	E239A	E239A	E527	E527	E416	E416	E419	E419	E419	E177	E177
SiO2	65.30	64.55	65.37	65.25	66.33	65.71	65.74	64.37	66.30	72.20	66.20	66.70
TiO2	0.19	0.13	0.00	0.00	0.08	0.10	0.11	0.11	0.00	0.04	0.05	0.11
Al2O3	19.56	18.01	19.20	19.20	19.74	18.34	18.42	18.09	18.50	14.80	18.50	18.50
FeO	0.25	0.00	0.18	0.13	0.31	0.16	0.04	0.14	0.30	0.21	0.10	0.31
MnO	0.15	0.10	0.02	0.03	0.02	0.10	0.00	0.06	0.00	0.00	0.00	0.12
MGO	0.00	0.20	0.24	0.26	0.27	0.00	0.00	0.00	0.00	0.00	0.00	0.00
CaO	0.14	0.00	0.05	0.15	0.06	0.03	0.00	0.00	0.12	0.15	0.11	0.00
Na2O	1.70	1.04	1.25	1.18	0.00	0.00	0.61	0.08	0.00	0.41	1.13	1.58
K2O	13.82	14.58	14.68	14.67	13.78	15.63	15.58	14.47	15.50	11.20	13.50	13.50
TOTAL	100.9	98.7	100.9	100.9	100.6	100.1	100.5	97.3	100.7	99.0	99.5	100.9
	Structural formulae calculated on the basis of 8 Oxygens.											
Si	2.98	2.95	2.98	2.98	3.03	3.00	3.00	2.94	3.02	3.30	3.02	3.05
Al	1.02	1.01	1.01	1.01	1.04	0.99	0.99	1.04	1.00	0.78	1.01	1.01
Ti	0.01	0.01	0.00	0.00	0.003	0.004	0.004	0.004	0.00	0.001	0.002	0.004
Fe	0.01	0.00	0.01	0.01	0.01	0.01	0.002	0.01	0.01	0.01	0.004	0.01
Mg	0.00	0.01	0.02	0.02	0.02	0.00	0.00	0.002	0.02	0.00	0.00	0.00
Mn	0.01	0.004	0.001	0.001	0.001	0.004	0.00	0.002	0.00	0.00	0.00	0.01
Ca	0.01	0.09	0.002	0.01	0.003	0.001	0.00	0.00	0.01	0.01	0.01	0.00
Na	0.15	0.10	0.11	0.10	0.00	0.00	0.05	0.01	0.00	0.08	0.10	0.14
K	0.80	0.90	0.91	0.90	0.78	0.95	0.94	0.90	0.93	0.69	0.83	0.83
Sum of cations	4.99	4.97	5.02	5.00	4.89	4.88	4.98	5.06	4.47	4.68	4.90	4.97

Table 4.7

Compositions, cation contents of probed Chlorite and epidote.

SAMPLE NUMBERS	Chlorite E419	E239A	E239A	E239A	E156	Epidote E419	E419
SiO2	27.30	26.96	28.91	29.36	37.64	37.34	37.28
TiO2	0.00	0.05	0.04	0.02	0.35	0.62	0.022
Al2O3	17.51	19.63	19.35	17.44	14.64	22.12	23.32
FeO*	19.90	22.33	18.58	18.80	11.88	13.93	14.78
MnO	0.24	0.43	0.40	0.37	0.19	0.32	0.39
MgO	17.37	15.08	16.25	18.24	22.61	0.17	0.01
CaO	n.d.	n.d.	0.18	0.23	0.49	23.25	22.96
Na2O	0.25	n.d.	n.d.	n.d.	n.d.	n.d.	n.d.
K2O	n.d.	0.13	0.20	0.21	2.24	n.d.	0.12
TOTAL	82.6	84.6	83.9	84.7	90.0	97.7	98.8
Where FeO*= Total iron as Fe2O3.	Structural formulae calculated on the basis of 22 Oxygens.					of 25 Oxygens.	
Si	5.93	5.78	6.09	6.17	7.30	6.24	6.16
Al	4.48	4.96	4.80	4.32	3.40	4.31	4.54
Ti	0.00	0.01	0.01	0.004	0.05	0.10	0.003
Fe	3.61	4.01	3.27	3.31	1.90	1.80	1.91
Mg	5.62	4.82	5.10	5.72	6.60	0.04	0.003
Mn	0.04	0.08	0.07	0.07	0.03	0.05	0.06
Ca	----	----	0.04	0.05	0.01	4.12	4.07
Na	0.11	----	----	----	----	----	----
K	----	0.04	0.05	0.06	0.60	----	0.03
Where n.d.= not detected							

Table 4.8

Compositions, cation contents of probed apatite , ilmenite and magnetite.

SAMPLE NUMBERS	Apatite		Ilmenite			magnetite
	E419	E177	E156	E419	A11	E156
SiO2	0.95	0.74	0.80	0.65	0.61	0.89
TiO2	n.d.	n.d.	51.15	48.33	49.51	0.51
Al2O3	0.27	0.27	0.15	0.15	0.00	0.81
FeO	0.22	0.22	46.20	46.40	46.17	97.16
MnO	0.05	n.d.	2.56	5.06	4.50	0.32
MgO	n.d.	0.16	n.d.	n.d.	n.d.	n.d.
CaO	53.6	53.4	n.d.	n.d.	n.d.	n.d.
Na2O	n.d.	1.15	n.d.	0.19	n.d.	n.d.
P2O5	41.3	42.8	n.d.	n.d.	n.d.	n.d.
Cl	0.76	n.d.	n.d.	n.d.	n.d.	n.d.
TOTAL	95.2	98.7	100.9	100.5	100.8	99.7
	Structural formulae calculated on the basis of 25 Oxygens		of 3 Oxygens			of 4 Oxygens
Si	0.17	0.12	0.02	0.02	0.02	
Al	0.06	0.05	0.004	0.01	0.00	
Ti	----	----	0.94	0.92	0.94	
Fe	0.03	0.03	0.95	0.99	0.98	
Mg	----	0.04	----	----	----	
Mn	0.01	----	0.05	0.11	0.10	
Ca	9.54	9.50	----	----	----	
Na	----	0.37	----	0.01	----	
P	5.78	5.99	----	----	----	
Cl	0.23	----	----	----	----	

where n.d.= not detected

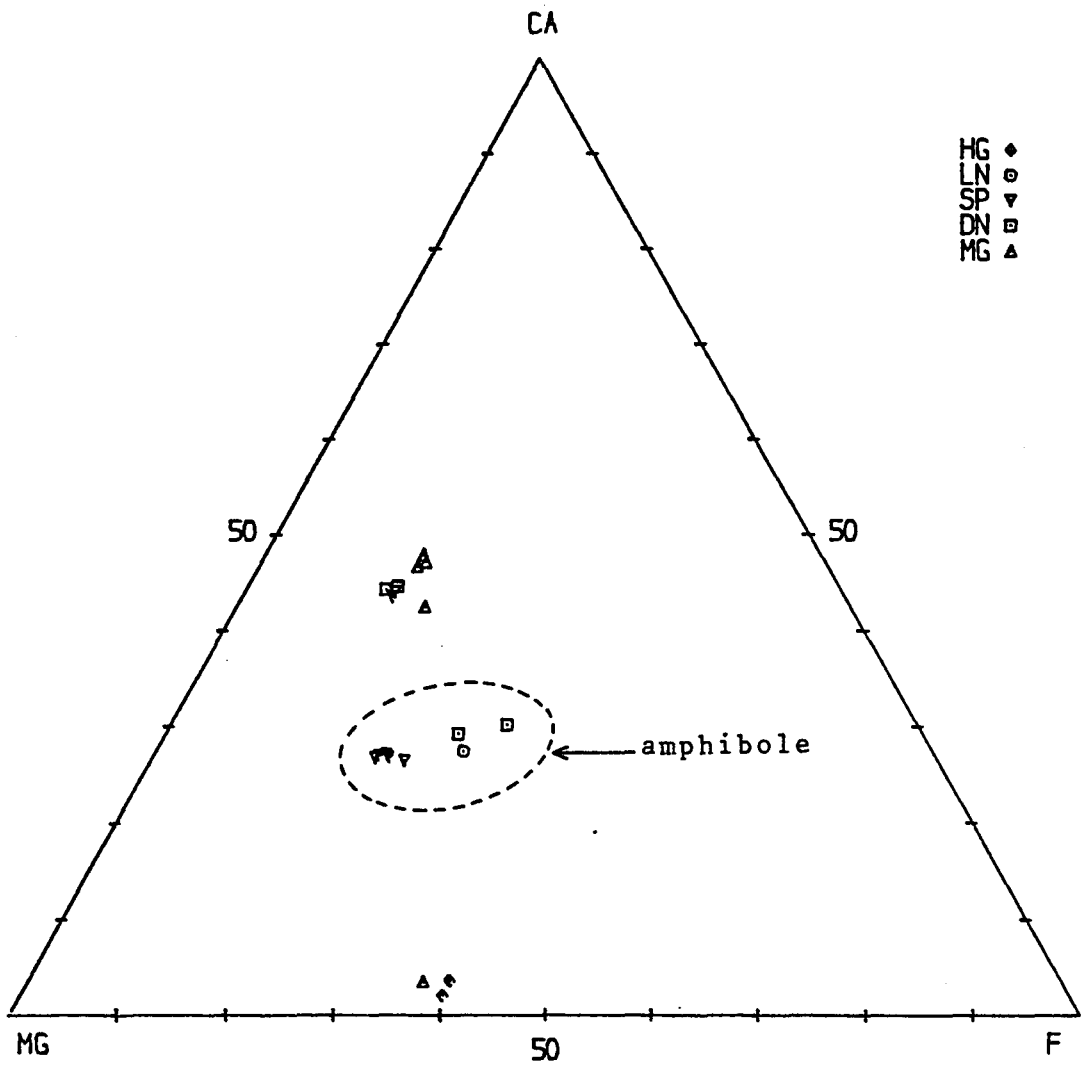

Fig. 4.1 Ternary plot of Ca-Mg-Fe + Mn(F) which show distinction of orthopyroxene, clinopyroxene and amphibole. Symbols as in figure (2.1)

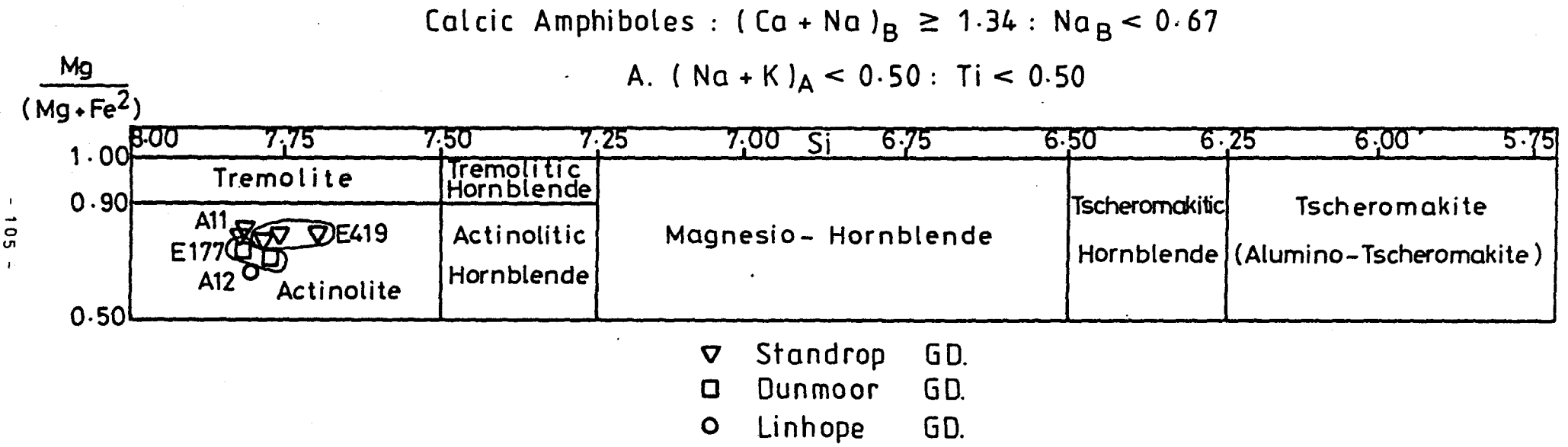

Fig. 4·2 Distinction and classification scheme of amphibole (after Leake, 1978). Symbols as in Fig. (2·1).

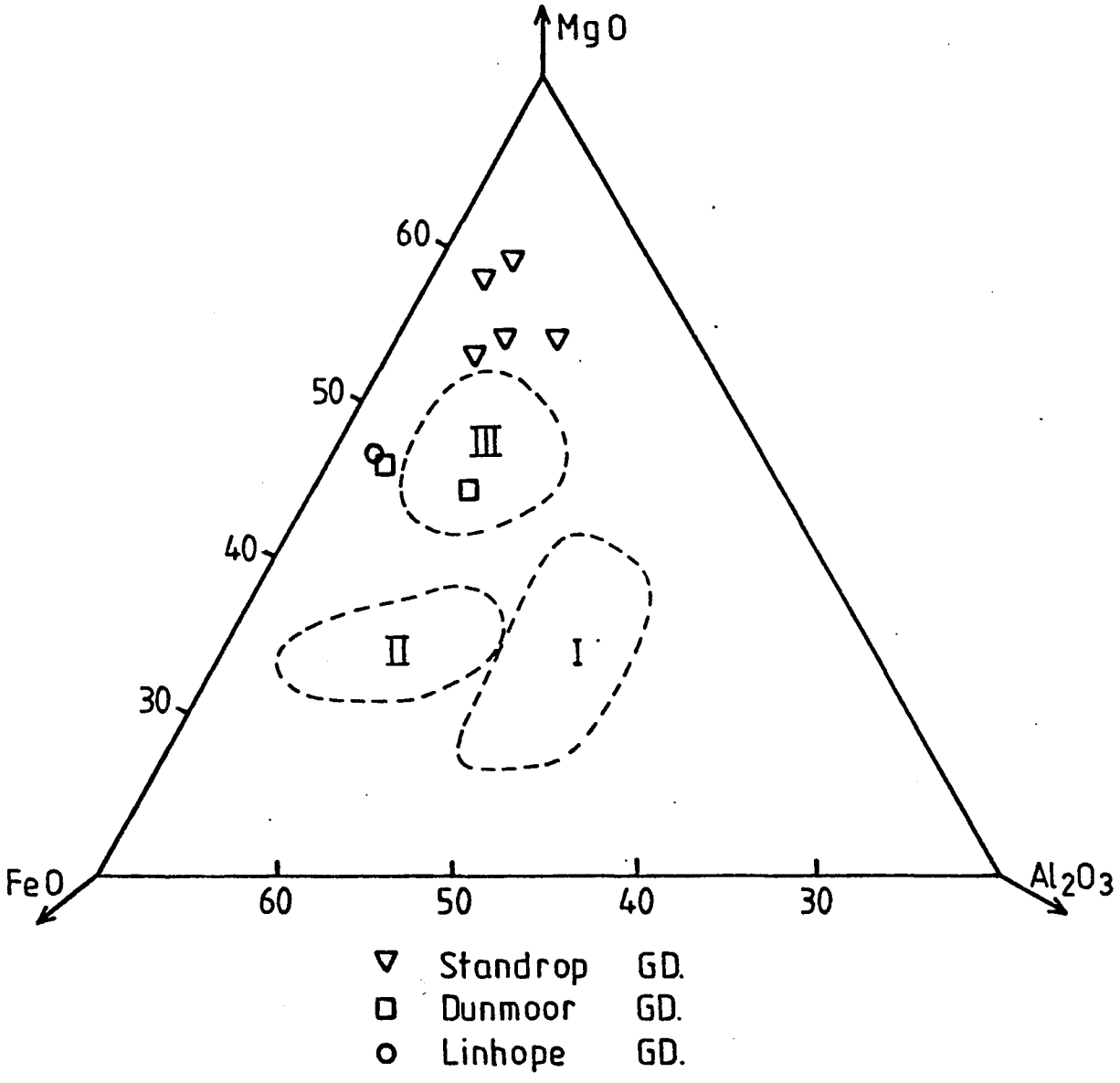

Fig. 4.3 Analysed amphiboles plotted in an FeO - MgO $-Al_2O_3$ diagram. Fields I, II and III are appinites and appinitic hornblendes, primary magmatic hornblendes and supposed secondary hornblendes respectively (Nockolds and Mitchell, 1948, p.559)

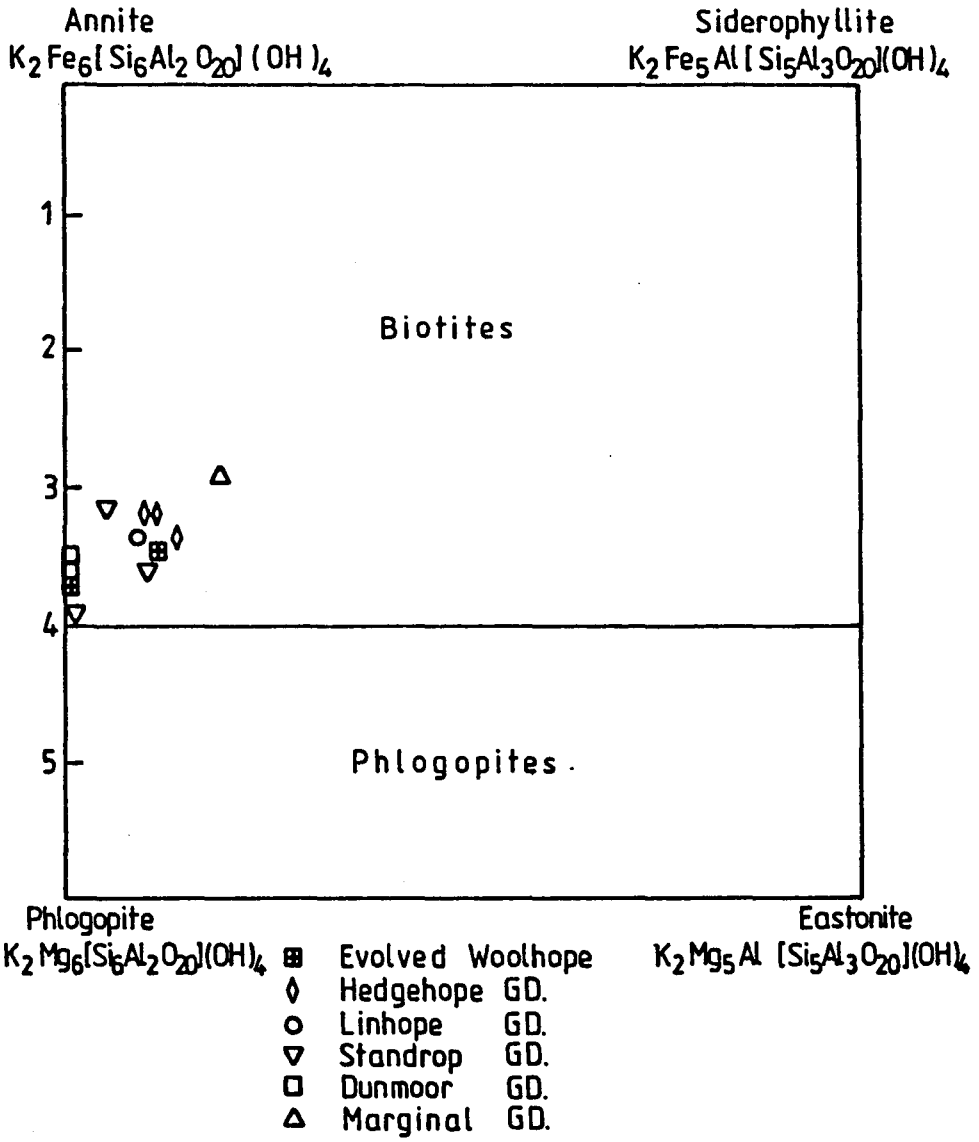

Fig. 4.4 Phlogopite-biotite compositional fields. Most phlogopites and biotites fall within these fields; the division between them is arbitrarily chosen to be where Mg : Fe = 2 : 1.
(After Deer et al., 1962), Symbols as in Fig. (2.1)

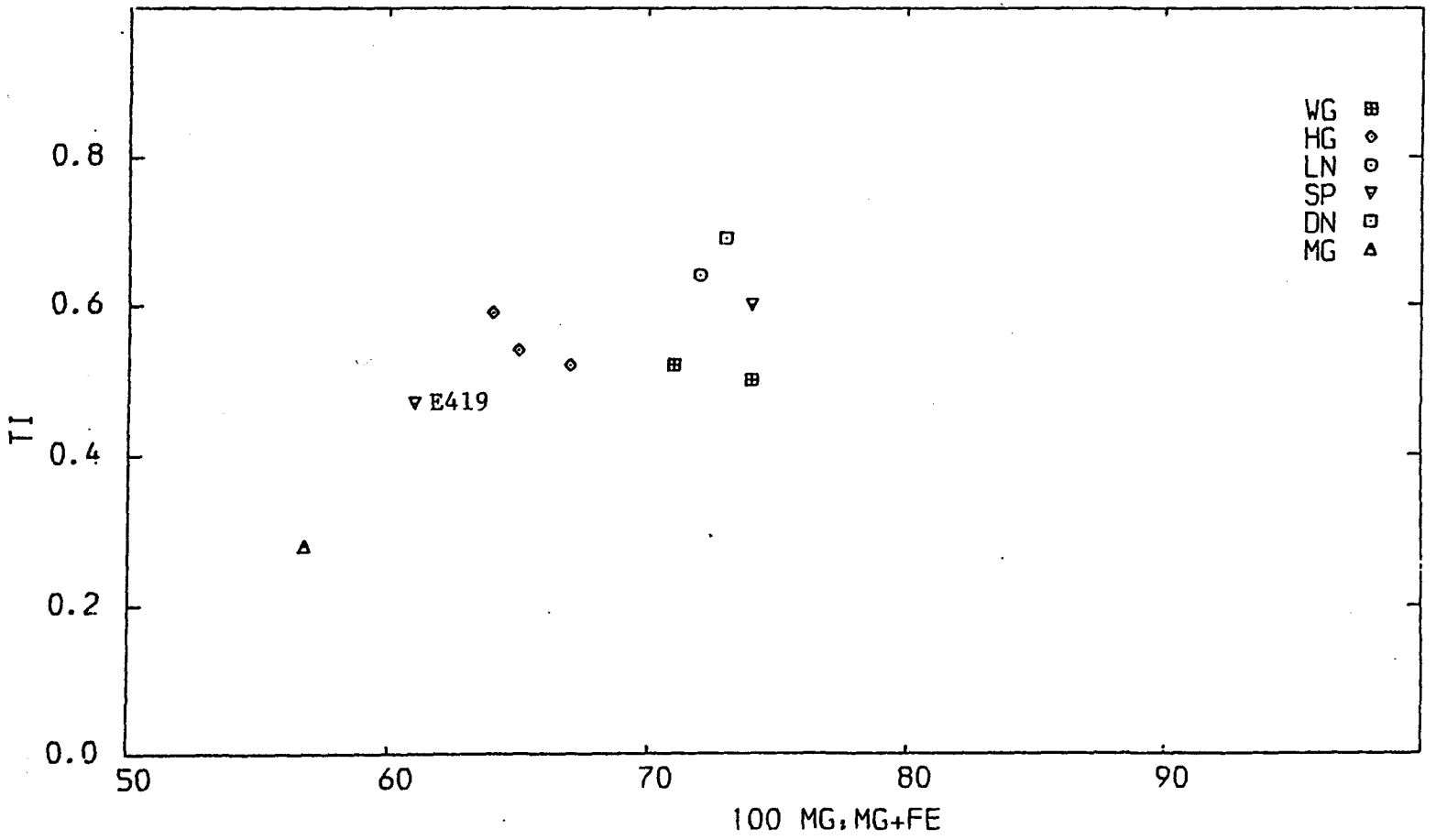

Fig. 4.5 Plot of the cationic ratio (100 Mg/mg + Fe) of 6 biotites from fresh granodiorites and granite and one from Standrop Granodiorite being affected by sericitic (2) alteration (E419).
Symbols as in figure (2.1).

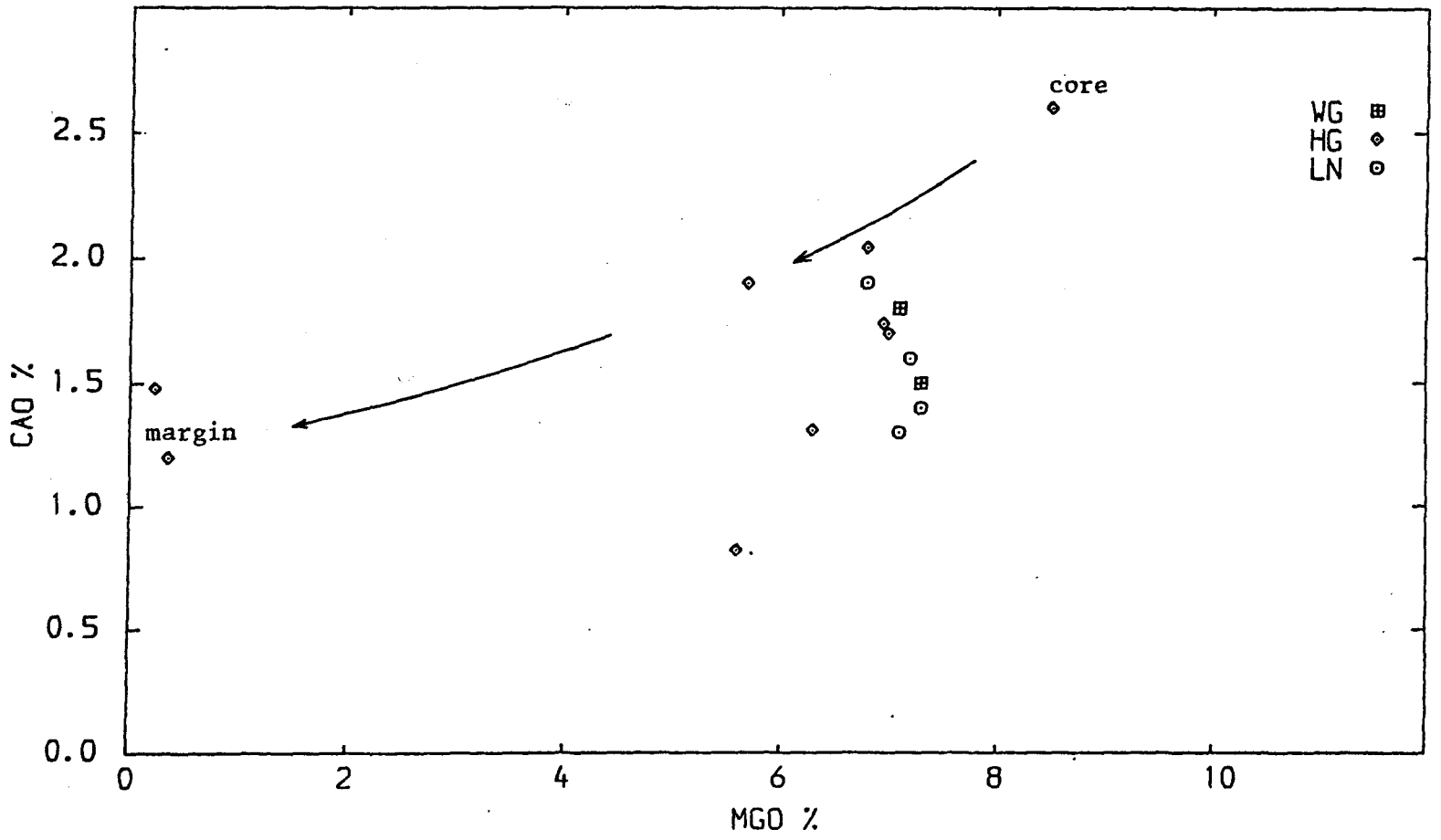

Fig. 4.6 Plot of CaO% against MgO% of tourmaline grains. Distinct chemical variation is shown by grain through a transect from core to margin (of sample E416)

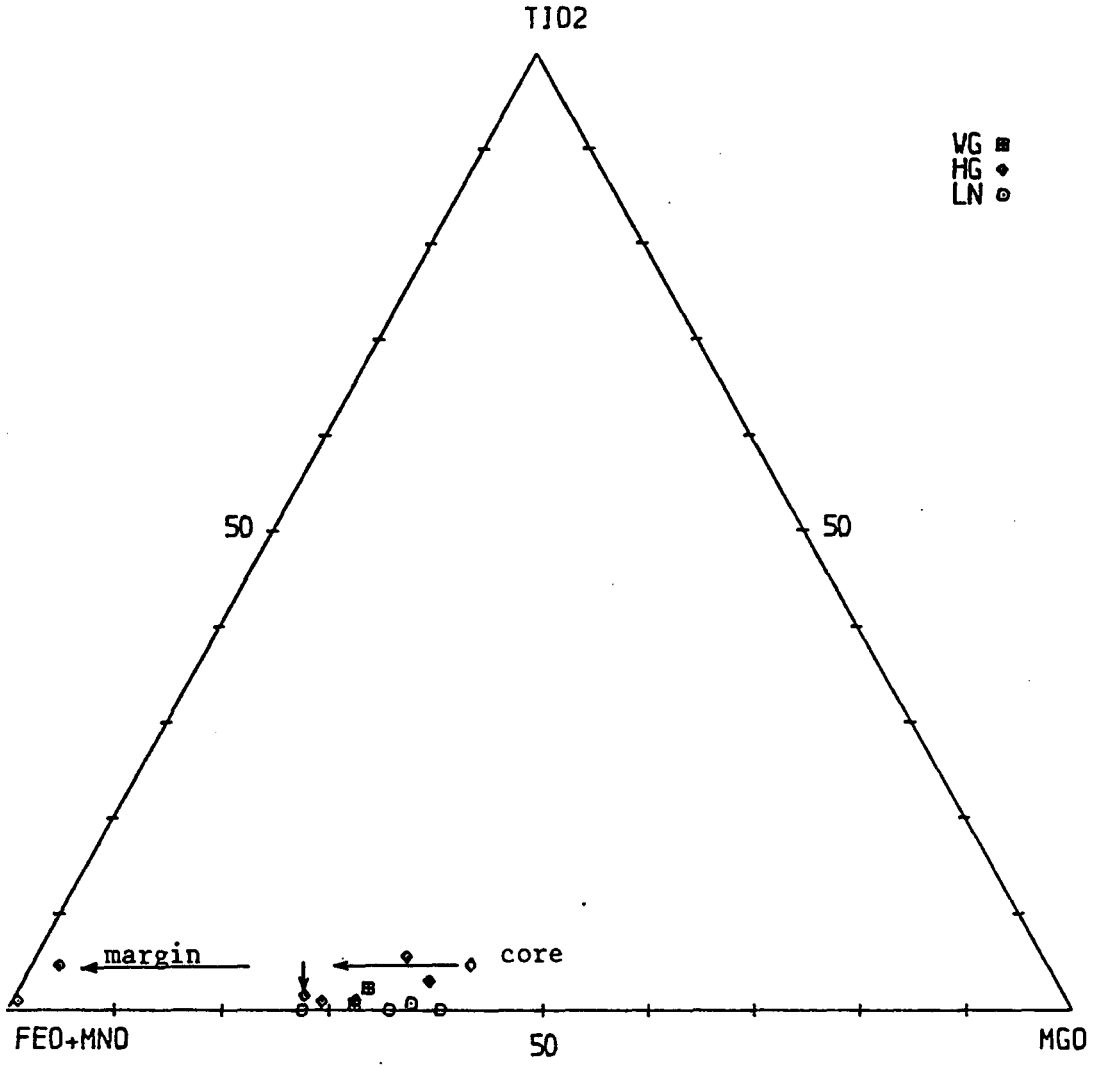

Fig. 4.7 Ternary plot of TiO_2 - FeO + MnO - MgO in tourmaline grains of different rock types with transect from core to margin of one grain (of sample E416)

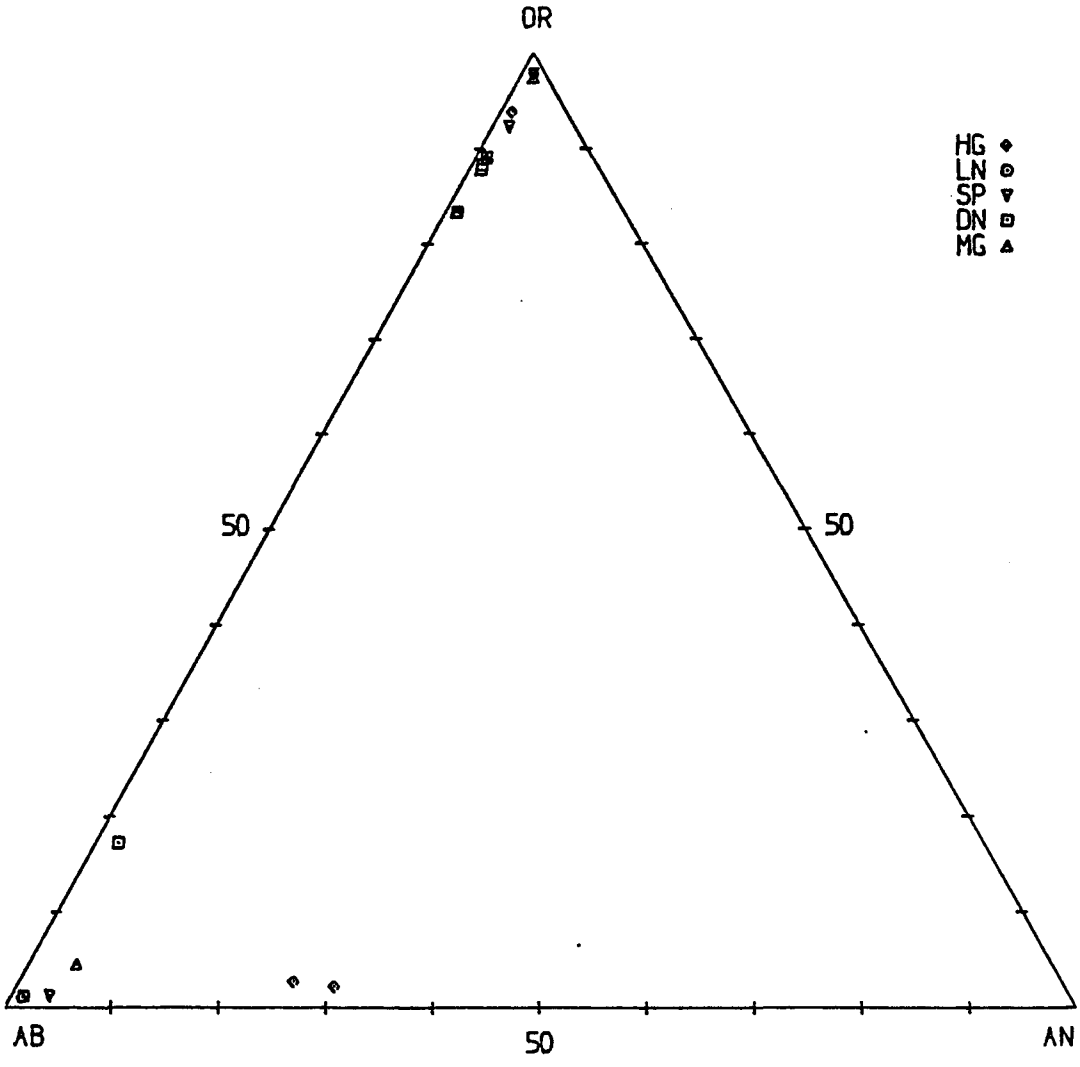

Fig. 4.8 Ternary plot of Or-Ab-An of orthoclase and plagioclase in both fresh and altered rocks.

CHAPTER FIVE

PRIMARY GEOCHEMISTRY

CHAPTER FIVE

PRIMARY GEOCHEMISTRY

5.1 ANALYTICAL METHODS AND SAMPLE SELECTION

5.1.1 ANALYTICAL METHODS

Major elements and a selection of trace elements were analysed on 122 rocks by atomic absorption spectrometry (A.A.S.), supplemented by colorimetry for some minor elements. The determination of a range of other trace elements, including rare earth elements (REE), was carried out using the Philips PW 1410 X-ray fluorescence instrument. A summary of the analytical techniques is as follows:

1. ATOMIC ABSORPTION SPECTROMETRY (A.A.S.):
   a. Major elements: Si, Al, total iron as Fe2O3, Na, K, Ca, Mg, Mn.
   b. Trace elements: Cr, Li, Ni, Co, Zn, Cu, Sr, Pb, Rb, Be, v.
2. COLORIMETRY
   Ti, P, Fe2+.
3. GRAVIMETRY
   Total water.
4. X-RAY FLUORESCENCE:
   a. Trace elements: Rb, Sr, Y, Zr, Nb, Mo, Pb, Th, U.
   b. Rare earth elements (REE): La, Ce, Pr, Nd, Sm, Eu, Gd, Er, Yb.

The details of the analytical procedures excluding REE, and of their precision and accuracy are given together with the analytical results and the calculated CIPW norms for the rocks in appendices A and D respectively. The details of the analytical procedures of rare earth elements together with the analytical results are given in Appendix B. The values recorded in the above appendices for pairs of duplicate analyses and for the standard rocks chosen are an indication for the good analytical precision of the methods used.

5.1.2 SAMPLE SELECTION

To give a representative sample of the least altered rocks for the interpretation of the primary geochemistry, forty specimens were chosen of the freshest rocks selected from each of the six rock groups. All forty have been analysed for major, minor and trace elements and six of these specimens (one sample from each rock unit) have been analysed for REE. In addition seven further samples were chosen for analysis, to investigate the granite veins cutting the complex, the hornfelsed andesites around the granite and a xenolith collected from within the Standrop Granodiorite. Below is a list of the rock types in order, together with the numbers of fresh samples selected. Altered rocks will be considered in chapter 6.

1.	Woolhope Granite	4 samples
2.	Hedgehope Granodiorite	6 samples
3.	Linhope Granodiorite	3 samples
4.	Standrop Granodiorite	13 samples
5.	Dunmoor Granodiorite	6 samples
6.	Marginal Granodiorite	8 samples
7.	Veins	3 samples
8.	Hornfelses	3 samples
9.	Xenoliths	1 sample
		47

The chemistry of the 40 fresh analysed samples of granodiorite and granite confirms the division into six groups with each group showing distinctive chemical characteristics. Chemical averages of each of the groups, are calculated and presented in Tables 5.1 and 5.2.

5.2 GENERAL FEATURES OF PRIMARY GEOCHEMISTRY

The averages of the six principal rock types are summarised in order in Table 5.1. These data are used to interpret processes of magmatic evolution where the roles of elements such as K, Ca, Na, Si together with Ni, and Cr are important. From each average the differentiation index (Thornton and Tuttle, 1960) was calculated as a

measure of the degree of evolution of each unit. The Marginal Granodiorite which forms the outermost intrusive phase is relatively the most basic and in this unit K, Na, and Si are lower and Ca, Ni, and Cr are higher than in the other bodies in the two cycles of igneous activity. The other granodiorites are rather similar in their degree of evolution, with Standrop Granodiorite the next least evolved, followed by the Linhope Granodiorite, the Dunmoor Granodiorite and the Hedgehope Granodiorite. The Woolhope Granite is much more evolved, and is chemically a true granite, as is shown by the considerable differences between its major and trace elements and those of the granodiorites. There is a clear progression towards more evolved compositions in both igneous cycles, both of which contain a relatively evolved porphyritic granodiorite. Three veins were analysed and their average is presented next to the average of the four samples of Woolhope Granite (Table 5.2). The chemistry of both is nearly identical which suggest that the Woolhope Granite was the source of the veins. Eventually fracturing, produced by the high volatile pressure characteristic of evolved melts such as the Woolhope magma (when exceeding the sum of minimum stress and tensile strength of the enclosing rock), followed by intrusion of the evolved Woolhope melt along the fractures gave rise to the veins of this composition. A similar effect is also seen in the Loch Doon Pluton (Tindle and Pearce, 1981). Table 5.2 shows a comparison of xenolith, hornfels and Marginal Granodiorite. All three rock types are very similar to one another, except that the xenolith is depleted relative to the other rock types in V, Cr, and Ni, to an extent unusual in

such a basic rock.

Field evidence show that these xenoliths are mainly found in the Standrop Granodiorite (which begins igneous cycle 2). The analysed xenolith might be a fragment of rock from cycle 1 caught up in the renewed igneous activity of cycle 2, or possibly a fragment of hornfels, but its anomalous compatible trace element chemistry would seem to rule out a very simple origin.

An AFM diagram plotted for the granodioritic and granitic samples (Figure 5.1) shows a typically calc-alkaline curve of variation (Nockolds and Allen, 1953- p.110). The analysis means show a tendency towards shoshonitic compositions, as demonstrated by the enrichment of K, Rb, and Sr relative to normal calc-alkaline rocks. The subdivision of calc-alkaline from shoshonitic magmas is generally carried out using the plot of Zr against Sr (Pearce, 1973), and such a plot (Figure 5.1a) confirms the nature of these analyses and their tendency towards shoshonite as they lie nearly on the borderline separating calc-alkaline from shoshonitic magmas. Shoshonites are known to erupt both at converging plate margins and in post-orogenic situations after subduction has ceased (Pearce and Cann, 1973; Pearce, 1976). A comparison of these rocks with the typical calc-alkaline rocks of the Cascade Province (basalt - andesite - dacite - rhyolite association), Northern United States (Turner and Verhoogen, 1960) shows that in the Cheviot K (or Rb) and Sr are higher relative to the abundances usual in calc-alkaline rocks.

Another comparison of these analyses, is made with the data given by Brown (1979) for the values of K2O/Na2O, Rb/Sr, K/Rb ratios and U content in the Caledonian Granites of North England and the Southern Uplands. Table 5.3 shows that when this comparison is made, the Southern Uplands data (and that for the Loch Doon in particular) seem to be more or less identical to the Cheviot data. Tindle and Pearce (1981) summarize the chemical analyses of the Loch Doon Pluton in Southern Scotland which is characterised by gradational contacts and a progressive change from more basic to more acid units towards the centre of the complex. So a chemical comparison of the individual bodies in each magmatic cycle from the two plutons is suggested (i.e. individual bodies of cycle 1 in the two Plutons are compared with each other and same with the magmatic phases comprising cycle 2 in both plutons). Consequently a group of samples were selected from Table 1 in Tindle and Pearce (1981) for this purpose as follows:

Loch Doon Samples	Cheviot Samples
1. Magma cycle 1	1. Magma cycle 1
a. 128	a. Marginal Granodiorite.
b. 157	b. Dunmoor Granodiorite.
2. Magma cycle 2	2. Magma cycle 2
a. 264	a. Standrop Granodiorite.
b. 288	b. Linhope Granodiorite.
c. 242	c. Hedgehope Granodiorite.
d. 250	d. Woolhope Granite.
The above are individual sample no.	Averages are taken to represent each unit.

Therefore samples 128 and 157 (of magma cycle 1) from the Loch Doon Pluton are compared with the averages of the Marginal and Dunmoor

Granodiorites respectively whereas samples 264, 288 and 242 are taken against components of igneous cycle 2 which are the Standrop, Linhope and Hedgehope Granodiorites respectively. Finally the Woolhope Granite is compared with sample 250. The selection of these samples is mainly based on their contents of SiO2, so that Loch Doon samples were chosen with SiO2 contents approximately those of the Cheviot unit averages.

The results of this comparison are:

- Units of cycle 1 in the Cheviot Pluton are found to be higher in Rb and lower particularly in Y and Zr and to a slight extent in MgO and CaO contents. Other elements (major, traces and REE) are more or less similar in the two cases (Table 5.4).
- Components of cycle 2 in the Cheviot Pluton are higher in Rb and Zr whereas other elements (including the REE) are more or less similar in both plutons (Table 5.4).

In addition pairs of Rb and Sr values from the Cheviot complex are found to fall on the line of the variation diagram of Sr against Rb for the Loch Doon Pluton (Brown, 1979). Finally a comparison can be made with the Newry Igneous Complex, County Down which is in a similar tectonic setting in Ireland. This is found to be poorer in K2O, Rb, Zr and richer in Sr for same SiO2 content than the Cheviot Pluton (Meighan and Neeson, 1979, Table 5.5).

5.3 RARE EARTH ELEMENTS -(REE)-

Six typically fresh samples of the Cheviot granodiorites and granite were analysed for REE using the method described in Appendix B, and were normalized to the chondritic average (Nakamura, 1974, Table 5.6). A slight modification has been made of some of the values quoted by Nakamura, to improve the between element relations here, bringing the values closer to those obtained by various workers. The normalized values (Table 5.7) are plotted against REE atomic number in Figure 5.4. The fresh granodiorites plot in a narrow band which is shown on Figure 5.4a. The Tb and Dy points have been omitted because of their rather large analytical error. The following observation can be made:

1. The granodiorites contain about the same REE content as, and have a comparable REE pattern to, other analysed granodiorites (Tindle and Pearce, 1981; Pankhurst, 1979). They show a typical enrichment in light REE with slight negative Eu anomaly, which is characteristic of some granodiorites (Towell, et al, 1965; Haskin, et al, 1966; Goles, 1968).
2. The Woolhope Granite differs strikingly from the granodiorites and is relative to them strongly depleted in light REE and to a lesser extent in heavy REE. The negative Eu anomaly is greater than that of granodiorite.
3. Figure 5.4 shows that progressive fractionation of the parent magma produces a slight increase in total REE with increasing evolution of the magma, as shown by Taylor (1965) and Haskin et

al. (1966). The sudden decrease in total REE (especially light REE) in passing from the granodiorites to the granite can be explained by the onset of crystallisation of minor REE-rich phases, such as apatite and zircon. In the granodiorites most of the REE are probably in the plagioclase feldspar, but as the concentration of P and Zr builds up in the magma, eventually early crystallisation of these REE-rich phases begins, and the REE content of the magma decreases. The progressive development of the Eu anomaly from the granodiorite to the granite is most readily explained in terms of the removal of significant amounts of plagioclase feldspar, which concentrates Eu^{2+} (Philpotts, 1970), during fractional crystallization.

5.4 TECTONIC ENVIRONMENT

5.4.1 DEPTH TO BENIOFF ZONE

A general correlation has been shown between the potassium content of basaltic andesite and andesitic lava at a given silica content and depth from the volcano to the inclined seismic zone, the Benioff zone, that dips away from the associated trenches into the mantle beneath volcanic arcs, by many workers in this field (Dickinson and Hatherton, 1967; Dickinson, 1975; Hatherton and Dickinson, 1969; Nielson and Stoiber, 1973). This approach can be applied here to examine whether it is possible that a Benioff zone underlies the

Cheviot at a reasonable depth. The K2O content at 60% SiO2 is measured from the potash-silica variation diagram of the averages (Figure 5.5, Table 5.1) by extrapolating the variation line. This value (K2O=2.75) is compared with the value measured by Nielson and Stobier (1973, P. 6890) at Java for high potash lavas at 60% SiO2. This suggests a depth of approximately 190 km. At a more sophisticated level, the following equations were calculated by Hutchinson (1976) based on the Indonesian arc and are applied here on both Marginal and Standrop Granodiorites which are relatively more basic than the other phases and are thus nearer in composition to the lavas used by Hutchinson. The three equations relate depth and SiO2 content separately to K2O, Rb, and Sr.

Depth = 397-(5.26 x %SiO2)+(35.04 x %K2O)

Depth = 373-(4.36 x %SiO2)+(0.73 x PPM Rb)

Depth = 110-(0.03 x %SiO2)+(0.14 x PPM Sr)

These give the following values for depth:

	Marginal Gd.	Standrop Gd.
D K2O	192 Km	191 Km
D Rb	220 Km	215 Km
D Sr	173 Km	164 Km

These values scatter somewhat, but are all consistent with an apparent depth to a Benioff Zone beneath Cheviot of about 190 km.

5.4.2 TECTONIC SETTING

Pearce et al. (in press) use discriminant functions to subdivide granites according to the tectonic setting of their intrusion into four main groups - Ocean Ridge Granites (ORG), Volcanic Arc Granites (VAG), Within Plate Granites (WPG) and Syn-Collision Granites (Syn-COLG) and the granites within each group may be further subdivided according to their precise settings and petrological characteristics. Discrimination of ORG, VAG, WPG and Syn-COLG is carried out on projections of Y - Nb, Yb - Ta, Rb - (Y+Nb) and Rb - (Yb+Ta). Figure 5.6 shows the Y-Nb plot, in which the Cheviot samples clearly fall into the combined VAG + Syn-COLG field. These two types of granite are discriminated on Figure 5.7, of Rb against (Y+Nb). Here the Cheviot granite falls very close to the border between the two types. Taken together with the results of the Benioff calculation, this might indicate that the Cheviot complex formed in an early collision environment, perhaps above a remnant slab of oceanic lithosphere still descending beneath the collision orogen. Such evidence is consistent with the regional stratigraphic and structural evidence (Phillips et al., 1976).

5.5 INDIVIDUAL GRANITE BODIES

The Cheviot Pluton grades into composition from granodiorite through to granite. These plutonic rocks are found to be calc-alkaline to shoshonitic in nature as mentioned above. The genetic relation between these phases are best shown on Harker Diagrams. These plots show that SiO2 content ranges nearly uninteruptedly from 63% to 69% for granodiorites corresponding to Marginal Granodiorite and Hedgehope Granodiorite respectively whereas in the granite, the Woolhope Granite, it ranges from 72% - 76%. Good positive correlations exist between K2O (or Rb) and SiO2 (Figures 5.2a & 5.3a). The Marginal Granodiorite is relatively the most basic member of the Cheviot Intrusive phases, and has the lowest K and Rb. Subsequent increase in K and Rb is due to the fractionation of mafic minerals such as pyroxene from the parent magma which in turn enriches the residual melt in both of these elements. On the other hand there is strong negative correlation between SiO2 and TiO2, Al2O3, P2O5, FeO*, MgO, CaO, Ni, Cr, Sr individually and to a slight extent with Na2O. This suggests a probable line of descent with progressive crystallization of ferromagnesian minerals, calcic plagioclase, apatite and Fe-Ti oxides (minor phases). Table 5.8, summarizes the grouping of plots according to positive or negative correlation, degree of scatter and nature of slope of the linear relation:

A plot of the C.I.P.W normative components, Q, Or and Ab, of the unit means (Figure 5.12, Table 5.9) shows the evolution towards granite within each cycle. The fractionation paths of the two cycles (cycle 1, from Marginal to Dunmoor and cycle 2 from Standrop to Linhope and Hedgehope Granodiorites and finally to the Woolhope Granite) are distinctly shown. The composition of the granite in the system Q-Or-Ab is close to the minimum melting composition. Tuttle and Bowen (1958) show that the composition of the minimum melting point in the granite is a function of the water vapour pressure. Figure 5.12 shows that the Woolhope Granite lies close to the point representing the minimum melting composition at 500 bars water vapour pressure, and that the compositions of the other units show a trend in the direction of that point. Figure 5.13 shows that at such a low water vapour pressure, the water content of the magma would be low (about 0.5%). The dry nature of the Cheviot magmas suggested by this evidence is consistent with the small quantity of hydrous phases in the fresh granites.

Figure 5.12 is also interesting because it clearly separates the two igneous cycles of the Cheviot complex. Such a distinction can also be seen on other chemical plots. On the plot of Zr against (CaO+MgO), (Figure 5.14b) where (CaO+MgO) is used as an index of evolution of the igneous rocks, there is an excellent separation of the two cycles, with cycle 1 showing a relatively higher Zr content than cycle 2. In addition the Zr values of cycle 1 decrease slightly from the more basic Marginal Granodiorite to the more evolved Dunmoor

Granodiorite, while the Zr values of cycle 2 show a more marked and persistent decrease with evolution from the Standrop Granodiorite to the Woolhope Granite, presumably as a result of precipitation of zircon from the evolving magma. A distinction can also be made on a plot of K2O against (CaO+MgO) (Figure 5.14a). This shows that cycle 1 is somewhat higher in K2O than cycle 2.

On both Figures 5.14a and b, the different units that go to make up the complex can be distinguished from one another very clearly, though the clusters of points from each unit do come close to one another. Some of the scatter in the clusters may be the result of analytical errors, but more may result from real variation in the local composition of the granite. Since the differences between the units are relatively small, this effect may bring samples from two different units very close in composition.

5.6 PETROGENESIS OF GRANODIORITES

It is now important to ask whether the change from relatively basic granodiorite to more evolved granodiorite during each cycle, and the eventual production of granite magma, can be explained by the operation of crystal fractionation processes, or whether other processes are required to operate as well as crystal fractionation or instead of it.

The smooth curves shown on the Harker diagrams of Figures 5.2, 5.3 and 5.8 to 5.11 are one piece of evidence. Mixing of magmas would tend to produce straight line Harker plots, for example. More quantitative evidence comes from log-log plots of trace elements. Figures 5.15 and 5.16 show that several important trace elements give straight line log-log Plots. Such straight line plots are required by ideal Rayleigh fractionation (Rayleigh, 1896). This assumes surface equilibrium between crystal and liquid, an assumption that is supported as reasonable in the present case because the complex oscillatory zoning in the plagioclases has been preserved during the solidification of the magmas. The Rayleigh fractionation equation for a single trace element is

$$C_l = C_o F^{(D-1)}$$

where C_l is the concentration of the element in the evolved Liquid, C_o that in the parent liquid, F the fraction of liquid remaining and D the bulk solid-liquid distribution coefficient for the element.

If two Rayleigh equations are written for two elements in the same rocks and F is eliminated between the equations, then the result is:

$$\log C_a = \frac{(D_a-1)}{(D_b-1)} \times \log C_b + r$$

where C_a is the concentration of element a in a liquid fraction, $\log C_b$ that of element b, D_a and D_b are the equivalent solid-liquid distribution coefficients and r is a complex function of the original compositions and distribution coefficients. Thus a plot of log C_a

against log C_b should define a straight line, with slope $(D_a-1)/(D_b-1)$, which passes through the point representing the original composition.

Though these arguments make a good case for the operation of crystal fractionation, it can be investigated further by examining whether a combination of plausible cumulate phases can explain quantitatively the change in composition during evolution of the magmas.

What cumulate phases might be precipitating from the granodiorite magmas?

First, there are the phases that appear as phenocrysts in the porphyritic granodiorites. The most common phenocryst phase is plagioclase, followed by biotite, augite and hypersthene in order of abundance. Clearly these may be phases forming part of the precipitated solid.

Second, there are minor phases. These are present in the granodiorites in small quantities, but not always clearly as early-crystallising phases. However, examination of the Harker diagrams indicates that some of them at least may form part of a precipitating solid. Ilmenite is present in the granodiorites as medium-sized rounded single crystals, possibly early crystallising, and TiO2 decreases steadily during evolution of the magma. On that basis, ilmenite seems a possible precipitating phase. Similarly a consistent decrease in Zr and P2O5 during evolution, coupled with the presence of well-sized zircon and apatite crystals suggests that

these phases too should be included for consideration. Finally, magnetite occurs in the granodiorites in similarly sized crystals to ilmenite, and should also be included in any calculation.

Now consider crystal fractionation in which the solid is made up of a mixture of all of these phases, so that defining:

bi = fraction of biotite in solid,
opx= fraction of orthopyroxene in solid,
cpx= fraction of clinopyroxene in solid,
pl = fraction of plagioclase in solid,
il = fraction of ilmenite in solid,
mt = fraction of magnetite in solid,
zc = fraction of zircon in solid,
ap = fraction of apatite in solid,

Then

$$bi + opx + cpx + pl + il + mt + zc + ap = 1$$

Since zircon and apatite are present in any solid in very small amounts and have very little effect on other elements than Zr and P they are omitted from calculation at this stage, so that we can set, nearly enough

$$bi + opx + cpx + pl + il + mt = 1 \qquad (1)$$

Now, if the oxide composition of the precipitated solid is expressed by:

SiO2=s
Al2O3=a
FeO=f
CaO=c
K2O=k
TiO2=t

then the proportions of phases and the percentages of oxides can be

related, assuming that the compositions of the phases are those determined by electron microprobe analysis (see Chapter 4 and Table 5.10 where the analyses are summarised.),

Thus:

$$t = 6bi + 0.3cpx + 0.3opx + 48il + 0plag+0mt \quad (2)$$

where the coefficients are the TiO2 contents of the appropriate phases from Table 5.10. Similarly we can write:

$$a = 13.5bi + 26.5pl \quad (3)$$
$$c = 22cpx + 20opx + 7.8pl \quad (4)$$
$$f = 12bi + 9cpx + 22opx + 46il + 92mt \quad (5)$$
$$k = 9.5bi + 1.1pl \quad (6)$$
$$s = 40bi + 52cpx + 52opx + 58pl \quad (7)$$

A further set of equations arise from the fact that any precipitating solid must lie on the projection to lower SiO2 values of the line connecting the least and most evolved granodiorites on all the Harker diagrams, and thus must satisfy the equation of the line connecting those two points. For this purpose the averaged data of Table 5.1 was used, rather than the individual analyses. The resulting straight line equations are:

$$t= -0.05s + 4.05 \quad (8)$$
$$a= -0.13s + 23.75 \quad (9)$$
$$c= -0.37s + 27.39 \quad (10)$$
$$f= -0.33s + 25.67 \quad (11)$$
$$k= 0.25s - 12.40 \quad (12)$$

We now have 12 equations for 12 unknowns. These are now solved, and after that, small adjustments are made to accommodate Zr and P. The Harker diagrams for Zr and P aginst SiO2 (Figure 5.5) are extrapolated to the SiO2 value obtained from the solution of the

twelve simultaneous equations above. The values of Zr and P obtained are those present in any precipitating solid and are 465 ppm for Zr and 0.58% for P2O5. From these values the appropriate contents in the precipitating solid of zircon and apatite can readily be calculated. The result of this calculation of the possible precipitating solid can either be expressed as a phase composition, when it is:

bi = 16.30 %
opx = 14.60 %
cpx = 13.84 %
pl = 55.27 %
il = 0.84 %
mt = 1.29 %
zc = 0.10 %
ap = 1.37 %

Or as the elemental composition:

SiO2 = 53.37 %
TiO2 = 1.46 %
Al2O3 = 17.06 %
FeO* = 8.00 %
MgO = 7.62 %
CaO = 7.64 %
Na2O = 3.59 %
K2O = 2.16 %
P2O5 = 0.58 %
Zr = 465 ppm

The precipitate that appears from this calculation is a biotite gabbro or biotite diorite, with rather over 50% of andesine plagioclase, and nearly equal amounts of biotite, orthopyroxene and clinopyroxene. The relative proportions of minerals calculated are close to the relative proportions of the phenocryst phases observed in the porphyritic granodiorites, and this suggests rather strongly

that such a precipitating solid might be the cause of the evolution from one end of the granodiorite range to the other. The precipitate itself would be rather similar to the distinctive rock kentallenite, a biotite-bearing olivine gabbro with sodic plagioclase and interstitial alkali feldspar. The Cheviot cumulate would not, however, contain olivine. It is certainly possible that kentallenite is a cumulate from a similar, but more undersaturated magma.

The major element geochemistry thus seems consistent with a relationship between the granodiorites based on crystal fractionation and precipitation of a sodic biotite gabbro. This possibility can be explored further using trace elements, by calculating a bulk solid-liquid distribution coefficient for the phase assemblage derived from major elements for a number of critical trace elements, and then comparing the result to distribution coefficients derived from log-log trace element plots, (Figures 5.17a, 5.17b, 5.18a and 5.18b)

For a precipitated solid made up of known phases in known proportions, the bulk solid-liquid distribution coefficient for any trace element is given by

$$C_s/C_l = D = \Sigma i D(i).X(i)$$

where C_s is the concentration of the element in the solid, C_l its concentration in the liquid, D(i) the solid-liquid distribution

coefficient for phase i and X(i) the weight fraction of phase i in the mixture.

In the present case the relation becomes; for any trace element:

$$D = pl.Dpl+opx.Dopx+cpx.Dcpx+il.Dil+mt.Dmt+2c.D2c+ap.Dap+zc.Dzc$$

where pl, opx etc take the values calculated above, expressed as fractions. Using values for D derived from Table 5.11 out of different references , the following values for bulk distribution coefficient between solid and liquid can be calculated:

Rb: 0.39	Eu: 1.66	Y: 1.40
La: 0.62	Yb: 0.89	
Ce: 0.67	Lu: 1.10	
Sm: 0.58	Cr: 4.39	

These values may be compared with values calculated using log/log plots of trace elements (Figures 5.17 to 5.18). As indicated above, in ideal Rayleigh fractionation log/log plots of pairs of trace elements will give a straight line relationship, with slope:

$$m = \frac{Da-1}{Db-1}$$

Often, in such cases, one of the elements can be assumed to be behaving so incompatibly that its distribution coefficient is effectively zero, in which case plots of other elements against that give slope of -(Da-1). In this case, no element could be found approaching this condition, so that an alternative approach had to be found. The distribution coefficient for Rb was assumed to be the same as that calculated above, (0.39) and the slope of log/log plots of other elements against Rb was taken as -(Da-1)/0.61. From this relationship , other distribution coefficients could be calculated, giving values as follows:

La:0.80	Cr:1.84
Ce:0.88	Y:1.00
Sm:0.84	

These values are not the same as these calculated above. Those for La, Ce, and Sm are higher and for Cr and Y lower than the values generated by the phase assemblage calculation. There are two possible explanations for this discrepency. Either crystal fractionation was supplemented (or even replaced) by another process, such as wall rock assimilation or magma mixing, in causing the evolution of the granodiorites from one type to another, or the quoted distribution coefficients for these elements into the appropriate phases might be in error. The latter certainly seems

possible. Values quoted for the distribution coefficient of Cr vary strongly with magma composition, ranging from 7 to 25 for clinopyroxene and from 2 to 5 for orthopyroxene. Choice of a different value in the range could markedly influence the calculation for Cr. The rare earths and yttrium are strongly partitioned into some of the minor phases, such as apatite and though the values of the distribution coefficient are known to be high they are not very well constrained. However, it is not particularly satisfactory that there should be this degree of divergence between the two sets of distribution coefficients, and the possibility that there is a process acting in addition to crystal fractionation cannot be ruled out. On the other hand, crystal fractionation seems very well able to explain the major element variation, and the balance of the evidence must be that it is the most important process operating.

5.7 PETROGENESIS OF THE GRANITE

The second magmatic cycle in the complex evolved as far as a granitic composition close to the ternary minimum in the Q-Ab-Or systems. This granite magma contrasts strongly with the most evolved granodiorite of this cycle (the Hedgehope Granodiorite) in its depletion in many elements. MgO, FeO*, Ni and Cr reach very low levels, as a consequence of the continued crystallisation of ferromagnesian minerals, and Ca and Sr are depleted as a result of plagioclase crystallisation. In addition, some of the elements characteristics of minor phases, such as Ti, P, Zr and REE are

severely depleted, apparently because of the increasing importance of the crystallisation of such phases as fractionation proceeds. This is particularly striking in the case of the REE, which hardly vary at all during the crystallisation that causes the variation in the granodiorites, but are markedly depleted in the Woolhope Granite. Because of the strong influence of the minor phases on the chemical fractionation in the granites, it did not seem appropriate to attempt a detailed fractionation calculation, but it seems qualitatively likely that this later stage fractionation would have been controlled by rather similar phases to those deduced above, though with a larger component of the minor phases present in the crystallising solid.

Table 5.1

Averages of the different fresh Cheviot Granodiorites (Gd.) and Granite (Gr.)

Average	Marginal Gd. (n=8)	Dunmoor Gd. (n=6)	Standrop Gd. (n=13)	Linhope Gd. (n=3)	Hedgehope Gd. (n=6)	Woolhope Gr. (n=4)
SiO2	64.42	67.50	65.90	66.17	68.32	73.72
TiO2	0.83	0.67	0.71	0.63	0.61	0.29
Al2O3	15.33	15.03	15.21	14.99	14.91	13.80
Fe2O3	1.67	1.53	1.71	1.46	1.49	1.45
FeO	2.68	1.79	2.14	2.33	1.51	0.46
MnO	0.09	0.07	0.08	0.10	0.06	0.04
MGO	2.94	1.82	2.49	2.48	1.67	0.70
CaO	3.53	2.42	2.99	2.56	2.02	0.47
Na2O	3.71	3.62	3.57	3.39	3.52	2.80
K2O	3.81	4.62	4.02	4.40	4.54	5.08
P2O5	0.30	0.21	0.28	0.27	0.23	0.09
H2O	1.01	0.82	1.10	1.27	1.01	1.19
TOTAL	100.3	100.1	100.2	100.1	99.9	100.1
Li	59	78	76	83	84	34
V	95	69	81	84	61	29
Cr	78	53	74	70	48	20
Co	35	40	39	37	47	57
Ni	41	31	40	40	26	11
Cu	24	20	21	21	16	6
Zn	74	75	78	81	55	32
Rb	175	224	177	214	239	256
Sr	467	336	401	384	307	134
Y	18	19	18	17	18	17
Zr	322	279	240	221	205	137
Nb	16	16	15	14	15	15
Mo	2	4	2	1	3	2
Pb	24	22	28	20	23	19
Th	28	33	27	29	28	30
U	6	7	6	7	8	7

Where * n = number of samples

Table 5.2

Comparison tables

1. Woolhope Granite with veins.
2. Marginal Granodiorite with Hornfels and Xenolith.

	- 1 -		- 2 -		
Average	Woolhope Gr. 4 samples	Veins 3 samples	Marginal GD. 8 samples	Hornfelses 3 samples	Xenolith 1 sample
SiO2	73.72	72.94	64.42	63.67	60.40
TiO2	0.29	0.40	0.83	1.00	1.05
Al2O3	13.80	13.86	15.33	15.61	16.20
Fe2O3	1.45	0.89	1.67	1.27	2.78
FeO	0.46	0.93	2.68	3.17	2.99
MnO	0.04	0.03	0.09	0.09	0.11
MGO	0.70	0.83	2.94	2.85	3.16
CaO	0.47	1.13	3.53	4.52	5.02
Na2O	2.80	3.67	3.71	3.57	3.90
K2O	5.08	5.03	3.81	3.29	3.30
P2O5	0.09	0.12	0.30	0.39	0.46
H2O	1.19	0.48	1.01	0.64	0.66
TOTAL	100.7	100.3	100.3	100.1	99.5
Li	34	61	59	37	64
V	29	37	95	130	15
Cr	20	26	78	76	4
Co	57	41	35	36	36
Ni	11	10	41	48	3
Cu	6	16	24	36	5
Zn	32	33	74	62	39
Rb	256	263	175	127	147
Sr	134	266	467	667	478
Y	17	13	18	20	24
Zr	137	132	322	336	289
Nb	15	14	16	15	18
Mo	2	4	2	2	3
Pb	19	39	24	31	20
Th	30	36	28	12	20
U	7	11	6	2	4

Table 5.3

Comparison between Cheviot Granite / Northern England and Southern Uplands granites.

	n	K2O/Na2O	Rb/Sr	K/Rb
Brown G.C.,1979.				
N England:				
a. Ordovician and Silurian:				
Ennerdale granophyre	4	0.43	1.23	279
Dufton microgranite	3	0.77	0.81	242
Threlkeld-st. John's microgranite	4	0.81	0.84	216
b. Lower Devonian:				
Skiddaw granite	2	1.28	1.96	117
Shap granite	10	1.34	0.97	139
Eskdale granite	8	1.46	2.38	111
Weardale granite	19	1.48	3.97	96
Southern Uplands:				
Loch Doon tonalite	21	1.26	0.29	234
Cairnsmore of Fleet granite	29	1.48	1.73	200
Criffel granodiorite	24	1.01	0.31	198
Cairnsmore of Carsphairn tonalite	5	0.84	0.24	228
Cheviot Granite (this Thesis)				
a. Cycle 1		1.03-1.28	0.37	180
b. Cycle 2 - Granodiorites		1.13-1.18	0.44	188
- Woolhope Granite		1.81	1.91	165

Table 5.4

Comparison between the Cheviot and the Loch Doon Plutons.

SAMPLE NUMBERS	Cycle 1				Cycle 2							
	MG GD	128	DN GD	157	SP GD	264	LN GD	288	HG GD	242	WG	250
SiO2	64.42	61.44	67.50	65.01	65.90	64.34	66.17	68.39	68.32	70.34	73.72	73.07
TiO2	0.83	1.16	0.67	0.89	0.71	0.75	0.63	0.54	0.61	0.41	0.29	0.21
Al2O3	15.33	15.55	15.03	15.40	15.21	14.89	14.99	14.52	14.91	14.47	13.80	14.63
FeO *	4.62	6.32	3.50	5.37	4.06	4.72	4.02	3.20	3.15	2.36	1.96	1.21
MnO	0.09	0.09	0.07	0.08	0.08	0.08	0.10	0.08	0.06	0.05	0.04	0.04
MGO	2.94	3.70	1.82	2.62	2.49	3.79	2.48	2.20	1.67	1.46	0.70	0.45
CaO	3.53	3.80	2.42	2.61	2.99	3.51	2.56	2.44	2.02	1.68	0.47	1.04
Na2O	3.71	3.71	3.62	3.60	3.57	3.65	3.39	3.62	3.52	3.59	2.80	3.75
K2O	3.81	3.87	4.62	4.00	4.02	3.82	4.40	4.51	4.54	5.15	5.08	5.32
P2O5	0.30	0.28	0.21	0.20	0.28	0.20	0.27	0.14	0.23	0.12	0.09	0.06
TOTAL +	100.3	99.9	100.1	99.8	100.2	99.8	100.1	99.6	99.9	99.6	100.1	99.8
Rb	175	157	224	144	177	135	214	185	239	210	256	208
Sr	467	359	336	306	401	452	384	354	307	251	134	182
Y	18	37	19	34	18	24	17	26	18	23	17	17
Zr	322	435	279	355	240	223	221	207	205	144	137	88
Nb	16	18	16	13	15	14	14	15	15	16	15	13
La	47	50	50	48	42	32	46	31	47	53	17	29
Ce	88	106	95	89	80	67	91	64	83	82	55	58
Nd	32	50	35	40	32	27	35	26	34	38	14	21
Sm	6	10	5.8	7.6	5.4	5.2	6.1	4.9	6.1	7	3.3	4.2
Eu	1.5	1.6	1.1	1.2	1.2	1.1	1.2	1	1.3	0.9	0.7	0.7
Gd	3.7	----	3.7	----	4.5	----	4.3	----	4.6	----	2.8	----
Tb	----	1.2	----	1.1	----	0.6	----	0.6	----	0.8	----	0.4
Tm	----	0.8	----	0.5	----	0.3	----	0.3	----	0.3	----	----
Yb	1.0	3.8	1.5	3.3	1.3	1.9	1.4	1.8	1.4	1.8	1.5	0.8
U	6	7.1	7	8	6	3.3	7	5.6	8	6.4	7	4.8
Th	28	25	33	19.6	27	18	29	26	28	27.8	30	20.5
Sc	6.1	12.8	4	13.2	4	12.1	5.1	13.2	3.5	9.6	1.4	3.2

The above numbers are Loch Doon sample number (After Tindle et al., 1981) whereas symbols represent the different intrusive phases in the Cheviot, see figure 5.1.

+ The total in the Cheviot Data is with water(H_2O+).

Table 5.5

Comparison between The Cheviot Dunmoor Granodiorite and Newry igneous complex.

LOCALITY	Newry	Cheviot
ROCK TYPE	Granodiorite	DN. Granodiorite
SiO2	67.80	67.50
K2O	2.54	4.62
La	28.80	50.00
Ce	59.10	95.00
Pr	5.80	10.30
Nd	19.60	35.00
Sm	3.20	5.80
Eu	0.90	1.10
Gd	2.30	3.70
Tb	2.30	-----
Dy	1.90	-----
Ho	0.30	-----
Er	1.50	1.90
Yb	1.03	1.50
Lu	0.19	-----
Rb	97.00	224.00
Sr	436.00	336.00
Zr	127.00	279.00
Ni	28.00	31.00
Zn	64.00	75.00

Table 5.6

Concentration (in ppm) of Rare Earth Elements (REE) in Chondrite.

Reference	Nakamura	Schmitt et al.
La	0.328	0.30
Ce	0.865	0.84
Pr	0.137	0.12
Nd	0.630	0.580
Sm	0.203	0.210
Eu	0.077	0.074
Gd	0.276	-----
Tb	0.052	0.049
Dy	0.343	-----
Ho	0.078	0.064
Er	0.196	-----
Tm	0.034	0.025
Yb	0.220	0.170
Lu	0.034	0.031
	0.19	-----
Y	1.90	-----

Table 5.7

Concentration in part per million over chondrite concentration (ppm/chond.) of the different types of intrusive phases of the Cheviot Granite.

Sample Number	Rare Earth Elements (REE)													
	La	Ce	Pr	Nd	Pm	Sm	Eu	Gd	Tb	Dy	Y	Er	Tm	Yb
B12	2.14	2.01	1.88	1.77	----	1.48	1.25	1.13	----	----	0.95	0.88	----	0.65
E177	2.18	2.04	1.88	1.74	----	1.45	1.16	1.13	----	----	0.95	0.96	----	0.83
A11	2.11	1.96	1.83	1.70	----	1.42	1.20	1.21	1.03	----	0.93	0.75	----	0.76
A12	2.15	2.02	1.87	1.75	----	1.47	1.19	1.19	----	----	0.95	0.83	----	0.78
E156	2.15	1.98	1.85	1.72	----	1.48	1.23	1.21	----	----	0.93	0.83	----	0.79
E150	1.71	1.80	1.49	1.36	----	1.20	0.97	0.99	----	----	0.87	0.90	----	0.83

Table 5.8 Summary of features of Harker Diagrams

---

a. Positive correlation: Slight scatter, steep slope
   K_2O , Rb.
b. Negative correlation:
   1. Slight scatter, steep slope: MgO, CaO, FeO*, Sr, P_2O_5.
   2. Slight scatter, moderate slope: Na_2O.
   3. Moderate scatter, steep slope: Cr, Ni, Al_2O_3 and TiO_2.

See Figures 5.2, 5.3 and 5.8-5.11.

Table 5.9

Norm composition (C.I.P.W) for averages (in Table 5.1)

Rock Type	Marginal GD.	Dunmoor GD.	Standrop GD.	Linhope GD.	Hedgehope GD.	Woolhope GD.
Q	16.47	21.00	19.76	20.20	24.03	36.21
Or	22.51	27.30	23.75	26.00	26.82	30.01
Ab	31.38	30.62	30.19	28.67	29.77	23.68
An	13.93	10.63	13.00	10.94	8.52	1.74
C	0.00	0.18	0.22	0.65	1.09	3.06
Di: Wo	0.68	0.00	0.00	0.00	0.00	0.00
En	0.47	0.00	0.00	0.00	0.00	0.00
Fs	0.15	0.00	0.00	0.00	0.00	0.00
Hy: En	6.85	4.53	6.20	6.17	4.16	1.74
Fs	2.19	1.05	1.49	2.22	0.65	0.00
Mt	2.42	2.22	2.48	2.12	2.16	0.77
He	0.00	0.00	0.00	0.00	0.00	0.92
Il	1.58	1.27	1.35	1.20	1.16	0.55
Ru	0.00	0.00	0.00	0.00	0.00	0.00
Ap	0.71	0.50	0.66	0.64	0.55	0.21
Q	23.4	26.6	26.8	27.0	29.8	40.3
Or	32.0	34.6	32.2	34.7	33.3	33.4
Ab	44.6	38.8	41.0	38.3	36.9	26.3

Table 5.10

Mineral phases and their oxides concentrations (Chapter 4, EDS analyses)

Mineral Phases	Biotite	Clinopyroxene	Orthopyroxene	Ilmenite	Plagioclase An38
SiO2	40.0	52.0	52.0	0.0	58.0
TiO2	6.0	0.3	0.3	48.0	0.0
Al2O3	13.5	1.0	0.5	0.0	26.5
FeO *	12.0	9.0	22.0	46.0	0.0
MgO	16.0	14.0	21.0	0.0	0.0
CaO	0.0	22.0	2.0	0.0	7.8
Na2O	0.0	0.0	0.0	0.0	6.5
K2O	9.5	0.0	0.0	0.0	1.1

Table 5.11

Mineral-liquid partition coefficients derived from references below.

Element	Mineral							
	Opx	Cpx	Plag	Il	Bi	Mt	Ap	Zc
Rb	0.04	0.04	0.1	0	2	0	0	0
Sr	0.1	0.5	4	0	0.2	0	---	0
La	0.1	0.3	0.3	0	0.3	0	25	3
Ce	0.2	0.5	0.3	0	0.3	0	25	3
Sm	0.2	0.5	0.15	0	0.3	0	25	4
Eu	0.15	1	2	0	0.25	0	25	3
Yb	0.80	2	0.05	0	0.40	0	25	50
Lu	0.80	2	0.05	0	0.40	0	25	250
Co	10	7	0	----	15	10	---	-----
Cr	5(2)	25 (7)	0	(5)	15	50	---	-----
Ni	10	20	0	(4)	10	7	---	----
Ti	0.4	0.7	0.05	----	----	12.5	0.1	----
Zr	0.2	0.6	0.1	0.3	----	0.8	0.1	----
Y	1	4	0.1	0	0.03	2	40	60
Nb	0.8	0.8	0.06	0.8	----	2.5	0.1	----
Cumulate Fraction	0.146	0.138	0.553	0.008	0.163	0.013	0.014	0.001

References:

1. Condie KC (1978)

2. Condie KC and Harrison NM (1976)

3. Condie KC and Hunter DR (1976)

4. Pearce JA and Norry MJ (1979)

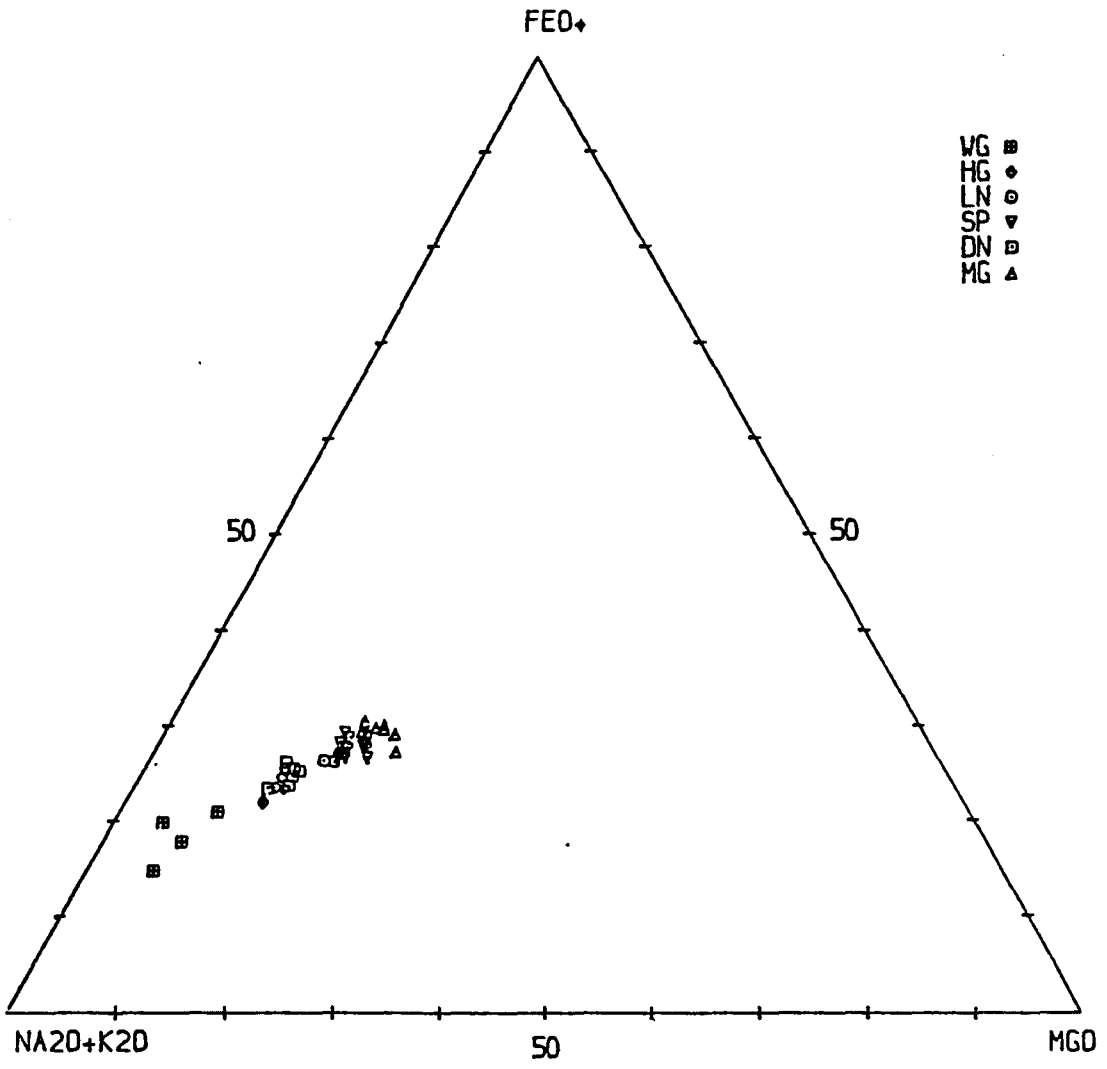

Fig. 5.1 AFM diagram for (40) fresh granodiorites and granites showing calc-alkaline trend,

where WG = Woolhope Granite
HG = Hedgehope Granodiorite
LN = Linhope Granodiorite
SP = Standrop Granodiorite
DN = Dunmoor Granodiorite
MG = Marginal Granodiorite

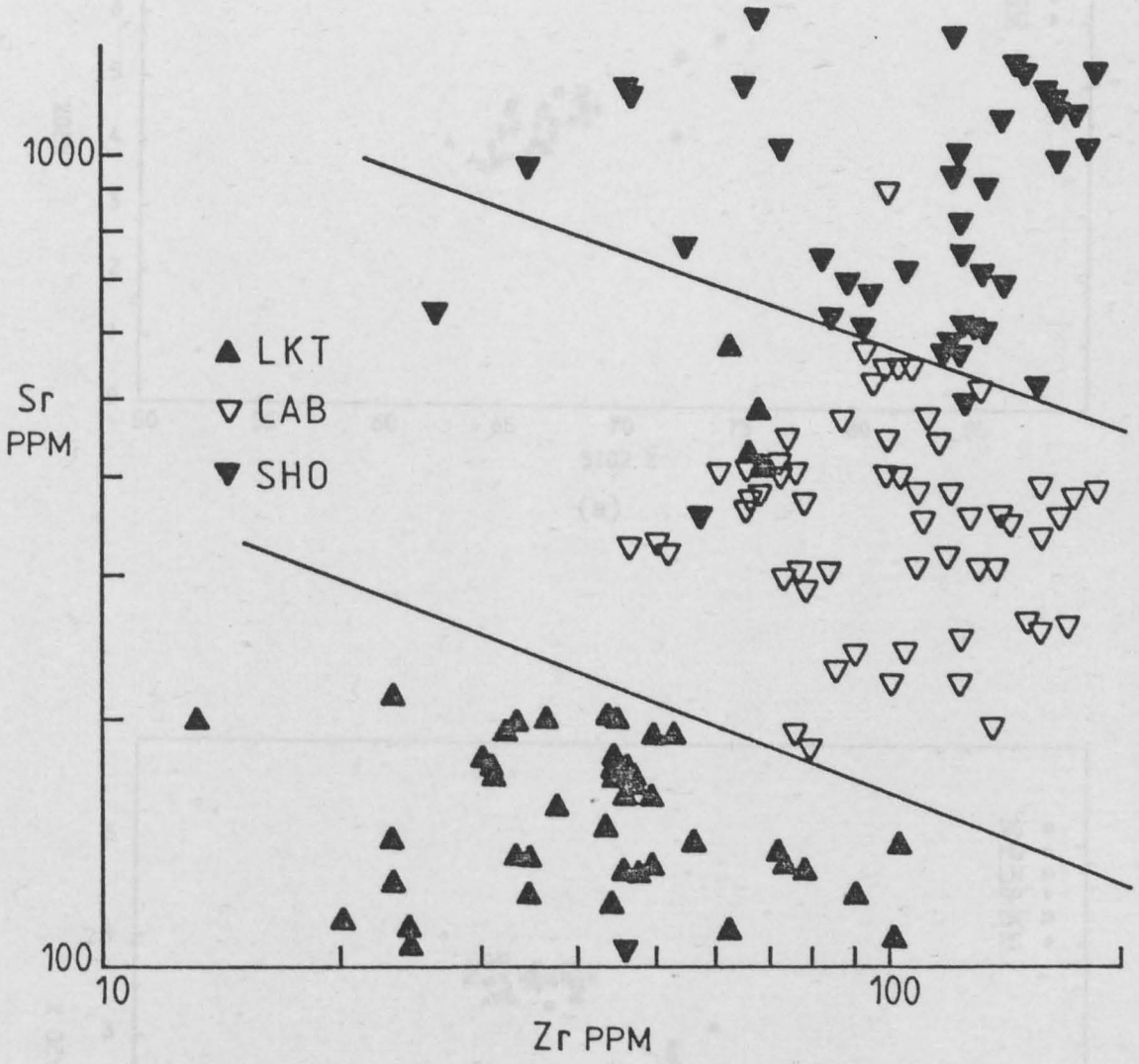

Fig. 5.1a Distinction of low-potassium tholeiites (LKT), calc-alkali basalts (CAB) and shoshonites (SHO) using Zr and Sr.
(After Pearce 1973).

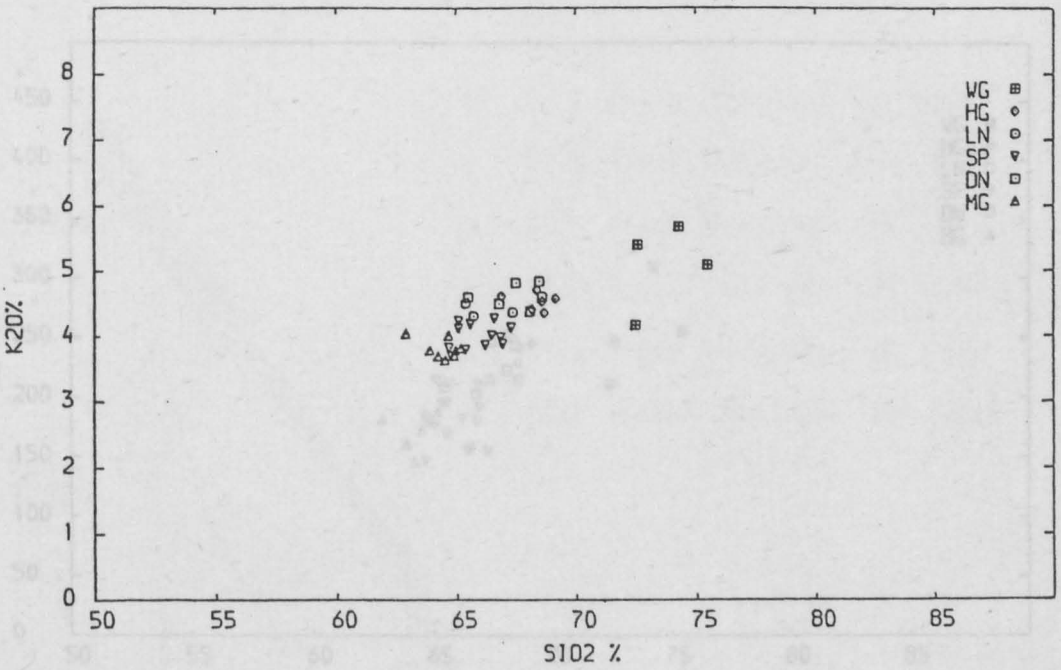

(a)

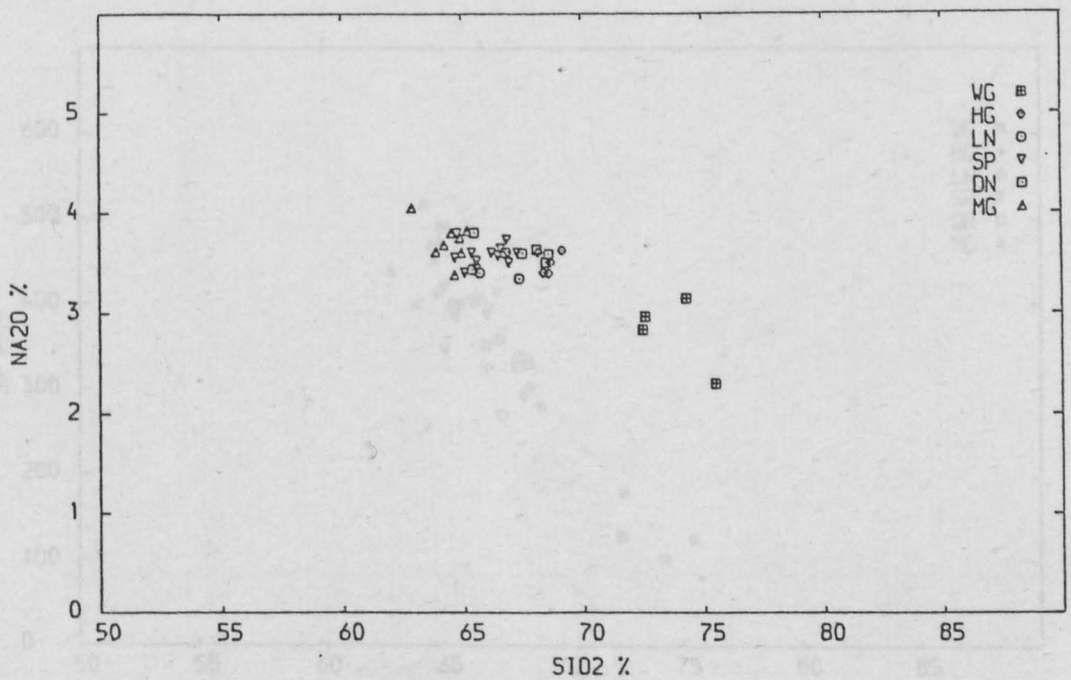

(b)

Fig. 5.2 Harker diagrams of 40 fresh granodiorites and granites

(a) $K_2O\%$ v. $SiO_2\%$

(b) $Na_2O\%$ v. $SiO_2\%$

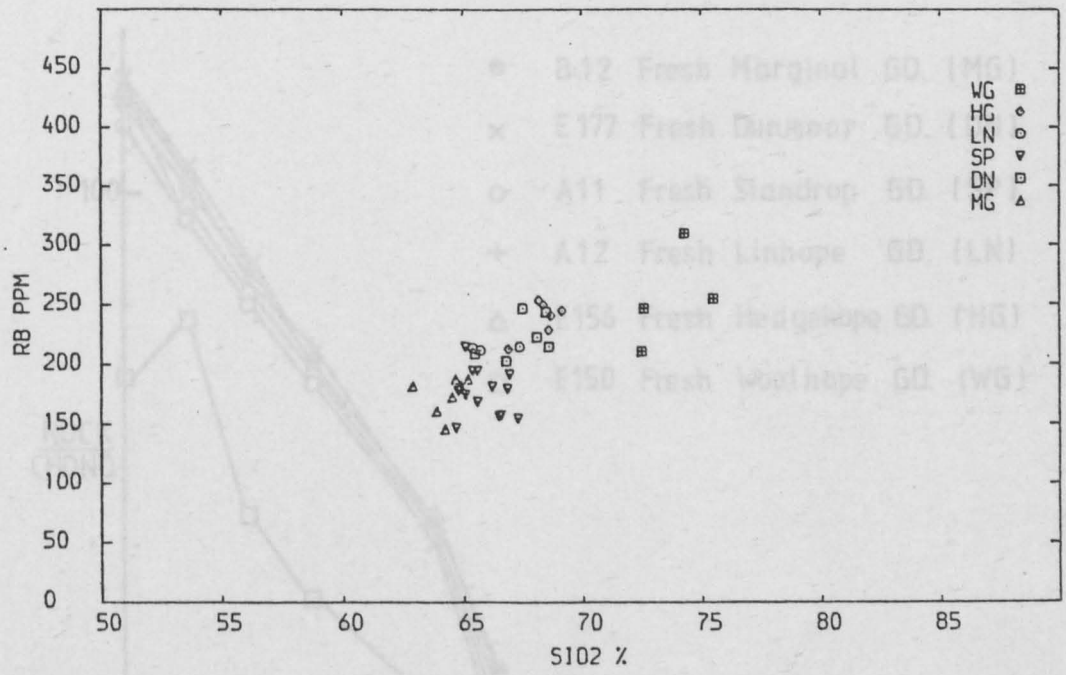

(a)

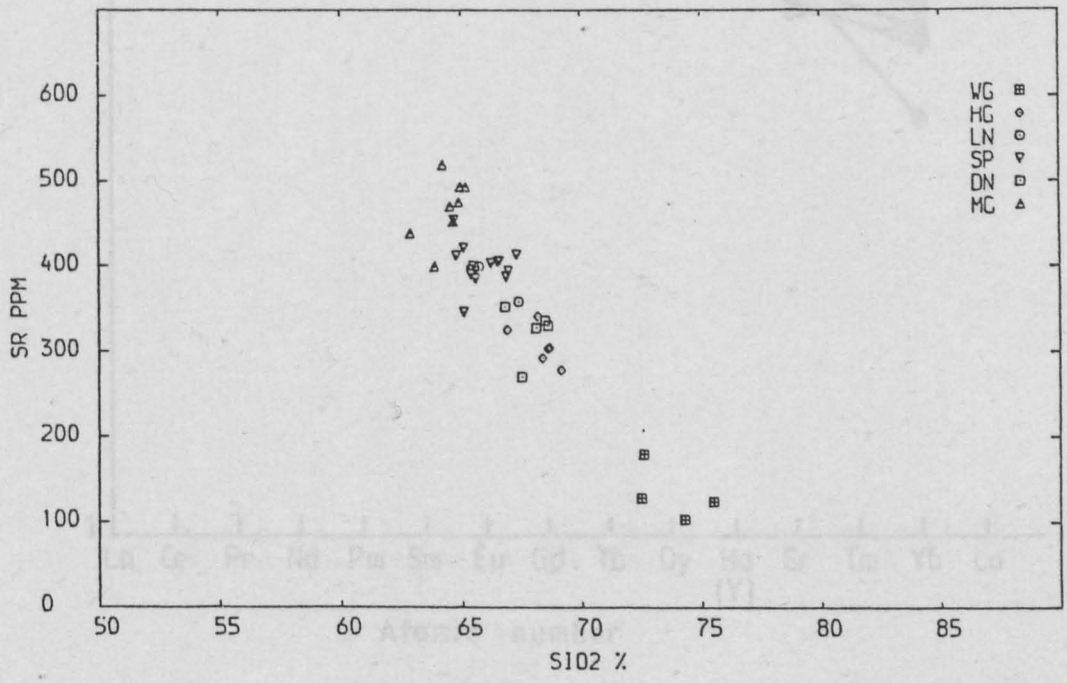

(b)

Fig. 5.3 Harker diagrams of 40 fresh granodiorites and granites

(a) Rb ppm v. SiO_2%

(b) Sr ppm v. SiO_2%

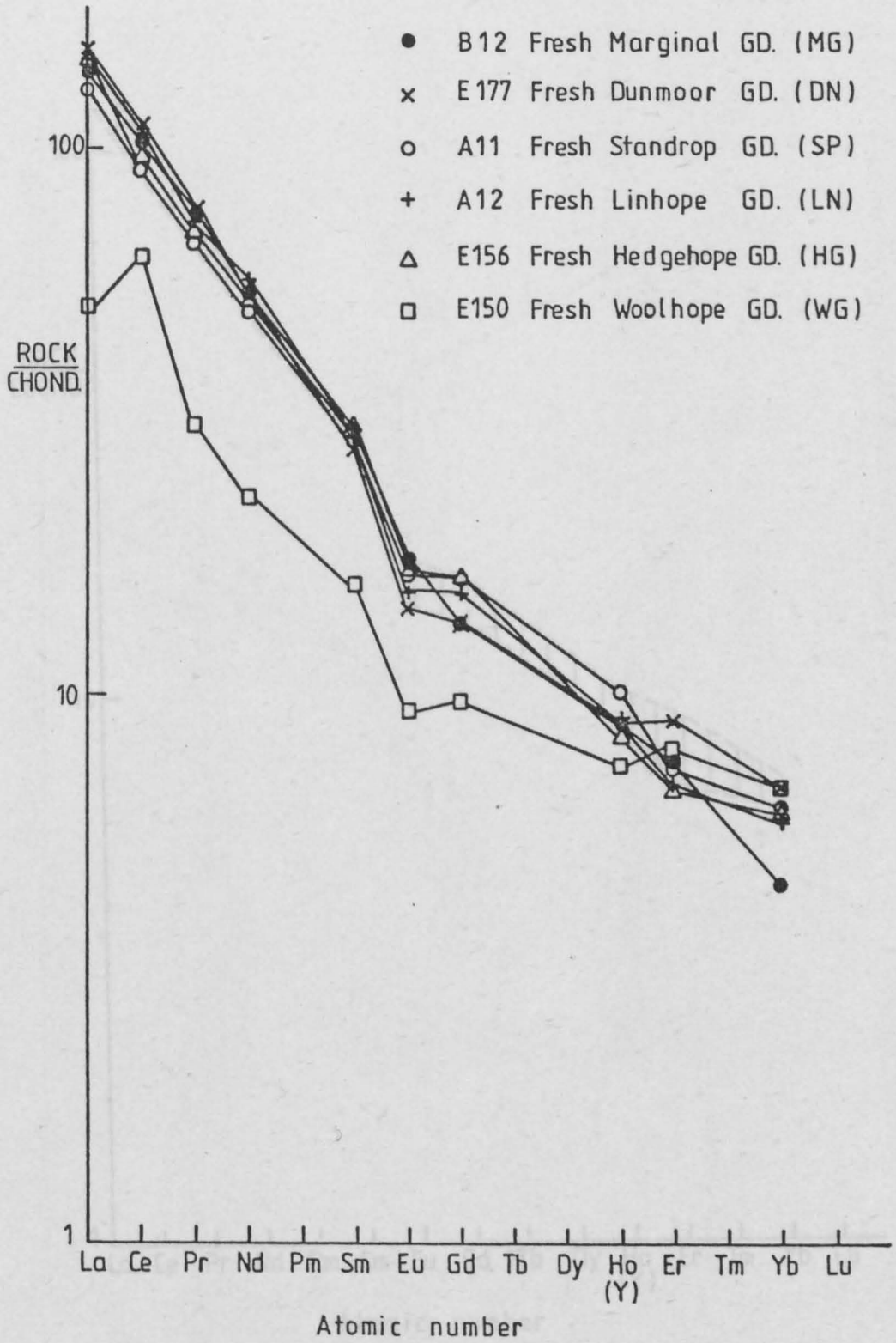

Fig. 5.4 Chondrite-normalised REE patterns for the fresh granodiorites and granite.

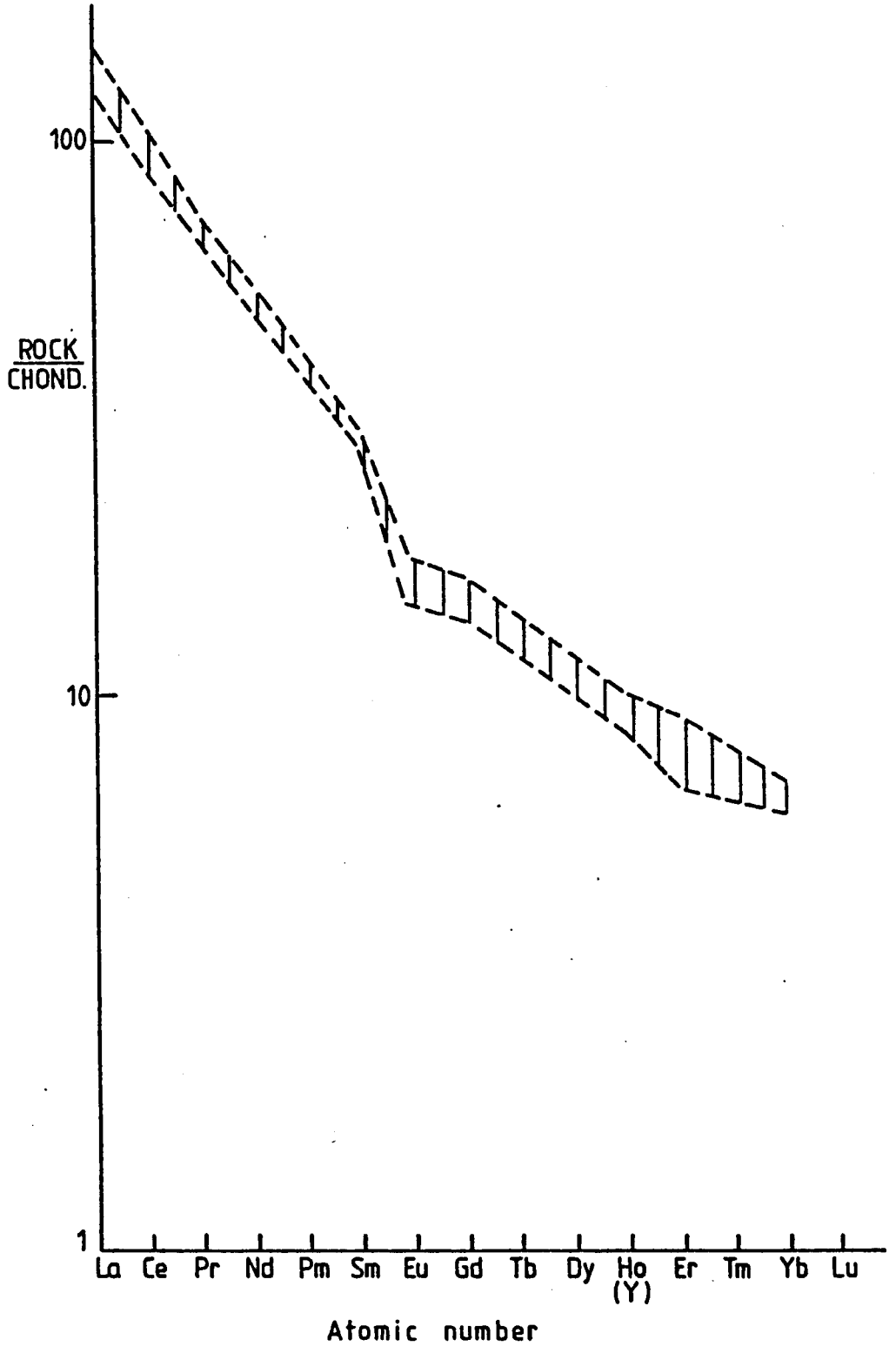

Fig. 5·4a The band occupied by REE patterns for fresh granodiorites.

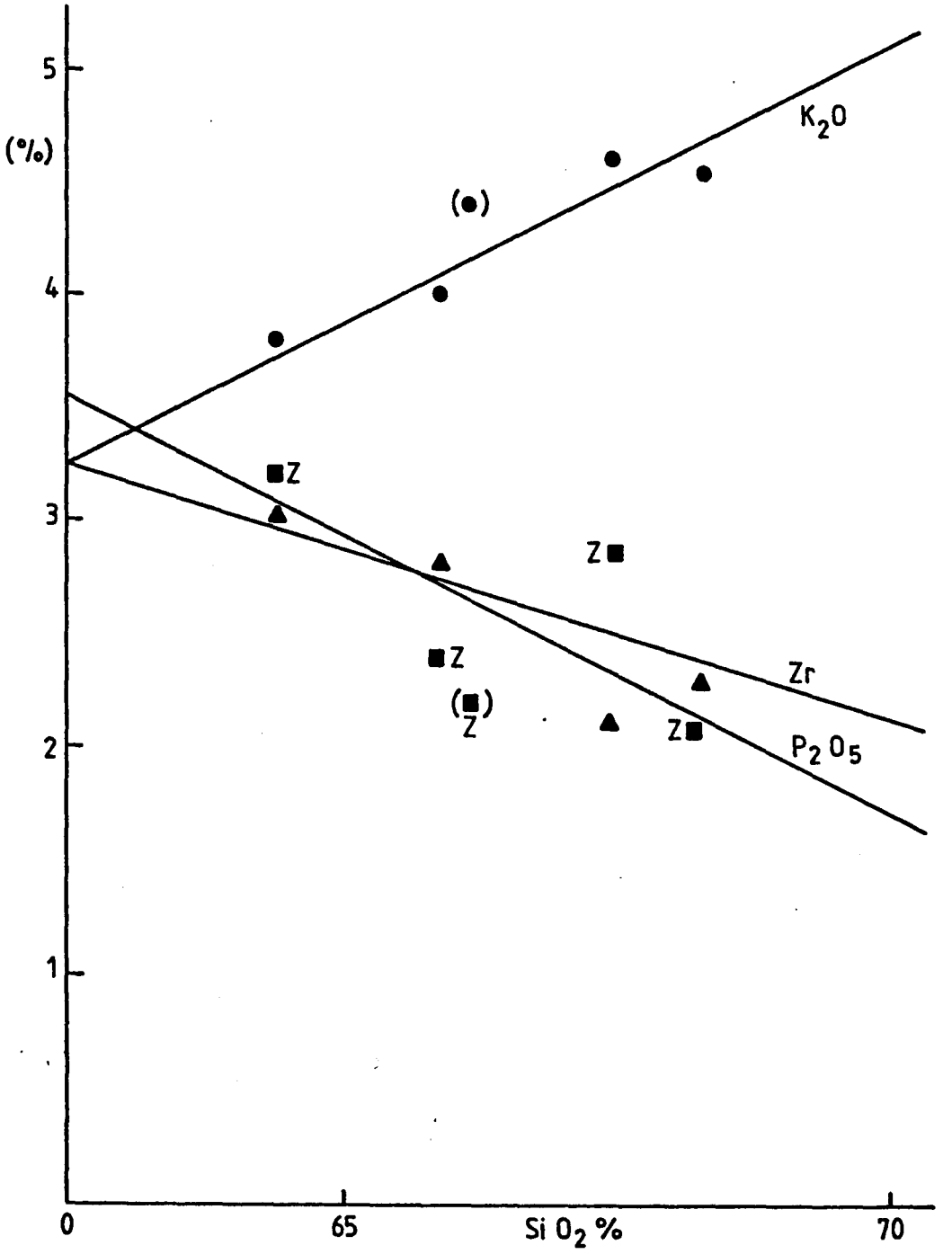

Fig. 5.5 Simplified variation diagram based on averages.

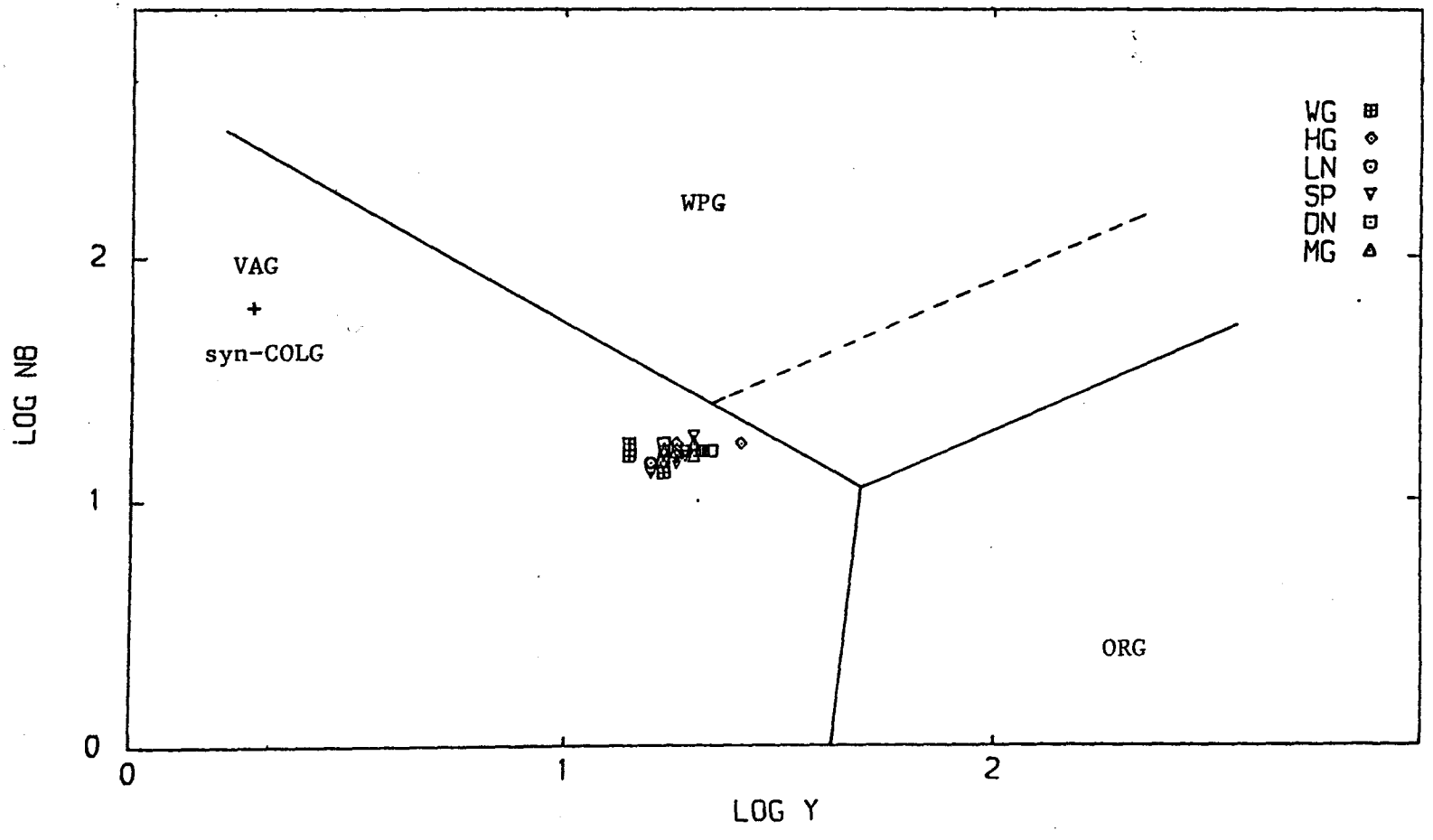

Fig. 5.6 Plot of Log (Y v. Nb) as tectonic discriminator diagram. Pearce et al, in press

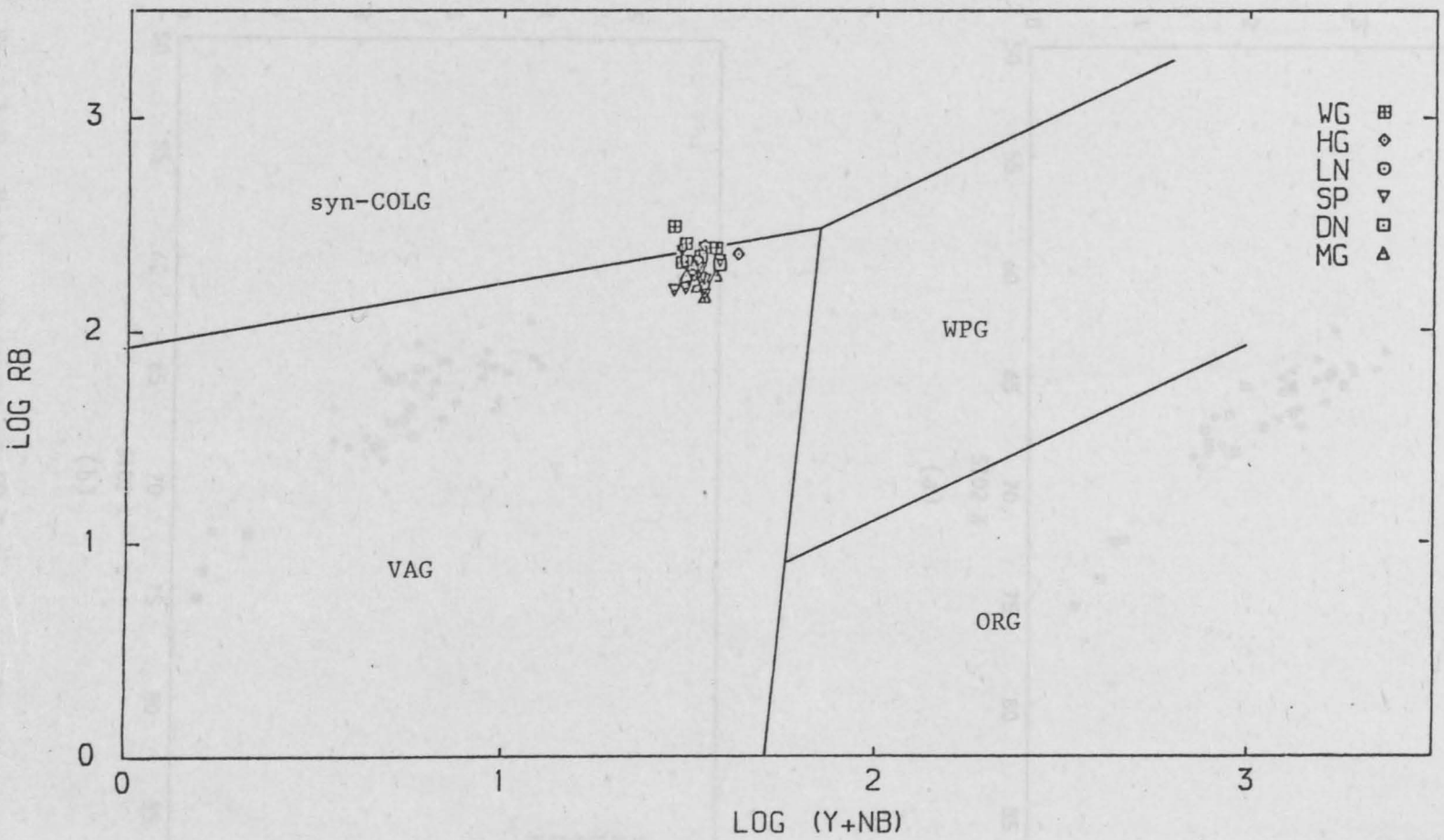

Fig. 5.7 Plot of log (Y + Nb) v. Rb as tectonic discriminator diagram Pearce et al, in press

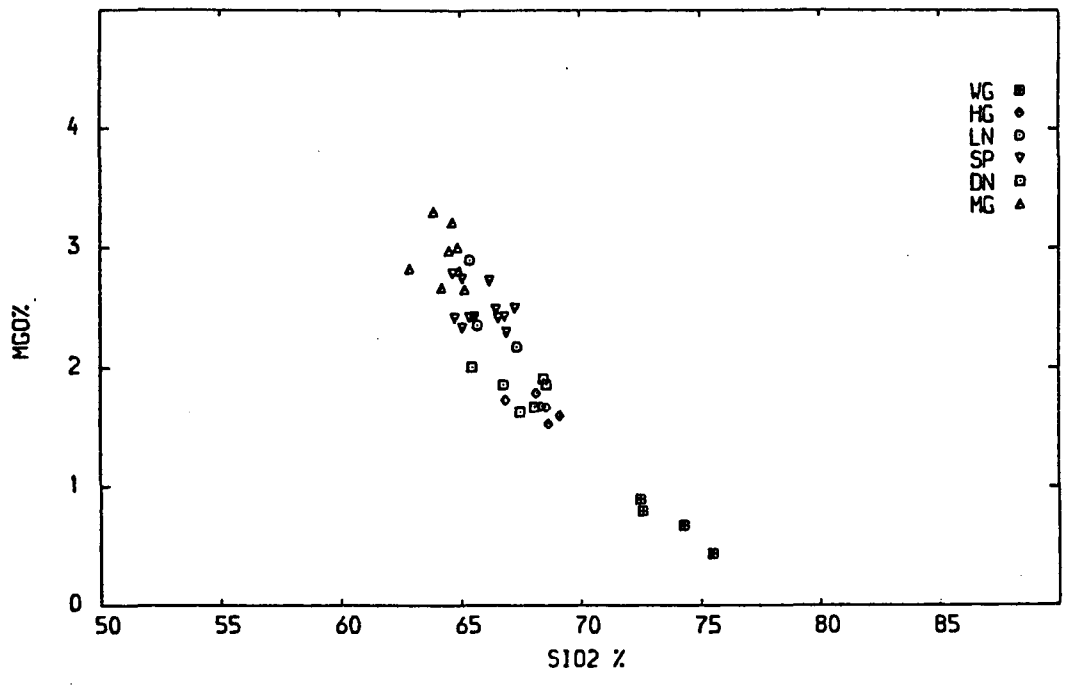

(a)

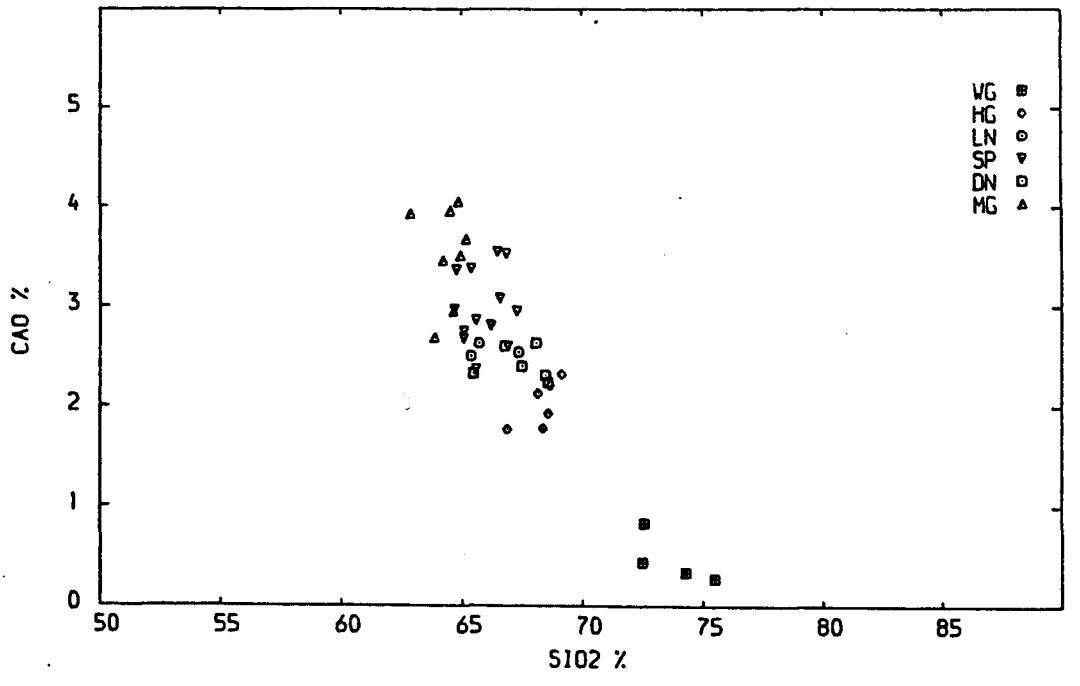

(b)

Fig. 5.8 Harker diagrams of 40 fresh granodiorites and granites

(a) MgO% v. SiO_2%

(b) CaO% v. SiO_2%

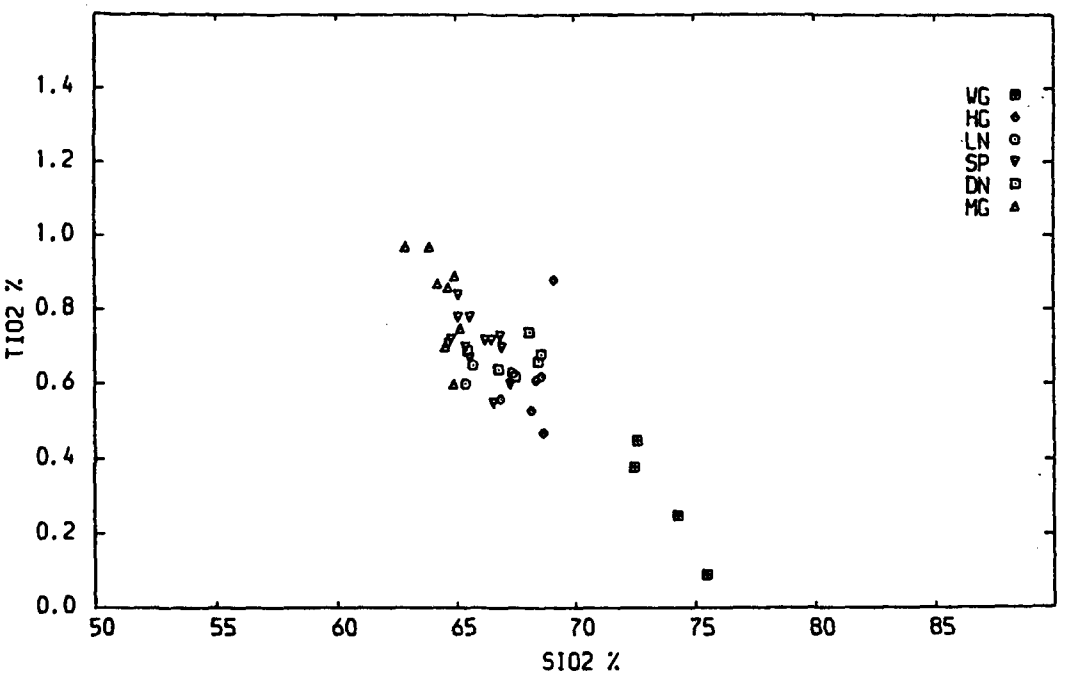

(a)

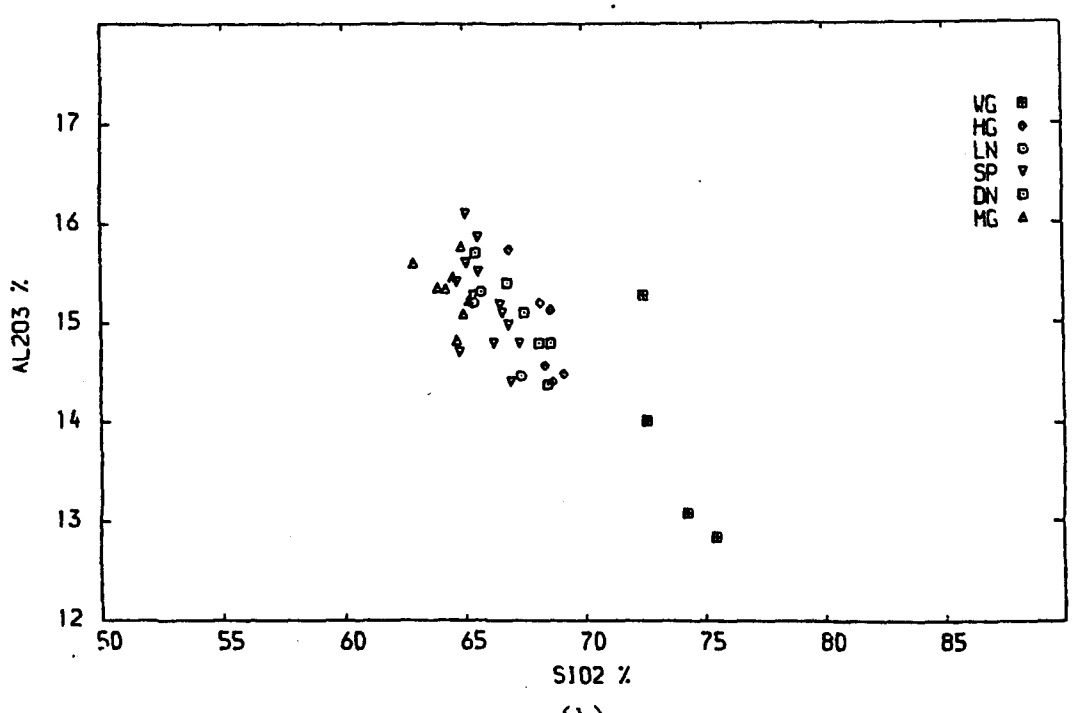

(b)

Fig. 5.9 Harker diagrams of 40 fresh granodiorites and granites

(a) TiO_2% v. SiO_2%

(b) Al_2O_3% v. SiO_2%

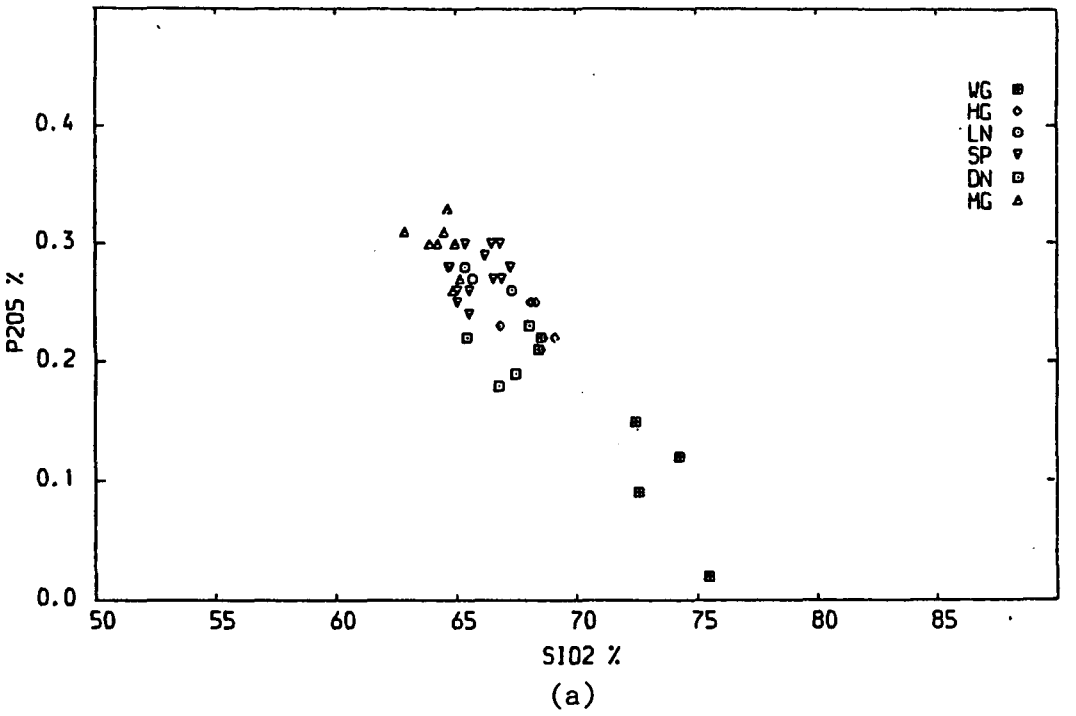

(a)

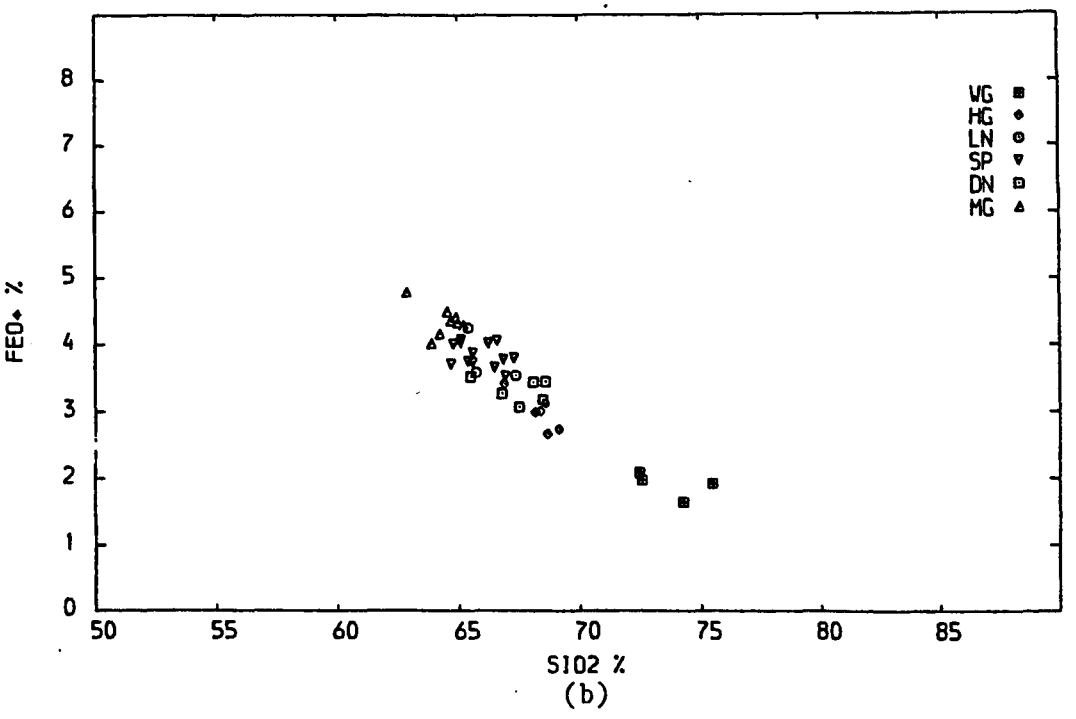

(b)

Fig. 5.10 Harker diagrams of 40 fresh granodiorites and granites

(a) P_2O_5% v. SiO_2%

(b) FeO*% v. SiO_2%

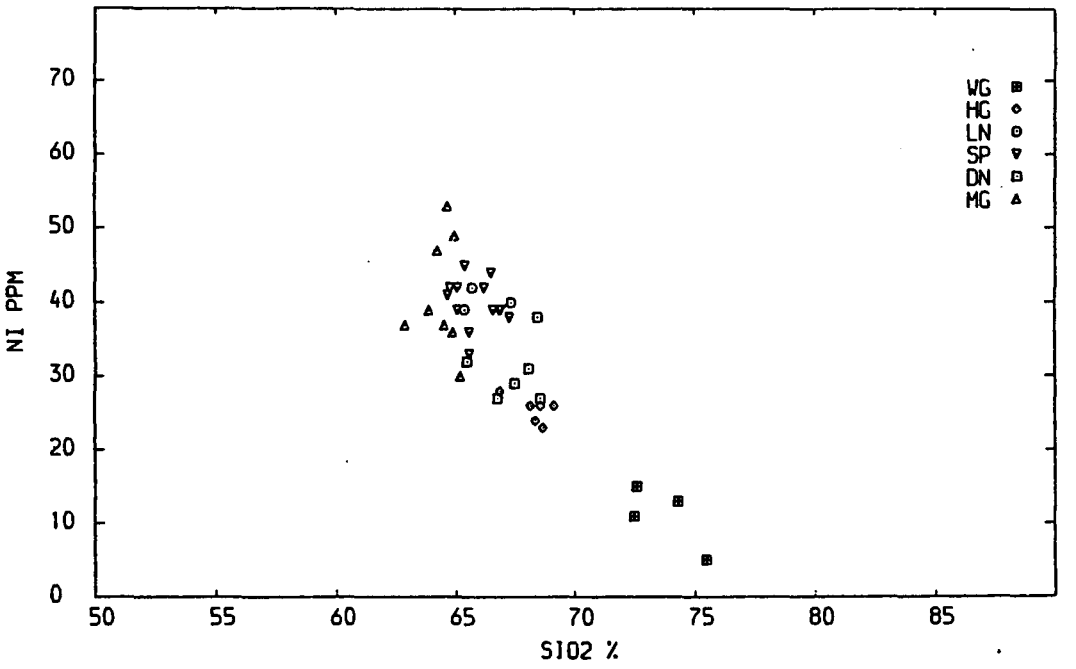

(a)

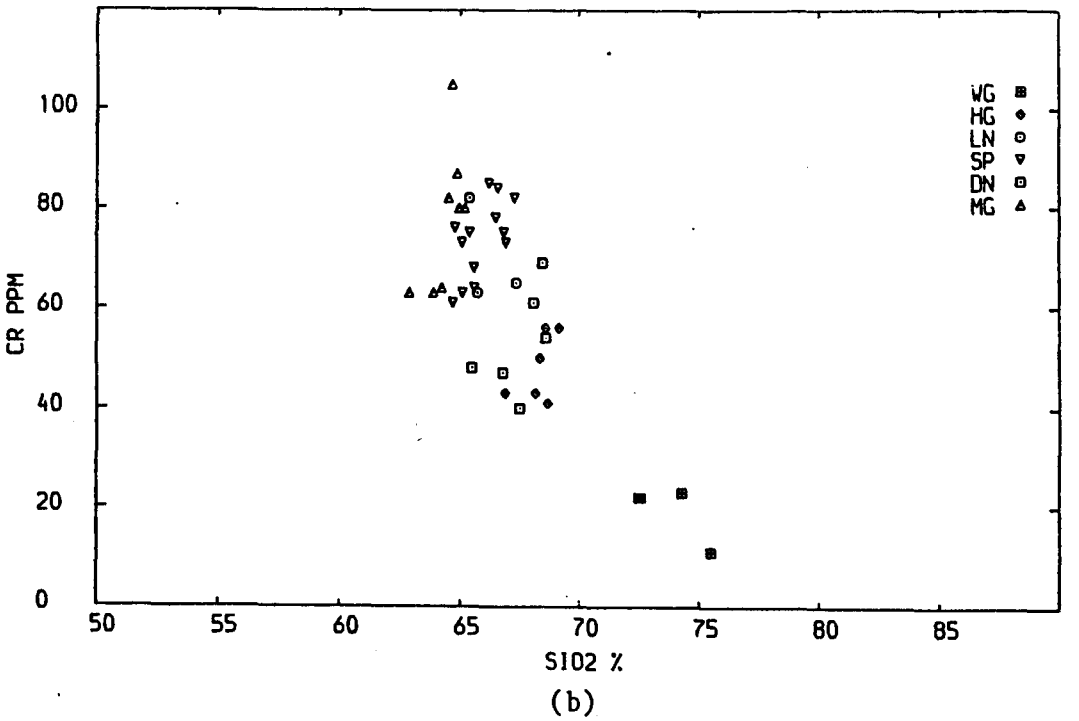

(b)

Fig. 5.11 Harker diagrams of 40 fresh granodiorites and granites

(a) Ni ppm v. SiO_2%

(b) Cr ppm v. SiO_2%

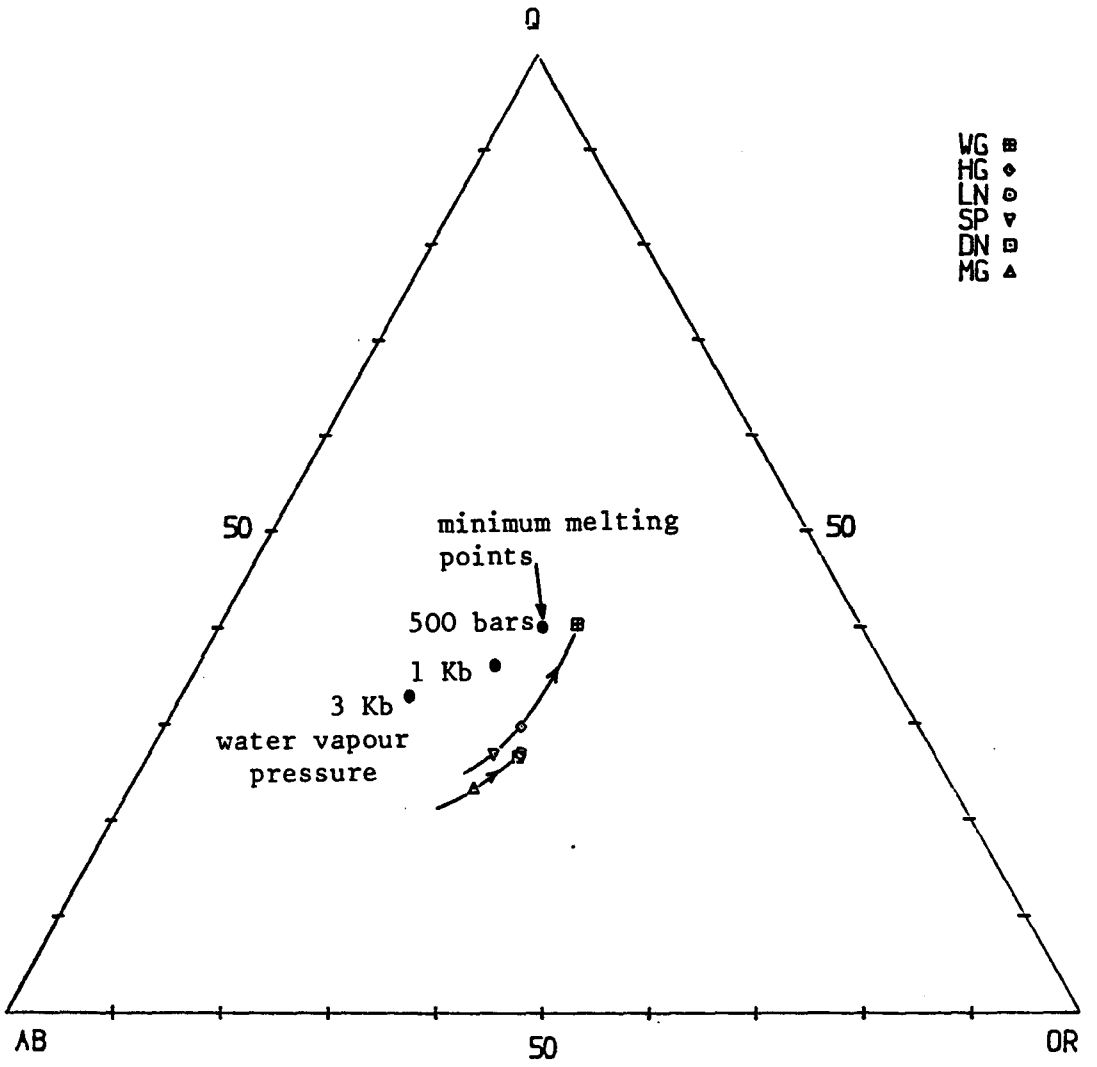

Fig. 5.12 Plot of the C.I.P.W. Norms (Q - Ab - Or), of the averages of the six types of intrusive phases, which indicates the fractionation and nature of the two magmas . Tuttle and Bowen, 1958.

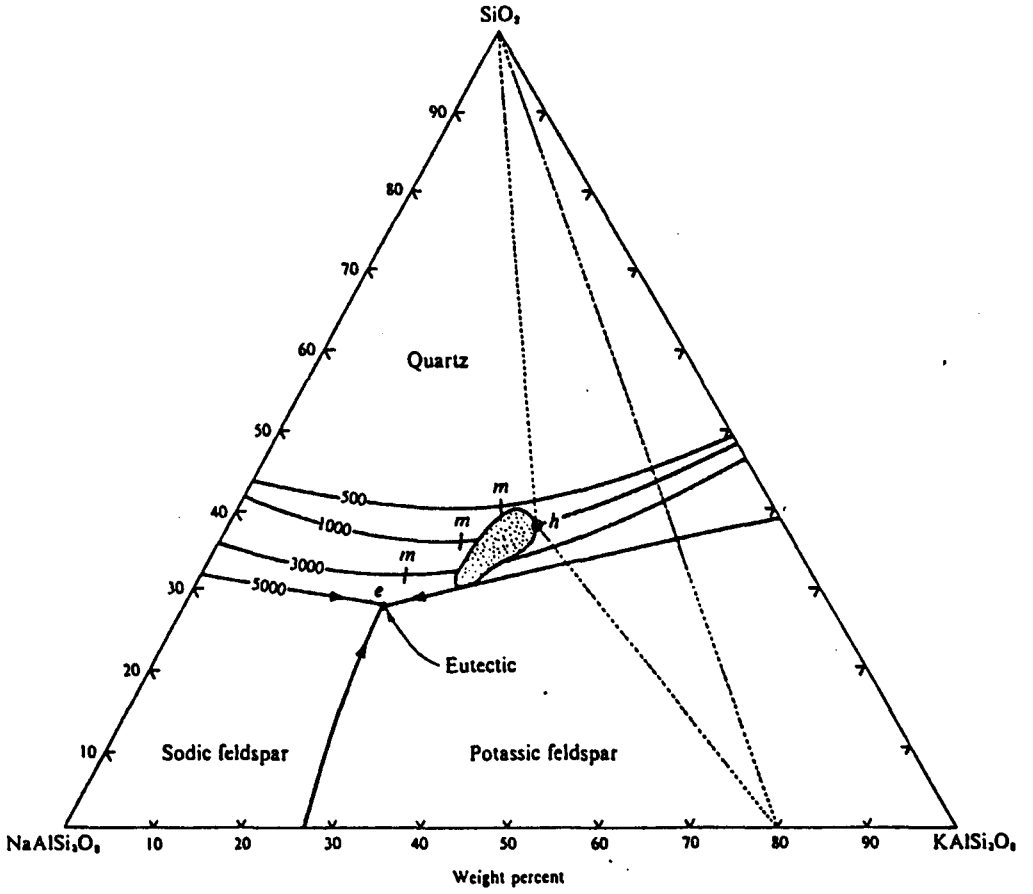

Fig. 5 · 13 Curves for water-saturated liquids in equilibrium with quartz and alkali feldspar at indicated confining pressures (500, 1000, 3000 and 5000 bars). Isobaric minima are labelled *m* except at 5000 bars, where a ternary eutectic *e* is generated by intersection of the alkali-feldspar solvus with the liquidus surface (Fig. 5·1)*. Plots of normative Q, or, and *ab* of analyzed granites concentrate in the stippled area. The dotted three-phase triangle illustrates the initial phases to precipitate from liquid *h* at 1000 bars.

*(Data from Tuttle and Bowen, 1958.)

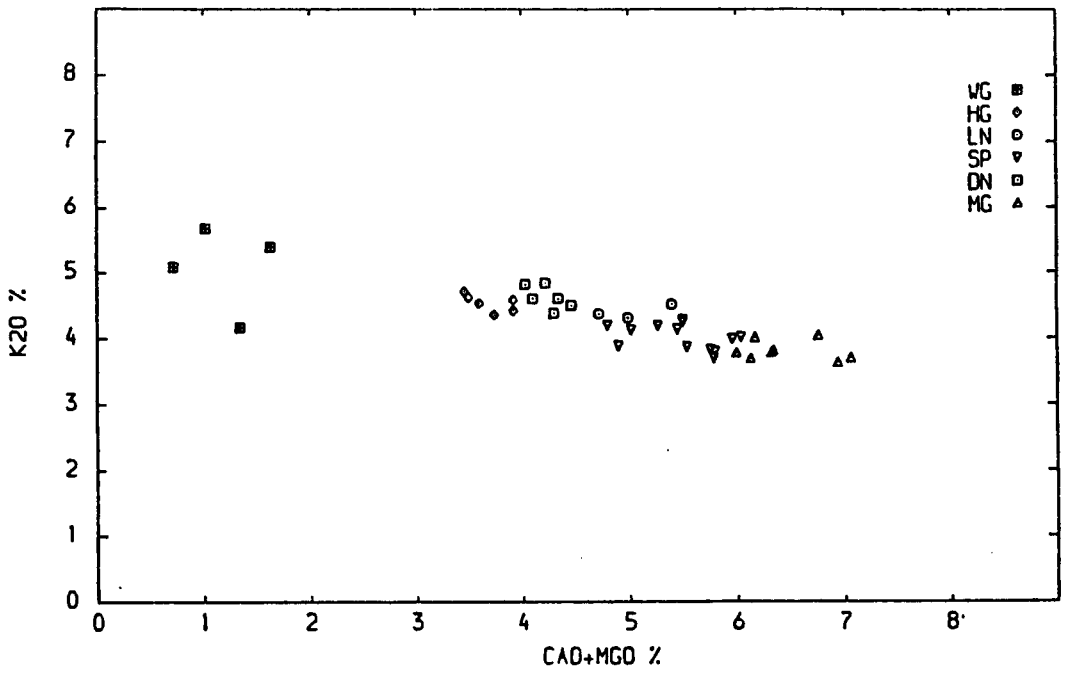

(a)

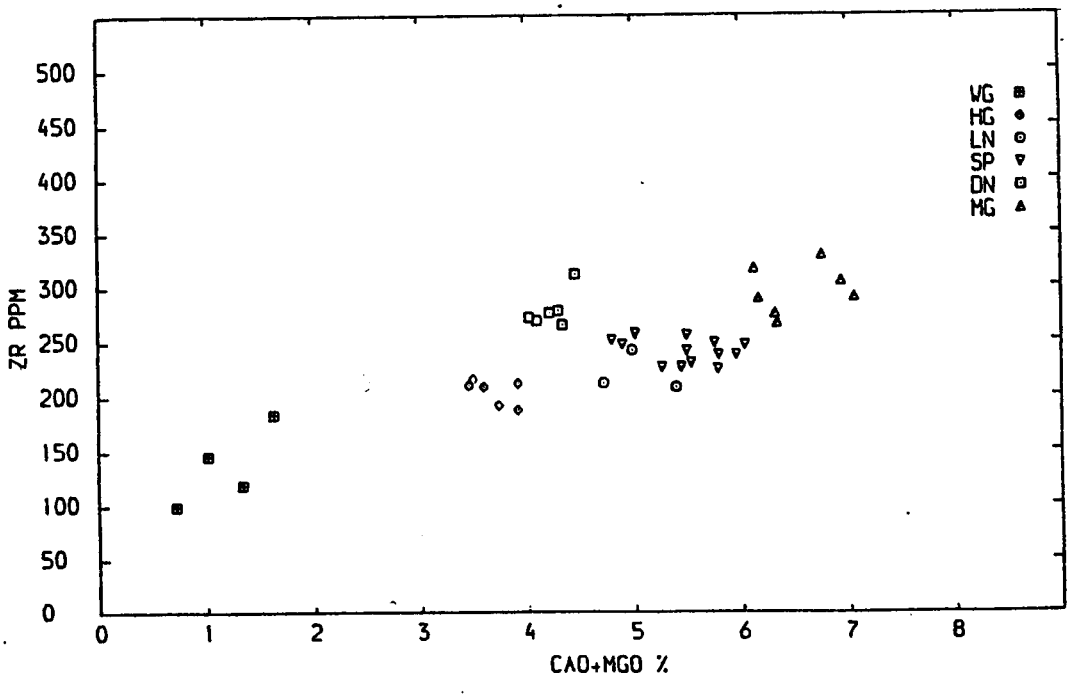

(b)

Fig. 5.14 Plots of (CaO+MgO)% v.

(a) K2O% (b) Zr ppm

which can be considered as discrimination diagrams of the two igneous cycles and their individual bodies.

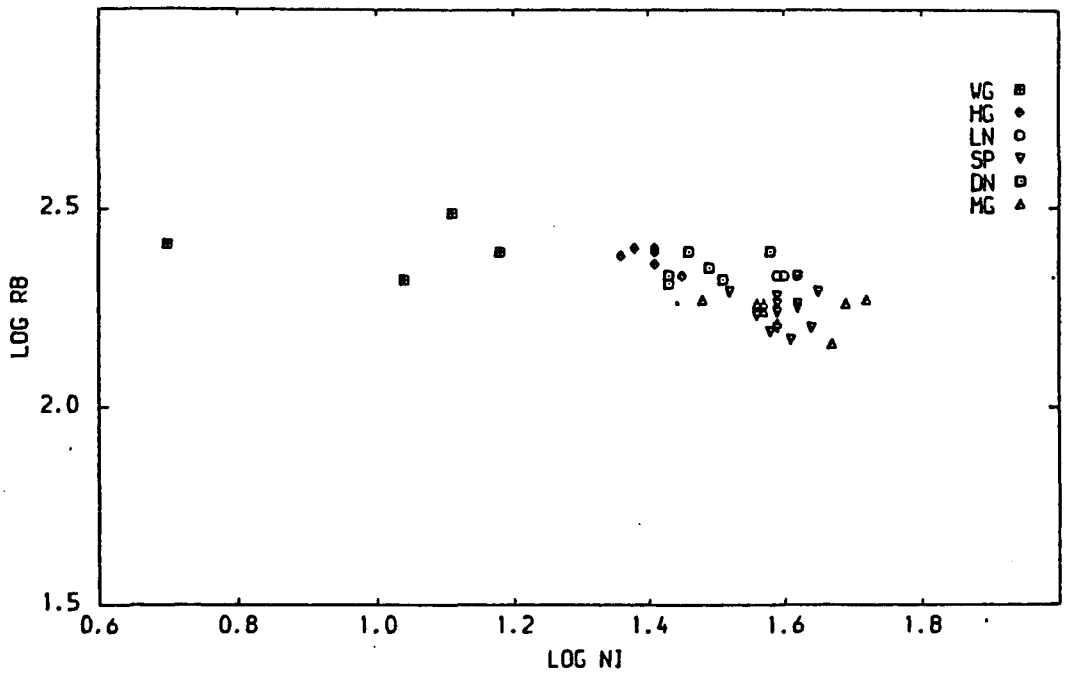

(a)

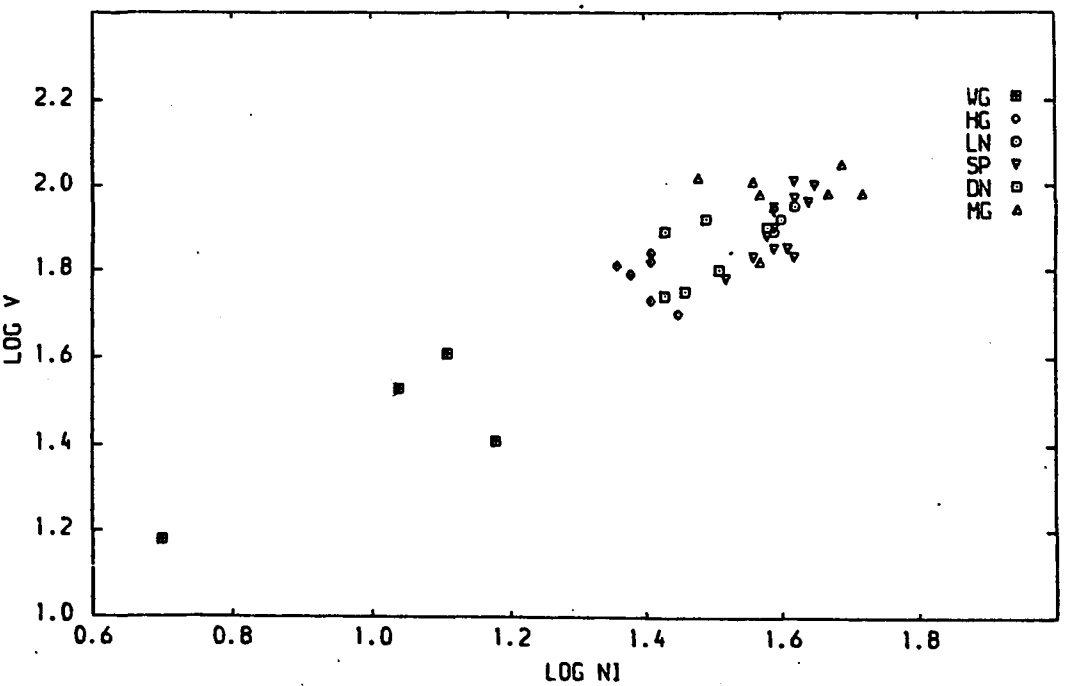

(b)

Fig. 5.15 Log relations of 40 fresh granodiorites and granites with a linear correlation

(a) Log Rb v. Log Ni.

(b) Log V v. Log Ni

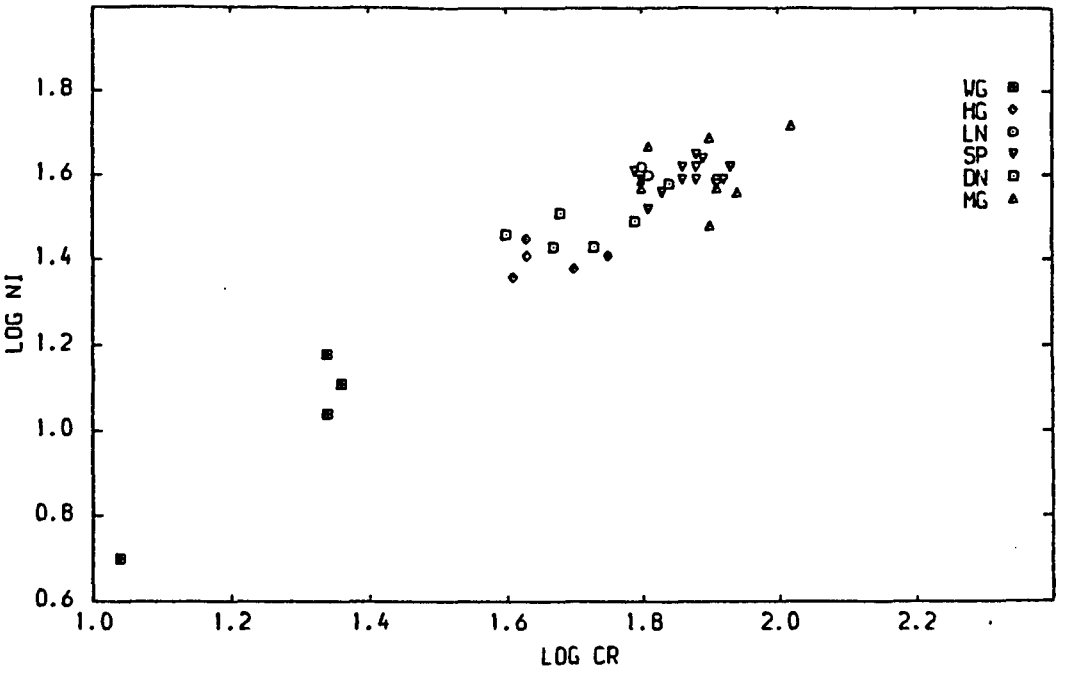

(a)

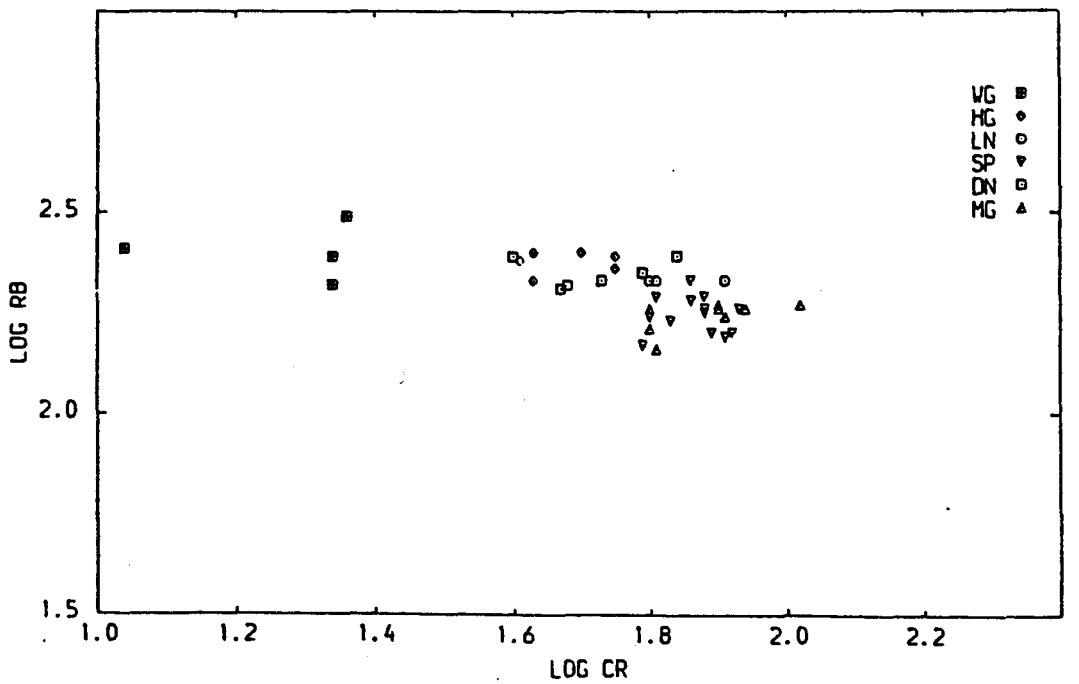

(b)

Fig. 5.16 Log relations of fresh granodiorites and granites with a linear correlation

(a) Log Ni v. Log Cr

(b) Log Rb v. Log Cr

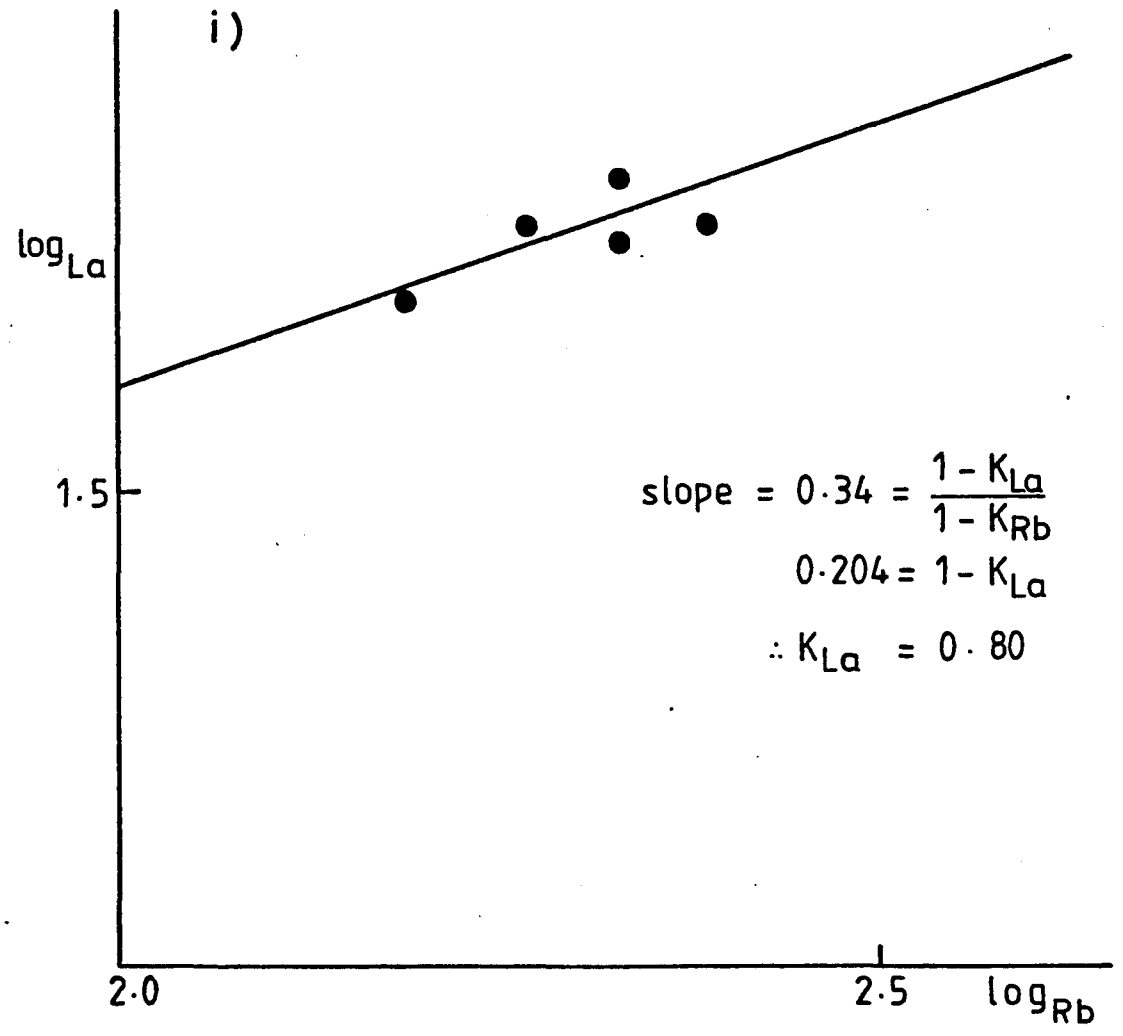

Fig. 5·17a Simplified log-log diagram based on average data.
i) $\log_{La}$ v. $\log_{Rb}$

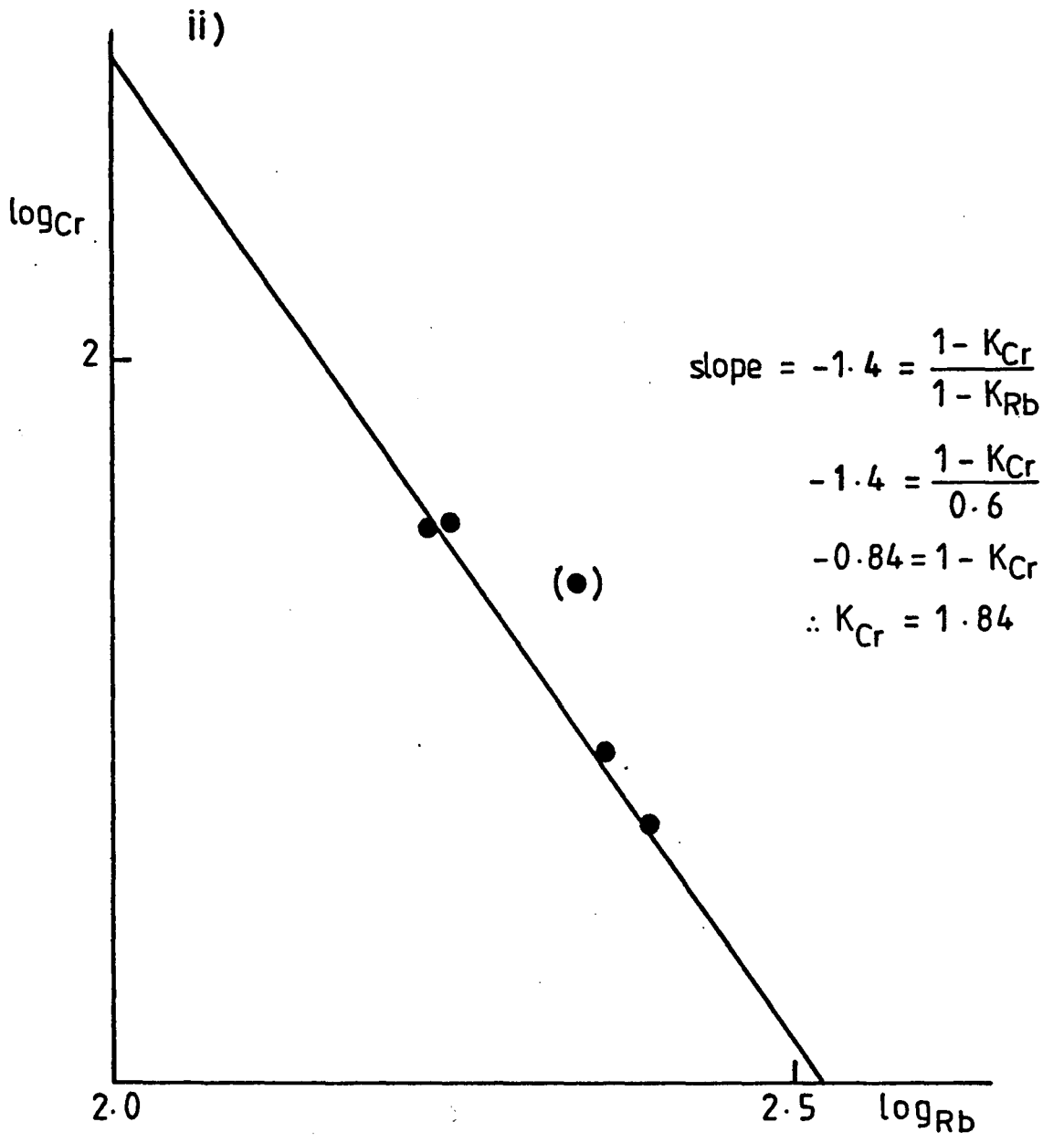

Fig. 5 · 17 b Simplified log-log diagram based on average data.
ii) $\log_{Cr}$ v. $\log_{Rb}$

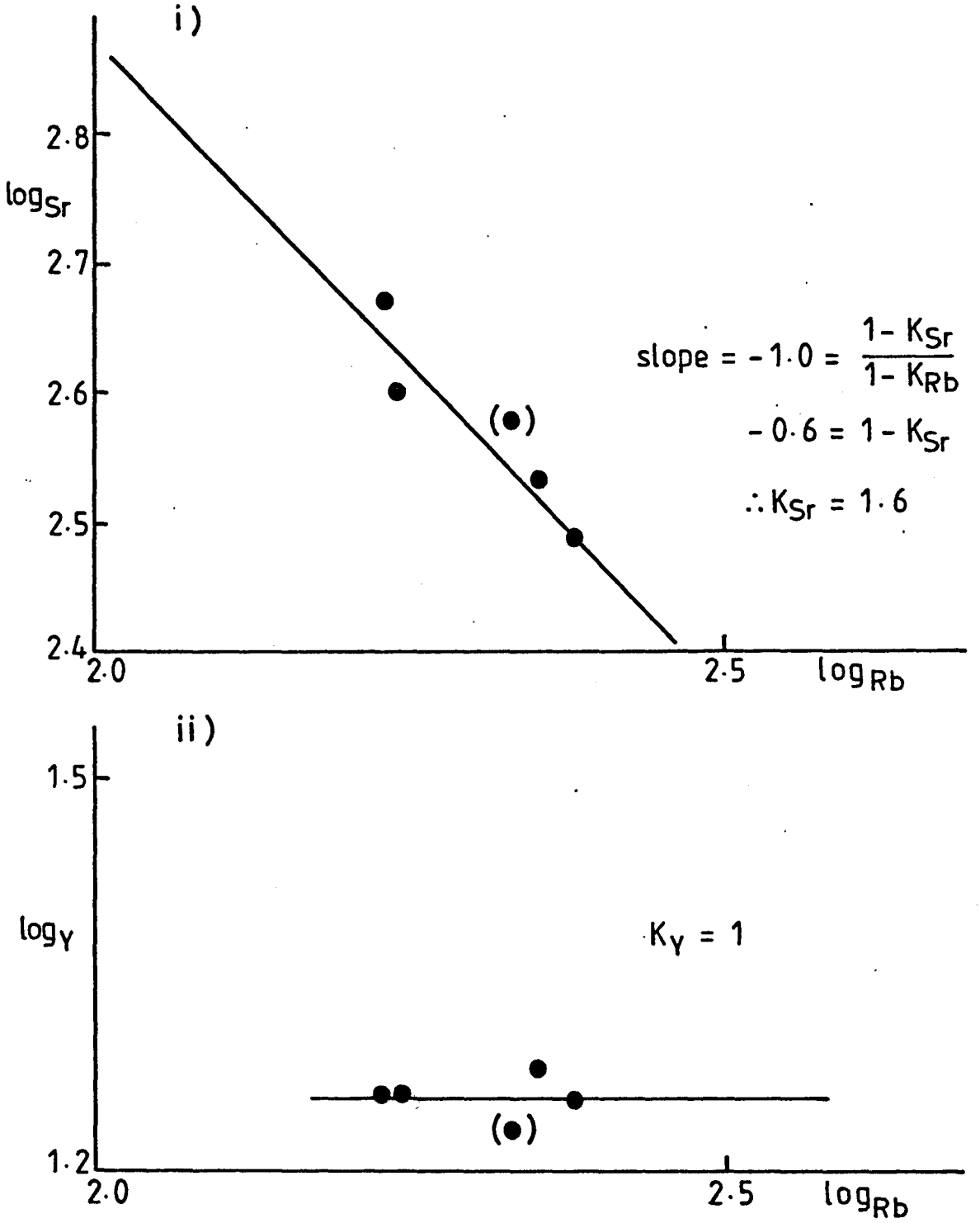

Fig. 5·18a Simplified log-log diagrams based on average data.
i) $\log_{Sr}$ v. $\log_{Rb}$ ii) $\log_{Y}$ v. $\log_{Rb}$

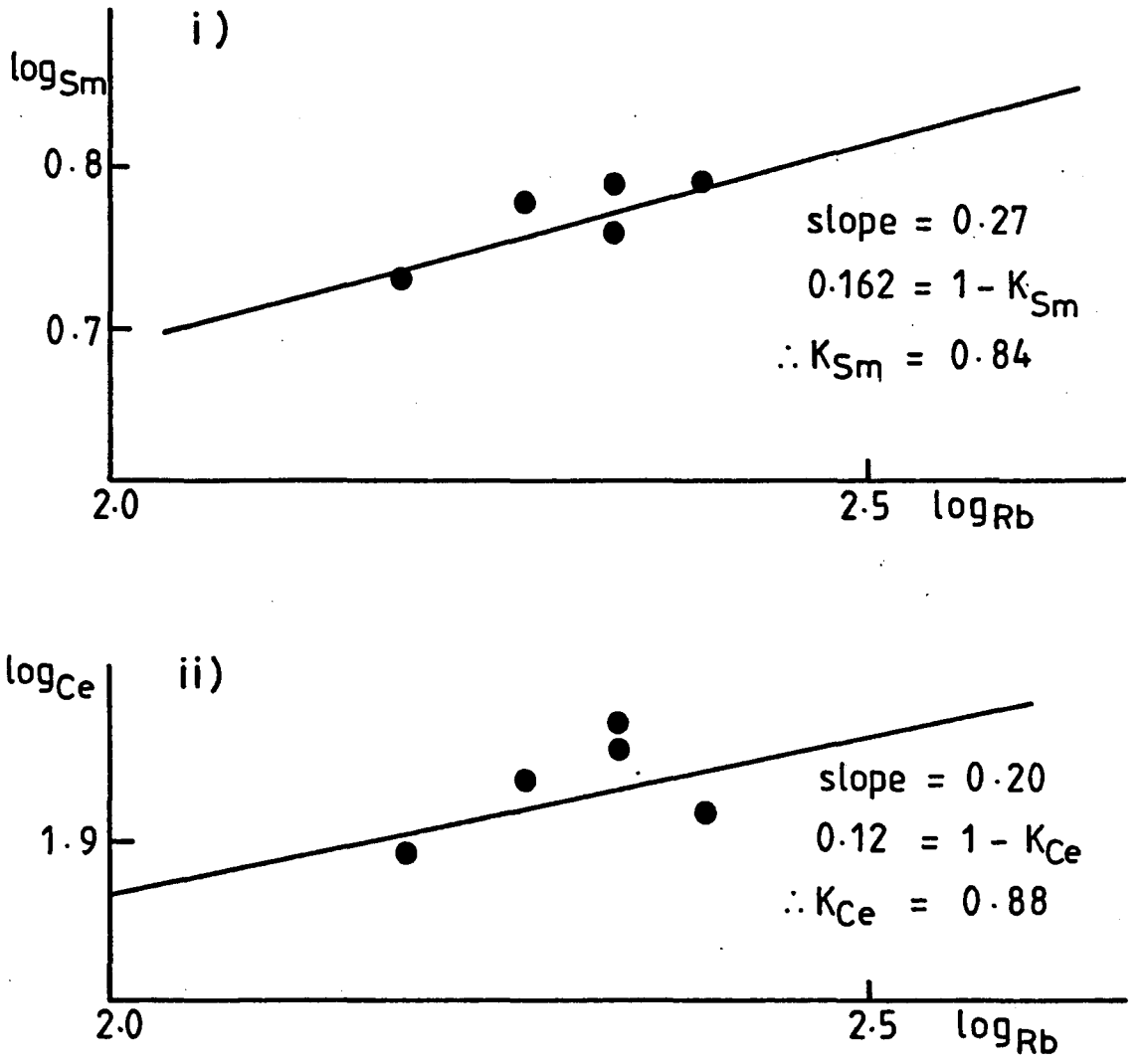

Fig. 5·18 b Simplified log - log diagrams based on average data.
i) $\log_{Sm}$ v. $\log_{Rb}$ ii) $\log_{Ce}$ v. $\log_{Rb}$

CHAPTER SIX

ALTERATION GEOCHEMISTRY

CHAPTER SIX

ALTERATION GEOCHEMISTRY

6.1 INTRODUCTION

In chapters 2 and 3 the field observations and petrography of alteration were discussed. In this chapter the geochemical changes during alteration will be considered. Briefly, the conclusions from the earlier chapters were that there were two episodes of hydrothermal circulation in the Cheviot complex, system A, associated with the intrusion of the Dunmoor Granodiorite ring dyke late in the history of igneous cycle 1, and system B, associated with the intrusion of the Hedgehope Granodiorite ring dyke towards the end of igneous cycle 2. These two episodes of hydrothermal circulation have given rise to five different alteration assemblages:

1. Potassic alteration of system A, (K1), developed sporadically near Bleakhope.
2. Sericitic alteration of system A (S1) developed more widely around the K1 centre.
3. Potassic alteration of system B (K2), found so far only at one place, E of Hedgehope Hill.
4. Sericitic alteration of system B (S2), widely, but patchily, developed within the northern part of the complex and within the Standrop Granodiorite to the south.
5. Propylitic alteration (P) probably developed in association with

both system A and system B, and widespread throughout the complex as well as in the surrounding hornfelses.

Samples were chosen for analysis to represent as far as possible the full range of petrographic variation present in the rocks of each assemblage. Major and trace element analyses (see Chapter 5 and Appendix D for details) were performed on 71 altered samples, divided between the alteration assemblages as follows:

1. K1 alteration: 6 samples, all altered from Dunmoor Granodiorite.
2. S1 alteration: 13 samples, altered from the Marginal and Dunmoor Granodiorites as well as from dykes intruding them.
3. K2 alteration: 2 samples, both altered from Hedgehope Granodiorite.
4. S2 alteration: 32 samples, altered from the Hedgehope and Standrop Granodiorites as well as from dykes intruding them.
5. P alteration: 18 samples, altered from the Marginal Granodiorite and the Linhope Granodiorite.

REE analyses were performed on a selection of 14 of these samples (4 from K1, 4 from S1, 1 from K2, 1 from S2 and 2 from P). Analytical procedures and accuracy are given, along with the full analytical results, in Appendix A (for major and trace analyses) and in Appendix B (for REE). In this chapter these results will be compared with the major and trace analyses of 44 fresh samples, and the REE analyses of the six representive fresh samples which were described in Chapter 5.

6.2 GRAPHICAL ASSESSEMENT OF GEOCHEMICAL CHANGES

The most important geochemical changes in whole-rock composition during hydrothermal alteration can be seen very well using three different kinds of plots.

1. Plots of individual elements against Al2O3 (Figures 6.1, 6.2, 6.3 and 6.4).

   In these plots, the content of Al2O3 is plotted as the Y coordinate. This was selected because it varies little in the fresh rocks and is relatively immobile during alteration. This can be well seen on Figure 6.4(b), a plot of Al2O3 against the normally immobile element Nb. The clustering of the points suggests strongly immobile behavior of Al2O3 as well. Each of the figures shows the variation of one element against Al2O3, and is made up of six plots, one for each of the intrusion phases. On each is shown the fresh rocks (as maltese crosses) and the different alteration assemblages that have affected the rock with appropriate symbols. The dispersion of altered rocks beyond the cluster of fresh rocks is a measure of the mobility of the element concerned. The elements selected for display in this Chapter are mostly those which show a large degree of dispersion caused by alteration. This system of plotting not only allows a comparison of fresh and altered rocks but also comparisons of the chemistry of different types of alteration.

2. Ratio plots. (Figures 6.5 and 6.6) Figure 6.5 plots the atomic

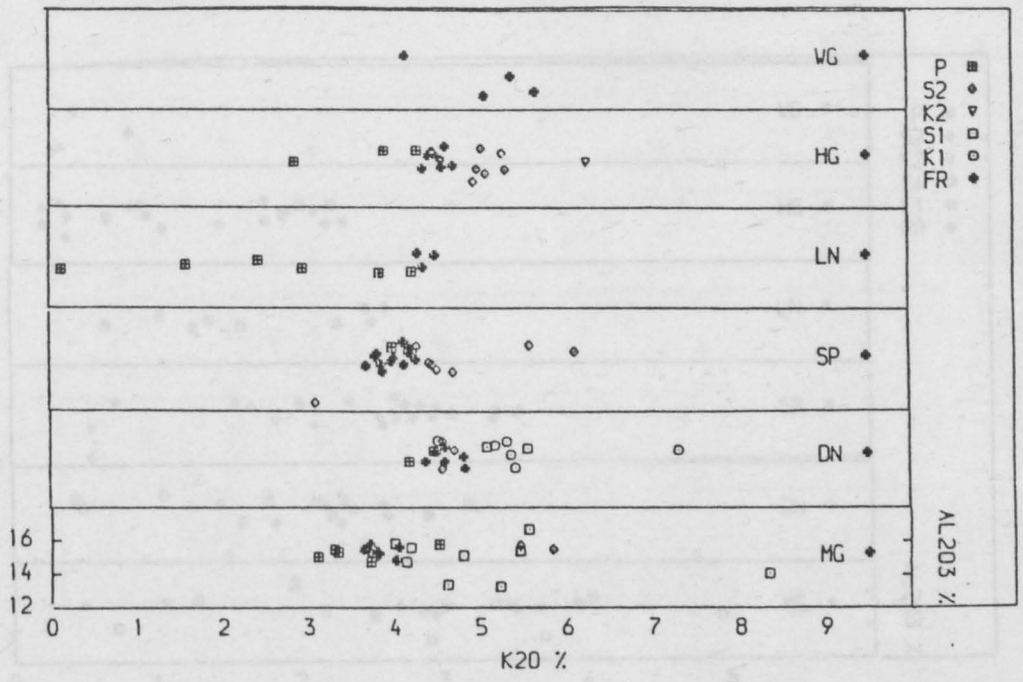

(a)

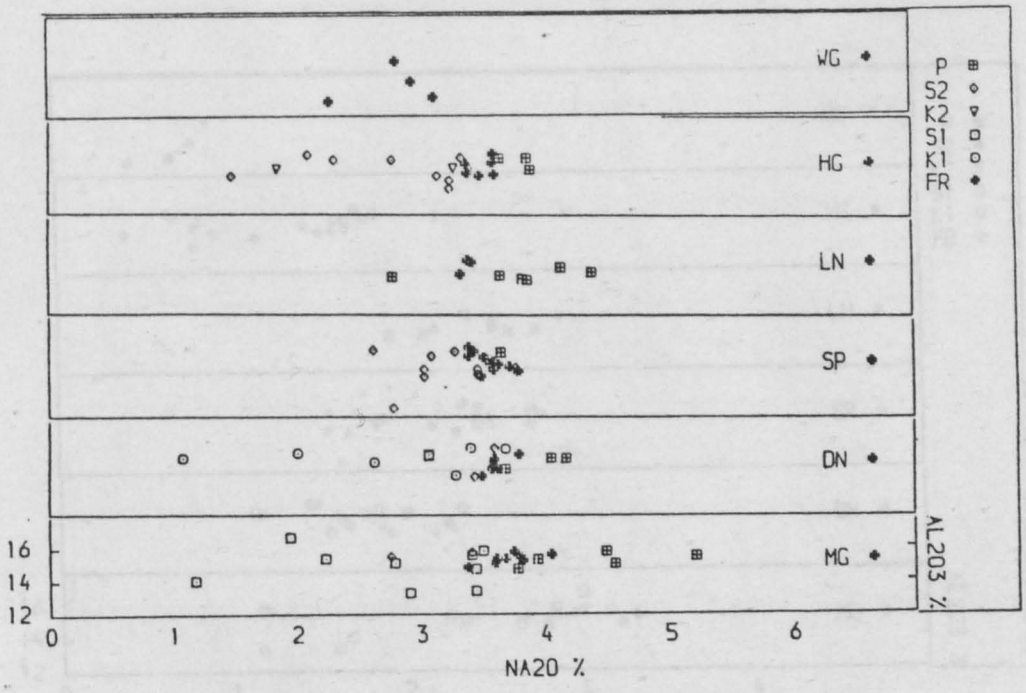

(b)

Fig. 6.1 Plots of the various alteration types against Al_2O_3%

(a) K_2O% v. Al_2O_3%

(b) Na_2O% v. Al_2O_3%

Symbols as in figure (2.1) and (3.1)

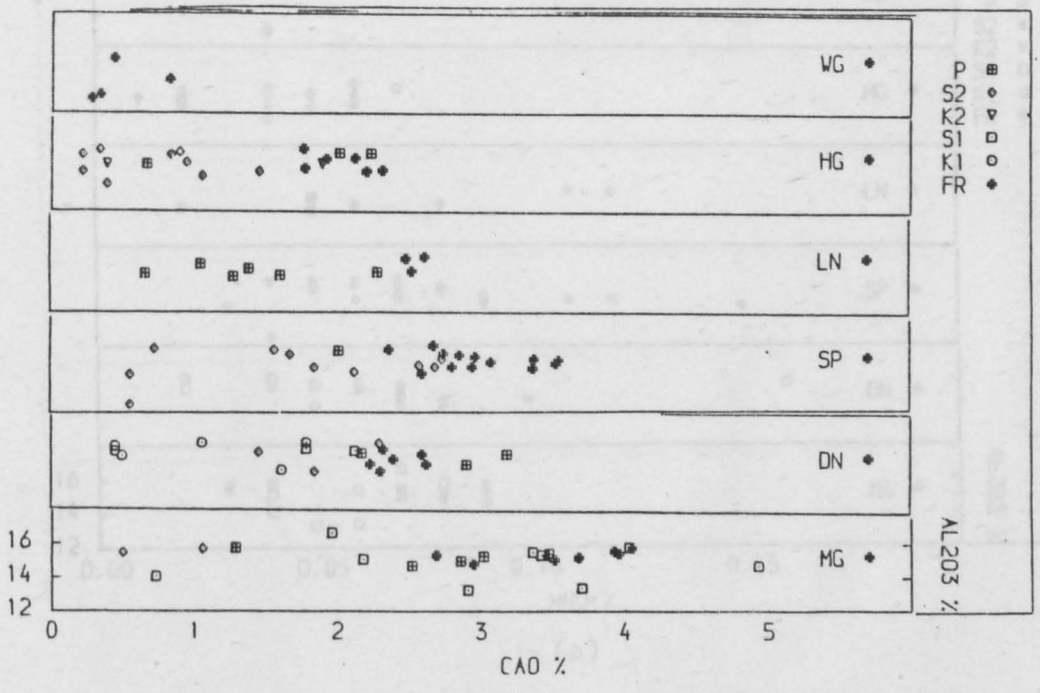

(a)

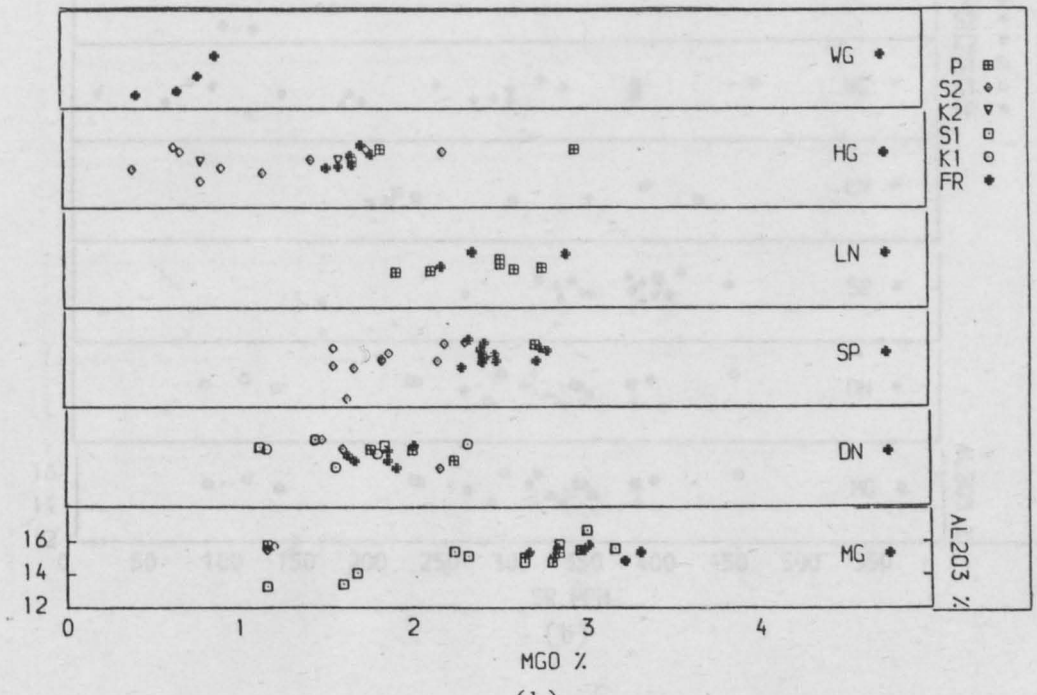

(b)

Fig. 6.2 Plots of the various alteration types against Al_2O_3%

(a) CaO% v. Al_2O_3%

(b) MgO% v. Al_2O_3%

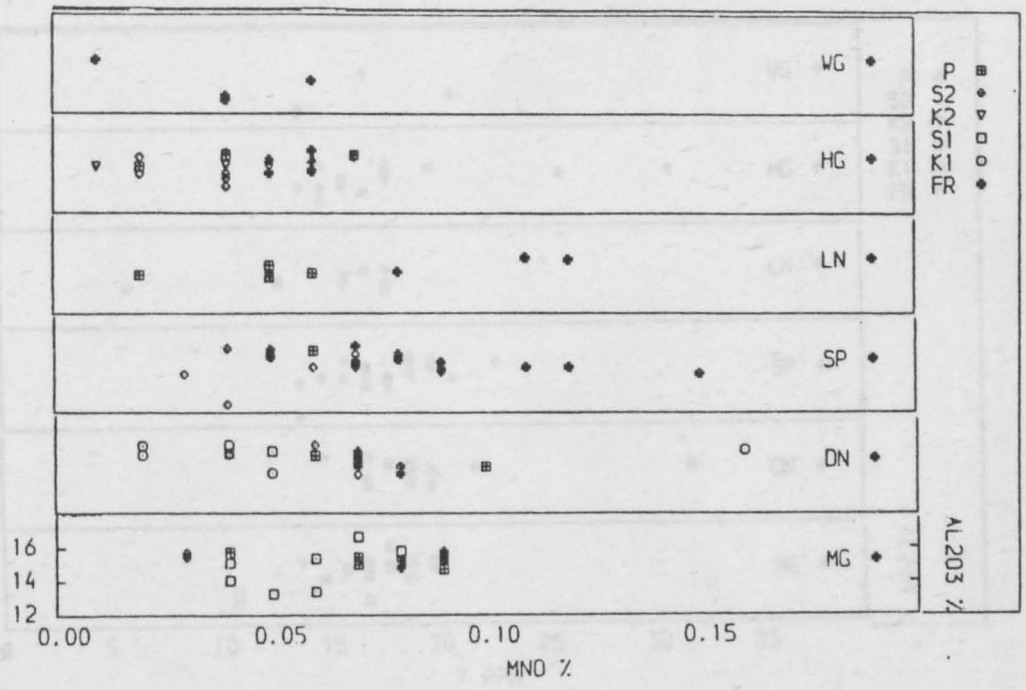

(a)

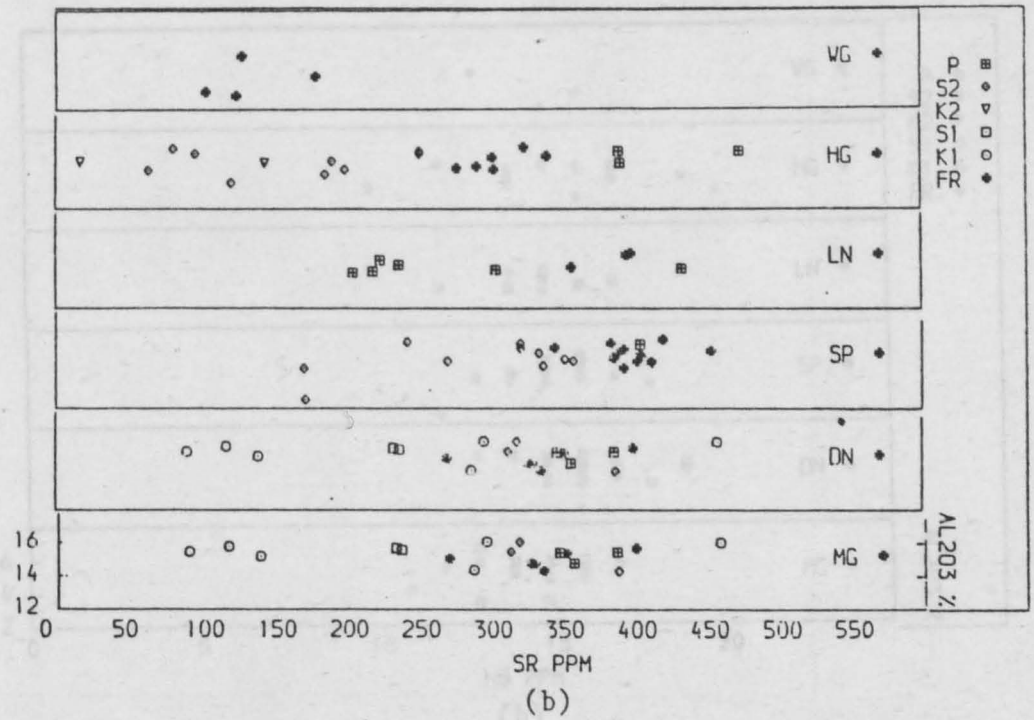

(b)

Fig. 6.3 Plots of the various alteration types against Al2O3%

(a) MnO% v. Al2O3%

(b) Sr ppm v. Al2O3%

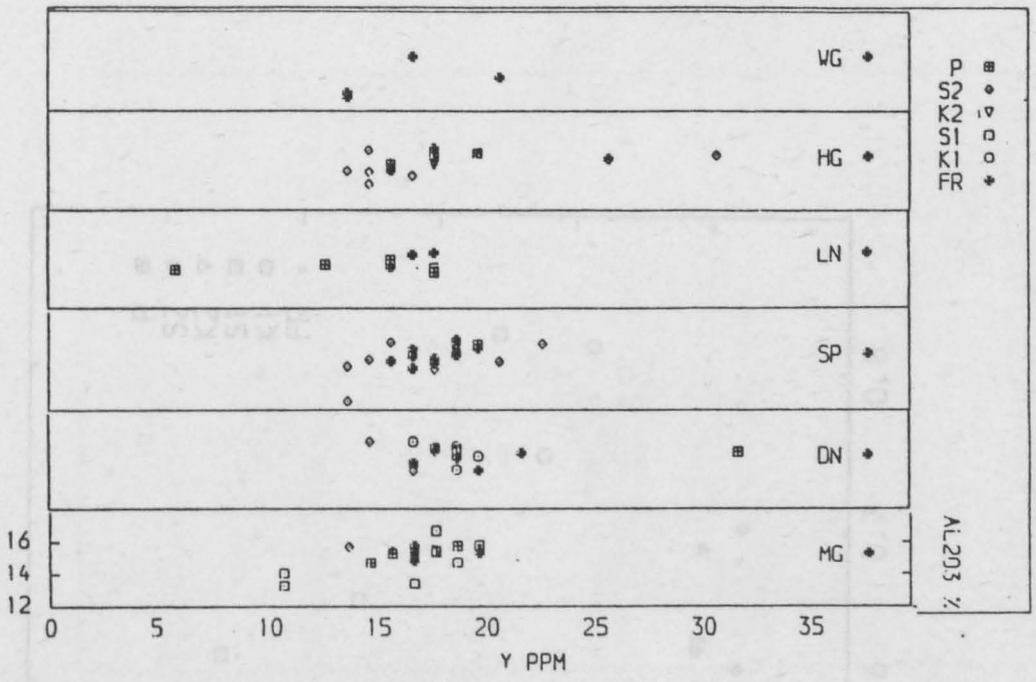

(a)

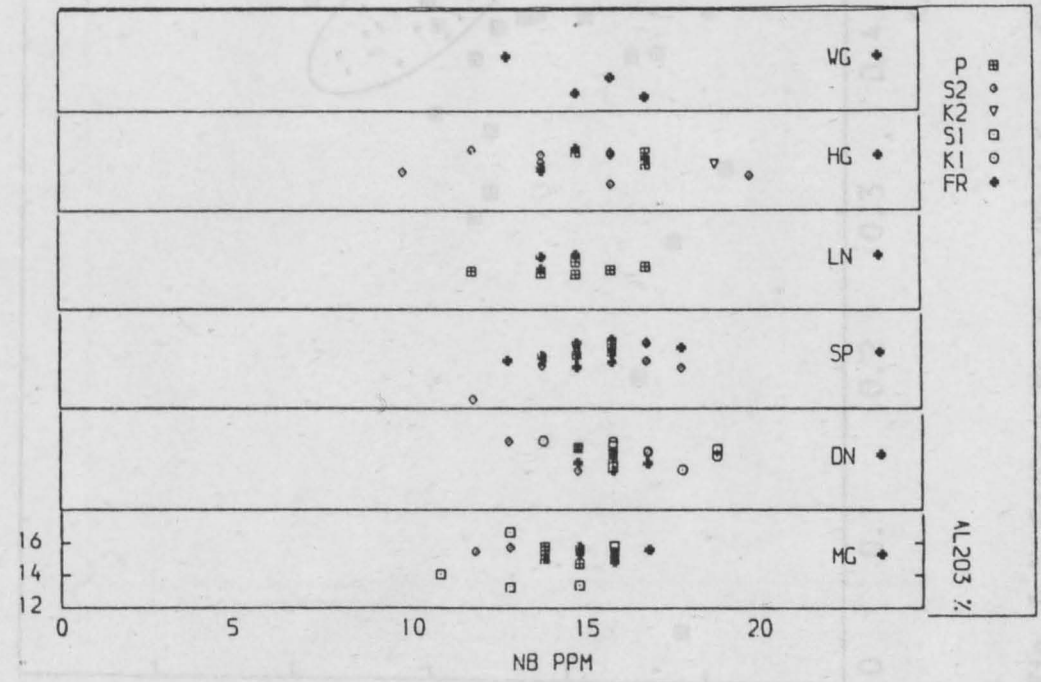

(b)

Fig. 6.4 Plots of the various alteration types against Al_2O_3%

(a) Y ppm v. Al_2O_3%

(b) Nb ppm v. Al_2O_3%

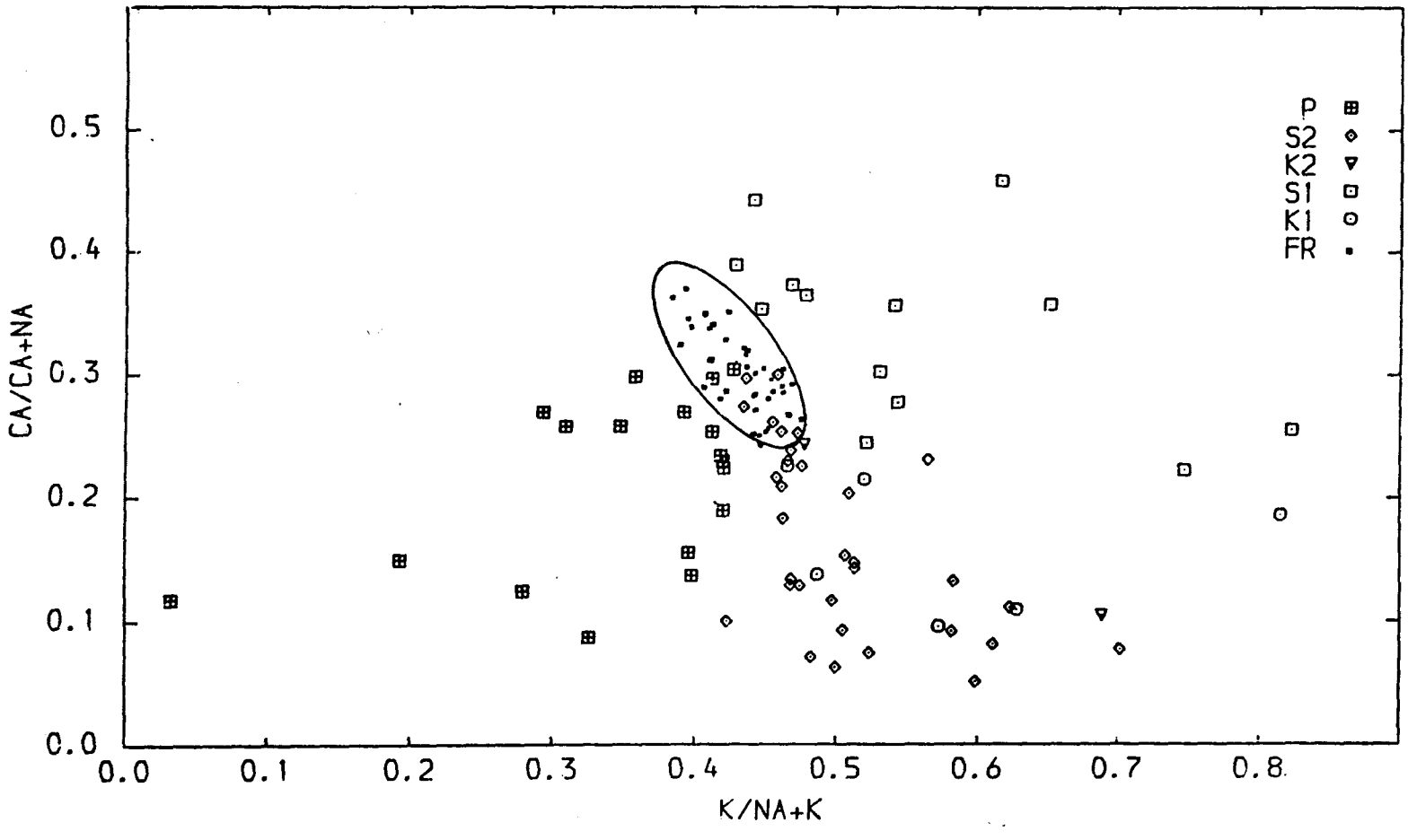

Fig. 6.5 Ca/Ca + Na v. K/Na + K as distinction diagram of the different alteration types and fresh rocks.

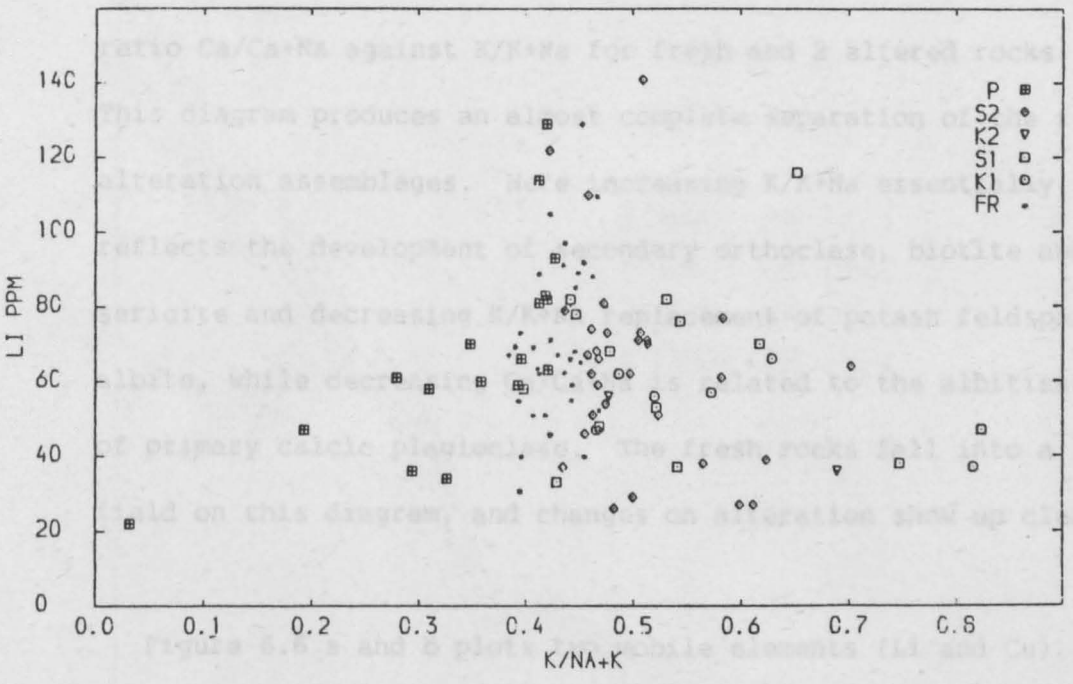

(a)

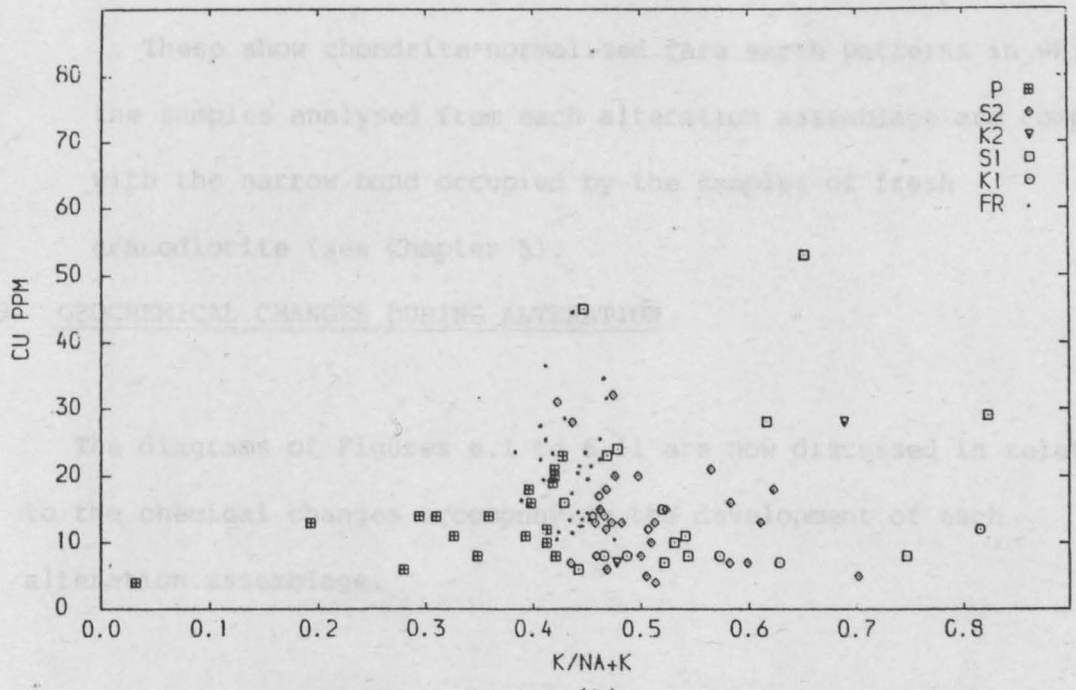

(b)

Fig. 6.6 Distinction diagrams of the different alteration types and fresh rocks

(a) Li ppm v. K/Na + K

(b) Cu ppm v. K/Na + K

ratio Ca/Ca+Na against K/K+Na for fresh and 2 altered rocks. This diagram produces an almost complete separation of the five alteration assemblages. Here increasing K/K+Na essentially reflects the development of secondary orthoclase, biotite and sericite and decreasing K/K+Na replacement of potash feldspar by albite, while decreasing Ca/Ca+Na is related to the albitisation of primary calcic plagioclase. The fresh rocks fall into a small field on this diagram, and changes on alteration show up clearly.

Figure 6.6 a and b plots two mobile elements (Li and Cu) against K/Na+K.

3. REE plots. (Figures 6.7-6.11)

These show chondrite-normalised rare earth patterns in which the samples analysed from each alteration assemblage are compared with the narrow band occupied by the samples of fresh granodiorite (see Chapter 5).

6.3 GEOCHEMICAL CHANGES DURING ALTERATION

The diagrams of Figures 6.1 to 6.11 are now discussed in relation to the chemical changes accompanying the development of each alteration assemblage.

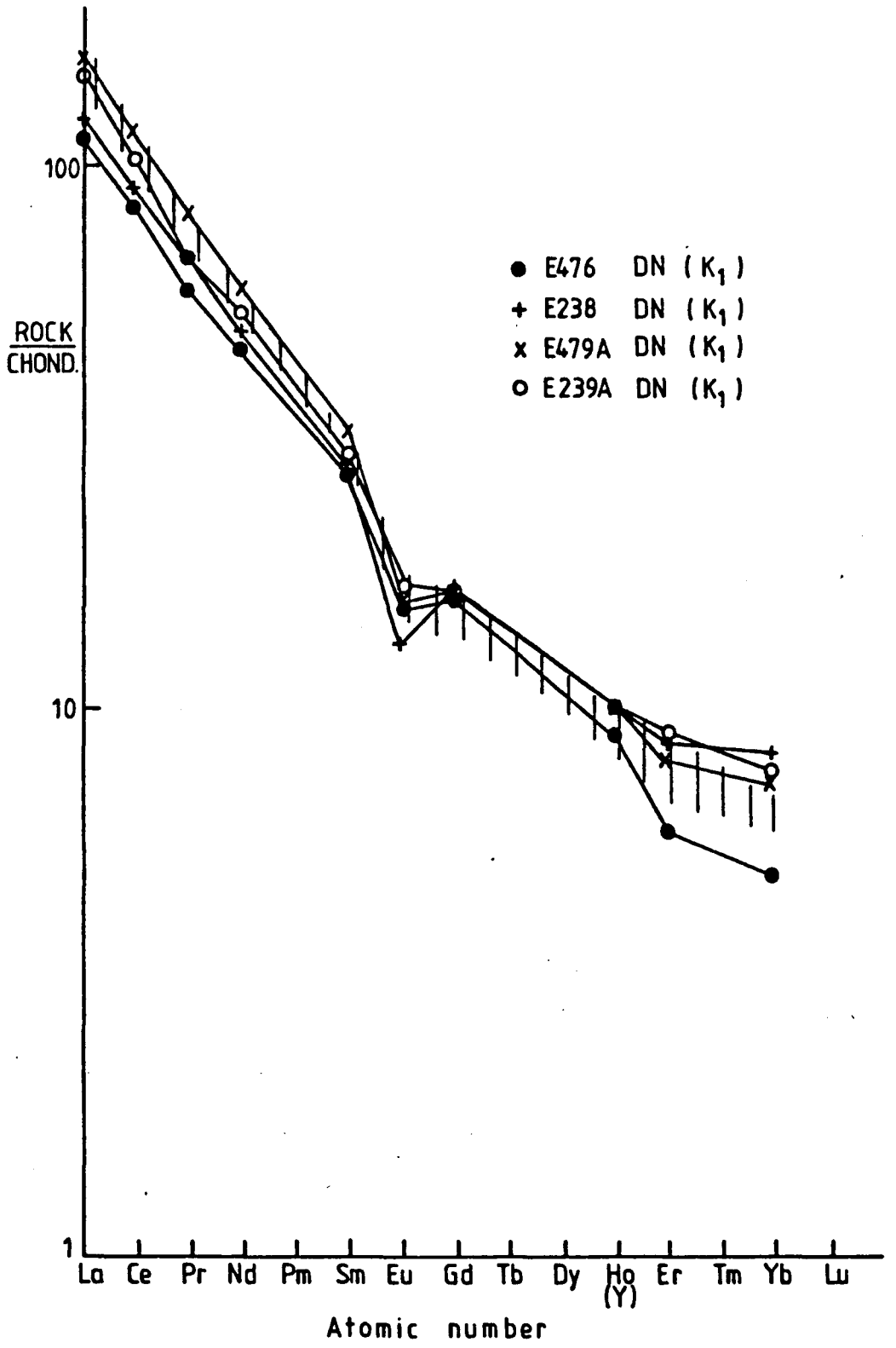

Fig. 6·7 Chondrite-normalized REE patterns for Dunmoor Granodiorites affected by K-silicate (1) alteration. Symbols as in Fig. (6·1).

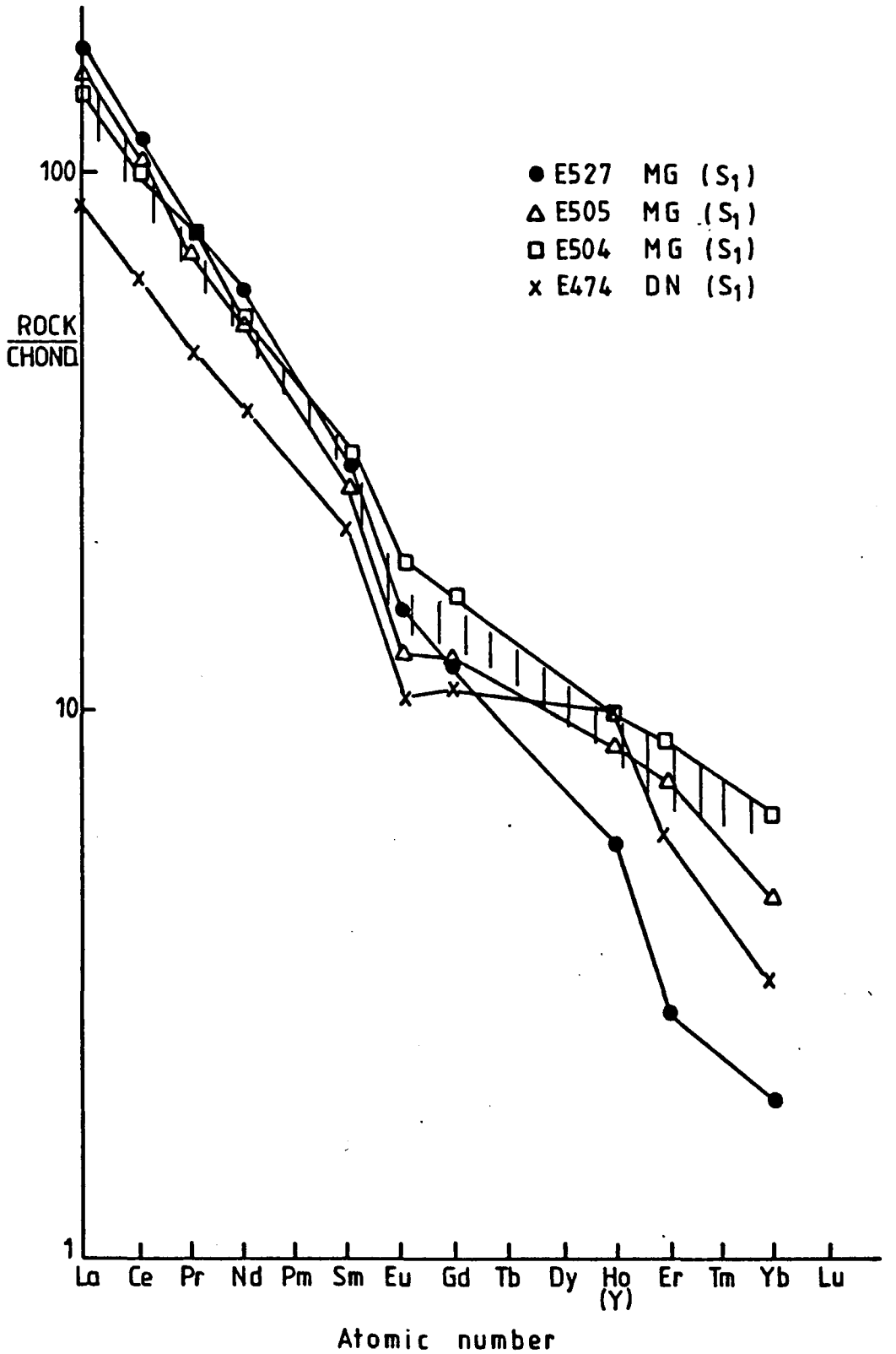

Fig. 6.8 Chondrite-normalized REE patterns for Marginal and Dunmoor Granodiorites affected by sericitic (1) alteration.

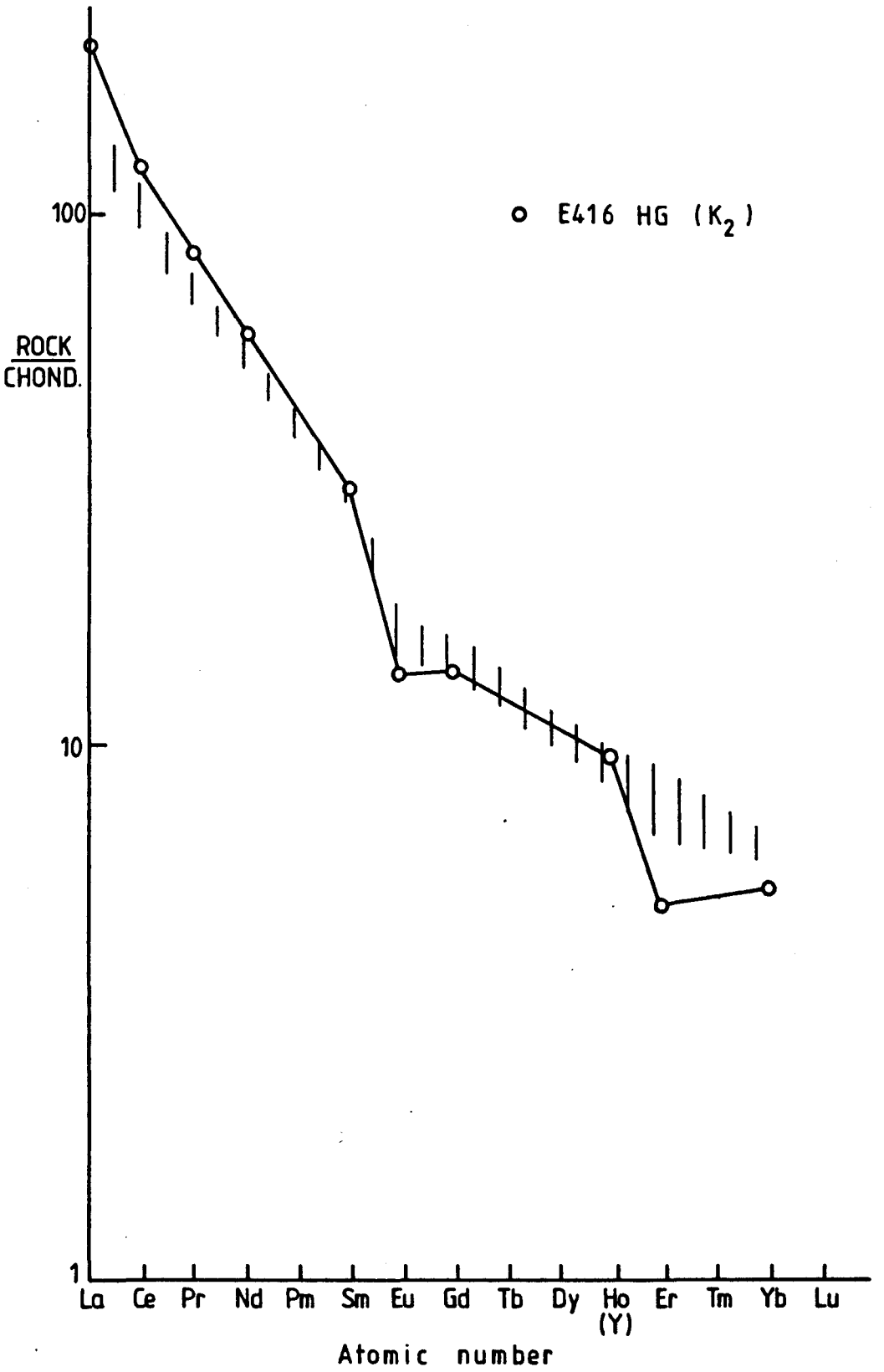

Fig. 6·9 Chondrite-normalized REE patterns for Hedgehope Granodiorite affected by K-silicate (2) alteration.

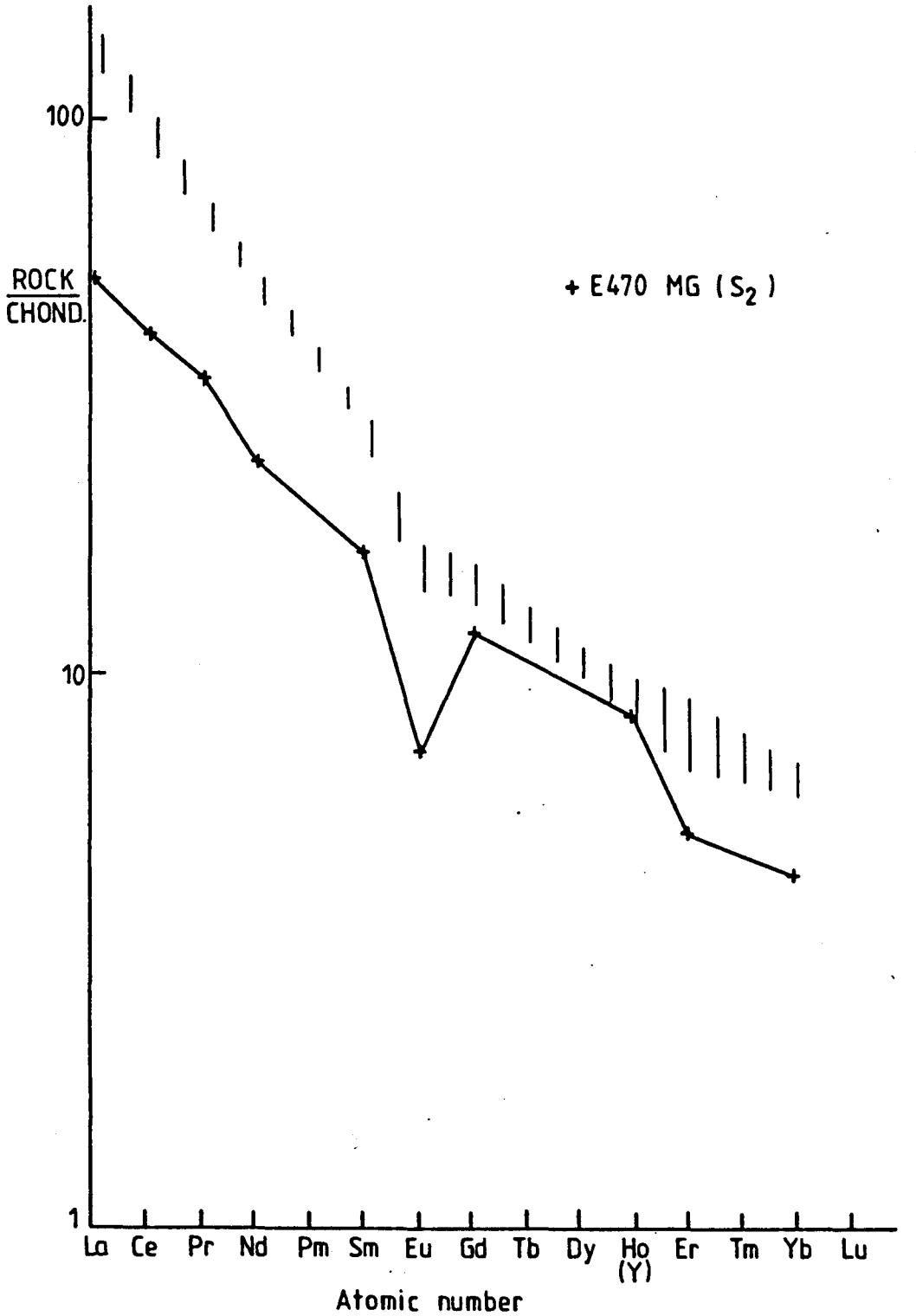

Fig. 6 · 10 Chondrite - normalized REE pattern for Marginal Granodiorite affected by sericitic (2) alteration.

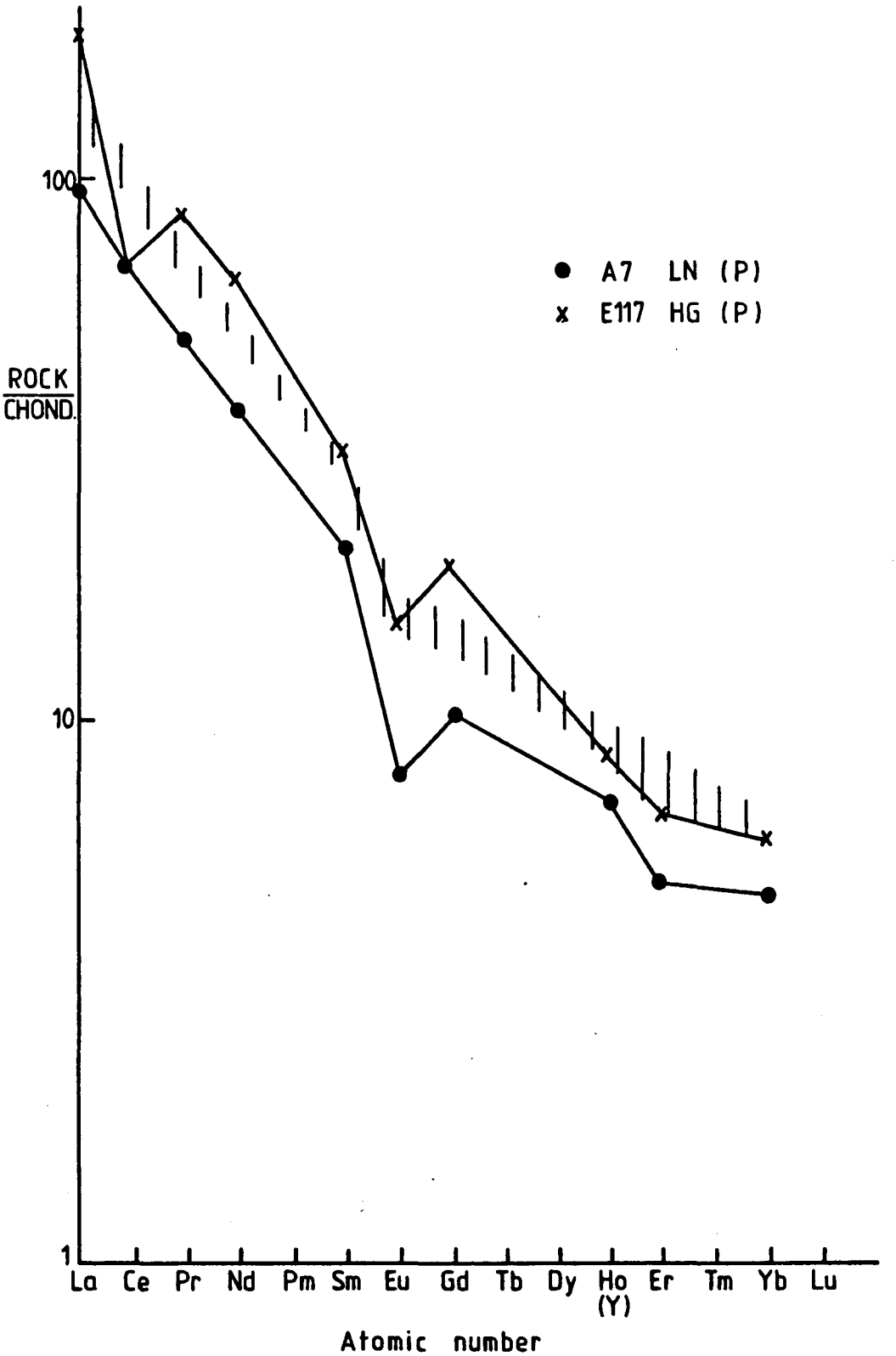

Fig. 6·11 Chondrite-normalized REE patterns for Linhope and Hedgehope Granodiorites affected by propylitic alteration.

6.3.1 POTASSIC ALTERATION 1 (K1)

The geochemical variations displayed by the different plots reflect the mineralogical changes which were described in Chapters 3 and 4. The chemical plots against Al2O3 demonstrate that K (and Rb) have been gained and accommodated in the secondary orthoclase and biotite (Figure 6.1a) whereas CaO, Na2O and Sr (partitioned into plagioclase) and to a slight extent MnO and MgO (partitioned in pyroxenes) have been removed into the fluid (Figures 6.2a, 6.1b, 6.3b, 6.3a, 6.2b) respectively, in agreement with the conclusion of Alderton, Pearce and Potts (1980). However variation in other elements (such as Y, Nb, Figures 6.4a, 6.4b) and P is not significant. The chemical gains and losses in this zone are again shown on the plot of K/K+Na against Ca/Ca+Na (Figure 6.5). Moreover there is a distinct variation in the Ca/Ca+Na ratio for this assemblage which divides the analysed K1 samples into two groups, one with a high Ca/Ca+Na trending towards that of S1, and the other with relatively low Ca/Ca+Na ratio. Petrographic studies of this assemblage reveal that this zone is overlapped partially by the next younger S1 assemblage which produces rocks of a relatively calcic nature (through production of calcite as well as chlorite and sericite) and this might explain the apparent subdivision. Bivariate plots of both Li and Cu against K/K+Na ratio are presented. These plots (Figures 6.6a, 6.6b) show that both elements are more or less depleted and removed into the fluid as alteration proceeds. The rare earth element plots show analyses of four of these samples, and

reveal no significant change in both light and heavy REE during alteration (figure 6.7). The immobility of REE, taken together with that of the elements P, Y, Nb and Ti mentioned above suggests that the original minor phases may have remained unaffected during this alteration episode.

6.3.2 SERICITIC ALTERATION 1 (S1)

The study of this assemblage in thin section shows that both feldspars are replaced by sericite or muscovite whereas pyroxene and biotite are replaced by calcite and chlorite respectively. The geochemical plots against Al2O3 show that K (and Rb) (which are concentrated in mica) are introduced into the system whereas the breakdown of pyroxene and biotite into calcite and chlorite causes a depletion in MgO and MnO. In addition the contents of Na2O and Sr (partitioned in plagioclase) are depleted as a result of the formation of sericite (particularly from plagioclase) and of chlorite (from biotite). However the variations in Nb, Ti and P are not significant which again suggests the resistance to alteration of the minor phases. The bivariate plot of the ratios K/K+Na against Ca/Ca+Na distinguishes a field for this zone which reflects the calcic nature of all of the samples belonging to this zone. This is apparently due to the production of calcite from pyroxene as shown petrographically. In addition the bivariate plots of Li and Cu against K/K+Na ratio show that Li (accommodated in Mica is enriched in most of the samples of this assemblage whereas Cu is depleted in

some samples and enriched in others. Finally the REE analyses reveal no significant change in the light REE but a marked depletion towards the heavy end together with a marked decrease in the size of the negative Eu anomaly (especially by sample E527). The depletion in heavy REE contrasts with the constancy of the other less mobile elements such as Nb, Ti and P, and may reflect a different structural position for the heavy REE.

6.3.3 POTASSIC ALTERATION 2 (K2)

This alteration assemblage is restricted to the Hedgehope Granodiorite, postdating its intrusion and predating the tourmalinization stage characteristic of the rest of alteration system B. This type reveals similar gains and losses in the analyses as does K1. The enrichment of K and Rb content in these rocks is due to the production of secondary orthoclase and biotite which accommodates them. On the other hand Na_2O, CaO, Sr (partitioned in plagioclase), and MgO and MnO (partitioned in pyroxenes) are depleted and removed into the fluid as a result of the instability of both plagioclase and pyroxenes during this stage. The bivariate plot of the ratios K/K+Na against Ca/Ca+Na shows a great deal of variation between the two analysed samples of this type which might be attributed to varying intensity of alteration (Figure 6.5). The other bivariate plots show that Li (partitioned in mica) is depleted and removed into the fluid (Figure 6.6a) whereas Cu is introduced to the system (Figure 6.6b). The REE analyses reveal no significant

change in both light REE and heavy REE (only one sample, E416, was analysed, see Figure 6.9).

6.3.4 SERICITIC ALTERATION 2 (S2)

Petrographic evidence for this assemblage indicates the production of tourmaline and sericite (or muscovite) from both feldspars, and plagioclase in particular. These mineralogical changes are reflected in the chemical variation as demonstrated by the plots against Al2O3 (Figures 6.1-6.4). These plots indicate that K2O, Rb are introduced to the system whereas Na2O, CaO, Sr and Y are depleted and removed into the fluid as a result of plagioclase alteration to sericite (or muscovite). The instability of mafic minerals (such as biotite and pyroxene) during this stage cause the production of tourmaline and to a less extent chlorite. These new minerals are unable to accommodate the same content of MgO and MnO as the primary minerals, so that a depletion in the content of these is recorded (Figures 6.2b, 6.3b respectively) and they are removed into the fluid. The bivariate atomic ratios plot of K/K+Na against Ca/Ca+Na (Figure 6.5) plays a very important role in separating S1 from S2. S1 is more calcic in nature (due to the production of calcite) whereas S2 is relatively less calcic. Rocks belonging to this zone are mainly composed of sericitic +/- secondary orthoclase, neither of which are unable to accommodate Ca, so it is removed into the fluid. The other bivariate plots of Li and Cu against K/K+Na show that both Li and Cu are more or less depleted in this assemblage. The REE plot of Figure 6.10

reveals a striking depletion in both light REE and heavy REE in the only sample analysed (E470). This shows the effect of two alteration types, S1 being overprinted by S2, identified by the presence of its characteristic tourmaline. The marked increase in the size of the negative Eu anomaly is a reflection of the intense alteration of feldspar (plagioclase in particular) to sericite.

6.3.5 PROPYLITIC ALTERATION (P)

The effect of this type of alteration is shown by almost all the granodiorites. Petrographic studies reveal the existence of chlorite, albite, epidote, actinolite +/- sericite +/- calcite +/- tourmaline (disseminated) as alteration products. These mineralogical variations are reflected in the chemical variations which are well shown by the plots against Al_2O_3 which indicate a removal of K_2O (and Rb) (partitioned in biotite and alkali feldspar) into the fluid together with CaO (Figure 6.2a) and Sr (Figure 6.3b) (partitioned in plagioclase). In contrast there is an introduction of Na_2O (accommodated into albite feldspar). Finally MnO (partitioned into pyroxene and biotite) and Y (in plagioclase) are both depleted and removed into the fluid, as reported by Alderton, Pearce and Potts (1980). The bivariate ratios plot of K/K+Na against Ca/Ca+Na isolates this type perfectly into a field of relatively low K/K+Na. The variation exhibited by samples of this type is mainly attributed to the intensity of alteration and consequently intensely altered rocks are mainly composed of albite (and disseminated

tourmaline) such as sample A6. The other bivariate plots of Li and Cu against K/K+Na indicate that Li and Cu are both depleted in this type (see Figures 6.6a, 6.6 b). The REE analyses reveal no significant change in both LREE and HREE except for a marked increase in the size of the negative Eu anomaly exhibited by sample E117 which is probably due to the production of sericite from plagioclase (Figure 6.11).

Figure 6.12 is a plot of Th against Al2O3. It is interesting, since 12 of the samples show substantial depletion in Th, and one sample enrichment. This mobility of Th seems to have occurred most often in S2 and P, and is particularly associated the development of tourmaline in the alteration assemblage. Clearly Th cannot be considered to be an immobile element under conditions of porphyry copper alteration, especially when tourmaline is present.

6.4 ELEMENT FLUXES DURING ALTERATION

The graphical presentation of the last section allows a qualitative view of chemical changes accompanying alteration. More quantitative conclusions come from comparing averages of highly altered rock with fresh samples. The averages of the fresh samples for each unit are summarised in Chapter 5, Table 5.1. Each alteration type was represented by an average of samples selected both to show intense alteration of that particular assemblage and to have originated from the same parent intrusive. Below are five

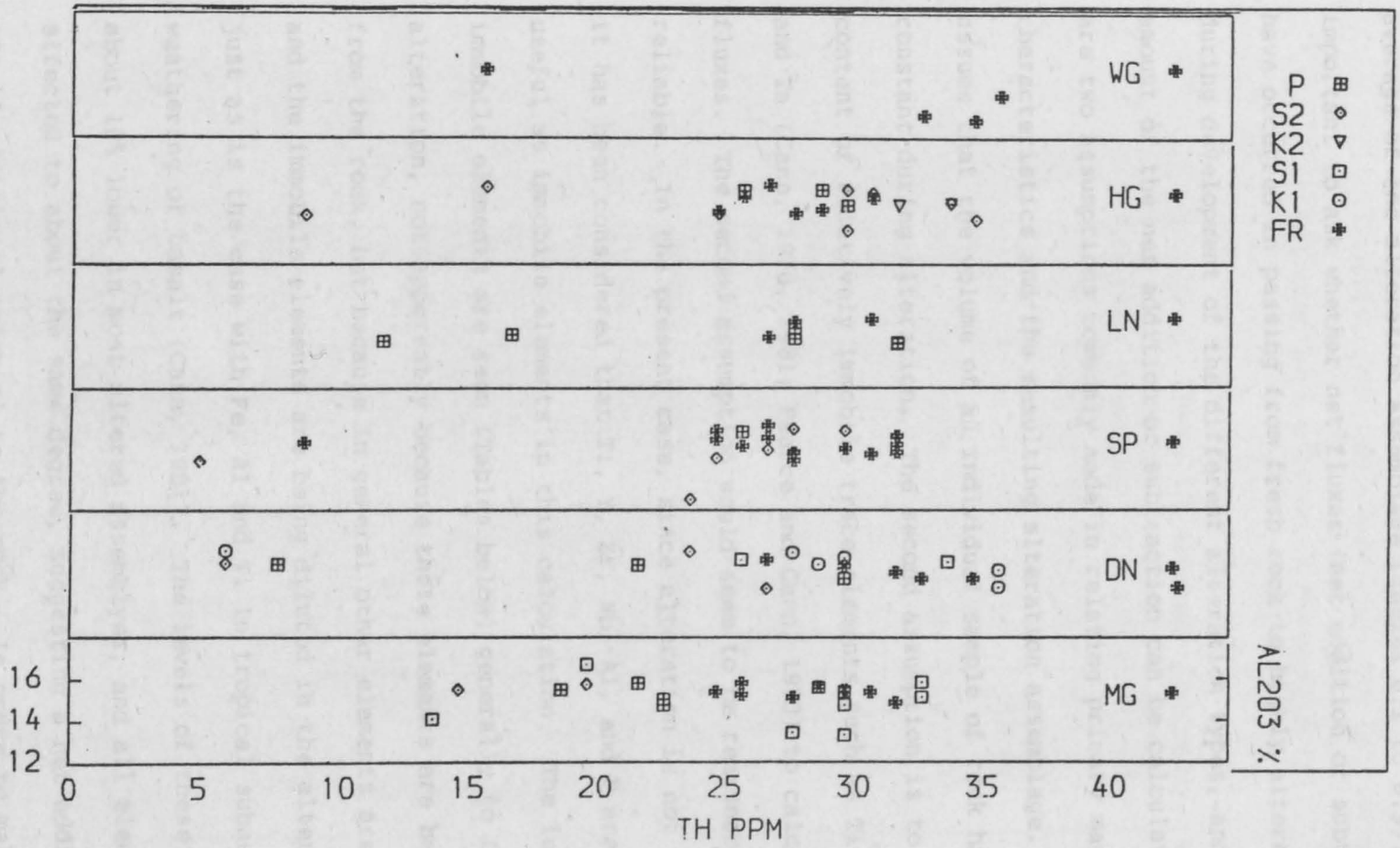

Fig. 6.12: Distinction diagram of the different alteration types and fresh rocks

tables each of which shows a fresh average and a corresponding average of one alteration assemblage (Tables 6.1 to 6.5). It is now important to ask whether net fluxes (net addition or subtraction) have occurred in passing from fresh rock to highly altered rock during development of the different alteration types, and whether the amount of the net addition or subtraction can be calculated. There are two assumptions commonly made in relating primary magmatic characteristics and the resulting alteration assemblage. One is to assume that the volume of an individual sample of rock has remained constant during alteration. The second assumption is to use the content of relatively immobile trace elements such as Ti, Y, Zr, Nb, and Ta (Cann, 1970, 1981; Pearce and Cann, 1973) to calculate net fluxes. The second assumption would seem to be reasonably simple and reliable. In the present case, since alteration is not too intense, it has been considered that Ti, Y, Zr, Nb, Al, and P are potentially useful as immobile elements in this calculation. The levels of these immobile elements are seen (Tables below) generally to fall during alteration, not apparently because these elements are being removed from the rock, but because in general other elements are being gained and the immobile elements are being diluted in the altered rocks, just as is the case with Fe, Al and Ti in tropical subaerial weathering of basalt (Cann, 1981). The levels of these elements are about 10% lower in most altered assemblyes, and all elements are affected to about the same degree, suggesting a net addition of about 10% of additional material to the rock. In order to make a valid comparison with the unaltered averages, then, the analytical results

Table 6.1

Chemical enrichment and depletion in Dunmoor Granodiorite affected by K silicate 1 alteration (K1).

Average	Fresh Dunmoor 6 samples	Altered Dunmoor 6 samples	Immobile Fresh/ Altered	Addition(+) Subtraction(-) in g/100 gm
SiO2	67.50	68.22		+ 0.72
TiO2	0.67	0.64	1.00	------
Al2O3	15.03	15.50	0.97	------
Fe2O3	1.53	1.55		+ 0.02
FeO	1.79	1.58		- 0.21
MnO	0.07	0.06		- 0.01
MgO	1.82	1.62		- 0.20
CaO	2.42	0.98		- 1.44
Na2O	3.62	2.68		- 0.94
K2O	4.62	5.52		+ 0.90
P2O5	0.21	0.22	0.95	------
H2O	0.82	1.74		+ 0.92
TOTAL	100.1	100.3	-----	mg/100 gm
Li	78	54		- 2.40
V	69	64	1.00	- 0.50
Cr	53	44		- 0.90
Co	40	46		+ 0.60
Ni	31	29		- 0.20
Cu	20	10		- 1.00
Zn	75	64		- 0.90
Rb	224	263		+ 3.90
Sr	336	231		-10.50
Y	19	19	1.00	------
Zr	279	259	1.10	------
Nb	16	17	0.94	------
Mo	4	3		- 0.10
Pb	22	18		- 0.40
Th	33	28		- 0.50
U	7	4		- 0.30

Altered Samples:

E466, E476, E479A, E478A, E238, E239A.

Table 6.2

Chemical enrichment and depletion in Marginal Granodiorite affected by sericitic 1 alteration (S1).

Average	Fresh Marginal 8 samples	Altered Marginal 7 samples	Immobile Fresh/ Altered	Altered x 1.1	Addition(+) Subtraction(-) in g/100 gm
SiO2	64.42	65.2		71.8	+ 7.34
TiO2	0.83	0.76	1.10	0.84	------
Al2O3	15.33	14.66	1.10	16.13	------
Fe2O3	1.67	1.09		1.20	+ 0.02
FeO	2.68	2.28		2.51	- 0.17
MnO	0.09	0.06		0.07	- 0.02
MgO	2.94	2.10		2.31	- 0.63
CaO	3.53	2.83		3.11	- 0.42
Na2O	3.71	2.56		2.82	- 0.89
K2O	3.81	5.45		6.00	+ 2.19
P2O5	0.30	0.26	1.10	0.29	------
H2O	1.01	2.16		2.38	+ 1.37
TOTAL	100.3	99.5	------	------	mg/100 gm
Li	59	69		76	+ 1.70
V	95	75		83	- 1.20
Cr	78	59		65	- 1.30
Co	35	34		37	+ 0.20
Ni	41	30		33	- 0.80
Cu	24	23		25	+ 0.10
Zn	74	60		66	- 0.80
Rb	175	265		292	+11.70
Sr	467	200		220	-24.70
Y	18	16	1.10	18	------
Zr	322	262	1.20	288	------
Nb	16	14	1.10	15	------
Mo	2	2		23	0.00
Pb	24	11		12	- 1.20
Th	28	26		29	+ 0.10
U	6	5		6	0.00

Altered Samples:

E510, E227, E222, E504, E505, E527, E502.

Table 6.3

Chemical enrichment and depletion in Hedgehope Granodiorite affected by K silicate 2 alteration (K2).

Average	Fresh Hedgehope 6 samples	Altered Hedgehope 2 samples	Immobile Fresh/ Altered	Altered x 1.1	Addition(+) Subtraction(-) in g/100 gm
SiO2	68.32	70.75		77.83	+ 9.51
TiO2	0.61	0.58	1.10	0.64	------
Al2O3	14.91	14.81	1.01	16.29	------
Fe2O3	1.49	1.08		1.19	- 0.30
FeO	1.51	0.82		0.90	- 0.61
MnO	0.06	0.02		0.02	- 0.04
MgO	1.67	1.20		1.32	- 0.35
CaO	2.02	1.14		1.25	- 0.77
Na2O	3.52	2.57		2.83	- 0.69
K2O	4.54	5.41		5.95	+ 1.41
P2O5	0.23	0.16	1.44	0.17	- 0.06
H2O	1.01	1.25		1.25	+ 0.24
TOTAL	99.9	99.7	------	------	mg/100 gm
Li	84	46		51	- 3.30
V	61	45		50	- 1.10
Cr	48	45		50	+ 0.20
Co	47	65		72	+ 2.50
Ni	26	21		23	- 0.30
Cu	16	18		20	+ 0.40
Zn	55	29		32	- 2.30
Rb	239	253		278	+ 3.90
Sr	307	81		89	-21.80
Y	18	9	2.00	10	------
Zr	205	197	1.04	217	------
Nb	15	18	0.83	20	------
Mo	3	3		3	------
Pb	23	18		20	- 0.30
Th	28	33		36	+ 0.80
U	8	9		10	+ 0.20

Altered Samples:

E415, E416.

Table 6.4

Chemical enrichment and depletion in Hedgehope Granodiorite affected by sericitic 2 alteration (S2).

Average	Fresh Hedgehope 6 samples	Altered Hedgehope 9 samples	Immobile Fresh/ Altered	Altered x 1.1	Addition(+) Subtraction(-) in g/100 gm
SiO2	68.32	71.08		78.20	+10.00
TiO2	0.61	0.47	1.30	0.51	------
Al2O3	14.91	14.79	1.00	16.27	------
Fe2O3	1.49	1.49		1.64	+ 0.15
FeO	1.51	0.94		1.03	- 0.48
MnO	0.06	0.04		0.04	- 0.02
MgO	1.67	1.11		1.22	- 0.45
CaO	2.02	0.71		0.78	- 1.24
Na2O	3.52	2.79		3.07	- 0.45
K2O	4.54	4.91		5.40	+ 0.86
P2O5	0.23	0.18	1.30	0.20	------
H2O	1.01	1.49		1.64	+ 0.65
TOTAL	99.90	100.2	------	------	mg/100 gm
Li	84	60		66	- 1.80
V	61	38		42	- 1.90
Cr	48	31		34	- 1.40
Co	47	52		57	+ 1.00
Ni	26	19		21	- 0.50
Cu	16	9		10	- 0.60
Zn	55	54		59	+ 0.40
Rb	239	249		274	+ 3.50
Sr	307	160		176	-13.10
Y	18	18	1.00	20	------
Zr	205	179	1.10	197	------
Nb	15	15	1.00	17	------
Mo	3	3		3	0.00
Pb	23	23		25	+ 0.20
Th	28	27		30	+ 0.20
U	8	6		7	- 0.20

Altered Samples:

E166, E372, E371, E521, E418, E383, E555, E541, E376.

Table 6.5

Chemical enrichment and depletion in Linhope Granodiorite affected by propylitic alteration (P).

Average	Fresh Linhope 3 samples	Altered Linhope 6 samples	Immobile Fresh/ Altered	Altered x 1.1	Addition(+) Subtraction(-) in g/100 gm
SiO2	66.17	68.79		75.67	+ 9.50
TiO2	0.63	0.50	1.30	0.55	------
Al2O3	14.99	14.41	1.00	15.85	------
Fe2O3	1.46	2.37		2.61	+ 1.15
FeO	2.33	1.64		1.80	- 0.53
MnO	0.10	0.05		0.06	- 0.04
MgO	2.48	2.41		2.65	+ 0.17
CaO	2.56	1.39		1.53	- 1.12
Na2O	3.39	3.79		4.17	+ 0.78
K2O	4.40	2.54		2.79	- 1.61
P2O5	0.27	0.24	1.10	0.26	------
H2O	1.27	1.37		1.51	+ 0.24
TOTAL	100.1	99.5	------	------	mg/100 gm
Li	83	58		64	- 1.70
V	84	80	1.10	88	------
Cr	70	63		69	- 0.10
Co	37	41		45	+ 0.80
Ni	40	39		43	+ 0.30
Cu	21	12		13	- 0.80
Zn	81	60		66	- 1.50
Rb	214	125		138	- 7.60
Sr	384	271		298	- 8.60
Y	17	15	1.10	17	------
Zr	221	212	1.00	233	------
Nb	14	145	0.90	17	------
Mo	1	2		2	+ 0.10
Pb	20	8		9	- 1.10
Th	29	25		28	- 0.10
U	7	5		6	- 0.10

Altered Samples:

A6, E127, E126A, E126B, E108, A7.

for the altered rocks should be multiplied by about 1.1, so that comparison is between 100 g of original rock and the material that the rock has now become after addition. If now the average of the fresh rock is subtracted from the adjusted average of the altered rock, then element or oxide fluxes can be calculated expressed as g or mg/100g of original rock. These values appear in the final column of each of Tables 6.1 to 6.5. Table 6.7 summarises the chemical fluxes calculated in tables 6.1-6.5. Most striking is the addition of SiO2 during alteration to all assemblages, and to all except K1 on a scale of about 10%. This net addition can explain almost all of the dilution shown by the relatively immobile elements. Also added to all assemblages is water, while Ca and Sr are removed from all assemblages. K and Rb are added to all assemblages except for P, and Na and Mg are conversely subtracted from all except P. The reasons for this are the mineralogical changes described in the last section. The K/Rb ratio in the material added or subtracted ranges from 150 to 300.

Li is removed from all assemblages except S1, a fact that is not readily explained by mineralogical changes. Of the more mobile elements of economic interest, Cu is removed from K1, S2 and P, and added to S1 and K2, though in rather small amounts, while Zn and Pb behave in parallel, being removed from all assemblages except S2. In Table 6.6 the averages of 36 samples of the granodiorites are presented next to the different alteration types. This table is as a summary from which we could determined using the above techniques,

Table 6.6

Chemical variation in the fresh Cheviot Granodiorite (GD.) affected by different alteration types.

Average	Fresh GD. 36 samples	P 6 samples	S2 10 samples	K2 2 samples	S1 7 samples	K1 6 samples
SiO2	66.26	68.79	71.08	70.75	65.24	68.22
TiO2	0.71	0.50	0.46	0.58	0.76	0.64
Al2O3	15.14	14.41	14.89	14.81	14.66	15.50
Fe2O3	1.61	2.37	1.45	1.08	1.09	1.55
FeO	2.11	1.64	1.02	0.82	2.28	1.58
MnO	0.08	0.05	0.04	0.02	0.06	0.06
MgO	2.34	2.41	1.08	1.20	2.10	1.62
CaO	2.82	1.39	0.61	1.14	2.83	0.98
Na2O	3.58	3.79	2.92	2.57	2.56	2.68
K2O	4.19	2.54	4.93	5.41	5.45	5.52
P2O5	0.26	0.24	0.17	0.16	0.26	0.22
H2O	1.04	1.37	1.51	1.14	2.16	1.74
TOTAL	100.1	99.5	100.2	99.7	99.5	100.3
Li	74	58	45	46	69	54
V	79	80	44	45	75	64
Cr	66	63	30	45	59	44
Co	39	41	47	65	34	46
Ni	36	39	16	21	30	29
Cu	20	12	13	18	23	10
Zn	73	60	67	29	60	64
Rb	198	125	251	253	265	263
Sr	388	271	168	81	200	231
Y	18	15	18	9	16	19
Zr	257	212	193	197	262	259
Nb	2	15	15	18	14	17
Mo	25	2	3	3	2	3
Pb	29	8	30	18	11	18
Th	29	25	28	33	26	28
U	6	5	6	9	5	4

Table 6.7

Summary of chemical changes accompanying the development of each alteration assemblage (+ is net addition, - is net subtraction; oxide fluxes are quoted in g/100g of parent, element fluxes as mg/100g of parent).

Average	K1	S1	K2	S2	P
SiO2	+ 0.7	+ 7.3	+ 9.5	+ 10.0	+ 9.5
MgO	- 0.2	- 0.6	- 0.4	- 0.5	+ 0.2
CaO	- 1.4	- 0.4	- 0.8	- 1.2	- 1.1
Na2O	- 0.9	- 0.9	- 0.7	- 0.5	+ 0.8
K2O	+ 0.9	+ 2.2	+ 1.4	+ 0.9	- 1.6
H2O	+ 0.9	+ 1.4	+ 0.2	+ 0.7	+ 0.2
Li	- 2.4	+ 1.7	- 3.3	- 1.8	- 1.7
Cu	- 1.0	+ 0.1	+ 0.4	- 0.6	- 0.8
Zn	- 0.9	- 0.8	- 2.3	+ 0.4	- 1.5
Rb	+ 3.9	+11.7	+ 3.9	+ 3.5	- 7.6
Sr	-10.5	-24.7	-21.8	- 13.1	- 8.6
Pb	- 0.4	- 1.2	- 0.3	+ 0.2	- 1.1

the estimated values of the net addition and subtraction in g/100g or in mg/100g for the different alteration types.

The contrast between the elemental fluxes during propylitic alteration and those during the development of the other assemblages suggests that possibly propylitic alteration may have been proceeding with potassic and sericitic alteration, and acting as a source of potassium and rubidium for the other alteration and a sink for sodium and magnesium released. In this case the cation sum of Mg and Na changes might be equal and opposite to the change in K and Rb, and the ratio of the change in K to that in Rb would be the same in all rock types. Both of these are approximately true, but not precisely enough to say whether this model is preferred to the more normal one where the propylitic alteration is produced later than the other alteration, and from meteoric rather than magmatic water. A rather extensive programme of isotopic analysis would be needed to make a definite decision.

CHAPTER SEVEN

CONCLUSION

CHAPTER SEVEN

CONCLUSION

7.1 INTRODUCTION

Since understanding of the geological history of the Cheviot Granite is the aim of this thesis, it is important at this stage to introduce the important events which set the present geology in the area.

7.2 GEOLOGICAL SETTING

In order to set the scene of the geological setting of the Cheviot Granite in relation to the regional Caledonian granites situated immediately N and S of the Iapetus suture (Phillips, et al. 1976) the following factors must be taken in consideration,

7.2.1 ORDOVICIAN-SILURIAN PALAEOGEOGRAPHY

Faunal and structural evidence (cited in McKerrow, et al. 1977) suggest that a wide ocean was present between the Southern Uplands of Scotland and the English Lake District, and this ocean was very broad in the early stages (Late Cambrian). During the Late Ordovician and Silurian periods the Southern Uplands were situated on the continental margin of North America, where the Iapetus Ocean was

being subducted and consequently narrowed. It is generally agreed that the active subduction zone dipped towards the NW during this period. The Southern Uplands has been divided stratigraphically into three units (Peach and Horne, 1899). The Southern Belt, in which both the Criffell pluton and the Cheviot pluton are situated, consists of Wenlock greywackes and shales, some of which contain graptolites. The Central Belt, in which Cairnsmore of Fleet pluton is situated, consists of greywackes overlying Moffat Shale successions of mid Ordovician to Llandovery (Lower Silurian) shales, ashes and cherts. In The Northern Belt, in which the Loch Doon complex lies, is entirely of Ordovician age. There mafic volcanics, bedded cherts and, in some places, graptolitic shales underlie greywackes. During the Ordovician and Silurian periods the Southern Uplands was an active margin similar to the modern active margins where a thick sediment cover exists on the ocean plate entering the subduction zone. Packets of sediment were sequentially offscraped from the undergoing plate, being far less dense than ocean-floor basalt. Where this process occurs for prolonged periods, a deformed pile of sediment, known as accretionary prism, builds up in the fore-arc region (Leggett, et al. 1979). However the initial detachment planes of the accreted packets of sediment are commonly manifested in seismic profile (e.g. Seely, et al. 1974) as regularly spaced major fault planes. These are initially-low angle features, later rotating to a higher angle as the accretionary complex builds up. In the Southern Uplands the major fault-bounded tracts in the area are interpreted as individual accreted packets of ocean floor

and trench sediment, added in sequence. Prolonged accretion gives rise to a ridge feature, the trench slope break (Dickinson, 1973) at the top of the tectonically rising lower trench slope, which formed in the Southern Uplands the continuous ridge known as Cockburnland. In the Southern Uplands, the trench slope break was probably completely below sea level during the late Ordovician. The first evidence for emergence is the appearance of the southerly-derived turbidites in the Lower Silurian in the Midland Valley. The modern active margin of NW Sumatra (Karig, et al. 1980) with its wide fore-arc basin can considered to be a representative modern analogue.

7.2.2 CALEDONIAN OROGENY

Generally the Caledonian orogenic cycle constituted a crucial event in the geological evolution of NW Europe. In the early stages of this cycle as mentioned above the continents were separated by Iapetus Ocean, which opened about the beginning of the Cambrian period and closed in the Late Silurian/Early Devonian (Dewey and Shackleton, 1984) as a result of a collision orogeny involving the large continental plates of Europe and the North Atlantic continents (composed of what are now Greenland and North America) together with a number of smaller massifs which became trapped in the Collision zone (Dewey 1969, as cited in Watson 1984). So by the end of the Caledonian cycle (Late Silurian-Early Devonian), the province had become a coherent entity welding the European and North Atlantic continents and was elevated to form a single large landmass (the Old

Red Sandstone continent). However the former site of the ocean is the present Iapetus suture which separates the English Lake District from the Scottish Southern Uplands via the Solway Firth.

At the end of the Caledonian Cycle the area was subjected to great erosion following folding and uplift giving rise to a mountain belt resulting from probable oversteeping of the prism (Leggett, et al. 1979). As a result part of the area north of the suture became a basin of deposition (N Scotland), the floor of which was occupied by one or more lakes in which were deposited the Old Red Sandstone strata which were laid down on the upturned edges of older rocks, and consist of sandstone and conglomerates. Great thicknesses of these sediment appear to have flowed into the lakes where they were later covered by sediments which were partly lacustrine and partly fluviatile in origin. The Cheviot Hills (immediately N of the suture) comprised a high mountain plateau with deeply dissected upturned Silurian strata on which the Cheviot volcanic pile was constructed. The volcanic pile is associated with unfossiliferous red sandstone and marl which is the only representative in the region of beds of possible Lower Devonian age.

7.2.3 THE SOUTHERN SCOTLAND AND NORTHERN ENGLAND IGNEOUS PROVINCE

Geographically the Cheviot Granite forms one of a group of granitic intrusions lying both north and south of the Iapetus suture, in the Southern Uplands, in the equivalent zone in Northern Ireland,

in the Lake District and in the Pennines. These granites provide a strong evidence of close links in space and time with the Cheviot Granite.

Location	Age	Determination Method	Ref.
Cheviot	390	K-Ar	5
SOUTHERN UPLANDS			
Criffell	397+/-2	Rb-Sr minerals	4
Cairnsmore of Fleet	392+/-2	Rb-Sr minerals	4
Loch Doon	408+/-2	Rb-Sr minerals	6
MIDLAND VALLEY			
Distinkhorn	390	Rb-Sr	8
IRELAND			
Newry	399+/-2	Rb-Sr	7
LAKE DISTRICT			
Eskdale	390	K-Ar	8
Shap	394+/-4	Rb-Sr whole rock	2
Skiddaw	399+/-4	K-Ar micas	3
Weardale	410+/-10	Rb-Sr whole rock	1
Carrock Fell	386+/-6	K-Ar	3

References:

1. Holland and Lambert (1970)
2. Wadge, et al. (1978)
3. Shepherd, et al. (1976)
4. Stephens and Halliday (1979)
5. Mitchell (1972)
6. Halliday, et al. (1980)
7. Meighan and Neeson (1979)
8. Halliday, et al. (1979)

As these granites are mainly high-level intrusions, the dates are probably close to their time of intrusion. Their age range from approximately 408 to 390 Ma, corresponding to the Lower Devonian on the time scale of Harland, et al. (1982), would place them as post-collisional, since the Caledonian orogeny took place in the latest Silurian. They are also unaffected by Caledonian deformation,

and the Cheviot lavas overlie uptilted Silurian strata. They are characterised by their large volumes and low densities as expressed by strong negative gravity anomalies display by some of them, e.g. Weardale (Bott, 1966). Before reaching the conclusion of how the Cheviot pluton relates to these plutons, three examples from the Southern Uplands are taken for illustration. These are the Loch Doon pluton (field observation, petrology and geochemical data), Criffell-Dalbeattie (field observation) and finally the Black Stockarton Moor complex (west of Criffell, for its porphyry copper affinity).

1. Loch Doon pluton

This is situated in the Northern Belt (Peach and Horne, 1899). It is a complex intrusion, mapped by Gardiner and Reynolds (1932) as having entirely gradational contacts between the different units. The earliest, and outermost, unit is composed of two patches of dioritic rock, formerly called norite by Gardiner and Reynolds (1932), in which hypersthene and augite occur together with plagioclase and minor biotite. Olivine occurs rarely in the chilled facies near the margin and secondary actinolite (after pyroxene), ilmenite and interstitial quartz are also present. Moving towards the centre of intrusion quartz diorite, tonalite (with xenolithic material), granodiorite, granite and microgranite occur (Tindle and Pearce, 1981). The geochemistry is very similar to that of the Cheviot pluton, showing a very high level of incompatible elements (see above, Chapter 5). The presence of a large granitic batholith below Loch Doon has been

suggested by Brown and Locke (1979) on the basis of a residual gravity anomaly with an approximate amplitude of -18 mgals. Tindle and Pearce (1981) concluded that the Loch Doon pluton was the product of in situ fractional crystallisation of two distinct magmas controlled by separation of plagioclase, orthopyroxene, clinopyroxene and biotite. The main differences between Loch Doon and the Cheviot are the reported presence of gradational contacts in the former and the progressive change from more basic to more acid units towards the centre of the complex. In the Cheviot the contacts are sharp, and the units form intersecting ring structures.

2. Criffell-Dalbeattie pluton

This pluton lies in the Southern Belt of Peach and Horne, (1899). It is characterised by an ovoid outcrop some 27 km x 11 km (Phillips 1956). Most of the area comprises two rock types- an outer zone of biotite-hornblende-granodiorite and an inner porphyritic variety with microperthite megacrysts termed biotite-granite by Stephens and Halliday (1979). They considered that these units have no sharp contact. However the clear petrographic and chemical distinction of the two units suggests two separate magma pulses with a sharp contact between them. The granodiorite is surrounded by a metamorphic aureole up to 1.5 km wide, consisting of hornblende-diopside hornfels with veins of granodiorite penetrating the country rock. The margin of the granodiorite is described as being sharp and unchilled and xenoliths of wall-rocks are locally abundant.

3. Black Stockarton Moor complex

Since the above two examples show no hydrothermal alteration similar to that of the Cheviot area, an attempt was made to find an example which lies geographically near the Cheviot and which has an affinity with its alteration style. This is the Black Stockarton Moor complex which lies west of the Criffell-Dalbeattie pluton. In this example copper-molybdenum mineralisation occurs in close association with sill-like minor granodiorite intrusives and a swarm of porphyrite dykes intruded into the Silurian mudstone, siltstones and greywacke of the country rocks. Geological mapping during follow-up of drainage geochemical anomalies revealed multiphase intrusion of minor intrusive rocks in a subvolcanic complex. A reconnaissance drainage survey of the Criffell-Dalbeattie area indicated that samples from some streams that drain northwards from the Black Stockarton Moor area contained anomalous levels of copper. Two reconnaissance soil lines sampled across the uncultivated moorland proved an anomalous zone with levels that reached 900 ppm Cu; and this was correlated (over most of the area) with deep overburden anomalies, with a general increase in copper levels with depth at anomalies sites (Leake and Brown, 1979).

Field relationships indicate that the intrusions are coeval with the Criffell-Dalbeattie complex (Leake and Brown, 1979) which has been dated at 397+/-2 M.Y. (Halliday, et al. 1980). At Black Stockarton Moor a linear zone of chloritic alteration (our

propylitic zone) is developed, in which hornblende/actinolite, epidote, calcite, pyrite, arsenopyrite and other minerals occur mostly in replacement and fissure-type veinlets in hornfelsed country rock. The extent of this zone appears to be related to the outcrop of the granodiorite. Immediately to the east of this is a narrow zone of pyrite enrichment in sericitically altered country rocks and granodiorite, and in some areas further east, low grade chalcopyrite-bornite-chalcocite-molybdenite mineralisation occurs in quartzose veinlets in sericitically altered granodiorite. Furthermore, the most heavily mineralized zones are located in highly brecciated sedimentary rocks. This brecciation thought to be produced at the time of intrusion either by retrograde boiling or perhaps by release of fluid after the rapid reduction of confining pressure as magma reached a relatively high crystal level (This is similar to the brecciation associated with both Dunmoor and Hedgehope Granodiorites). The nature of alteration and mineralisation bears a resemblance to the porphyry-type mineralisation of Lowell and Guilbert (1970).

There are a number of similarities between the Cheviot pluton and these three examples:

1. Within each pluton there is gradation in composition of different intrusive phases characteristic of calc-alkaline terrains.
2. Two phases of magmatism are involved in generating each pluton.
3. The Loch Doon geochemistry (major and trace elements) of both

magmatic cycles 1 and 2 show a great similarity with the Cheviot intrusive phases as shown in Table 5.4.

Our field observations in the Cheviot area show some clear differences:

1. The Cheviot Granite is a comparatively simple type of multiple ring structures in which the two major cycles of magmatic activity can readily be distinguished.
2. Field evidence demonstrates that the present level of erosion is near the roof (see later), which shows the Cheviot Granite to be located at a higher structural level than the other plutons of the Southern Uplands, leading to intrusion into comagmatic andesites.
3. There are clear internal contacts between the different phases of granitic intrusion.
4. There is no sign of mineralization in the Cheviot area (in particular in the SE area-south east of the Harthope Fault), although hydrothermal alteration occurs.

It seems probable that these differences are due to the fact that the Cheviot Granite occurs at a high level relative to the other plutons of the Southern Uplands. Other N England / S Scotland granites are different from the Cheviot Granite. The intrusions considered are the Weardale Granite (Dunham, et al. 1965; Holland, 1967); the Cairnsmore of Fleet granite (Parslow, 1964) and the Skiddaw Granite (Hitchen, 1934). Of

these, Read (1961) has included the Skiddaw and Cairnsmore of Fleet granites in his category of "Forceful Newer Granites". The similarity of the Cairnsmore of Fleet granite trace element pattern to that of the Skiddaw Granite extends to the major element and mineralogy (Parslow, 1964; Hitchen, 1934). The Weardale Granite is also very similar to the Skiddaw Granite - Dunham, et al. (1965) stated "The Weardale granite is most like the Skiddaw granite (Hitchen, 1934) in its mineralogy and composition". These intrusions in turn are very granitic in composition and are clearly very different to the broadly granodioritic composition of the Cheviot Granite.

The minor element abundance pattern in the Shap Granite (Grantham, 1928) is clearly very similar to that of the Cheviot Granite, though the Shap Granite displays the presence of the well-known large feldspars. Comparison of the Criffell Dalbeattie (Macgregor, 1937) with the Cheviot Granite shows that the earliest stage of the Criffell Dalbeattie multiple intrusive corresponds in composition very closely to the Marginal Granodiorite of the Cheviot Granite. However the differentiation trend in the Criffell Dalbeattie complex is very different from the Cheviot trend which might be attributed to the precipitation of hornblende instead of the pyroxene characteristic of the Cheviot. Nonetheless, the similarities of the Cheviot, Shap and the earliest stage of the Criffell Dalbeattie granites are sufficiently marked to suggest that the magma source of these

plutons may have been related. However there is still the possibility that some of the features that have been found in the Cheviot during this work will now be discovered in the other complexes.

7.3 IGNEOUS HISTORY OF THE CHEVIOT COMPLEX

Stratigraphical and palaeogeographical evidence points to the conclusion that the Iapetus Ocean was effectively closed before the end of the Silurian period (Watson 1984). If, as seems probable, active subduction beneath the Cheviot and the Southern Uplands region had ceased by this time (408 Ma on the time scale of Harland, et al. 1982) it is difficult to envisage a direct role for the subduction process in the formation of volcanicity in this region. In Chapter 5 it was shown that the Cheviot Granite falls very close to the border between the VAG + syn-CoLG field on the Rb against (Y+Nb) diagram of Pearce et al. (in press), Figure 5.7. Taken together with the Benioff zone calculation (190 km), this might indicate that the Cheviot complex formed in an early collision environment, perhaps above a remnant slab of oceanic lithosphere still descending beneath the collision orogen. Such evidence is consistent with the regional stratigraphic and structural evidence (Phillips, et al. 1976). The geochemical affinities between the Cheviot lavas and the modern arc volcanoes, and perhaps the evidence for lateral geochemical variations in lower Devonian magmatism (Thirlwall 1981) can be reconciled with the relationships outlined

above if we adopt a two-stage process like that favoured for some modern arc volcanism (e.g. Gill 1982). In this model fluids expelled from a down-going slab of oceanic crust rise into and metasomatically alter the overlying mantle wedge during the stage of active subduction. Partial melting in the pickled mantle may subsequently give rise to volcanic and plutonic suites with arc characteristics. Block movements (e.g. subsidence of blocks bounded by circular ring-fractures) on dislocations may be propagated down into the mantle from above and cause the partial melting of the metasomatised mantle, permitting the ascent of magma into the space potentially provided as permitted or passive intrusions (Read, 1961). It would follow from these proposals that lateral variations may have been developed in the lithospheric mantle as a result of variation in volume and chemical composition of the fluids introduced from an underlying subduction zone (Watson 1984) and that variation in composition of the post-orogenic magmas (Thirlwall, 1981) would be related to the variations in composition generated in the mantle.

The earliest evidence of magmatic activity from the Cheviot volcano comes from the andesite lavas. Forty samples of the Cheviot andesite were analysed for major and trace elements by Thirlwall (1981). Their average is compared with the mean composition of the Marginal Granodiorite in Table 7.1. This comparison show that the average andesite is slightly more basic than the Marginal Granodiorite. Thus from the earliest period of volcanism there is evidence for the existence of magma very similar to that which formed

Table 7.1

Comparison between The Cheviot Marginal Granodiorite (present study) and mean of 40 andesitic samples from The Cheviot Hills (Thirlwall, 1981).

ROCK TYPE	Marginal Granodiorite	Andesite (Thirlwall, 1981)
SiO2	64.42	63.20
TiO2	0.83	0.91
Al2O3	15.33	16.01
FeO *	4.35	4.92
MnO	0.09	0.07
MgO	2.94	3.00
CaO	3.53	3.85
Na2O	3.71	3.57
K2O	3.81	3.94
P2O5	0.30	0.31
H2O	1.01	----
Total	100.30	99.78
Cr	90	78
Ni	41	54
V	95	91
Sc	6.1	13
Cu	24	21
Zn	74	92
Sr	467	490
Rb	175	140
Th	28	23
Zr	322	289
Nb	16	15
La	47	58
Ce	88	118
Nd	32	45
Y	18	20

the later granodiorite intrusions. This reveals the existence of a long lived magma chamber of nearly constant composition which was responsible for the early part of the Cheviot igneous history, and continued in being through certainly the first and perhaps also the second plutonic cycle seen in the granite complex at the present levels of erosion. Chapter 5 has given evidence that individual granodiorite bodies have evolved from one another by crystal fractionation, with particularly strong evidence from major element variation, and the balance of evidence must be that it is the most important process operating.

At a very early stage a cauldron subsidence probably formed when a block of greywacke and argillites perhaps overlain unconformably by a sequence of Old Red Sandstone rocks, subsided on a ring fault such as in the Glencoe Cauldron (Roberts, 1974). This episode of cauldron subsidence at depth was accompanied by the extrusion of lavas (andesite, rhyolite and ignimbrite), welling up the sides of the sinking block, thereby building up the early caldera with lava flows stretching at least 20 km from its centre. With time, the volcano rose possibly between 2.5-4 km above surrounding plateau to judge from the dimensions of modern volcanoes with a similar diameter at the base. The eruption of ignimbrite (at Knock Hill 990170) points out the culmination of the volcanic activity and the formation of the caldera. The association of andesite lava with rhyolite suggests that the composition of the magma in the chamber was approximately similar to that of the Marginal Granodiorite with occasional

development of granitic magma by extreme fractionation. An immense out-pouring of lavas occurred at this stage which even after extensive erosion covers an area of 600 square km. Non of the previous workers record possible feeders to the andesite lavas in the Cheviot, and it seems probable that subsequent events in the geological history of the cauldron would have destroyed the evidence whereby these feeders could be recognised.

The emptying of the magma chamber in this way allowed the central block to subside further into the magma chamber while the magma intruded towards the surface (Figure 2.4) metamorphosing the andesite which resulted from this subsidence. The essential elements of the mapping for this thesis showed that the complex is made up by cauldron subsidence, where a centrally placed granodioritic pluton is enclosed within a multi-component ring dykes (Figure 2.1). Within this cauldron, repeated subsidence and intrusion has led to the progressive obliteration of the initial stages of its evolution, resulting in the rocks concerned (the Marginal, Dunmoor, and Standrop Granodiorites) being preserved as remnants (Figures 2.1 and 2.3). However from their distribution and on the basis of the evidence of the chilled contacts of the units that pass across variable topography with little deflection, intrusive margins are clearly dipping rather steeply. It appears that migration of the magma upward has taken place along a ring fractures such as that cutting the andesite at Cunyan Crags where it was intruded by the Marginal Granodiorite. It is likely that this magmatic mass could go on

rising up to a shallow level until the pressure of water vapour in the liquid became equal to the total pressure, and the liquid reached the wet melting curve for granite, a curve which granite cannot pass as a liquid (Cann, 1970). In the case of the Marginal Granodiorite, Figure 5.12 suggests that it contained a rather high content of water. Once the Marginal Magmatic mass, which did not seem to migrate far away from the magma chamber, rose upward it reached the wet melting curve, at which it started crystallising until it was completely solid producing rocks of equigranular texture and releasing water as pegmatitic fluid of lower melting point, which could percolate upwards until it eventually solidified in the form of the quartz veins associated this body such as those at Linhope Spout Waterfall 959169.

The Marginal Granodiorite forms the outermost and oldest member of the complex , and is a fine - to medium-grained grey granodiorite, allotriomorphic, slightly more basic in its mineral assemblages than the other granodiorites. It is composed of subhedral feldspar (zoned plagioclase) typically amounting to about 50 per cent of the rock, subordinate orthoclase and perthite 10- to 12 per cent and allotriomorphic quartz 17- to 19 per cent. The principal dark minerals are clinopyroxene (augite up to 4 per cent), orthopyroxene (hypersthene up to 3 per cent) and biotite (up to 11 per cent). Accessory minerals are zircon, apatite, ilmenite and magnetite. Finally this granodiorite is characterised by the presence of an aggregations of interlocked pyroxene crystals which appear as dark

spots in the hand specimen, and were interpreted as very small xenoliths by Jhingran (1942), though there is no clear evidence that this is the case.

After its intrusion, the Marginal Granodiorite probably crystallised completely, as shown by the chilling against it of the next intrusive phase, and the straight and clear trace of that contact. After that period of hiatus in volcanic activity, another ring-fracture subsidence took place, allowing more fractionated magma from the underlying magma chamber to rise up to form the Dunmoor Granodiorite, which is the last intrusion of the first igneous cycle in the Cheviot area. It appears that the magmatic mass rose more or less along an adiabat, with its temperature decreasing as the confining pressure diminshes, until it reached the state at which total pressure was equal to water vapour pressure (Cann 1970). However, since this magmatic mass was not saturated with water vapour, it did pass the appropriate melting curve (Cann 1970) by partly crystallising, producing the crystallised solid, now seen as phenocrysts of pyroxenes, plagioclase and biotite, which contained less water than the Dunmoor magmatic liquid, so that the water content of the remaining liquid was increased. When the vapour pressure of water in the magma again reached the confining pressures the result now seems to have been the sudden release of water as a separate fluid phase, drying out the magma, raising its melting point, and thus causing very rapid crystallisation of the remaining liquid to produce a fine-grained groundmass. Such a two-stage

process would account for the porphyritic texture of the rock in which the phenocrysts are much larger, and the groundmass much finer grained, than the grain size of the crystals in the equigranular Marginal Granodiorite. The sudden release of water and the immediate crystallisation of the groundmass was associated with the development of the first hydrothermal alteration episode that brought to a close the first igneous cycle (see below).

The Dunmoor Granodiorite forms a crescentic intrusion in the south part of the Cheviot Granite (south of the Harthope Fault). North of its outcrop it has been obliterated by younger events. It represents the culminating phase of first igneous cycle. It is well exposed and its contact with the earlier Marginal Granodiorite can be clearly defined. Along its outer margin it is intrusive into the Marginal Granodiorite and the attitude of the contact is either vertical or of a very steep outward dip. On the inner margin it is, in turn, intruded by the coarse-grained Standrop Granodiorite which is the first intrusion of second igneous cycle. The Dunmoor Granodiorite is of porphyritic texture with large phenocrysts of plagioclase feldspar (zoned andesine), the plagioclase (i.e. both as phenocrysts and groundmass components) amounting to about 47 per cent of the rock , pyroxenes (both augite and hypersthene) amounting to about 5 per cent and finally biotite to about 7 per cent. The ground mass is usually composed of granophyric texture with quartz (both as interstitial and intergrowth part) between 22 to 29 per cent being intergrown with perthite alkali feldspar (up to 11 per cent) together with biotite

and plagioclase whereas accessory minerals are zircon, apatite, magnetite and ilmenite.

The emplacement of the second igneous cycle was preceded by a period of hiatus in volcanic activity during which the Dunmoor Granodiorite was completely consolidated. During this time, the underlying magma chamber was replenished by one or more injections of more basic magma, and the composition was returned to one very close to that of the Marginal Granodiorite. This new batch of magma had some what different K and Zr contents than the previous one, so that the relationships between K, Zr and (CaO+MgO) were displaced during the second cycle from those of the first cycle (see later). At this stage another subsidence on a ring fault seems to have taken place, when a thick accumulation of igneous material, consisting of components of the first igneous cycle and perhaps some andesites, subsided into the underlying magma chamber and permitted the magma to migrate upwards and form the largest intrusion in the Cheviot complex at the present time which is the Standrop Granodiorite. The rocks from the hills of Great and Little Standrop, where this intrusion phase is particularly well developed, display the typical petrographic feature of this group. It is again well exposed and its contact with the earlier Dunmoor Granodiorite can seen locally such as at (918168) near Shielcleugh Edge and with the later Linhope Granodiorite at Linhope Burn (948172) where the chilling contact of the Linhope Granodiorite against the Standrop Granodiorite is extremely clear. These granodiorites (the Standrop and Linhope) are

the coarsest phases in the complex but it is very difficult to distinguish between their weathering surfaces in the field. Their coarse grained characteristics indicate that the magma began to crystallise at a relatively deeper level (i.e. deeper than the Marginal magmatic mass) when its water pressure was equal to the total pressure. The crystallisation path followed by this intrusion is very similar to that displayed by the Marginal Granodiorite. Therefore a slow crystallisation occurred giving rise to coarse grained rocks and releasing the excess water as pegmatitic fluid of lower melting point, which percolated upward and solidifies to form those large quartz veins attached to and associated with this intrusion phase. Thin sections show that the Standrop Granodiorite is coarse and granular with plagioclase feldspar (zoned andesine), typically amounting to about 50 per cent of the rock, pyroxenes (both augite and hypersthene up to 6 per cent) together with biotite (up to 12 per cent), quartz (up to 21 percent) and alkali feldspar (up to 10 per cent). Accessory minerals are apatite, zircon, ilmenite and magnetite. Finally the apparent filling of the centre of the complex by this phase of intrusion and the abundance of large xenoliths of hornfels (perhaps roof pendants) in the area east of Langleeford (9521 and 9621) indicate that stoping occured in addition to block subsidence during the emplacement of this granodiorite.

The Linhope Granodiorite that succeeds the Standrop Granodiorite is only seen at two places in the floor of the valley of the Linhope Burn, in one of which (948172) a flat horizontal contact is seen ,

with the Linhope Granodiorite chilled from below against the Standrop Granodiorite above. The Linhope Granodiorite thus may form a ring dyke, the top of which is near the present level of erosion. The Linhope granodiorite is less evolved chemically than the Hedgehope Granodiorite, and thus is believed to predate it. The crystallisation of the Linhope Granodiorite, a coarse, equigranular rock, probably followed a similar course to that of the Standrop Granodiorite. Thin sections show that this granodiorite is coarse, granular in texture with plagioclase (zoned andesine, up to 49 per cent), pyroxenes (both augite and hypersthene up to 5 per cent), biotite (up to 8 per cent) together with quartz (up to 23 per cent) and alkali feldspar (both orthoclase and perthite up to 12 per cent) whereas accessory minerals are apatite, zircon, magnetite and ilmenite.

Following the intrusion and complete consolidation of the Linhope Granodiorite another block subsidence on a ring fault caused the emplacement of a horse-shoe shaped ring dyke which is entirely enclosed by the Standrop Granodiorite. The chilling relation against it is seen locally as on the NW side of Hedgehope Hill at 938203. This granodiorite is well developed on Hedgehope Hill.

The Hedgehope Granodiorite is porphyritic with large phenocrysts of plagioclase (zoned andesine which amount up, both as phenocrysts and groundmass constituent, to 45 per cent) , pyroxenes (both augite and hypersthene which amount up to 5 per cent) in a groundmass of

quartz (up to 23 per cent), orthoclase microperthite (up to 20 per cent) and biotite (up to 6 per cent). Accessory minerals are zircon, apatite, ilmenite and magnetite. The crystallisation path undergone by the Hedgehope Granodiorite magmatic mass must have been very similar to that of the porphyritic Dunmoor Granodiorite (see above). An earlier phase of crystallisation at deeper levels was succeeded by rapid expulsion of water coupled with crystallisation of the finer groundmass as the magma reached its present structural levels. This was responsible for producing the porphyritic texture and also for initiating the second hydrothermal cycle.

The final igneous phase is not very well exposed in the southern part of the complex and its contacts with the earlier intrusive phases are not seen. However its evolved chemical composition and fine equigranular grain size suggest that it is the last liquid from the magma chamber. This is the Woolhope Granite which comprises the culminating phase of the second magmatic cycle and is well developed at Woolhope Crag 924223. This phase is most probably, like the previous intrusions, emplaced along a ring fault as a result of block subsidence, though the field evidence is not clear. The Woolhope Granite is a widespread rock type NW of the Harthope Fault. In chapter 2 it was argued that there it and the Hedgehope Granodiorite form flat intrusive sheets, demonstrated by contacts keeping close to contours, which overlie the subsiding blocks of earlier intrusive phases (see Figure 2.2). On this interpretation the SE part of the complex would represent a lower structural level than the NW part,

elevated during later movements on the Harthope Fault. If this is so, similar sheets of Woolhope Granite and Hedgehope Granodiorite would have previously overlain the SE part of the complex. Veins of Woolhope Granite type are found within the Marginal Granodiorite both at Dunmoor Hill 967174 and at Bellyside Hill 907222 as well as with in the Dunmoor Granodiorite at Dunmoor Hill 967177. These veins may represent the feather edge of intrusion of the Woolhope Granite in a South-easterly and a North-Westerly directions. Thin sections show that this granite is fine grained and composed mainly of quartz (up to 40 per cent), orthoclase (up to 20 per cent), plagioclase (mostly albite , up to 20 per cent) and biotite (between 10- to 13 per cent). In addition disseminated tourmaline with or without sericite occurs which is mostly an alteration product of biotite and feldspar (plagioclase in particular). In addition accessory minerals such as apatite, magnetite, zircon and ilmenite occur.

Discrimination diagrams are displayed in Chapter 5 in which Zr and K2O are plotted against (Cao+MgO), where (CaO+MgO) is used an index of evolution of the igneous rocks. An excellent separation of the two cycles is produced, with cycle 1 showing a relatively higher Zr and K2O contents than cycle 2. In addition to that Zr values of cycle 1 decrease slightly from the more basic Marginal Granodiorite to the more evolved Dunmoor Granodiorite, while the Zr values of cycle 2 show a more marked and persistent decrease with evolution from the Standrop Granodiorite to the Woolhope Granite, presumably as a result of precipitation of zircon from the evolving magma (Figures

5.14a and b). Another clear separation between the two igneous cycles of the complex is shown by the Q, Or and Ab diagram (Figure 5.12).

The strong contrast in chemical analysis between the latest phase (the Woolhope Granite) and the most evolved granodiorite in cycle 2 (the Hedgehope Granodiorite) can be attributed to the strong influence of the minor phases on the chemical fractionation in the granites, though it did not seem appropriate to attempt a detailed fractionation calculation. However it seems qualitatively likely that this later stage fractionation would have been controlled by rather similar phases to those deduced in the granodiorites, though with a larger component of the minor phases present in the crystallising solid.

Two hydrothermal systems are recorded in the area of which the space-time relationships can be summarised as follows.

1. Hydrothermal System A:

   The emplacement of the porphyritic Dunmoor Granodiorite as a high level ring dyke was accompained by radial fracturing, as shown by the groups of dykes with the same composition and petrography as the Dunmoor Granodiorite which are found cutting the Marginal Granodiorite.

Much of the hydrothermal alteration associated with system A is apparently similarly fracture-controlled, either by the Breamish Fault or by related fractures in the Bleakhope region. It was argued above that the porphyritic nature of the granodiorite was connected with its releasing large volume of water as it crystallised. The fractures created by the intrusion seemed to have acted to localise the hydrothermal alteration effects. Both juvenile water released from the magma and meteoric water were probably involved, as has been demonstrated by isotope studies on other areas of porphyritic alteration, but the necessary evidence to prove this was not collected in the Cheviot.

The highest temperature alteration was in the K1 zone, where solutions, probably dominantly igneous, acted to replace plagioclase by secondary orthoclase and pyroxenes by secondary biotite, and strip both calcium and sodium from the parent rocks. This zone is spatially centred on the west end of the outcrop of the Dunmoor Granodiorite. The K1 zone is surrounded by, and partly overprinted by, the S1 sericitic alteration zone, which is found also in isolated occurrences nearby. This type of alteration affects the Dunmoor Granodiorite, the dykes it sends off into the Marginal Granodiorite, and the Marginal Granodiorite itself, , transgressing lithological boundaries. The overprinting on the K1 zone shows that, while the S1 alteration may have started at the same time as the K1 alteration, it

continued after the K1 alteration stopped. Rocks belonging to this zone can show wholesale replacement of primary silicates by sericite, quartz, calcite, chlorite and albite, and destruction of original igneous textures. There seems a special association of this type of alteration with the dykes sent off by the Dunmoor Granodiorite, and it is possible that they may have been able to act as pathways for the solutions shortly after their intrusion. The chemistry of this type of alteration involves retention of calcium in the rock to some extent, because of the presence of calcite as an alteration mineral. Potassium and rubidium are introduced and accommodated into the secondary mica (sericite). The solution acted to replace both feldspar (plagioclase in particular) by sericite and pyroxene and biotite by secondary calcite and chlorite, and strip both magnesium, manganese, sodium and strontium from the parent rock.

2. Hydrothermal System B:

As in the case of system A, this system seems to have been initiated by the rapid expulsion of water from granodiorite magma, producing sudden crystallisation of the magma to give a porphyritic texture, together with the release of juvenile water. The highest temperature style of alteration here, the K2 zone of potassic alteration, is confined to a single small area set in the Hedgehope Granodiorite, the porphyritic intrusive that appears to have initiated hydrothermal alteration. In this zone, secondary orthoclase and biotite, with or without albite, are characteristic alteration minerals. Again it is likely that

juvenile water was predominant during this alteration. Surrounding this zone, and also occurring in scattered places widely over the central part of the complex, is the sericitic style of alteration associated with this system, S2 (see Figure 3.1). This affects the Hedgehope Granodiorite itself, the dykes it sends off into the complex, and both of the granodiorites forming earlier in cycle 2, the Standrop and Linhope varieties. This type of alteration has as its most characteristic mineral tourmaline, and its most common occurrence as associated with networks of narrow veins cutting the granodiorites. The alteration destroys the primary texture of the rocks and replaces it with the assemblage sericite (or muscovite), tourmaline, chlorite, albite +/- epidote +/- calcite. This type of alteration, though sometimes associated with major fractures, is more disseminated than the earlier phase of sericitic alteration, being often associated with micro-veining or incipient brecciation of the rocks. Such a mode of occurrence is more typical of porphyry-style alteration in general.

Alteration of S2 type, though closely associated with the Hedgehope Granodiorite, apparently continued to remain active up to the time of emplacement of the Woolhope Granite. The occurrence of tourmaline in the granite seems to be related to contemporaneous hydrothermal circulation of this type.

The chemistry of the S2 alteration episode is markedly different from that of the S1 episode, though both have a sericitic petrography. The calcite characteristic of S1 is much less developed in S2. This is indicated by the relative stripping of calcium, sodium, strontium and lithium, where the solution acted to replace plagioclase to sericite, minor calcite, tourmaline and epidote.

Surrounding the sericitic alteration areas, and sometimes overprinted on them, is the lower temperature propylitic alteration. Though probably active during earlier phases of hydrothermal activity, the propylitic style continued after the higher temperature circulation had finished, and the system, probably containing mostly meteoric water, gradually encroached on the earlier zones as the overall temperature fell and the magmatic water became exhausted. Typical propylitic assemblages are actinolite + epidote + albite + chlorite +/tourmaline +/- sericite +/- calcite, essentially those characteristic of greenschist facies metamorphism. Tourmaline is patchy in its occurrence within this system, but in some places is clearly an integral part of alteration assemblage. The geochemistry of the propylitic alteration is dominated by depletion in Ca (and Sr) and enrichment in Na resulting from the mineralogical changes. Among these changes are the replacement of plagioclase by albite and epidote, biotite by chlorite and pyroxenes by secondary actinolite.

Finally it is interesting to ask why the Cheviot granite complex is not a host to a porphyry copper deposit. Most of the complex has

an appropriate granodioritic composition, and each igneous cycle contains a porphyritic member which is associated with a system of porphyry-style hydrothermal alteration. The level of erosion seems appropriate: many porphyry copper deposits seem at a similar level-with the granite intruding the lower part of the volcanic pile. Yet Haslam (1975) and Leake and Haslam (1978) found very small geochemical anomalies. The stream sediment samples (Haslam, 1975) showed an area of weak anomalies in the SW corner of the complex near Low Bleakhope, and milder anomalies still in one or two places in the north part of the complex. The panned concentrates (Leake and Haslam, 1978) showed mild copper anomalies near low Bleakhope as well, but little in the northern area. Thus if there is some copper mineralisation it is likely to be in the SW part of the complex associated with hydrothermal system A. The same area is also anomalous in Zn, Ba and Pb, and this association suggests that any mineralisation there is not likely to be of porphyry copper type, but low-temperature vein mineralisation of the kind found scattered widely in the area.

The altered granites are remarkably poor in sulphides. Sericitic alteration associated with porphyry copper deposits is usually accompained by the development of abundant pyrite disseminated through the rock. There is little pyrite now to be seen in sericitically altered samples in the Cheviot and no sign that much more was ever present. The key problem thus seems to be a general lack of metal sulphides, not just of copper. There are two ways in

which such a situation might arise -if the circulating solutions were poor in sulphide, or if they were very rich in sulphides and could not transport metals as well. The second possibility seems less likely. If the solutions were so sulphide-rich, then they would be expected to have sulphurised the iron oxides in the rock, and yet these remain apparently in their primary state.

Sulphide in porphyry copper deposits has been shown by S isotope analysis to be most probably magmatic in origin (Ohmoto and Rye, 1979). Sulphur-poor hydrothermal solutions in the Cheviot thus suggest sulphur-poor magmas feeding the complex.
Why might the magmas have contained so little sulphur? Could it have been because the volcanism was not in a normal subduction zone environment, but in a post-collisional tectonic setting? Further research may give the answer.

APPENDIX A

ANALYSIS METHODS (EXCLUDING RARE EARTH ELEMENTS)

Appendix A

ANALYSIS METHODS

SUMMARY OF TECHNIQUES

1. X-RAY FLUORESCENCE ANALYSIS (XRF)

   For trace elements Pb, Th, Rb, U, Sr, Y, Zr, Nb, Mo.

2. ATOMIC ABSORPTION SPECTROMETRY (AAS) / COLORIMETRY

   For major elements Si, Al, Fe, Ti, Ca, Mg, Na, K, Mn, P.

3. ATOMIC ABSORPTION SPECTROMETRY

   For trace elements Zn, Cr, Cu, Pb, Ni, Co, Li, Rb, Sr, V.

4. GRAVIMETRIC METHOD

   For combined H_2O.

PREPARATION OF THE ROCK POWDER

Rock samples were prepared for analysis by reducing a suitable-sized hand-specimen to approximately 0.5cm-sized fragments with a hammer. These were shattered using a tungsten carbide mallet and plate, and then ground to a fine powder (less than 75μ) in a tungsten carbide-lined TEMA mill. Grinding time was kept to a minimum (30 seconds) to minimize contamination and oxidation caused by heating effects during grinding.

A-1 XRF TRACE ELEMENT DETERMINATION

A-1.1 OUTLINE

Samples in the form of pressed powder pellets were irradiated using an X-ray tube with tungsten anode; for Rb, Sr, Y, Zr, Nb, and Mo the characteristic emitted K_a radiation was measured, while for Pb, Th and U the L_a or L_b lines were counted. After correction for overlapping lines, the peak/background ratio was used to measure concentration of each element. Spiked rocks of similar overall composition were analysed to calibrate the instrument.

A-1.2 PELLET PREPARATION

Each sample pellet was prepared for analysis by the following method:

1. Approximately 12g of the rock powder was weighed out (enough to give a pellet infinitely thick to X-rays).
2. A small amount (approximately 21 drops) of a binding agent (Poly-vinyl alcohol solution) was added to the rock powder and well mixed.
3. The mixed powder was then placed between polished 4cm diameter dies and pelleted in a hydraulic press at 12 tons for a period of two minutes.
4. The powder pellet was then dried at approximately 34°C overnight, and stored in a desiccator.

A-1.3 EQUIPMENT AND OPERATING PARAMETERS

Spectrometer	Philips PW1410, with PW1730 generator, PW1930 channel control and W/X-ray tube.
Tube potential	60 kV
Tube current	40 mA
Spinner	On
Collimator	Coarse
Filter	Out
X-ray path	Air
Crystal	LiF 200
Counter	Scintillation (counter potential 1810 v)
Dead time corrector	On
Gain	128
Window settings :	Lower level 390
	Window 400
Counting time	40 sec

The optimum wavelength setting (i.e 2θ value)for each element was determined by scanning over a 2θ range using a spiked quartz sample. Pulse height conditions (window settings) were determined by an energy scan with the same sample. Background counts were measured at 5 angular positions (spread over the whole range) which show minimum overlap by the principal peaks (see tables A.1, A.1a for complete set of 2θ values).

A-1.4 CALIBRATION

1. Determination of Background Curvature:

Blank samples (i.e materials containing none of the elements being determined) were counted at all peak and background positions to determine the shape of the background curve and enable the background at each peak position to be calculated from the (corrected) value of a nearby background position. For each element a background correction factor (BCF) is calculated from the blank results such that

corrected background (CBKGRD)

CBKGRD = (BCF) x Corrected background at background position

2. Determination of Overlap Factors:

Corrections were made for peak overlaps on other peak and background positions e.g. Rb K_b on Y K_a, Sr K_b on Zr K_a (see Table A.1a for complete list). To determine these, quartz samples spiked with 1000 ppm of each element (separately) were counted at the principal peak and overlapping peak positions. The background count rates at each position were measured using a pure quartz sample. For each overlap, overlap correction factor (OF)

$$OF = \frac{\text{Counts on spiked sample at OP - Bkgrd at OP}}{\text{Counts on spiked sample at PrPP - Bkgrd at PrPP}}$$

where OP = Overlap position, PrPP = Principal peak position
BKGRD = Background

So that:
Overlap correction at OP for element M
= (OF) x Counts at PrPP for element M

3. Calculation of concentration:

As mentioned above, peak/background was used as a measure of concentration, i.e.

$$\text{Conc. (Z ppm)} = K \times \frac{\text{Peak counts /40 seconds}}{\text{Bkgrd counts /40 seconds}}, \quad \text{eqn.(1)}$$

where K = slope of calibration line for each element, i.e. K1, K2, K3, ...etc. for Pb, Th, Rb, ...etc.

Hence it was necessary first to calculate true peak and background values and measure K by analyses of spiked rocks. The corrected peak and background values for each element were obtained by solving a set of 18 simultaneous equations derived as follows (using lead as an example):

Let C = Counts, and as in Table A.1,

P Pb = recorded C/40 sec for Pb L_b peak,

Obs. B_e = recorded C/40 sec for B_e bkgrd position,

Corr. B_e = true C/40 sec for B_e position,

X1,X2,X3 ...etc = true C/40 sec for Pb, Th, Rb ...etc peaks,

X11,X12,X13 ...etc = true C/40 sec for bkgrd at Pb, Th, Rb, ...etc, peak positions.

Then, from Table A.1,

$$P\ Pb = X1 + X11 + 0.004.X2 \qquad \text{eqn.(2)}$$

Similarly considering the background position B , again from table A.1

$$X11 = 1.080 \times (\text{corr. } B_e) \text{ and}$$

$$\text{Corr. } B_e = \text{obs. } B_e - (0.020 \times X1)$$

Hence, eliminating corr. B_e,

$$\text{Obs. } B_e = 0.020\ X1 + 0.926\ X11 \qquad \text{eqn.(3)}$$

In a similar manner, a further 16 equations can be derived by considering the other 8 elements. Solving the set of equations using a computer programme gave values for the true peak and true background for each element of every sample analysed. Hence by determining the value of K in equation (1) (for each element),the elemental concentration could be calculated. Each slope (K1 for Pb, K2 for Th etc.) was determined by analysing a series of spiked samples of a rock (of similar type i.e granitic) containing 0, 100, 250, and 1000 ppm of each element, with 2 to 4 elements spiked together in each series (i.e. Rb, Sr, Nb, Mo in one series, Y, Zr in another and Pb, Th, U in a third)

By processing the spiked rock data the corrected peak and background values were obtained e.g. the values of X3 (peak) and X13(background) for rubidium for each level of spiking. By plotting X3/X13 against the spiked addition the slope K3 was

obtained (see Diagram A.1):

From eqn.(1), Z3 (ppm) = K3 . X3/X13

therefore K3 = Z3 / X3/X13 = AB/BC in diagram.

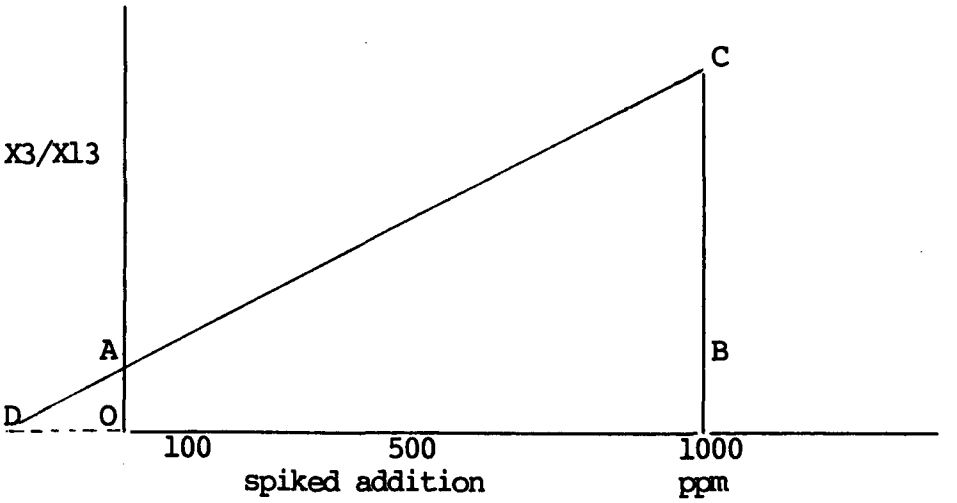

Diagram A.1: Measurement of slope K1 for Rb.

Intercept OD on axis = concentration in unspiked rock.

This process was carried out for each spiked element in turn and the slope values were inserted into the computer programme to enable analytical results to be directly calculated.

4. Analysis of samples:

Each sample was analysed twice and a mean result calculated. Performance of the machine was monitored by regularly checking standard samples (for results see Table A.2 for standard rocks described in Table A.3; reproducibility is shown in table A.4).

A-2 ATOMIC ABSORPTION SPECTROMETRY

A-2.1 MAJOR ELEMENT ANALYSIS

The following procedure was used. It is a slightly modified version of that described by Bernas (1968).

1. The rock powder was dried at 110°C for two hours.
2. Approximately 100mg of the rock powder was accurately weighed and placed in a Teflon vessel. The sample was moistened with 0.5ml of Aqua Regia (1:3 mixture of Analar conc. nitric and hydrochloric acids) and 5ml of hydrofluoric acid (48% Analar) was added with swirling. The teflon vessel was then sealed in a stainless steel bomb and heated in an oven at 110-120°C for about 4 hours.
3. The bomb was allowed to cool and then the contents were examined. If any powder remained, the bomb was resealed and reheated for a further period of time. Otherwise the vessel was removed from its steel case and its contents carefully transfered into a polystyrene vial containing 2g of boric acid. The vessel was washed out several times with hot distilled water and the washing transfered to the vial. The vial was then placed in a warm place until all precipitated fluorides had dissolved.
4. After cooling the solution was diluted with water to 200ml in a volumetric flask, and then this MAIN SOLUTION was transfered to a polyethylene bottle for storage.

The main solution was used to determine MnO, Al2O3, SiO2 by (AAS) and Ti colorimetrically. Further dilution (10 times) was required for AAS determination of total Fe (as Fe2O3) , MgO, CaO, Na2O and K2O. Any samples with excessively high or low concentrations of an element, were either further diluted, or the concentrated solution was used. 40ml of the MAIN SOLUTION was used for the colorimetric determination of Titanium (see later)

A-2.2 AAS ANALYSIS

The concentration of the major elements (except Titanium, P2O5 and H2O) were determined using a Varian AA-575 atomic absorption spectrophotometer on the sample solution at the appropriate dilution. Table A.5 shows the machine conditions for each element. Calibration of the machine was carried out using the international standard rocks TB, GS-N, GA, JG1, NIMG, GM, and SY1, which were prepared using the same technique as the samples. For each element the most appropriate of these rocks was used as the primary standard (Std), whilst the others enabled the accuracy of the method to be ascertained. The comparative values are shown in table A.6. The machine was calibrated by running the primary standard initially to obtain an absorbance reading for one of the elements after first zeroing the machine using distilled water. The concentration (in μg/ml) of that elemental oxide in the standard (from published data; eg. Abbey, 1974) was entered into the machine, and using this the microcomputer constructed a calibration curve. For elements with a wide range of

concentrations, or if the calibration curve was not a staight line, two or three primary standards could be used. A blank was also prepared and run using exactly the same procedure as the samples and standards. If the blank was significantly greater than zero, allowance was made for this in the calibration and subsequent calculations.

Throughout the sample run recalibration was performed regularly, to counteract any variability in the machine conditions. The machine produced reading in concentration units (μg/ml) , based on the standards being used. These were converted to weight per cent by using the following formula

$$\text{Wt \%} = \frac{\text{Concentration } (\mu\text{g/ml}) \times 20 \times \text{dilution}}{\text{Sample weight (mg)}}$$

Detection limits and reproducibilities of this method are shown in table A.4.

A-2.3 TRACE ELEMENT ANALYSIS

To prepare the solution for trace element analysis the following procedure was used:

1. 1g of sample powder was weighed into a 50ml squat Teflon beaker and moistened with a few drops of water. The following were then added successively : 2ml nitric acid (ARISTAR S.G. 1.42), 2ml hydrochloric acid (ARISTAR S.G. 1.18), and 6ml hydrofluoric acid (ARISTAR, 48% HF)

2. The beaker was covered and heated gently for about 1 hour on a low temperature hot plate to dissolve silicates. The lid was then removed and heating was increased to reduce the solution to a volume of 2-3ml.
3. 4ml hydrofluoric acid (ARISTAR 40%) and 3ml perchloric acid (ARISTAR, 60%) were added. The solution was evaporated until fumes of perchloric acid were evolved; the beaker was covered and fuming continued for about 5 minutes.
4. The beaker sides and the lid were washed down with a few ml of water and the solution evaporated heated until fumes of perchloric acid reappeared. Fuming was continued (with lid replaced) for 15 minutes or until a minimum unattacked residue remained
5. 0.5ml perchloric acid and 20ml water were added and the solution was boiled to dissolve salts.
6. The solution was transfered to a 250ml glass conical beaker and boiling continued if necessary to complete solution. After cooling, the solution was diluted to 100ml in a volumetric flask. This solution , the TRACE SOLUTION, was stored in a polystyrene vial, and used for the direct AAS determination of all trace elements, and for the colorimetric determination of P2O5.

All the trace elements except Sr, Rb and V were measured against a composite standard solution made up by combining suitable standard solutions of Li, Ni, Co, Cr, Cu, Zn, Pb. This composite solution was diluted to give a set of standards with a range of concentrations for

each element. For Sr, Rb and V an ionisation suppressant was added to standards and samples. A 0.3% (v/v) lanthanum addition (as lanthanum chloride) was made for Sr and a 0.5% sodium addition (as sodium perchlorate) for Rb and V measurement.

All elements were determined by AAS in exactly the same way as for major elements. Operating parameters are given in Table A.5. Accuracy and precision of the method are shown by Table A.7.

A-3 COLORIMETRY

All absobance measurements were carried out using a Pye-Unicam SP600 spectrophotometer.

1. TITANIUM (as TiO2)

Titanium was determined using the yellow complex formed between Ti and hydrogen peroxide. The titanium colorimetric reagant was made up thus:

50ml concentrated sulphuric acid (Analar) was mixed with 50ml water and allowed to cool. This was followed by addition of 100ml orthophosphoric acid (Analar) and 200ml hydrogen peroxide solution (100 vols, Analar). The mixture was diluted to 600ml.

10 ml of the reagent were placed in a dry 50ml volumetric flask and then made up to the mark with 40ml of the MAIN SOLUTION (A2.1). The absorbance was measured at 400nm, 15-30 minutes after mixing using 4cm cells. Standard rocks were used as

calibration standards (Table A.6).

2. PHOSPHORUS (as P2O5)

Phosphorus was determined on the Trace Solution (A2.3) using the "molybdenum blue" complex formed in a reducing solution of ammonium molybdate of controlled acidity. The colorimetric reagent "Reducing Solution" was be made up immediately before use, as follows:

125ml 3N sulphuric acid (Analar, 8% v/v) was mixed with 38ml ammonium molybdate solution (Analar, 20g/l) and 60ml ascorbic acid solution (Analar 18 g/l). The mixture was diluted to 250 ml.

20ml of the reducing solution was placed in a 50ml volumetric flask and a suitable volume of sample solution (usually 2ml) was added. The solution was made up to the mark with distilled water and the blue colour allowed to develop for at least 24 hours. Absorbance was measured at 827nm in 1cm cells. A standard solution containing 50 g/ml P2O5 (as potassium dihydrogen orthophosphate) was used for calibration.

3. FERROUS IRON (as FeO)

On the basis of the total iron figure obtained by AAS, a suitable quantity of each sample was weighed into a small polystyrene vial, aiming to obtain 500μg FeO. 0.1ml ammonium vanadate solution (16 g/l in 5% v/v sulphuric acid) was added followed by 1ml hydrofluoric acid (42% Analar). The vial was closed with a tight-fitting plastic cap and allowed to stand

overnight. 5ml beryllium sulphate solution (50% w/v) was added and the vial shaken until all precipitated fluorides had dissolved. The solution was then transfered to a 100ml volumetric flask containing a mixture of 5ml dipyridyl solution, (0.15% w/v), 10ml ammonium acetate solution (50% w/v) and about 50ml water. After making up to volume with distilled water the solution was allowed to stand at least 30 min. to allow the coloured complex to develop. The absorbance was measured at 525nm in 1cm cells.

Samples were analysed in duplicate if the expected FeO content was greater than 10% and standard rocks were analysed with each batch of samples for calibration.

A-4 GRAVIMETRIC TECHNIQUES

1. COMBINED WATER

Samples were dried at 110°C for 2hr before analysis, so that total water determined =combined water content. Total water was determined by the Penfield method. A portion of sample powder was weighed into the lower bulb of a Penfield tube and the middle bulb wrapped with wet tissue. The sample bulb was heated to bright red heat with an oxygen-gas torch to completely drive off water which condensed in the cooled bulb. The lower bulb was completely removed by fusing the tube and pulling it off. After

cooling , the outside of the truncated tube was carefully wiped dry and the tube weighed. It was then dried for 2 hours in an oven at 110 C and reweighed thus:

$$\text{Total water (\%)} = \frac{W1 - W2}{W0} \times 100$$

Where

W1=Weight of truncated tube before oven drying (g)
W2=Weight of dried truncated tube (g)
W0=Initial weight of sample (g)

Table A.1

Summary of 2THETA angles, background correction factors overlap factors (Table below, A.1a) and symbols used in calculation.

LINE	2THETA	OBS. C/40 S	TRUE C/40 S		BCKGRD CORRECTION FACTOR	CONC. PPM
			BKGRD	PEAK		
Mo K_a	20.33	PMo	X19	X9	X19=1.15xCorr. B_A	Z 9
B_A	20.88	Obs. B_A	corr. B_A			
Nb K_a	21.40	PNb	X18	X8	X18=0.390xCorr. B_A	Z 8
Zr K_a	22.55	PZr	X17	X7	X17=1.120xCorr. B_B	Z 7
B_B	23.27	Obs. B_B	Corr. B_B			
Y K_a	23.74	PY	X16	X6	X16=1.113xcorr. B_C	Z 6
B_C	24.48	Obs. B_C	Corr. B_C			
Sr K_a	25.15	PSr	X15	X5	X15=0.892xCorr. B_C	Z 5
U L_a	26.14	PU	X14	X4	X14=1.142xCorr. B_D	Z 4
Rb K_a	26.62	PRb	X13	X3	X13=1.070xCorr. B_D	Z 3
B_D	27.05	Obs. B_D	Corr. B_D			
Th L_a	27.43	PTh	X12	X2	X12=0.930xCorr. B_D	Z 2
Pb L_b	28.26	PPb	X11	X1	X11=1.080xCorr. B_E	Z 1
B_E	28.73	Obs. B_E	Corr. B_E			

...contd/

Table A.1a

OVERLAP FACTORS (OF)

LINE	OF
Mo K_a	Nb K_a0.002,Zr K_b0.041,U L_b0.144
B_A	Mo K_a0.009,Nb K_a0.003,Zr K_b0.005,Y K_b0.047,U L_b0.183
Nb K_a	Mo K_a0.005,Zr K_a0.003,Y K_b0.093,U L_b0.203,Th L_b0.014
Zr K_a	Nb K_a0.005,Sr K_b0.180,U L_b0.032,Th L_b0.220
B_B	Zr K_a0.007,Y K_a0.003,Sr_bK 0.003,Rb K_b0.016,U L_a0.006, Th L_b0.010,Pb L_c0.048
Y K_a	Zr K_a0.004,Rb K_b0.262,Th L_b0.032,Pb L_c0.036
Bc	Y K_a0.005,Sr K_a0.003,Rb K_b0.003,Th L_b0.032
Sr K_a	Y K_a0.003
U L_a	Sr K_a0.003,Rb K_a0.004
Rb K_a	U L_a0.072
B_D	Rb K_a0.010,U L_a0.003,Th L_a0.015
Th L_a	Rb K_a0.003,Pb L_b0.033
Pb L_b	Th L_a0.004
B_E	Pb L_b0.020

Table A.2

Standard rock data (X.R.F.)

Accuracy and precision of the method. International standard values at top, analyses from this study at bottom.

STANDARD ROCKS	Concentration of elements in ppm.								
	Rb	Sr	Y	Zr	Nb	Pb	Th	U	Mo
BOB1	4	193	26	111	4	4	4	—	—
	6	190	23	105	6	7	5	2	4
WS1	22	370	—	—	—	<10	—	—	—
	20	360	24	170	19	6	3	3	5
JG1	185	185	31	110	—	26	14	3	2
	184	181	28	118	13	33	12	2	3
I1	130	170	—	60	—	74	—	—	—
	126	170	6	72	5	74	9	6	5
F2	510	140	—	—	—	220	—	—	—
	432	120	2	68	2	270	1	2	5
GD1	135	650	—	—	—	30	—	—	—
	125	624	11	167	12	36	17	5	3
G2	170	480	12	300	14	29	24	2	1
	171	470	10	363	13	38	36	1	2
GSP1	250	230	32	500	29	53	105	2	1
	242	223	23	589	27	66	118	3	3
GM	250	135	26	145	—	30	35	—	1
	259	131	24	149	22	44	45	9	1
NIMG	325	10	147	300	53	40	52	15	3
	318	11	128	317	54	56	64	19	3
PKN	850	40	13	—	—	240	—	—	—
	852	38	6	1	1	300	1	4	2

Table A.3

The International Standard Rocks used in this thesis for the different methods of geochemical analyses are as follows

1. BOBl Ocean Floor Basalt, Birmingham University.
2. FKN Potash Feldspar, C.R.P.G., Nancy - France.
3. F2 Feldspar F2
4. GA Granite, C.R.P.G., France.
5. GDl Granodiorite, Geological Survey of Japan.
6. GM Granite, Z.G.I, Berlin.
7. GSN Granite, C.R.P.G., Nancy - France.
8. GSPl Granodiorite, U.S. Geological Survey.
9. G2 Granite, U.S. Geological Survey.
10. Il Aplitic Granite, Queen Mary College.
11. JGl Granodioritic, Geological Survey of Japan.
12. NIMG Granite, S. African Bureau of Standards.
13. SYl Syenite, Canadian Certified Reference Materials.
14. TB Shale, Tonschiefer, Z.G.I., Berlin.
15. WSl Whin Sill, Barrasford Quarry.

Where C.R.P.G. = Centre de Recherches Petrographiques et Geochimiques.

Z.G.I. = Zentroles Geologisches Institute .

Table A.4

Reproducibility and detection limits (where appropriate) for the A.A.S, Colorimetric, Gravimetric and X.R.F methods.

Reproducibility = 2 sigma , LID = Lower limit of detection.

A.A.S. Major Elements (WT%)	2 sigma
SiO2	+/- 1
Al2O3	+/- 0.3
FeO*	+/- 0.05
MgO	+/- 0.05
CaO	+/- 0.05
Na2O	+/- 0.1
CaO	+/- 0.05
Na2O	+/- 0.1
K2O	+/- 0.1
TiO2	+/- 0.05
MnO	+/- 0.01
H2O+	+/- 0.05

2 sigma for Fe2O3 between (0-3%) is 0.15
2 sigma for FeO between (0-3%) is 0.1
Therefore reproducibility of Fe2O3 is higher than for FeO as it is calculated as the difference between total Fe and FeO.

A.A.S. Trace Elements (ppm)	LID	2 Sigma
Co	5	+/- 10
Cr	5	+/- 5
Cu	3	+/- 3
Li	3	+/- 3
Ni	5	+/- 3
Pb	5	+/- 5
Rb	5	+/- 10
Sr	10	+/- (10-20)
V		+/- 10

i.e. +/- 5ppm (<100ppm), or +/- 5% (>100ppm) of content except V=+/- 10ppm (<100ppm) or +/- 10% (>100ppm). Some elements may be better eg. Li, Cu (~2ppm for conc. of 50 ppm.)

X.R.F. Trace Elements (ppm)	LID
Y	2
Zr	2
Mo	2
Nb	2
Rb	2
Sr	2
U	5
Th	5
Pb	5

Table A.5

Atomic absorption machine condition (VARIAN AA-575)

ELEMENT	WAVE LENGTH (nm)	FLAME		BAND PASS (nm)	LAMP CURRENT (mA)	BKGRD. CORRECTOR
		TYPE	CONDITIONS			
Si	251.6	C2H2 96/N2O 50	Fuel rich	0.2	20	Off
Al	309.3	C2H2 96/N2O 60	Fuel rich	0.5	7	Off
Fe	248.3	C2H2 16/Air 52	Lean	0.2	7	Off
Mn	279.5	C2H2 16/Air 52	Lean	0.2	5	Off
Mg	285.2	C2H2 75/N2O 46	Fuel rich	0.5	3.5	Off
Ca	422.7	C2H2 75/N2O 46	Fuel rich	0.5	3.5	Off
Na	589.0	C2H2 16/Air 62	Lean	0.5	5	Off
K	766.5	C2H2 16/Air 62	Lean	1.0	7	Off
Li	670.8	C2H2 10/Air 66	Lean	1.0	5	Off
Cu	324.7	C2H2 10/Air 50	Lean	0.5	5	Off
Zn	213.9	C2H2 08/Air 47	Lean	1.0	5	On
Pb	217.0	C2H2 11/Air 40	Lean	1.0	3.5	Off
Co	240.7	C2H2 08/Air 48	Lean	0.2	7	On
Ni	232.0	C2H2 09/Air 50	Lean	0.2	3.5	Off
Cr	357.9	C2H2 85/N2O 53	Fuel rich	0.2	5	Off
V	318.5	C2H2 89/N2O 43	Fuel rich	0.5	20	Off
Rb + 0.5% Na	780.0	C2H2 10/Air 48	Lean	0.2	7	Off
Sr + 0.3% La	670.8	C2H2 72/N2O 52	Lean	1.0	5	Off

Where BKGRD = Background
C2H2 = Acetylene
N2O = Nitrous oxide
So the type of flame is either 1. Nitrous oxide-acetylene
2. Air-acetylene

Table A.6

Standard rock data (A.A.S and Colorimetric for major elements)

Accuracy and precision of the method. International standard values at top, results from this study at the bottom.

OXIDES WT%	STANDARD ROCKS						
	TB	GSN	GA	JGl	NIMG	GM	SYI
SiO2	60.3	65.7	70.0	72.4	75.7	73.6	59.5
	61.3	65.3	69.8	STD	75.8	STD	61.3
TiO2	0.93	0.68	0.38	0.27	0.09	0.21	0.49
	----	0.68	0.31	----	-----	0.20	----
Al2O3	20.6	14.7	14.5	14.2	12.1	13.5	9.6
	STD	14.6	14.4	14.2	12.2	13.7	9.4
FeO *	6.92	3.75	2.77	2.16	2.00	2.02	8.21
	STD	3.76	2.76	2.15	2.08	2.02	8.20
MnO	0.05	0.06	0.09	0.06	0.02	0.04	0.40
	0.05	0.06	STD	0.07	0.02	0.05	0.40
MgO	1.94	2.30	0.95	0.76	0.06	0.38	4.2
	1.86	STD	0.92	0.76	0.04	0.30	STD
CaO	0.33	2.50	2.45	2.17	0.78	1.04	10.2
	0.25	STD	2.46	2.17	0.70	0.94	STD
K2O	3.85	4.63	4.03	3.96	34.99	4.74	2.67
	3.94	4.62	4.04	3.96	STD	4.78	2.79
P2O5	0.10	0.28	0.12	0.09	0.02	0.06	0.22
	----	----	----	----	----	0.05	----
H2O+	3.82	1.07	0.87	0.54	0.49	0.35	0.47
	----	----	----	0.50	0.57	----	----

Where STD = Standard used for that element.

Table A.7

Standard rock data (A.A.S for Trace elements)

Accuracy and precision of the method: International standard values at top, results from this study at the bottom.

STANDARD ROCKS	Concentration of elements in ppm.									
	Zn	Cr	Cu	Pb	Ni	Co	Li	Rb	Sr	V
WS1	120	80	62	8	57	60	9	23	375	380
	120	82	62	9	52	57	9	20	380	370
BOB1	70	270	62	5	105	55	9	<5	200	300
	68	272	63	4	102	53	8	4	203	289

APPENDIX B

RARE EARTH ELEMENTS (REE)

Appendix B

RARE EARTH ELEMENTS: ANALYTICAL METHOD AND RESULT TABLES

B-1 DETERMINATION OF RARE EARTH ELEMENTS IN SILICATE ROCKS

B-1.1 OUTLINE OF METHOD

The rock sample was dissolved in an acid mixture and evaporated with perchloric acid to remove other volatile acids. Rare earth elements (REE) were separated by double precipitation as oxalates, followed by double precipitation as hydroxides, together with Al as carrier which were finally collected on a filter paper disc. The individual rare earths were determined by XRF using the paper disc as sample and measuring emitted L_a radiation. Corrections were applied for overlapping lines. Calibration was carried out with precipitations of known amounts of each rare earth. Lutetium was added to each as an internal standard to check and correct for incomplete recovery. This method was developed in Newcastle by P. J. Oakley and N. M. Al. Hafdh by combining ideas from Sen Gupta (1976, 1977, 1981)

B-1.2 PROCEDURE FOR PREPARATION OF DISCS FOR XRF MEASUREMENT

1. INITIAL TAKE-UP

A 2.00g sample of each rock was weighed and transfered to 50ml teflon beaker. 3ml nitric acid (ARISTAR, S.G. 1.42), 3ml hydrochloric acid (ARISTAR, S.G. 1.18) and 10ml hydrofluoric acid (ARISTAR, 48%) were added successively. The beaker was covered and heated on low temperature hotplate for 1 hr followed by an evaporation to leave a moist residue. After cooling, 6ml hydrofluoric acid and 5ml perchloric acid (ARISTAR, 72%) were added and the solution evaporated to fumes of perchloric acid and fumed for 5 minutes. After washing down beaker sides with a few ml water the evaporation was repeated. When cool 30ml nitric acid (10%)/ hydrogen peroxide (5%) solution was added and the solution heated to dissolve salts. It was transfered to a 400 ml conical beaker and boiling continued to complete solution.

2. OXALATE PRECIPITATIONS

Sufficient calcium (as Ca nitrate solution 1ml = 0.02gm Ca) was added to total 0.2g Ca in the solution. Oxalates were precipitated by first adding, with stirring, 15ml alcoholic methyl oxalate solution (400μg/l) to the boiling solution, then adjusting pH to 2.0-2.5 with (50%) v/v ammonia solution. After digesting at near boiling point, for 4 hours keeping pH 2.5 (PH paper), the solution was allowed to cool , settle overnight and filtered (540 paper). The precipitate was washed with (1%) ammonium oxalate solution discarding filtrate and washings. The

precipitate was dissolved through the paper with 70ml boiling nitric acid (20% v/v) into a 400ml conical beaker. The paper was washed with 60ml hot (5%) nitric acid, collecting washings with the filtrate. 3ml perchloric acid was added and the solution evaporated to a moist residue. Take up by redissolved by heating with 30 ml nitric acid (10%)/ hydrogen peroxide (5%) solution and diluted to 150ml with water. The oxalates were precipitated exactly as before, and filtered. The precipitate was washed with (1%) ammonium oxalate solution and redissolved in nitric acid as before. 3ml perchloric acid, was added, the solution evaporated to a moist residue and redissolved by boiling with 30ml nitric acid (10%)/ hydrogen peroxide (5%) solution.

3. HYDROXIDE PRECIPITATIONS

The solution was diluted to 100ml with water, 5.0ml standard Al solution (1ml= 1mg Al) was added and 2ml saturated sulphur dioxide solution to reduce Ce. It was made alkaline (pH 11) with ammonia solution (50% v/v) and fitered (541 paper) after standing for 1hr. The precipitate was washed with water and redissolved through the paper with 20ml hot nitric acid (20% v/v) into a 400ml conical beaker. The solution was boiled, cooled and 2ml saturated sulphur dioxide solution was added, together with 0.25ml lutetium solution (1ml= 1mg Lu). The hydroxide were reprecipitated with ammonia as before. After standing for 1hr the precipitate was filtered off on a 541 filter paper disc (40mm dia. to fit the XRF sample holder) , washed with water (2x10ml) , dried at 60^{o}c, and stored in a desiccator for XRF measurements.

B-1.3 XRF EQUIPMENT AND OPERATING CONDITIONS

Spectrometer	Full details as in A1.3+
	rhodium tube
Tube potential	60 KV
Tube current	40 mA
Spinner	On
Collimator	Fine REE+bkgrd
	Coarse Sc +bkgrd
Filter	Out
X ray path	Vacuum (pressure 0.03 torr)
Crystal	LiF 200
Counter	Flow (counter potential 1600 V)
Dead time corrector	On
Gain	128
Window Settings :	Lower level 210
	Window 120
Counting time	40 Sec

Wave length scan with single element on paper was carried out to select proper angles. Pulse height conditions (window settings) were determined by an energy scan with the same samples. For REE, background counts were measured at two positions, one towards each

end of the series in positions not seriously overlapped. A separate background position was used for Sc. The background curve was effected by Fe, Ni, Mn (see Table B.1 for complete set of 2θ values) radiation from the tube, giving rise to increased background around 49.07°(Ni K_a), 52.63°(Fe K_b), 56.63°(Fe K_a),and 63.60°(Mn K_a).

B-1.4 CALIBRATION

In essence the calibration procedure was the same as for the XRF trace elements (Appendix A, section A1.4).

1. DETERMINATION OF BACKGROUND CURVATURE

Blank samples (containing 5mg alumina only) were counted at all peaks and background positions to determine the shape of the background curve and to enable the background at each peak position to be calculated from the corrected value of one or other of the two background positions (Table B.1). For each element a background correction factor (BCF) was calculated from the blank results such that

Corrected background at peak position

= (BCF) x corrected background at background position

Background correction factors are listed in the Table B.1

2. DETERMINATION OF OVERLAP FACTORS

Corrections were made for overlaps as with the determination of Rb, Sr, etc (Appendix A, section A1.4). They were measured exactly as in A1.4 using 250 g single element spikes (with 5mg Al2O3) as hydroxides on filter paper discs. A complete list of overlaps found is in Table B.1.

3. CALCULATION OF RESULTS

250μg single element spikes were used as standards. From several replicate counts a mean (peak-background) value was calculated for each elemental standard. Corrected (peak-background) values for each element in each sample were calculated using the background correction and overlap factors, working in sequence through all the elements. Then for each element

$$\mu g \text{ in sample} = \frac{\text{(Peak-Background) for sample}}{\text{(Peak-Background) for standard}} \times 250$$

$$\text{and for 2gm samples, ppm} = \frac{\mu g \text{ in sample}}{2}$$

Examples of this procedure are shown in Table B.2 and full results in Table B.3.

Table B.1

Main XRF elemental overlaps using LiF200 analysing crystal.

LINE	2THETA	F	OVERLAP CORRECTIONS
Lu La	47.43	1.4310	Er 0.006; Ho 0.103; Dy 0.085;
Yb La	49.06	1.4906	Er 0.005; Ho 0.013; Dy 0.014 Tb 0.013; Eu 0.008; Sm 0.003
Tm La	50.79	1.3968	Dy 0.039; Tb 0.007; Gd 0.002 Sm 0.083
Er La	52.60	1.4218	Tb 0.187; Eu 0.002;
Ho La	54.54	1.2847	Lu 0.012; Gd 0.544; Eu 0.002;
Dy La	56.59	1.6404	Yb 0.002; Eu 0.042;
Tb La	58.79	1.2724	Sm 0.011; Pr 0.004;
Gd La	61.10	1.0307	Nd 0.021; Ce 0.109; La 0.034
B_A	61.95	------	Er 0.002; Ho 0.006; Tb 0.004 Gd 0.010; Eu 0.002; La 0.003 Nd 0.004; Pr 0.003; Ce 0.003;

...contd/

Table B.1

Main XRF elemental overlaps using LiF200 analysing crystal.

LINE	2THETA	F	OVERLAP CORRECTIONS
Eu L_a	63.57	1.0245	Nd 0.050; Pr 0.181;
Sm L_a	66.23	0.7455	Nd 0.003; Pr 0.009; Ce 0.040;
Nd L_a	72.13	1.2888	Ce 0.032; La 0.004;
Pr L_a	75.42	1.0813	Sm 0.002; La 0.389
B_B	77.60	------	Pr 0.005; Ce 0.004
Ce L_a	79.01	0.9364	----------
La L_a	82.91	0.8319	Nd 0.009
B_C	90.00		
Sc K_a	97.70		

Where F = Background Correction Factor , B = Background
Background under peak = FxB or B .
Background B is used to calculate Background under peak from Lu to Sm.
Background B is used to calculate Background under peak from Nd to La.
Background B is used to calculate Background under peak for Sc.

Table B.2

Three examples on the calculation of the results of which overlap corrections are taken from Table B.1 .

Samp. No. / ELEMENTS	All	E476	E476/1
Sc	22215 10 4 5	15480 7 3.1 3.5	16738 7.6 3.3 3.8
Ce	41491 196 80 98	33529 158 71 79	35476 167 72 84
Nd	19934 78 32 39	16352 64 29 32	17100 67 29 34
La	18101 103 42 52	14299 81 37 41	14986 85 37 43
Pr	5439 23 9.7 12	4349 18 8.1 9	4488 19 8.2 9.5
Sm	3953 13.4 5.4 6.7	3515 12 5.4 6	3525 12 5.2 6
Eu	911 3 1.2 1.5	809 2.6 1.2 1.3	711 2.3 1.0 1.2
Gd	3592 11 4.5 5.5	3147 9.7 4.4 4.9	2748 8.5 3.7 4.3
Tb	584 1.7 0.7 0.9	377 1.1 0.5 0.6	242 0.7 0.3 0.4
Dy	3129 9.2 3.7 4.6	3106 9.1 4.1 4.6	3328 9.8 4.2 4.9
Ho	----------	----------	----------
Er	942 2.7 1.1 1.4	1009 2.9 1.4 1.5	836 2.4 1.0 1.2
Tm	----------	----------	----------
Yb	1078 3.1 1.3 1.6	823 2.4 1.1 1.2	866 2.5 1.1 1.3
Lu	107242 308 125 154	96807 278 125 139	100606 289 125 145

The numbers in each box of the above table is laid out as:

1. True (Peak-Background)	2. μg of the element
4. Corrected ppm	3. Concentration ppm

Table B.3

REE concentration in the different fresh and altered Cheviot Granodiorites and Granites with accuracy and precision of the method indicated by the international standard rock NIMG .

SAMPLE NUMBER	RARE EARTH ELEMENT CONCENTRATIONS (PPM)													
	Sc	La	Ce	Pr	Nd	Sm	Eu	Gd	Tb	Dy	Ho	Er	Tm	Yb
All	4.0	42	80	10	32	5.0	1.2	4.5	0.7	3.7	—	1.1	—	1.3
E419	3.9	40	80	10	32	6.0	1.3	4.5	0.6	5.6	—	1.4	—	1.4
E420	3.3	31	53	6.0	22	4.2	0.9	2.8	0.1	4.2	—	1.2	—	1.2
E476A	3.3	37	72	8.2	29	5.2	1.0	3.7	0.3	4.2	—	1.0	—	1.1
E476	3.1	37	71	8.1	29	5.4	1.2	4.4	0.5	4.1	—	1.4	—	1.1
E527	3.8	56	100	11	38	5.8	1.2	3.3	0.3	3.0	—	0.5	—	0.5
E505	3.4	51	92	10	34	5.0	1.0	3.4	0.8	3.1	—	1.5	—	1.0
E504	4.7	46	88	11	35	6.3	1.5	4.6	0.8	5.5	—	1.8	—	1.4
E470	1.2	17	36	4.6	15	3.5	0.6	3.3	0.3	3.4	—	1.0	—	1.0
B12	6.1	47	88	11	32	6.0	1.5	3.7	0.1	4.7	—	1.5	—	1.0
A12	5.1	46	91	10	35	6.1	1.2	4.3	0.5	3.5	—	1.4	—	1.4
A7	4.2	32	62	7.0	23	4.1	1.6	2.8	0.3	2.3	—	1.0	—	1.0
E117	3.7	61	62	12	41	6.6	1.1	5.4	0.6	2.7	—	1.3	—	1.3
E416	3.2	66	104	11	37	10	1.0	3.7	0.4	2.9	—	1.0	—	1.2
E156	3.5	47	83	9.8	34	6.1	1.3	4.6	0.8	5.0	—	1.3	—	1.4
E150	1.4	17	55	4.2	14	3.3	0.7	2.8	0.1	3.4	—	1.5	—	1.5
E239A	3.2	48	89	9.6	34	5.7	1.3	4.5	0.6	3.5	—	1.8	—	1.7
E479A	5.0	53	100	11	38	6.5	1.2	4.9	0.6	5.4	—	1.6	—	1.6
E238	2.3	41	79	9.6	31	5.6	1.0	4.5	0.6	3.6	—	1.7	—	1.8
E177	4.0	50	95	10	35	5.8	1.1	3.7	0.8	3.2	—	1.9	—	1.5
E474	2.2	29	55	4.4	23	4.4	0.8	3.0	0.2	3.0	—	1.2	—	0.7
NIMG *	0.5	107	198	19	70	18	0.4	10	3.0	16	3.0	10	2.0	14
NIMG +	0.3	99	174	20	64	13	0.1	13	2.2	16	2.6	11	1.1	11

Where * = Standard values of the Granite NIMG, S. African Bureau of Standards

\+ = Analysis results

APPENDIX C

SAMPLE SUMMARY WITH NATIONAL GRID REFERENCES

APPENDIX:- C -:

SAMPLE SUMMARY WITH NATIONAL GRID REFERENCES.

- A -

SAM. NO.	NAT. GRID	LOCALITY	ROCK TYPE	POL. SEC.	TH. SEC.	CHEM. ANAL.
A1	993165	KNOCK HILL	IGNIMBRITE		X	
A2	993165	KNOCK HILL	AGGLOMERATE		X	
A3	953170	LINHOPE B.	MARGINAL GD.		X	
A4	958171	LINHOPE B.	SI. VEIN		X	
A5	956171	LINHOPE B.	P-TOURM. LN.		X	
A6	955170	LINHOPE B.	P-TOURM. LN.		X	X
A7	951171	LINHOPE B.	P-TOURM. LN.	X	X	X
A8	951171	LINHOPE B.	DYKE		X	
A9	951171	LINHOPE B.	LINHOPE GD.		X	
A11	947172	LINHOPE B.	STANDROP GD.	X	X	X
A12	947172	LINHOPE B.	LINHOPE GD.		X	X
A13	954180	LINHOPE B.	HEDGEH. GD.		X	
A14	954180	DUNMOOR B.	SI. VIEN		X	
A15	967175	DN. HILL	VEIN		X	X
A16	977180	CUNYAN CS.	VEIN		X	
A17	977180	CUNYAN CS.	MARGINAL GD.		X	X
A18	977180	CUNYAN CS.	MARGINAL GD.		X	
A19	977178	CUNYAN CS.	MARGINAL GD.		X	
A20	978175	DN. HILL	HORNFELS		X	
A21	978175	DN. HILL	HORNFELS		X	
B1	992166	KNOCK HILL	ANDESITE		X	
B2	992165	KNOCK HILL	AGGLOMERATE		X	
B3	992166	KNOCK HILL	PYROCLAST		X	
B4	992167	KNOCK HILL	PYROCLAST		X	
B5	994166	KNOCK HILL	ANDESITE		X	
B6	990166	KNOCK HILL	BOULDER VN.		X	X
B7	981182	CUNYAN CS.	ANDESITE		X	
B8	981182	DN. HILL	DYKE		X	
B9	981182	DN. HILL	BRECC. DYKE		X	
B10	981183	DN. HILL	MARGINAL GD.		X	
B11	981183	DN. HILL	MARGINAL GD.		X	X
B12	981184	DN. HILL	MARGINAL GD.	X	X	X
B13	978183	DN. HILL	MARGINAL GD.			
B14	978183	DN. HILL	MARGINAL GD.		X	
B15	978183	DN. HILL	MARGINAL GD.		X	
B16	978183	DN. HILL	MARGINAL GD.		X	
B17	968181	DN. HILL	STANDROP GD.		X	X
B18	969178	DN. HILL	STANDROP GD.		X	X
B19	966183	DN. HILL	STANDROP GD.		X	
B20	958189	DN. HILL	STANDROP GD.		X	
B21	965181	DN. HILL	STANDROP GD.		X	
C101	985179	CUNYAN CS.	HORNFELS		X	
C102	985180	CUNYAN CS.	HORNFELS		X	
C103	984179	CUNYAN CS.	HORNFELS		X	
C104	984180	CUNYAN CS.	HORNFELS		X	

SAM. NO.	NAT. GRID	LOCALITY	ROCK TYPE	POL. SEC.	TH. SEC.	CHEM. ANAL.
C105	983180	CUNYAN CS.	HORNFELS		X	
C106	983179	CUNYAN CS.	HORNFELS		X	
C107	982180	CUNYAN CS.	MARGINAL GD.		X	
C108	981179	CUNYAN CS.	MARGINAL GD.		X	
C109	981181	CUNYAN CS.	MARGINAL GD.		X	
C110	980182	CUNYAN CS.	MARGINAL GD.		X	
C111	979182	CUNYAN CS.	MARGINAL GD.		X	
C112	979182	CUNYAN CS.	MARGINAL GD.		X	
C113	977182	CUNYAN CS.	MARGINAL GD.		X	
C114	976182	CUNYAN CS.	MARGINAL GD.		X	
C115	976182	CUNYAN CS.	MARGINAL GD.		X	
C116	976183	CUNYAN CS.	MARGINAL GD.		X	X
C117	974180	CUNYAN CS.	P-TOURM. MG.		X	X
C118	973178	CUNYAN CS.	MARGINAL GD.		X	
C119	975177	CUNYAN CS.	MARGINAL GD.		X	
C120	975174	CUNYAN CS.	MARGINAL CS		X	
C121	975174	CUNYAN CS.	FELSITE VEIN		X	
C122	975173	CUNYAN CS.	MARGINAL GD.		X	
D100	971170	DN. HILL	DYKE		X	
D101	971170	DN. HILL	DYKE		X	
D102	970170	DN. HILL	MARGINAL GD.		X	X
D103	968170	DN. HILL	DYKE		X	
D104	969172	DN. HILL	MARGINAL GD.		X	
D105	968172	DN. HILL	MARGINAL GD.		X	X
D106	967172	DN. HILL	MARGINAL GD.		X	X
D107	966173	DN. HILL	DYKE		X	
D108	966174	DN. HILL	DYKE		X	
D109	966174	DN. HILL	DYKE		X	
D110	967175	DN. HILL	VEIN (IGN.)		X	X
D111	968175	DN. HILL	MARGINAL GD.		X	
D112	968177	DN. HILL	DUNMOOR GD.		X	
D113	969177	DN. HILL	DUNMOOR GD.		X	X
D114	969179	DN. HILL	DUNMOOR GD.		X	
D115	969178	DN. HILL	DUNMOOR GD.		X	X
D116	971178	DN. HILL	DUNMOOR GD.		X	
E100	947172	LINHOPE B.	STANDROP GD.		X	
E101	975172	DN. HILL	MARGINAL GD.		X	
E102	970180	DN. HILL	STANDROP GD.		X	X
E103	967182	DN. HILL	STANDROP GD.		X	X
E104	967176	DN. HILL	DUNMOOR GD.		X	
E105	965173	DN.HILL	DUNMOOR GD.		X	
E106	948171	LINHOPE B.	LINHOPE GD.		X	
E107	948172	LINHOPE B.	LINHOPE GD.		X	
E108	949171	LINHOPE B.	LINHOPE GD.		X	X
E109	948171	LINHOPE B.	LINHOPE GD.		X	
E110	946178	GREAT SP.	STANDROP GD.		X	
E111	944181	GREAT SP.	STANDROP GD.		X	X
E112	944178	GREAT SP.	STANDROP GD.		X	X
E113	944173	LINHOPE B.	HEDGEHP. GD.		X	
E114	944173	LINHOPE B.	HEDGEHP. GD.		X	

SAM. NO.	NAT. GRID	LOCALITY	ROCK TYPE	POL. SEC.	TH. SEC.	CHEM. ANAL.
E115	945173	LINHOPE B.	HEDGEHP. GD.		X	X
E116	945173	LINHOPE B.	HEDGEHP. GD.			
E117	946173	LINHOPE B.	HEDGEHP. GD.		X	X
E118	946173	LINHOPE B.	HEDGEHP. GD.		X	
E119	946173	LINHOPE B.	HEDGEHP. GD.			
E120	947173	LINHOPE B.	HEDGEHP. GD.			
E121	947173	LINHOPE B.	HEDGEHP. GD.		X	X
E122	947173	LINHOPE B.	STANDROP GD.		X	
E123	958171	LN. SPT	MARGINAL GD.		X	
E124	952171	LINHOPE B.	LINHOPE GD.		X	
E125	951171	LINHOPE B.	LINHOPE GD.		X	X
E126	951171	LINHOPE B.	DYKE		X	X
E127	950171	LINHOPE B.	LINHOPE GD.	X	X	X
E128	947173	LINHOPE B.	HEDGEHP. GD.		X	
E129	941175	LINHOPE B.	HEDGEHP. GD.		X	X
E130	940174	LINHOPE B.	LINHOPE GD.			
E131	938174	LINHOPE B.	LINHOPE GD.			
E132	938173	LINHOPE B.	LINHOPE GD.		X	
E133	939168	S/LN. B.	DUNMOOR GD.		X	X
E134	938168	S/LN. B.	DUNMOOR GD.		X	X
E135	938163	S/LN. B.	DUNMOOR GD.			
E136	937163	S/LN. B.	DUNMOOR GD.			
E137	936162	BROOMY CL.	MARGINAL GD.			
E138	937162	BROOMY CL.	MARGINAL GD.		X	X
E139	938161	BROOMY CL.	MARGINAL GD.			
E140	938161	BROOMY CL.	DYKE		X	X
E141	971178	DN. HILL	DUNMOOR GD.		X	
E142	972178	DN. HILL	MARGINAL GD.		X	
E143	972179	DN. HILL	DUNMOOR GD.		X	
E144	971180	DN. HILL	DUNMOOR GD.			
E145	970179	DN. HILL	DUNMOOR GD.			
E146	969179	DN. HILL	DUNMOOR GD.			
E147	968175	N/CAT CS	MARGINAL GD.		X	
E148	967176	LONG CS	MARGINAL GD.		X	X
E149	965176	W/LONG CS	MARGINAL GD.		X	
E150	959180	DUNMOOR B.	WOOLHOPE GR.	X	X	X
E151	958180	DUNMOOR B.	WOOLHOPE GR.			
E152	959181	DUNMOOR B.	WOOLHOPE GR.			
E153	959182	DUNMOOR B.	WOOLHOPE GR.		X	X
E155	981184	CUNYAN CS	MARGINAL GD.		X	
E156	971188	KITTY CS	HEDGEHP. GD.	X	X	X
E157	967183	DN. HILL	STANDROP GD.		X	
E158	967172	CAT CRAGS	DYKE		X	
E159	967173	CAT CRAGS	DUNMOOR GD.		X	
E160	967174	DN. HILL	MARG./DN.GD.		X	
160A	967174	DN. HILL	DUNMOOR GD.		X	
E161	989180	CUNYAN CS	HORNFELS		X	X
E162	986184	CUNYAN CS	HORNFELS		X	
E163	987194	HARELAW	STANDROP GD.		X	
E164	988207	DOD HILL	VEIN (IGN.)		X	

SAM. NO.	NAT. GRID	LOCALITY	ROCK TYPE	POL. SEC.	TH. SEC.	CHEM. ANAL.
E165	975215	MIDDLE. CS	HORNFELS		X	X
E166	977210	STEEL CS	VEIN (IGN.)		X	X
E167	995196	DOD HOUSE	STANDROP GD.			
E168	007196	E/DOD HSE.	ANDESITE		X	
E169	994202	N/DOD HSE.	STANDROP GD.		X	X
E170	965211	TATHEY CS.	HORNFELS		X	
170A	965211	TATHEY CS.	HN./SP. GD.		X	
E171	964211	TATHEY CS.	STANDROP GD.		X	X
E172	964212	TATHEY CS.	HORNFELS		X	X
E173	957218	HOUSEY CS.	HORNFELS		X	
E270	956217	HOUSEY CS.	HORNFELS			
E174	960163	RITTO HIL	MARGINAL GD.		X	
E175	960162	RITTO HIL	HORNFELS		X	
E176	960162	RITTO HIL	DYKE		X	
E177	953169	S/LN. B.	DUNMOOR GD.	X	X	X
E178	947172	LINHOPE B.	LINHOPE GD.		X	X
E179	947172	LINHOPE B.	STANDROP GD.		X	X
E180	951176	GREAT SP.	HEDGEHP. GD.		X	
E181	969165	N/LN. SPOU	VEIN (IGN.)		X	X
E182	968164	N/LN. SPOU	HORNFELS		X	
E183	955181	E/HET BURN	STANDROP GD.		X	
E184	946195	HG. HILL	HEDGEHP. GD.		X	
E185	945196	HG. HILL	HEDGEHP. GD.		X	X
E186	942184	LITTLE SP.	STANDROP GD.		X	
E187	941175	LINHOPE B.	HEDGEHP. GD.		X	
E188	958161	RITTO HILL	DYKE		X	
E189	959162	RITTO HILL	HORNFELS		X	
E190	952166	S/LN. B.	MARGINAL GD.		X	X
E191	948168	S/LN. B.	DUNMOOR GD.		X	X
E192	955164	RITTO HILL	MARGINAL GD.		X	X
E193	956160	RITTO HILL	MARGINAL GD.		X	
E194	951161	SW/ RITTO	HORNFELS		X	
E195	951162	SW/ RITTO	SI/CHL. VEIN		X	X
E196	945160	SW /RITTO	DYKE		X	X
E197	937159	SW/ RITTO	DYKE		X	X
E198	956170	LN. SPOUT	SI.VEIN/MG.		X	
E199	959163	RITTO HILL	MARGINAL GD.		X	
E200	942171	S/LN. BURN	STANDROP GD.		X	
E201	946173	LINHOPE B.	HEDGEHP. GD.			
E202	935157	LOW CANTLE	HORNFELS		X	
E203	934156	LOW CANTLE	MARGINAL GD.		X	X
E204	934156	LOW CANTLE	HORNFELS		X	
E205	932157	LOW CANTLE	HORNFELS		X	
E206	931158	L-H.CANTLE	DYKE		X	
E207	931158	L-H.CANTLE	DYKE		X	
E208	931157	L-H.CANTLE	HORNFELS		X	
E209	931158	L-H.CANTLE	DYKE		X	
E210	931159	L-H.CANTLE	DYKE		X	
E211	931159	L-H.CANTLE	DYKE		X	
E212	927162	HI. CANTLE	DYKE		X	X

SAM. NO.	NAT. GRID	LOCALITY	ROCK TYPE	POL. SEC.	TH. SEC.	CHEM. ANAL.
E213	927162	HI. CANTLE	DYKE		X	
E214	926163	SHIEL CL.	DUNMOOR GD.		X	X
E216	932178	W/SP. B.	STANDROP GD.		X	
E217	963160	S/ RITTO	HORNFELS		X	
E218	960158	S/ RITTO	DYKE		X	
E219	929154	COW CLEUGH	HORNFELS		X	
E220	928154	COW CLEUGH	HORNFELS		X	
E221	927156	CAT CLEUGH	DYKE		X	
E222	927156	CAT CLEUGH	MARGINAL GD.	X	X	X
E223	927157	CAT CLEUGH	MARGINAL GD.		X	
E224	927157	HI. BLKHP.	MARGINAL GD.		X	
E225	926157	HI. BLKHP.	DYKE		X	
E226	926158	HI. BLKHP.	MARGINAL GD.		X	
E227	925158	HI. BLKHP.	MARGINAL GD.		X	X
E228	925158	HI. BLKHP.	MARGINAL GD.		X	
E229	922159	BLACK CL.	MARGINAL GD.		X	
E230	921159	BLACK CL.	MARGINAL GD.		X	
E231	919157	BLACK CL.	HORNFELS		X	
E232	921161	BLACK CL.	MARGINAL GD.		X	
E233	921161	BREAMISH R	DYKE		X	
E234	920162	BREAMISH R	MARGINAL GD.		X	
E235	920162	SHIEL CL.	MARGINAL GD.		X	
E236	921163	SHIEL CL.	DUNMOOR GD.		X	
E237	921164	SHIEL CL.	DUNMOOR GD.		X	
E238	922164	SHIEL CL.	DUNMOOR GD.		X	X
238A	922164	SHIEL CL.	DUNMOOR GD.		X	
238B	922164	SHIEL CL.	DUNMOOR GD.		X	
E239	923165	SHIEL CL.	DUNMOOR GD.		X	
239A	923165	SHIEL CL.	DUNMOOR GD.	X	X	X
E240	916166	SHIEL CL.	MARGINAL GD.		X	
E241	917172	WHITE WELL	STANDROP GD.		X	
E242	917173	WHITE WELL	STANDROP GD.		X	
E243	918173	WHITE WELL	STANDROP GD.			
E244	919187	COMB FELL	STANDROP GD.		X	
E245	949176	GREAT SP.	STANDROP GD.		X	
E246	948175	GR. STDRP.	STANDROP GD.		X	
E247	949176	GR. STDRP.	STANDROP GD.		X	
E248	948177	GR. STDRP.	STANDROP GD.		X	
E249	947178	GR. STDRP.	STANDROP GD.		X	X
E250	960159	S/RITTO H.	DYKE		X	
E251	961158	S/RITTO H.	MARGINAL GD.		X	
E252	961158	S/RITTO H.	DYKE		X	
E253	962158	S/RITTO H.	DYKE		X	
E254	961159	S/RITTO H.	MARGINAL GD.		X	
E255	962159	S/RITTO H.	HORNFELS		X	
E256	963158	S/RITTO H.	MARGINAL GD.		X	
E257	963158	S/RITTO H.	MARGINAL GD.		X	X
E259	959158	S/RITTO H.	DYKE		X	
E260	957158	S/RITTO H.	DYKE		X	
E261	951180	GREAT SP.	STANDROP GD.		X	
E262	950178	GREAT SP.	STANDROP GD.		X	

SAM. NO.	NAT. GRID	LOCALITY	ROCK TYPE	POL. SEC.	TH. SEC.	CHEM. ANAL.
E263	950178	GREAT SP.	STANDROP GD.		X	
E264	950177	GREAT SP.	STANDROP GD.		X	
E265	949176	GREAT SP.	STANDROP GD.		X	
E266	945177	GREAT SP.	STANDROP GD.			
E267	943178	GREAT SP.	STANDROP GD.		X	
E268	943176	GREAT SP.	STANDROP GD.		X	
E269	944176	GREAT SP.	STANDROP GD.		X	X
F100	946176	GREAT SP.	STANDROP GD.			
F101	943180	GREAT SP.	STANDROP GD.			
F102	948172	GREAT SP.	STANDROP GD.			
E271	968182	DN. HILL	STANDROP GD.			
E272	968182	DN. HILL	STANDROP GD.			
E273	968182	DN. HILL	STANDROP GD.			
E274	967178	DN. HILL	DUNMOOR GD.		X	
E275	967177	LONG CS.	DUNMOOR GD.			
E276	971188	KITTY CS.	HEDGEHP. GD.		X	
E277	971171	DN. HILL	DYKE			
E278	971171	DN. HILL	MARGINAL GD.			
E279	971171	DN. HILL	DYKE			
E280	969179	DN. HILL	DUNMOOR GD.			
E281	968182	DN. HILL	STANDROP GD.			
E282	968182	DN. HILL	STANDROP GD.			
E284	(971172)	DN. HILL	MARGINAL GD.			
E285	(971172)	DN. HILL	MARGINAL GD.		X	
E286	(971172)	DN. HILL	MARGINAL GD.			
E287	(971172)	DN. HILL	MARGINAL GD.			
E288	969171	DN. HILL	DYKE			
E289	968171	DN. HILL	MARGINAL GD.			
E290	968171	DN. HILL	MARGINAL GD.			
E291	968170	DN. HILL	VEIN (IGN.)			
E292	971170	DN. HILL	MARGINAL GD.		X	
E293	971170	DN. HILL	MARGINAL GD.			
E294	970170	DN. HILL	MARGINAL GD.		X	
E295	970171	DN. HILL	MARGINAL GD.			
E296	969171	DN. HILL	DYKE			
E297	970171	DN. HILL	DYKE			
E298	971172	DN. HILL	MARGINAL GD.			
E299	970171	DN. HILL	DYKE			
E300	969172	DN. HILL	MARGINAL GD.			
E301	969172	DN. HILL	DYKE			
2302	968174	DN. HILL	VEIN			
E303	968174	DN. HILL	DYKE		X	
E304	972179	NE/LONG CS	STANDROP GD.			
E305	972179	NE/LONG CS	STANDROP GD.			
E306	975179	CUNYAN CS	MARGINAL GD.		X	
E307	977182	CUNYAN CS	MARGINAL GD.			
E308	970179	LONG CRAGS	DUNMOOR GD.		X	
E309	967177	LONG CRAGS	VEIN (IGN.)			
E310	968177	E/LONG CS	VEIN (IGN.)			

SAM. NO.	NAT. GRID	LOCALITY	ROCK TYPE	POL. SEC.	TH. SEC.	CHEM. ANAL.
E311	968177	E/LONG CS	DN./SI-VEIN		X	
E312	970172	DN. HILL	DYKE			
E313	969171	DN. HILL	DYKE			
E314	968172	DN. HILL	MARGINAL GD.			
E315	968173	CAT CRAGS	DYKE		X	
E316	968173	CAT CRAGS	DYKE			
E317	967172	CAT CRAGS	MARGINAL GD.			
E318	967172	CAT CRAGS	MARGINAL GD.			
E319	968172	CAT CRAGS	DYKE/SI- VN.			
319A	968172	CAT CRAGS	VEIN(WG.)/MG			
319B	968172	CAT CRAGS	VEIN(WG)/MG.			
319C	968172	CAT CRAGS	MOD. (P) MG.			
E320	968173	CAT CRAGS	MOD. (P) MG.			
E321	967173	CAT CRAGS	DYKE			
E322	966172	CAT CRAGS	DYKE		X	
E323	968172	S/CAT CS.	DYKE			
E324	968172	CAT CRAGS	VEIN(WG)/MG.			
E325	969173	S/LONG CS	DYKE			
E326	970174	NE/CAT CS	MARGINAL GD.			
E327	969174	N/CAT CS	MARGINAL GD.			
E328	968175	N/CAT CS	MARGINAL GD.			
E329	969177	NE/LONG CS	DUNMOOR GD.			
E330	968175	S/LONG CS	DYKE			
E331	968174	N/CAT CS	DYKE			
E332	968173	E/CAT CS	DYKE			
E333	958171	LN. SPT.	MARGINAL GD.			
E334	958171	LN..SPT.	MARGINAL GD.			
E335	958172	LN. SPT.	MARGINAL GD.		X	
335A	958172	LN. SPT.	DUNMOOR GD.		X	
E336	958172	LN. SPT.	MARGINAL GD.		X	
E337	958171	LN. SPT.	MARGINAL GD.			
337A	958171	LN. SPT.	VEIN (IGN.)		X	X
337C	958171	LN. SPT.	MARGINAL GD.			
E338	952172	LINHOPE B.	LINHOPE GD.			
E339	951171	LINHOPE B.	DYKE			
E340	951171	LINHOPE B.	LINHOPE GD.			
E341	948171	LINHOPE B.	P-TOURM.LN.			
E342	947172	LINHOPE B.	STANDROP GD.			
E343	947172	LINHOPE B.	STANDROP GD.			
E344	947172	LINHOPE B.	XENOLITH/SP.			
E345	947172	LINHOPE B.	HEDGEHP. GD.		X	X
E346	947172	LINHOPE B.	HEDGEHP. GD.			
E347	947172	LINHOPE B.	HEDGEHP. GD.			
E348	947173	LINHOPE B.	HEDGEHP. GD.			
E349	945173	LINHOPE B.	HEDGEHP. GD.			
E350	941175	LINHOPE B.	HEDGEHP. GD.			
E351	940175	LINHOPE B.	LINHOPE GD.		X	
E352	939175	LINHOPE B.	LINHOPE GD.		X	
E353	939174	LINHOPE B.	LINHOPE GD.		X	
E354	937173	LINHOPE B.	LINHOPE GD.	X	X	X
E355	956177	E/ HET B.	HEDGEHP. GD.			

SAM. NO.	NAT. GRID	LOCALITY	ROCK TYPE	POL. SEC.	TH. SEC.	CHEM. ANAL.
E356	960175	DUNMOOR B.	STANDROP GD.			
E357	959175	DUNMOOR B.	STANDROP GD.		X	X
E358	959175	DUNMOOR B.	STANDROP GD.		X	
E359	959174	DUNMOOR B.	STANDROP GD.		X	X
E360	959174	DUNMOOR B.	DUNMOOR GD.			
E361	959174	DUNMOOR B.	DUNMOOR GD.		X	X
E362	959173	DUNMOOR B.	DUNMOOR GD.			
E363	959173	DUNMOOR B.	DUNMOOR GD.		X	
E364	959173	DUNMOOR B.	DUNMOOR GD.		X	
E365	959172	DUNMOOR B.	DUNMOOR GD.			
E366	966164	NE/LN. HSE	ANDESITE			
E367	959172	DUNMOOR B.	MARG. /DUNM.			
E368	959172	DUNMOOR B.	DUNMOOR GD.			
E369	959178	DUNMOOR B.	HEDGEHP. GD.		X	
369A	959178	DUNMOOR B.	HEDGEHP. GD.		X	X
E370	959179	DUNMOOR B.	HEDGEHP. GD.		X	
E371	959180	DUNMOOR B.	HEDGEHP. GD.		X	X
E372	959180	DUNMOOR B.	HEDGEHP. GD.		X	X
E373	959182	DUNMOOR B.	WOOLHOPE EV.			
E374	952180	HET B.	STANDROP GD.		X	X
E375	951181	HET B.	STANDROP GD.		X	X
E376	949183	HET B.	DYKE		X	X
E377	949184	HET B.	STANDROP GD.		X	
E378	948184	HET B.	STANDROP GD.			
E379	947185	HET B.	STANDROP GD.			
E380	936182	SP. BURN	HEDGEHP. GD.			
E381	937180	SP. BURN	HEDGEHP. GD.		X	
E382	938179	SP. BURN	HEDGEHP. GD.		X	X
E383	938179	SP. BURN	HEDGEHP. GD.	X	X	X
E384	940177	SP. BURN	DYKE			
E385	940176	SP. BURN	VEIN			
E386	941178	GREAT SP.	STANDROP GD.			
E387	939171	SE/LN. B.	STANDROP GD.			
E388	933184	LITTLE SP.	HEDGEHP. GD.		X	
E389	936183	LITTLE SP.	HEDGEHP. GD.			
E390	936186	LITTLE SP.	WOOLHOPE GR.		X	X
E391	936187	LITTLE SP.	STANDROP GD.			
E392	935186	LITTLE SP.	WOOLHOPE GR.	X	X	X
E393	950160	W/RITTO H.	MG. GD/DYKE		X	
E394	951161	W/RITTO H.	MARGINAL GD.			
E395	951162	W/RITTO H.	MARGINAL GD.			
E396	952162	W/RITTO H.	DYKE		X	
E397	953162	W/RITTO H.	DYKE		X	
E398	953162	W/RITTO H.	MARGINAL GD.			
E399	953162	W/RITTO H.	MARGINAL GD.			
E400	954162	W/RITTO H.	DYKE		X	
E401	954161	W/RITTO H.	MARGINAL GD.			
E402	954160	W/RITTO H.	MARGINAL GD.		X	
E403	969175	S/LONG CS	DUNMOOR GD.			
E404	967174	S/LONG CS	DUNMOOR GD.			
E405	967174	S/LONG CS	DYKE			

SAM. NO.	NAT. GRID	LOCALITY	ROCK TYPE	POL. SEC.	TH. SEC.	CHEM. ANAL.
E406	967173	N/CAT CS	DUNMOOR GD.			
E407	968173	N/CAT CS	DYKE		X	
E408	969173	E/CAT CS	DYKE			
E409	968172	S/CAT CS	DYKE		X	
E410	967175	NE/CAT CS	DUNMOOR GD.		X	X
E411	967174	SE/LONG CS	DUNMOOR GD.			
E412	967174	N/CAT CS	DYKE			
E413	963185	NW/DN. H.	STANDROP GD.		X	
E414	959195	THREEST.B.	HEDGEHP. GD.		X	
E415	959196	THREEST.B.	HEDGEHP. GD.		X	X
E416	959196	THREEST.B.	HEDGEHP. GD.		X	X
E417	959197	THREEST.B.	HEDGEHP. GD.			
E418	959197	THREEST.B.	HEDGEHP. GD.	X	X	X
E419	957198	THREEST.B.	STANDROP GD.	X	X	X
E420	957198	THREEST.B.	STANDROP GD.	X	X	X
421A	949199	HEDGEHP.H.	HEDGEHP. GD.			
421B	949197	HEDGEHP.H.	HEDGEHP. GD.			
E422	935173	SHANK SIKE	STANDROP GD.			
E423	935177	SW/SP. B.	STANDROP GD.			
E424	928184	COMB FELL	STANDROP GD.			
E425	934198	HEDGEHP.H.	HEDGEHP. GD.			
E426	941201	HG. HILL	HEDGEHP. GD.			
E427	943202	HEDGEHP.H.	HEDGEHP. GD.			
E428	942203	HEDGEHP.H.	HEDGEHP. GD.			
E429	940202	HEDGEHP.H.	CHILLED HED.			
E431	943203	HEDGEHP. H	HEDGEHP. GD.			
E432	948199	HEDGHP. H.	STANDROP GD.			
E433	949199	HEDGEHP.H.	STANDROP GD.			
E434	952198	THREEST. B	STANDROP GD.			
E437	982203	= HSE	STANDROP GD.			
E438	980205	= HSE	STANDROP GD.			
E439	977210	STEEL CS	VEIN - IGNS.		X	
E440	974214	MIDDLE. CS	HORNFELS			
E441	965217	LANGLEE CS	HORNFELS			
E443	958218	HOUSEY CS	HORNFELS		X	
E444	957218	HOUSEY CS	HORNFELS			
E445	955217	HOUSEY CS	HORNFELS			
E446	955215	N/LONG CS	HORNFELS		X	
E447	957214	LONG CS	STANDROP GD.			
E448	954218	HOUSEY CS	STANDROP GD.			
E449	953218	HOUSEY CS	STANDROP GD.		X	
E450	954212	LONG CS	STANDROP GD.			
E451	946208	HEDGEHP.H.	STANDROP GD.			
E452	942210	HEDGEHP.H.	STANDROP GD.			
E453	940207	HEDGEHP.H.	STANDROP GD.			
E454	938207	HEDGEHP.H.	STANDROP GD.		X	X
E455	937206	LANGLEE HP	STANDROP GD.			
E456	957209	LONG CS	STANDROP GD.			
E457	966204	THREEST.B.	STANDROP GD.			
E458	928172	COLDLAW B.	STANDROP GD.		X	X

SAM. NO.	NAT. GRID	LOCALITY	ROCK TYPE	POL. SEC.	TH. SEC.	CHEM. ANAL.
E459	927176	COLDLAW B.	STANDROP GD.			
E460	919173	SHIEL CL.	STANDROP GD.			
E461	920167	SHIEL CL.	STANDROP GD.			
E462	920169	SHIEL CL.	STANDROP GD.			
E463	920169	SHIEL CL.	DUNMOOR GD.		X	
E464	920167	SHIEL CL.	SP./DUNM.GD			
E465	915165	BREAMISH R	DUNMOOR GD.			
E466	915168	WHITEWELL	DUNMOOR GD.		X	X
E467	914168	INNER Q.CL	DUNMOOR GD.	X	X	X
E468	906172	OUTER Q.CL	STANDROP GD.		X	X
E469	911169	INNER Q.CL	DUNMOOR GD.		X	X
E470	911168	INNER Q.CL	MARGINAL GD.	X	X	X
E471	909170	INNER Q.CL	MARGINAL GD.			
E472	910167	INNER Q.CL	DYKE		X	
E473	920163	BREAMISH R	MARGINAL GD.			
E474	921163	SHIEL CL.	DUNMOOR GD.	X	X	X
E475	921163	SHIEL CL.	DUNMOOR GD.			
E476	921164	SHIEL CL.	DUNMOOR GD.	X	X	X
E477	922165	SHIEL CL.	DUNMOOR GD.			
E478	922165	SHIEL CL.	DUNMOOR GD.	X	X	X
E479	923165	SHIEL CL.	DUNMOOR GD.		X	X
479A	923165	SHIEL CL.	DUNMOOR GD.		X	
E480	923165	SHIEL CL.	DUNMOOR GD.			
E481	923162	S/SHIEL CL	DUNMOOR GD.			
E482	911169	INNER Q.CL	DUNMOOR GD.		X	
E483	912160	AINSEY B.	HORNFELS			
E484	918163	AINSEY B.	DYKE			
E485	913161	AINSEY B.	HORNFELS		X	
E487	960159	S/RITTO H.	MARGINAL GD.		X	
E488	960159	S/RITTO H.	MARGINAL GD.			
E489	961159	S/RITTO H.	DYKE		X	X
E490	961159	S/RITTO H.	DYKE			
E491	960158	S/RITTO H.	MARGINAL GD.		X	
E492	960158	S/RITTO H.	MARGINAL GD.		X	
493A	959159	S/RITTO H.	MARGINAL GD.			
E494	959159	S/RITTO H.	DYKE			
E495	958159	S/RITTO H.	MARGINAL GD.		X	
E496	958158	S/RITTO H.	DYKE		X	
E497	956159	S/RITTO H.	MARGINAL GD.			
E498	955159	S/RITTO H.	DYKE		X	
E499	955160	S/RITTO H.	DYKE		X	X
E500	955160	S/RITTO H.	MARGINAL GD.		X	
E501	954160	S/RITTO H.	HORNFELS		X	
E502	954160	S/RITTO H.	MARGINAL GD.	X	X	X
E503	927157	CAT CL.	MARGINAL GD.			
E503	927157	CAT CL.	MARGINAL GD.			
E504	927156	CAT CL.	MARGINAL GD.	X	X	X
E505	927156	CAT CL.	MARGINAL GD.	X	X	X
E506	926155	CAT CL.	DYKE		X	
E507	926155	CAT CL.	MARGINAL GD.		X	

SAM. NO.	NAT. GRID	LOCALITY	ROCK TYPE	POL. SEC.	TH. SEC.	CHEM. ANAL.
E508	926154	CAT CL.	MARGINAL./HN		X	
E509	920158	BLACK CL.	MARGINAL GD.		X	
E510	922158	BLACK CL.	MARGINAL GD.		X	X
E511	922159	BLACK CL.	MARGINAL GD.	X	X	
E512	919164	BREAMISH R	DUNMOOR GD.		X	
E513	919163	BREAMISH R	MARGINAL GD.	X	X	X
E514	918168	SHIEL CL.	DN./SP. GD.			
E515	918168	SHIEL CL.	STANDROP GD.			
E516	918168	SHIEL CL.	CHILLED STD.			
E517	920167	SHIEL CL.	CHILLED STD.			
E518	990168	KNOCK H.	ANDESITE			
E519	933156	LOW CANTLE	MARGINAL GD.			
E520	930154	COW CLEUGH	HORNFELS			
E521	944202	HEDGEHP. H	STANDROP GD.		X	X
521A	944202	HEDGEHP. H	HEDGEHP. GD.	X	X	X
E522	944202	HEDGEHP. H	STANDROP GD.		X	
E523	945199	HEDGEHP. H	HEDGEHP. GD.			
E524	938194	HEDGEHP.H.	STANDROP GD.			
E525	926156	CAT CLEUGH	MARGINAL GD.		X	
E526	926156	CAT CLEUGH	MARGINAL GD.		X	
E527	930154	COW CLEUGH	MARGINAL GD.	X	X	X
E528	924155	HI. BLKHP.	MARGINAL GD.			
E529	925157	HI. BLKHP.	MARGINAL GD.			
E530	923165	SHIEL CL.	DUNMOOR GD.		X	
E540	960258	SE/WATCH H	DYKE			
E541	948249	SE/WATCH H	DYKE		X	X
E542	955257	BROADST.B.	DYKE			
E543	954254	BROADST.B.	STANDROP GD.			
E544	949254	BROADST.B.	STANDROP GD.			
E545	948254	BROADST.B.	STANDROP GD.			
E546	947253	BROADST.B.	STANDROP GD.			
E547	946252	BROADST.B.	STANDROP GD.			
E548	945251	BROADST.B.	XENOLITH			
E549	944253	BROADST.B.	DYKE			
E550	943253	BROADST.B.	STANDROP GD.			
E551	929236	LAMBDEN B.	HEDGEHP. GD.			
E552	927228	LAMBDEN B.	TOURM./ EPD.			
E553	927227	LAMDEN B.	HEDGEHP. GD.			
E554	927225	LAMBDEN B.	WOOLHOPE GR.			
E555	928223	LAMBDEN B.	WOOLHOPE GR.		X	X
E556	941227	BLACKSEAT	HEDGEHP. GD.			
N1	951227	HAWSEN B.	WOOLHOPE GR.		X	
N2	951228	HAWSEN B.	WOOLHOPE GR.		X	
N3	951229	HAWSEN B.	WOOLHOPE GR.		X	
N4	949232	HAWSEN CS	DYKE		X	
N5	950228	HAWSEN CS	WOOLHOPE GR.		X	
N6	949228	HAWSEN B.	WOOLHOPE GR.		X	
N1	951227	HAWSEN B.	WOOLHOPE GR.		X	
N2	951228	HAWSEN B.	WOOLHOPE GR.		X	
N3	951229	HAWSEN B.	WOOLHOPE GR.		X	
N4	949232	HAWSEN CS	DYKE		X	
N5	950228	HAWSEN CS	WOOLHOPE GR.		X	
N6	949228	HAWSEN B.	WOOLHOPE GR.		X	
N7	948229	HAWSEN B.	WOOLHOPE GR.		X	

SAM. NO.	NAT. GRID	LOCALITY	ROCK TYPE	POL. SEC.	TH. SEC.	CHEM. ANAL.
N8	949228	HAWSEN B.	WOOLHOPE GR.		X	
N9	949229	HAWSEN B.	WOOLHOPE GR.		X	
N10	949229	HAWSEN B.	DYKE		X	
N11	947230	HAWSEN B.	WOOLHOPE GR.		X	
N12	947231	HAWSEN B.	WOOLHOPE GR.		X	
N13	945230	HAWSEN B.	WOOLHOPE GR.		X	
N14	944230	HAWSEN B.	TOURM./ QZ.			
N15	944231	HAWSEN B.	TOURM./ QZ.			
N16	943231	HAWSEN B.	HEDGEHP. GD.		X	
N17	943231	HAWSEN B.	HEDGEHP. GD.		X	
N18	941231	HAWSEN B.	HEDGEHP. GD.		X	
N19	940230	HAWSEN B.	HEDGEHP. GD.		X	
N20	940230	HAWSEN B.	HEDGEHP. GD.		X	
N21	941227	BLACKSEAT	HORNFELS		X	
N22	937225	NEW BURN	STANDROP GD.		X	
N23	941224	NEW BURN	HORNFELS		X	
N24	941224	NEW BURN	HORNFELS		X	
N25	941224	NEW BURN	HORNFELS		X	
N26	941224	NEW BURN	DYKE/WG.		X	
N27	942224	NEW BURN	WOOLHOPE GR.		X	
N28	942224	NEW BURN	HORNFELS		X	
N29	943224	NEW BURN	WOOLHOPE GR.		X	
N30	945224	NEW BURN	WOOLHOPE GR.		X	
N31	946224	NEW BURN	WOOLHOPE GR.		X	
N32	947224	NEW BURN	WOOLHOPE GR.		X	
N33	947224	NEW BURN	WOOLHOPE GR.		X	
N34	947225	NEW BURN	WOOLHOPE GR.		X	
N35	925263	COMMON HSE	DYKE		X	
N36	924263	COMMON HSE	ANDESITE			
N37	911255	COMMON B.	ANDESITE		X	
N38	915256	COMMON B.	ANDESITE			
N39	916256	COMMON B.	ANDESITE			
N40	917257	COMMON B.	DYKE		X	
N41	918258	COMMON B.	DYKE		X	
N42	919258	COMMON B.	HEDGEHP. GD.		X	
N43	920259	COMMON B.	HEDGEHP. GD.		X	
N44	921258	COMMON B.	HEDGEHP. GD.		X	
N45	921258	COMMON B.	HEDGEHP. GD.			
N46	920258	COMMON B.	HEDGEHP. GD.		X	
N47	921260	COMMON B.	HORNFELS		X	
N48	922261	COMMON B.	DYKE		X	
N49	922261	COMMON B.	HG. GD. (S2)		X	
N50	925262	COMMON B.	HORNFELS		X	
N51	926262	COMMON B.	HG. GD. (S2)		X	
N52	930264	COMMON B.	HG. GD. (S2)		X	
N53	930265	COMMON B.	HG. GD. (S2)		X	
N54	933267	COMMON B.	HG. GD. (S2)		X	
N55	934267	COMMON B.	HEDGEHP. GD.		X	
N56	935267	COMMON B.	HEDGEHP. GD.		X	
N57	938266	COMMON B.	HEDGEHP. GD.		X	

SAM. NO.	NAT. GRID	LOCALITY	ROCK TYPE	POL. SEC.	TH. SEC.	CHEM. ANAL.
N58	944267	COMMON B.	DYKE		X	
N59	945248	HAZELY B.	DYKE		X	
N60	945248	HAZELY B.	STANDROP GD.			
N61	945247	HAZELY B.	STANDROP GD.			
N62	945246	HAZELY B.	STANDROP GD.			
N63	945246	HAZELY B.	STANDROP GD.		X	
N64	945245	HAZELY B.	STANDROP GD.			
N65	945245	HAZELY B.	STANDROP GD.		X	
N66	945244	HAZELY B.	STANDROP GD.			
N67	945244	HAZELY B.	STANDROP GD.			
N68	944244	HAZELY B.	STANDROP GD.		X	
N69	944243	HAZELY B.	STANDROP GD.			
N70	944243	HAZELY B.	STANDROP GD.			
N71	944242	HAZELY B.	STANDROP GD.		X	
N72	944242	HAZELY B.	STANDROP GD.		X	
N73	944241	HAZELY B.	STANDROP GD.			
N74	944241	HAZELY B.	STANDROP GD.			
N75	944240	HAZELY B.	STANDROP GD.			
N76	944240	HAZELY B.	STANDROP GD.			
N78	944239	HAZELY B.	STANDROP GD.			
N79	944239	HAZELY B.	STANDROP GD.			
N80	943239	HAZELY B.	STANDROP GD.			
N81	943238	HAZELY B.	STANDROP GD.			
N83	927233	BROADSTR.	HEDGEHP. GD.		X	
N84	922231	LAMBDEN B.	WOOLHOPE GR.		X	
N85	921232	LAMBDEN B.	WOOLHOPE GR.		X	
N86	921231	LAMBDEN B.	WOOLHOPE GR.		X	
N87	926231	LAMBDEN B.	WOOLHOPE GR.			
N88	927230	LAMBDEN B.	HEDGEHP. GD.		X	
N89	927229	LAMBDEN B.	HEDGEHP. GD.		X	
N90	927229	SE/LAMB.B.	HEDGEHP. GD.			
N91	928228	SE/LAMB.B.	HEDGEHP. GD.		X	
N92	927228	SE/LAMB.B.	HEDGEHP. GD.			
N93	926223	SE/LAMB.B.	HEDGEHP. GD.		X	
N94	926210	SE/LAMB.B.	HEDGEHP. GD.		X	
N95	926219	SE/LAMB.B.	HEDGEHP. GD.		X	
N96	925218	SE/LAMB.B.	HEDGEHP. GD.		X	
N97	930221	N/SCALD H.	HEDGEHP. GD.		X	
N98	930222	N/SCALD H.	HEDGEHP. GD.		X	
N99	928232	BROADSTR.	HEDGEHP. GD.		X	
N100	935248	BROADST.B.	STANDROP GD.		X	
N101	940252	BROADST.B.	STANDROP GD.		X	
N102	941253	BROADST.B.	DYKE		X	
N103	943253	BROADST.B.	STANDROP GD.		X	
N104	946253	HAZELY B.	STANDROP GD.			
N105	967248	N/SNEAR H.	DYKE			
N106	967249	N/SNEAR H.	ANDESITE			
N107	959248	STEELY CS	ANDESITE			
N108	956244	CARLING CS	ANDESITE			
N109	956243	CARLING CS	ANDESITE			

SAM. NO.	NAT. GRID	LOCALITY	ROCK TYPE	POL. SEC.	TH. SEC.	CHEM. ANAL.
N110	955249	STEELY CS	ANDESITE			
N111	946253	BROADST.B.	STANDROP GD.		X	
N112	946253	BROADST.B.	STANDROP GD.		X	
N113	947253	BROADST.B.	STANDROP GD.		X	
N114	947253	BROADST.B.	STANDROP GD.		X	
N115	947254	BROADST.B.	STANDROP GD.		X	
N116	947254	BROADST.B.	STANDROP GD.		X	
N117	948254	BROADST.B.	STANDROP GD.		X	
N118	948254	BROADST.B.	STANDROP GD.		X	
N119	949254	BROADST.B.	STANDROP GD.		X	
N120	949254	BROADST.B.	STANDROP GD.		X	
N121	949254	BROADST.B.	STANDROP GD.		X	
N122	950254	BROADST.B.	STANDROP GD.		X	
N123	950254	BROADST.B.	STANDROP GD.			
N124	950254	BROADST.B.	STANDROP GD.		X	
N125	951254	BROADST.B.	DYKE		X	
N126	950254	BROADST.B.	DYKE		X	
N127	952254	BROADST.B.	VEIN (IGN.)		X	
N128	952254	BROADST.B.	STANDROP GD.		X	
N129	952254	BROADST.B.	STANDROP GD.		X	
N130	953254	BROADST.B.	DYKE		X	
N131	953254	BROADST.B.	STANDROP GD.		X	
N132	953254	BROADST.B.	STANDROP GD.			
N133	953254	BROADST.B.	CHILLED STD.		X	
N134	954255	BROADST.B.	DYKE		X	
N136	962257	CAREY BURN	DYKE		X	
N140	946223	HAWSEN B.	WOOLHOPE GR.		X	
N141	923223	WOOL. CS	WOOLHOPE GR.		X	
N142	922222	WOOL. CS	WOOLHOPE GR.		X	
N143	922221	WOOL. CS	WOOLHOPE GR.		X	
N144	922220	WOOL. CS	WOOLHOPE GR.		X	
N145	921223	WOOL. CS	ANDESITE		X	
N146	920223	WOOL. CS	WOOLHOPE GR.		X	
N147	915213	NE/CHV. H.	WOOLHOPE GR.		X	
N148	914212	NE/CHV. H.	WOOLHOPE GR.		X	
N149	913211	NE/CHV. H.	WOOLHOPE GR.		X	
N150	912210	NE/CHV. H.	WOOLHOPE GR.		X	
N246	948219	LANGLEE HS	STANDROP GD.		X	
N247	945217	LANGL. HSE	STANDROP GD.		X	
N248	931220	LANGLE.HP.	STANDROP GD.		X	
N249	931220	LANGLE.HP.	STANDROP GD.		X	
N250	951224	NEW BURN	HEDGEHP. GD.		X	
N251	951224	NEW BURN	HEDGEHP. GD.		X	
NH1	934214	N.BROAD. F	STANDROP GD.			
NH2	933213	N.BROAD. F	STANDROP GD.			
NH3	932213	N.BROAD. F	STANDROP GD.			
NH4	930213	N.BROAD. F	STANDROP GD.			
NH5	930213	N.BROAD. F	STANDROP GD.			
NH6	929212	N.BROAD. F	STANDROP GD.			

SAM. NO.	NAT. GRID	LOCALITY	ROCK TYPE	POL. SEC.	TH. SEC.	CHEM. ANAL.
NH7	929212	N.BROAD. F	STANDROP GD.			
NH8	928212	N.BROAD. F	STANDROP GD.			
NH9	925207	N.BROAD. F	STANDROP GD.			
NH10	923205	SE/CHV. H.	STANDROP GD.			
NH11	921205	SE/CHV. H.	STANDROP GD.			
NH12	919204	SE/CHV. H.	STANDROP GD.			
NH13	917204	SE/CHV. H.	STANDROP GD.			
NH14	914203	SE/CHV. H.	STANDROP GD.			
NH15	914201	SE/CHV. H.	STANDROP GD.			
NH16	914209	SE/CHV. H.	HEDGEHP. GD.			
H13A	915203	SE/CHV. H.	WOOLHOPE GR.			
DB1	901229	DUNSDALE				
DB2	903226	DUNSDALE	DYKE			
DB3	903227	DUNSDALE	ANDESITE			
DB4	904226	DUNSDALE	ANDESITE			
DB5	905225	DUNSDALE	DYKE			
DB6	905225	DUNSDALE	ANDESITE			
DB7	905225	DUNSDALE	ANDESITE			
DB8	905224	DUNSDALE	MARGINAL GD.			
DB9	905224	DUNSDALE	MARGINAL GD.			
DB10	906223	DUNSDALE	MARGINAL GD.			
DB11	906222	DUNSDALE	MARGINAL GD.			
DB12	908220	DUNSDALE	MARGINAL GD.			
DB13	909218	DUNSDALE	MARGINAL GD.			
DB14	910218	DUNSDALE	XENOLITH(HN)			
DB15	910214	DUNSDALE	MARGINAL GD.			
DB16	908212	DUNSDALE	MARGINAL GD.			
DB17	907211	BELLYSIDE	MARGINAL GD.			
DB18	905210	BELLYS. CS	MARGINAL GR.			
DB19	905210	BELLYS. CS	MARGINAL GR.			
DB20	905215	BELLYS. CS	WOOLHOPE GR.			
DB21	905216	BELLYS. CS	WOOLHOPE GR.			
DB22	906217	BELLYS. CS	WOOLHOPE GR.			
S44	988173	USWAY BURN	STANDROP GD.			
S45	987173	USWAY BURN	VEIN (IGN.)			
S46	987173	USWAY BURN	DYKE			
S47	986172	USWAY BURN	HORNFELS			

ABBREVIATIONS IN THESE TABLES ARE:

/	:WITH
ANAL.	:ANALYSES
B	:BURN
BELLYS	:BELLYSIDE
BLKHP	:BLAKEHOPE
BRECC	:BRECCIATED
BROAD	:BROADHOPE

...CONTD/

ABBREVIATIONS USED ABOVE:

BROADSTR	:BROADSTRUTHER
CHEM.	:CHEMICAL
CHL	:CHLORITE
CHV	:CHEVIOT
CL(CL.)	:CLEUGH
CS(CS.)	:CRAGS
DN	:DUNMOOR
E	:EAST
EPD	:EPIDOTE
F	:FAULT
GD	:GRANODIORITE
GR	:GRANITE
H	:HILL
HG:HEDGEHP	:HEDGEHOPE
HI	:HIGH
HP	:HOPE
HSE(HS)	:HOUSE
IGN	:IGNEOUS
L-H	:LOW-HIGH
LAMB	:LAMBDEN
LN	:LINHOPE
MG	:MARGINAL
MIDDLE	:MIDDLETON
N	:NORTH
P-TOURM	:PROPYLITIC ALTERATION WITH TOURMALINE
POL.	:POLISHED
Q	:QUECKING
R	:RIVER
S	:SOUTH
SP	:STANDROP
SPT	:SPOUT
ST	:STRAND
SI	:SILICEOUS
S2	:SERICITIC(2)
TH.	:THIN
W	:WEST
WG	:WOOLHOPE GRANITE
WOOL	: = =
X	:FEATURE DONE

APPENDIX D

GEOCHEMISTRY TABLES

APPENDIX D

GEOCHEMISTRY TABLES

SUMMARY OF TECHNIQUES

1. ATOMIC ABSORPTION SPECTROMETRY(AAS):
    a. MAJOR ELEMENTS: Si, Al, Fe as Fe , Na, K, Ca, Mg, Mn.
    b. TRACE ELEMENTS: Cr, Li, Ni, Co, Zn, Cu, Sr, Pb, Rb, Be, V.
2. COLORIMETRY: Ti, P, Fe2+
3. GRAVIMETRY: Total water (combined water).
4. X RAY FLUORESCENCE: Other trace elements excluding REE (Appendix B); Y, Zr, Nb, Mo, Pb,Th, U, Rb and Sr.

Chemical analyses and C.I.P.W norms of samples of the main granite varieties of the Cheviot complex (both fresh and altered) together with dykes, veins and hornfelses are listed below. (Major oxides wt.% ; trace elements, parts per million).

APPENDIX:- D -:

GEOCHEMISTRY TABLES

SAMPLE NUMBERS	FRESH MARGINAL GRANODIORITE							
	Bl2	Bl1	Al9	Cl17	El92	E203	El90	El06A
SiO2	65.20	64.54	64.90	62.90	64.97	64.24	64.68	63.90
TiO2	0.75	0.70	0.60	0.97	0.89	0.87	0.86	0.97
Al2O3	15.22	15.46	15.77	15.60	15.09	15.34	14.83	15.35
Fe2O3	1.43	1.47	1.26	1.74	1.95	1.47	2.00	2.08
FeO	2.87	3.03	3.16	3.05	2.38	2.69	2.36	1.94
MnO	0.09	0.09	0.09	0.09	0.08	0.08	0.08	0.09
MGO	2.66	2.98	3.01	2.83	2.81	2.67	3.22	3.31
CaO	3.68	3.96	4.05	3.93	3.51	3.46	2.95	2.69
Na2O	3.82	3.80	3.75	4.05	3.60	3.68	3.38	3.61
K2O	3.82	3.64	3.71	4.05	3.79	3.70	4.02	3.79
P2O5	0.27	0.31	0.26	0.31	0.30	0.30	0.33	0.30
H2O	0.68	0.60	0.26	0.98	0.78	1.50	1.29	2.03
TOTAL	100.5	100.6	100.8	100.5	100.2	100.0	99.8	100.1
Li	74	68	56	32	52	41	80	70
V	105	95	103	66	111	96	96	90
Cr	80	82	87	63	80	64	105	63
Co	25	22	39	40	36	43	35	37
Ni	30	37	36	37	49	47	53	39
Cu	16	24	19	16	28	19	45	23
Zn	75	90	68	74	62	73	70	79
Rb	188	173	183	182	180	146	188	161
Sr	493	470	475	438	493	519	452	399
Y	17	17	17	20	17	20	17	17
Zr	266	305	290	329	275	317	289	507
Nb	16	15	15	17	14	15	16	16
Mo	3	1	2	5	1	1	2	3
Pb	37	37	41	23	15	14	10	16
Th	26	30	26	29	28	31	32	25
U	6	8	6	4	7	7	8	3
C.I.P.W. NORMS								
Q	16.65	15.64	15.37	11.95	18.38	17.21	19.10	18.38
Or	22.57	21.51	21.92	23.93	22.39	21.86	23.75	22.39
Ab	32.31	32.14	31.72	34.25	30.45	31.12	28.59	30.53
An	13.11	14.38	15.25	12.43	13.83	14.42	12.18	11.38
C	———	———	———	———	———	———	0.46	1.14
Di:Wo	1.41	1.35	1.31	2.10	0.68	0.33	0.00	0.00
En	0.91	0.87	0.81	1.40	0.51	0.22	0.00	0.00
Fs	0.41	0.39	0.43	0.54	0.10	0.08	0.00	0.00
Hy:En	5.72	6.55	6.68	5.64	6.49	6.43	7.77	8.24
Fs	2.60	2.97	3.51	2.18	1.33	2.36	1.41	0.41
Mt	2.07	2.13	1.83	2.52	2.83	2.13	2.90	3.02
He	———	———	———	———	———	———	———	———
Il	1.42	1.33	1.14	1.84	1.69	1.65	1.63	1.84
Ru	———	———	———	———	———	———	———	———
Ap	0.64	0.74	0.62	0.74	0.71	0.71	0.78	0.71

SAMPLE NUMBERS	FRESH DUNMOOR GRANODIORITE						FRESH STANDROP GRANODIORITE	
	E134	E191	E177	E410	E105	D113	E543	E169
SiO2	68.48	65.50	68.60	67.50	68.10	66.80	64.70	66.50
TiO2	0.66	0.69	0.68	0.62	0.74	0.64	0.71	0.72
Al2O3	14.37	15.70	14.80	15.10	14.80	15.40	15.41	15.18
Fe2O3	1.42	1.83	1.95	0.91	1.69	1.40	1.20	1.50
FeO	1.76	1.69	1.50	2.16	1.75	1.87	2.51	2.16
MnO	0.08	0.07	0.07	0.07	0.08	0.07	0.05	0.07
MGO	1.91	2.01	1.86	1.63	1.67	1.86	2.79	2.49
CaO	2.31	2.33	2.24	2.40	2.63	2.60	2.97	3.55
Na2O	3.50	3.80	3.58	3.59	3.63	3.60	3.55	3.57
K2O	4.84	4.60	4.60	4.82	4.38	4.50	3.83	4.02
P2O5	0.21	0.22	0.22	0.19	0.23	0.18	0.28	0.30
H2O	0.82	1.15	0.95	0.67	0.62	0.74	1.80	0.62
TOTAL	100.4	99.6	101.0	99.7	100.3	99.7	99.8	100.7
Li	81	81	63	111	67	66	64	72
V	80	63	77	56	84	55	71	91
Cr	69	48	54	40	61	47	61	78
Co	40	40	30	40	29	60	30	39
Ni	38	32	27	29	31	27	41	44
Cu	11	15	15	35	21	20	37	12
Zn	56	66	67	99	79	82	79	62
Rb	244	209	215	247	223	203	147	157
Sr	336	400	330	270	327	352	454	405
Y	20	18	17	19	17	22	19	19
Zr	276	265	269	272	278	312	248	246
Nb	16	15	15	16	17	16	16	16
Mo	2	4	1	5	2	5	5	2
Pb	16	26	15	33	17	23	3	14
Th	43	27	33	32	35	30	25	32
U	10	4	6	6	7	6	6	7
C.I.P.W. NORMS								
Q	22.10	18.18	23.17	20.10	22.51	20.21	18.53	19.60
Or	28.60	27.18	27.18	28.48	25.88	26.59	22.63	23.75
Ab	29.60	32.14	30.28	30.36	30.70	30.45	30.02	30.19
An	9.21	10.12	9.67	10.66	11.16	11.72	12.90	13.53
C	———	0.76	0.39	0.07	———	0.31	0.70	———
Di:Wo	0.37	0.00	0.00	0.00	0.16	0.00	0.00	0.89
En	0.27	0.00	0.00	0.00	0.12	0.00	0.00	0.64
Fs	0.06	0.00	0.00	0.00	0.02	0.00	0.00	0.17
Hy:En	4.49	5.00	4.63	4.06	4.04	4.63	6.95	5.56
Fs	1.05	0.58	0.15	2.32	0.72	1.35	2.54	1.50
Mt	2.06	2.65	2.83	1.32	2.45	2.03	1.74	2.17
He	———	———	———	———	———	———	———	———
Il	1.25	1.31	1.29	1.18	1.41	1.22	1.35	1.37
Ru	———	———	———	———	———	———	———	———
Ap	0.50	0.52	0.52	0.45	0.55	0.43	0.66	0.71

SAMPLE NUMBERS	FRESH STANDROP GRANODIORITE							
	E249	E112	E374	E375	E468	E179	A11	E359
SiO2	66.95	66.86	65.10	65.60	65.60	66.23	67.30	65.10
TiO2	0.70	0.73	0.78	0.67	0.78	0.72	0.60	0.84
Al2O3	14.40	14.98	15.60	15.51	15.86	14.80	14.80	16.10
Fe2O3	1.22	1.59	1.76	1.72	1.87	1.55	1.70	2.35
FeO	2.31	2.19	2.27	2.02	2.01	2.47	2.10	1.73
MnO	0.15	0.07	0.08	0.05	0.05	0.11	0.12	0.07
MGO	2.30	2.43	2.75	2.41	2.43	2.73	2.50	2.34
CaO	2.60	3.53	2.75	2.86	2.37	2.81	2.95	2.68
Na2O	3.50	3.73	3.40	3.52	3.44	3.60	3.60	3.40
K2O	3.89	3.99	4.24	4.19	4.20	3.87	4.14	4.13
P2O5	0.27	0.30	0.26	0.24	0.26	0.29	0.28	0.25
H2O	1.08	0.43	1.78	1.20	1.39	1.06	0.90	1.91
TOTAL	99.4	100.8	100.8	100.0	100.3	100.3	101.0	100.9
Li	106	63	90	98	60	90	68	56
V	88	90	68	60	68	103	76	70
Cr	73	75	73	64	68	85	82	63
Co	38	24	55	58	51	29	26	42
Ni	39	39	42	33	36	42	38	39
Cu	21	20	24	12	13	26	29	22
Zn	83	64	61	186	55	72	85	65
Rb	192	180	215	195	169	182	155	175
Sr	394	387	346	394	385	403	413	421
Y	17	18	20	17	19	18	16	19
Zr	247	237	255	226	251	230	226	257
Nb	15	15	18	16	15	14	13	16
Mo	1	1	4	4	3	1	1	3
Pb	27	19	20	105	24	17	41	17
Th	28	30	32	27	25	28	32	27
U	4	8	8	5	4	4	8	5
C.I.P.W. NORMS								
Q	22.41	19.52	19.14	19.49	21.14	20.19	20.69	21.01
Or	22.98	23.57	25.05	24.76	24.81	22.86	24.46	24.40
Ab	29.60	31.55	28.76	29.77	29.09	30.45	30.45	28.76
An	11.13	12.35	11.94	12.62	10.06	12.04	12.00	11.66
C	0.35	———	1.04	0.56	1.97	0.28	———	1.77
Di:Wo	0.00	1.33	0.00	0.00	0.00	0.00	0.33	0.00
En	0.00	0.96	0.00	0.00	0.00	0.00	0.24	0.00
Fs	0.00	0.26	0.00	0.00	0.00	0.00	0.06	0.00
Hy:En	5.73	5.09	6.85	6.00	6.05	6.80	5.98	5.83
Fs	2.36	1.37	1.58	1.27	0.95	2.27	1.62	0.00
Mt	1.77	2.31	2.55	2.49	2.71	2.25	2.46	3.37
He	———	———	———	———	———	———	———	0.03
Il	1.33	1.39	1.48	1.27	1.48	1.37	1.14	1.60
Ru	———	———	———	———	———	———	———	———
Ap	0.64	0.71	0.62	0.57	0.62	0.69	0.66	0.59

SAMPLE NUMBERS	FRESH STANDROP GRANODIORITE			FRESH LINHOPE GRANODIORITE			FRESH HEDGEHOPE GRANODIORITE	
	E103	B17	E102	E130	E178	A12	E129	E121
SiO2	65.40	66.60	64.79	67.37	65.73	65.40	68.69	68.18
TiO2	0.70	0.55	0.72	0.63	0.65	0.60	0.47	0.53
Al2O3	15.27	15.10	14.71	14.46	15.31	15.20	14.40	15.20
Fe2O3	1.56	2.23	1.95	1.29	1.45	1.65	1.09	1.44
FeO	2.19	1.83	2.06	2.25	2.14	2.60	1.58	1.55
MnO	0.08	0.09	0.09	0.08	0.11	0.12	0.05	0.05
MGO	2.42	2.42	2.42	2.18	2.36	2.90	1.53	1.79
CaO	3.38	3.08	3.37	2.54	2.63	2.50	2.21	2.13
Na2O	3.60	3.64	3.80	3.34	3.40	3.43	3.50	3.60
K2O	3.80	4.28	3.70	4.37	4.31	4.51	4.36	4.42
P2O5	0.30	0.27	0.28	0.26	0.27	0.28	0.22	0.25
H2O	0.47	0.91	0.80	1.07	1.29	1.44	0.74	1.12
TOTAL	99.2	101.0	98.7	99.8	99.7	100.6	98.8	100.3
Li	82	63	70	67	93	89	80	86
V	100	79	93	84	90	78	64	69
Cr	75	84	76	65	63	82	41	43
Co	45	16	51	46	38	26	29	48
Ni	45	39	42	40	42	39	23	26
Cu	20	18	17	15	22	26	15	13
Zn	71	67	68	55	101	88	61	35
Rb	195	158	178	215	212	214	241	254
Sr	390	406	412	358	399	396	304	341
Y	19	17	18	16	18	17	16	18
Zr	237	241	224	212	242	208	192	212
Nb	15	14	16	14	15	14	14	17
Mo	1		2	2	1	1	2	2
Pb	16	27	16	12	19	30	21	19
Th	32	26	31	27	31	28	28	26
U	9	6	9	7	9	5	7	8
C.I.P.W. NORMS								
Q	19.26	19.55	18.58	22.29	20.24	18.12	24.67	23.42
Or	22.45	25.29	21.86	25.82	25.46	26.65	25.76	26.11
Ab	30.45	30.79	32.14	28.25	28.76	29.01	29.60	30.45
An	14.29	12.23	12.16	10.90	11.28	10.57	9.53	8.93
C	———	0.00	———	0.24	0.92	0.80	0.43	1.22
Di:Wo	0.22	0.54	1.14	0.00	0.00	0.00	0.00	0.00
En	0.15	0.42	0.86	0.00	0.00	0.00	0.00	0.00
Fs	0.04	0.05	0.16	0.00	0.00	0.00	0.00	0.00
Hy:En	5.87	5.60	5.17	5.43	5.88	7.22	3.81	4.46
Fs	1.68	0.72	0.99	2.17	1.86	2.64	1.32	0.87
Mt	2.26	3.23	2.83	1.87	2.10	2.39	1.58	2.09
He	———	———	———	———	———	———	———	———
Il	1.33	1.04	1.37	1.20	1.23	1.14	0.89	1.01
Ru	———	———	———	———	———	———	———	———
Ap	0.71	0.64	0.66	0.62	0.64	0.66	0.52	0.59

	FRESH HEDGEHOPE GRANODIORITE				WOOLHOPE GRANITE			
SAMPLE NUMBERS	E156	E369A	E115	E345	E392	E390	E150	E153
SiO2	69.16	68.60	68.38	66.90	72.60	72.50	74.30	75.50
TiO2	0.88	0.62	0.61	0.56	0.45	0.38	0.25	0.09
Al2O3	14.48	15.13	14.57	15.74	14.02	15.27	13.08	12.84
Fe2O3	1.16	1.68	1.71	1.84	1.53	1.48	1.06	1.73
FeO	1.58	1.45	1.30	1.58	0.45	0.61	0.59	0.20
MnO	0.06	0.06	0.06	0.06	0.06	0.01	0.04	0.04
MGO	1.60	1.67	1.68	1.73	0.80	0.90	0.68	0.44
CaO	2.32	1.93	1.78	1.77	0.83	0.44	0.34	0.28
Na2O	3.62	3.39	3.40	3.61	2.96	2.83	3.14	2.29
K2O	4.58	4.53	4.71	4.62	5.40	4.17	5.68	5.09
P2O5	0.22	0.21	0.25	0.23	0.09	0.15	0.12	0.02
H2O	0.44	1.26	1.04	1.48	1.40	1.39	0.98	0.99
TOTAL	100.1	100.5	99.5	100.1	100.6	100.1	100.3	99.5
Li	130	66	73	67	52	28	36	19
V	66	54	61	50	26	34	41	15
Cr	56	56	50	43	22	22	23	11
Co	27	62	45	68	65	65	73	23
Ni	26	26	24	28	15	11	13	5
Cu	14	18	20	13	7	3	8	4
Zn	55	54	56	70	46	26	35	19
Rb	245	229	250	213	247	211	310	255
Sr	278	303	292	325	179	128	103	124
Y	16	26	16	18	21	17	14	14
Zr	188	209	210	216	184	119	146	99
Nb	14	17	14	15	16	13	15	17
Mo	2	4	2	3	3	3	2	1
Pb	21	39	16	23	26	13	28	9
Th	25	31	29	27	36	16	33	35
U	8	10	7	7	8	2	9	10
C.I.P.W. NORMS								
Q	23.66	25.37	24.95	22.26	32.02	38.23	32.91	41.52
Or	27.06	26.76	27.83	27.30	31.90	24.64	33.56	30.07
Ab	30.62	28.67	28.76	30.53	25.03	23.94	26.56	19.37
An	9.74	8.20	7.20	7.28	3.53	1.20	0.90	1.26
C	-----	1.65	1.24	2.14	2.01	5.66	1.44	3.10
Di:Wo	0.14	0.00	0.00	0.00	0.00	0.00	0.00	0.00
En	0.11	0.00	0.00	0.00	0.00	0.00	0.00	0.00
Fs	0.02	0.00	0.00	0.00	0.00	0.00	0.00	0.00
Hy:En	3.38	4.16	4.18	4.31	1.99	2.24	1.69	1.10
Fs	0.59	0.36	0.08	0.57	0.00	0.00	0.00	0.00
Mt	1.68	2.44	2.48	2.67	0.34	0.90	1.31	0.38
He	-----	-----	-----	-----	1.29	0.86	0.16	1.47
Il	1.67	1.18	1.16	1.06	0.85	0.72	0.47	0.17
Ru	-----	-----	-----	-----	-----	-----	-----	-----
Ap	0.52	0.50	0.59	0.55	0.21	0.36	0.28	0.05

SAMPLE NUMBERS	K SILICATE ALTERATION 1 (K1)						SERICITIC ALTERATION 1 (S1)	
	E466	E476	E479A	E478A	E238	E239A	C116	E257
SiO2	67.00	67.70	65.70	69.00	70.30	69.60	63.10	63.20
TiO2	0.47	0.57	0.82	0.73	0.55	0.73	1.01	0.72
Al2O3	16.04	16.10	15.80	15.21	14.40	15.48	15.81	15.56
Fe2O3	1.88	1.78	1.75	1.02	1.07	1.77	1.01	1.35
FeO	1.13	1.33	2.53	2.25	1.47	0.84	3.37	3.16
MnO	0.02	0.04	0.16	0.07	0.05	0.02	0.08	0.09
MGO	1.44	1.45	2.33	1.81	1.56	1.14	2.83	3.16
CaO	1.06	1.81	0.46	0.52	1.62	0.44	4.03	3.38
Na2O	3.68	3.40	2.03	2.62	3.30	1.10	3.51	3.40
K2O	5.30	4.54	5.16	5.39	5.42	7.28	4.01	4.18
P2O5	0.20	0.25	0.28	0.21	0.18	0.20	0.31	0.28
H2O	1.53	1.46	2.68	1.83	0.82	2.15	0.58	1.26
TOTAL	99.8	100.4	99.7	100.7	100.7	100.8	99.7	99.7
Li	62	47	66	57	56	37	33	78
V	58	56	73	75	53	69	89	91
Cr	47	37	62	43	36	40	59	80
Co	45	45	43	56	34	53	48	37
Ni	31	22	44	29	25	23	39	46
Cu	8	8	7	8	15	12	16	45
Zn	71	45	97	67	45	57	73	88
Rb	270	239	252	245	202	368	179	189
Sr	458	296	117	139	287	90	441	503
Y	17	17	19	20	19	19	20	18
Zr	262	216	263	272	249	292	340	303
Nb	16	14	16	19	18	17	16	14
Mo	2	3	2	3	2	4	4	2
Pb	16	20	20	10	17	23	29	26
Th	28	24	30	36	36	29	33	29
U	2	6	4	4	9	3	7	3
C.I.P.W. NORMS								
Q	21.48	25.19	29.51	28.92	24.64	33.28	14.16	14.63
Or	31.31	26.82	30.49	31.84	32.02	43.01	23.69	24.70
Ab	31.12	28.76	17.17	22.16	27.91	9.30	29.69	28.76
An	3.95	7.35	0.45	1.21	6.86	0.88	15.55	14.86
C	2.80	2.90	6.71	4.62	0.59	5.47	———	———
Di:Wo	0.00	0.00	0.00	0.00	0.00	0.00	1.01	0.03
En	0.00	0.00	0.00	0.00	0.00	0.00	0.62	0.02
Fs	0.00	0.00	0.00	0.00	0.00	0.00	0.34	0.01
Hy:En	3.58	3.61	5.80	4.51	3.88	2.84	6.43	7.85
Fs	0.00	0.11	2.14	2.21	1.00	0.00	3.50	3.66
Mt	2.35	2.58	2.54	1.48	1.55	0.66	1.46	1.96
He	0.26	———	———	———	———	1.32	———	———
Il	0.89	1.08	1.56	1.39	1.04	1.39	1.92	1.37
Ru	———	———	———	———	———	———	———	———
Ap	0.47	0.59	0.66	0.50	0.43	0.47	0.74	0.66

SAMPLE NUMBERS	SERICITIC ALTERATION 1 (S1)							
	E195	E235	E510	E227	E222	E504	E505	E527
SiO2	80.72	84.71	62.40	70.05	64.54	60.40	67.30	69.10
TiO2	0.27	0.43	0.87	0.57	0.86	0.83	0.63	0.58
Al2O3	8.12	7.12	15.37	13.27	15.10	14.72	13.39	14.07
Fe2O3	0.27	0.51	1.34	0.74	1.62	1.07	0.99	0.72
FeO	1.37	1.15	2.64	1.49	2.84	2.97	1.78	1.61
MnO	0.07	0.04	0.06	0.05	0.04	0.09	0.06	0.04
MGO	1.28	0.74	2.25	1.14	2.33	2.66	1.62	1.69
CaO	1.97	0.36	3.40	2.90	2.19	4.92	3.69	0.72
Na2O	1.89	0.66	2.23	2.90	2.79	3.44	3.45	1.17
K2O	2.65	2.91	5.45	5.25	4.80	4.14	4.61	8.36
P2O5	0.11	0.11	0.30	0.15	0.30	0.27	0.19	0.34
H2O	1.13	0.94	2.85	1.36	2.59	2.34	1.68	1.34
TOTAL	99.9	99.7	99.2	99.9	100.0	97.9	99.4	99.7
Li	68	38	70	37	82	82	48	47
V	35	44	83	51	98	76	54	66
Cr	28	30	65	27	67	64	50	86
Co	53	60	24	34	33	29	36	50
Ni	16	16	33	17	37	38	26	35
Cu	24	8	28	11	10	6	23	29
Zn	50	46	66	32	87	67	41	45
Rb	133	171	265	244	260	200	212	399
Sr	143	74	284	208	202	258	171	132
Y	8	8	18	11	17	19	17	11
Zr	156	112	314	268	293	223	251	213
Nb	8	8	16	13	16	15	15	11
Mo	2	1	2	1	1	2	2	2
Pb	30	9	10	7	11	16	6	16
Th	20	18	30	30	33	30	28	14
U	6	3	5	5	6	3	6	4
C.I.P.W. NORMS								
Q	53.57	67.70	17.70	26.27	21.49	11.48	21.21	26.54
Or	15.66	17.19	32.20	31.02	28.36	24.46	27.24	49.39
Ab	15.98	5.58	18.86	24.53	23.60	29.09	29.18	9.90
An	5.85	1.07	14.91	7.69	8.90	12.50	7.44	1.35
C	———	2.49	0.34	———	2.05	———	———	2.60
Di:Wo	1.34	0.00	0.00	2.39	0.00	4.23	4.02	0.00
En	0.79	0.00	0.00	1.54	0.00	2.64	2.70	0.00
Fs	0.49	0.00	0.00	0.69	0.00	1.34	1.02	0.00
Hy:En	2.40	1.84	5.60	1.30	5.80	3.98	1.34	4.21
Fs	1.49	1.05	2.42	0.59	2.53	2.03	0.50	1.48
Mt	0.39	0.74	1.94	1.07	2.35	1.55	1.44	1.04
He	———	———	———	———	———	———	———	———
Il	0.51	0.82	1.65	1.08	1.63	1.58	1.20	1.10
Ru	———	———	———	———	———	———	———	———
Ap	0.26	0.26	0.71	0.36	0.71	0.64	0.45	0.81

SAMPLE NUMBERS	SERICITIC ALTERATION 1 (S1)			K SILICATE 2 (K2)		SERICITIC ALTERATION 2 (S2)		
	E502	E469	E474	E415	E416	E454	E458	E420
SiO2	62.90	66.60	65.60	69.40	72.10	67.50	66.70	73.70
TiO2	0.98	0.64	0.66	0.57	0.60	0.78	0.82	0.59
Al2O3	16.67	15.60	15.70	14.85	14.78	14.78	15.84	12.51
Fe2O3	1.15	1.86	1.72	1.20	0.94	1.49	1.98	1.48
FeO	2.61	0.99	1.84	1.17	0.51	2.17	1.98	1.51
MnO	0.07	0.04	0.05	0.04	0.01	0.07	0.05	0.04
MGO	2.99	1.12	1.86	1.59	0.81	2.17	2.19	1.65
CaO	1.96	2.14	1.76	1.91	0.38	1.87	1.57	0.54
Na2O	1.94	3.08	3.14	3.28	1.87	3.05	3.28	2.78
K2O	5.57	5.56	5.08	4.59	6.28	4.14	4.28	3.00
P2O5	0.29	0.19	0.26	0.21	0.12	0.26	0.28	0.21
H2O	2.95	1.57	2.24	1.16	1.13	1.92	1.33	2.06
TOTAL	100.1	99.4	99.9	100.0	99.5	100.2	100.3	100.1
Li	116	76	53	56	36	81	62	122
V	94	66	73	50	39	73	65	49
Cr	55	34	44	49	41	71	63	49
Co	32	42	53	55	75	51	49	55
Ni	27	30	31	27	14	33	34	30
Cu	53	8	7	7	28	13	15	31
Zn	85	46	61	36	21	91	65	86
Rb	278	267	288	234	271	188	197	127
Sr	143	237	233	242	144	271	322	172
Y	18	19	18	17	18	21	23	14
Zr	275	288	253	191	203	266	246	201
Nb	13	19	15	17	19	17	17	12
Mo	2	3	2	3	3	3	3	3
Pb	10	20	13	26	10	24	20	13
Th	20	34	26	34	32	28	30	24
U	6	3	7	13	5	4	6	6
C.I.P.W. NORMS								
Q	21.41	21.71	21.67	26.77	35.52	26.70	25.09	42.74
Or	32.91	32.85	30.01	27.12	37.10	24.46	25.29	17.72
Ab	16.41	26.05	26.56	27.74	15.82	25.80	27.74	23.51
An	7.83	9.37	7.03	8.10	1.10	7.58	5.96	1.31
C	4.58	1.08	2.46	1.52	4.50	2.51	3.63	4.21
Di:Wo	0.00	0.00	0.00	0.00	0.00	0.00	0.00	0.00
En	0.00	0.00	0.00	0.00	0.00	0.00	0.00	0.00
Fs	0.00	0.00	0.00	0.00	0.00	0.00	0.00	0.00
Hy:En	7.44	2.79	4.63	3.96	2.02	5.40	5.45	4.11
Fs	2.35	0.00	0.96	0.29	0.00	1.60	0.74	0.65
Mt	1.67	1.47	2.49	1.74	0.00	2.16	2.87	2.15
He	———	0.85	———	———	0.94	———	———	———
Il	1.86	1.22	1.25	1.08	1.10	1.48	1.56	1.12
Ru	———	———	———	———	0.02	———	———	———
Ap	0.69	0.45	0.62	0.50	0.28	0.62	0.66	0.50

SAMPLE NUMBERS	SERICITIC ALTERATION 2 (S2)							
	E467	E517	E376	E541	E555	E383	E418	E521
SiO2	64.50	70.20	71.00	72.00	74.90	67.60	67.60	71.60
TiO2	0.77	0.82	0.47	0.27	0.09	0.76	0.73	0.62
Al2O3	15.93	14.36	15.34	15.64	14.33	15.36	15.50	14.09
Fe2O3	2.53	1.30	2.29	1.43	0.80	1.75	2.56	1.34
FeO	1.92	1.83	0.87	0.30	0.32	1.72	0.97	1.23
MnO	0.04	0.03	0.02	0.04	0.02	0.07	0.07	0.04
MGO	2.30	1.67	0.70	0.64	0.40	2.20	1.78	1.17
CaO	0.71	0.56	0.24	0.36	0.25	0.86	0.88	1.05
Na2O	2.62	3.05	2.34	2.12	1.48	2.80	3.36	3.24
K2O	5.60	4.71	5.28	5.06	5.31	4.46	4.48	5.11
P2O5	0.28	0.23	0.16	0.19	0.17	0.25	0.19	0.14
H2O	2.50	1.53	2.06	2.13	1.55	2.16	1.77	0.81
TOTAL	99.7	100.3	100.8	100.2	99.6	100.0	99.9	100.4
Li	77	71	27	27	64	70	59	73
V	69	48	33	25	58	103	53	46
Cr	65	55	14	23	71	85	46	32
Co	39	60	41	28	59	29	60	63
Ni	43	30	7	14	52	42	30	15
Cu	16	5	7	13	4	26	12	12
Zn	100	37	71	59	50	72	95	50
Rb	261	244	273	245	175	182	202	269
Sr	243	171	96	81	252	403	252	186
Y	16	18	31	15	18	18	20	17
Zr	237	267	219	146	245	230	203	248
Nb	17	18	14	12	16	14	16	20
Mo	3	2	3	2	3	1	3	4
Pb	17	20	3	10	7	17	33	36
Th	28	28	31	16	31	28	30	35
U	3	5	6	5	2	4	5	6
C.I.P.W. NORMS								
Q	23.58	30.96	36.09	39.13	29.58	20.19	26.93	29.53
Or	33.09	27.83	31.20	29.90	26.35	22.86	26.47	30.19
Ab	22.16	25.80	19.79	17.93	12.52	23.68	28.42	27.40
An	1.69	1.28	0.15	0.55	0.13	2.63	3.12	4.29
C	4.94	3.78	5.72	6.48	6.10	4.96	3.98	1.66
Di:Wo	0.00	0.00	0.00	0.00	0.00	0.00	0.00	0.00
En	0.00	0.00	0.00	0.00	0.00	0.00	0.00	0.00
Fs	0.00	0.00	0.00	0.00	0.00	0.00	0.00	0.00
Hy:En	5.73	4.16	1.74	1.59	1.00	5.48	4.43	2.91
Fs	0.24	0.99	0.00	0.00	0.00	0.59	0.00	0.20
Mt	3.67	1.88	1.51	0.32	0.84	2.54	1.24	1.94
He	———	———	1.25	1.21	0.22	———	1.71	———
Il	1.46	1.56	0.89	0.51	0.17	1.44	1.39	1.18
Ru	———	———	———	———	———	———	———	———
Ap	0.66	0.55	0.38	0.45	0.40	0.59	0.45	0.33

SAMPLE NUMBERS	SERICITIC ALTERATION 2 (S2)							
	E371	E372	E181	E140	E197	E499	E489	E470
SiO2	73.60	70.10	72.90	67.70	68.68	72.20	72.20	69.00
TiO2	0.42	0.52	0.32	0.63	0.73	0.25	0.27	0.36
Al2O3	13.59	14.89	14.63	15.07	15.43	15.19	14.92	15.48
Fe2O3	0.99	1.63	0.41	1.49	1.84	0.73	1.37	1.05
FeO	0.74	1.07	1.57	1.82	1.54	0.69	0.99	1.45
MnO	0.04	0.05	0.04	0.05	0.04	0.03	0.04	0.03
MGO	0.80	1.42	0.66	1.86	1.51	0.68	0.72	1.14
CaO	0.40	0.96	0.44	0.80	0.95	0.50	0.42	0.48
Na2O	3.24	3.40	3.10	3.30	3.56	3.65	1.97	2.76
K2O	4.94	4.57	5.19	4.93	4.90	5.18	4.99	5.84
P2O5	0.13	0.17	0.19	0.25	0.25	0.14	0.17	0.26
H2O	0.78	1.36	1.26	1.84	1.58	0.99	1.74	1.78
TOTAL	99.7	100.1	100.7	99.7	101.0	100.2	99.8	99.6
Li	29	47	51	62	54	26	39	61
V	30	44	44	78	88	23	38	44
Cr	21	40	15	45	53	12	12	24
Co	74	53	51	32	32	39	29	59
Ni	11	24	8	27	31	7	5	10
Cu	8	6	15	20	32	13	18	7
Zn	39	40	114	70	106	29	102	50
Rb	268	240	301	240	241	266	266	287
Sr	121	191	141	266	261	154	58	161
Y	15	16	16	17	19	15	20	16
Zr	152	175	219	271	343	120	217	145
Nb	16	14	14	15	18	12	14	12
Mo	3	4	1	4	1	2	2	3
Pb	62	26	14	12	16	42	54	48
Th	30	34	35	32	47	15	28	15
U	7	10	11	8	11	4	6	5
C.I.P.W. NORMS								
Q	34.18	29.16	32.68	25.35	25.58	29.33	40.02	28.05
Or	29.19	27.00	30.66	29.13	28.95	30.60	29.48	34.50
Ab	27.40	28.76	26.22	27.91	30.11	30.87	16.66	23.34
An	1.14	3.65	0.94	2.34	3.08	1.57	0.97	0.68
C	2.50	3.01	3.57	3.45	3.14	3.01	5.92	4.37
Di:Wo	0.00	0.00	0.00	0.00	0.00	0.00	0.00	0.00
En	0.00	0.00	0.00	0.00	0.00	0.00	0.00	0.00
Fs	0.00	0.00	0.00	0.00	0.00	0.00	0.00	0.00
Hy:En	1.99	3.54	1.64	4.63	3.76	1.69	1.79	2.84
Fs	0.00	0.00	2.09	1.16	0.18	0.31	0.31	1.26
Mt	1.30	2.10	0.59	2.16	2.67	1.06	1.99	1.52
He	0.09	0.18	———	———	———	———	———	———
Il	0.80	0.99	0.61	1.20	1.39	0.47	0.51	0.68
Ru	———	———	———	———	———	———	———	———
Ap	0.31	0.40	0.45	0.59	0.59	0.33	0.40	0.62

	SERICITIC ALTERATION 2 (S2)									
SAMPLE NUMBERS	E513	E361	E166	E215	E214	E419	E111	E186	B18	E269
SiO2	69.00	66.70	71.19	68.58	67.46	66.60	68.43	68.20	69.53	69.23
TiO2	0.46	0.73	0.35	0.49	0.70	0.65	0.57	0.79	0.60	0.48
Al2O3	15.72	15.50	14.38	16.08	14.32	15.57	14.80	15.27	14.90	14.50
Fe2O3	1.41	2.10	0.65	1.09	1.33	1.78	1.13	1.17	1.32	1.01
FeO	1.00	1.24	1.31	1.58	1.98	1.53	1.90	1.94	1.89	1.82
MnO	0.03	0.04	0.04	0.06	0.07	0.07	0.06	0.08	0.07	0.09
MgO	1.18	1.62	0.94	1.49	2.15	1.55	1.85	1.90	1.84	1.55
CaO	1.06	1.44	1.48	2.31	1.87	1.83	2.67	2.73	2.58	2.11
Na2O	3.40	3.60	3.15	3.60	3.45	3.12	3.47	3.60	3.78	3.47
K2O	5.46	4.70	4.99	4.58	4.57	6.12	4.49	4.23	4.44	4.52
P2O5	0.21	0.21	0.20	0.22	0.23	0.22	0.24	0.23	0.23	0.21
H2O	1.50	1.49	0.81	0.61	1.28	1.22	0.93	0.63	0.57	0.56
TOTAL	100.4	99.4	99.5	100.7	99.4	100.3	100.5	100.8	101.8	99.6
Li	71	51	141	46	68	38	110	79	37	74
V	49	71	41	64	83	58	65	85	70	50
Cr	28	36	31	41	58	43	57	58	67	58
Co	61	41	51	34	39	40	33	54	25	39
Ni	16	29	14	47	31	23	29	31	23	27
Cu	13	15	10	14	14	21	8	28	7	17
Zn	45	56	47	56	69	63	38	77	54	88
Rb	303	198	290	229	178	222	200	209	169	249
Sr	261	313	200	319	388	322	359	335	353	338
Y	14	18	14	15	17	19	21	17	15	14
Zr	178	271	169	216	234	197	206	218	245	199
Nb	13	17	14	13	15	15	16	16	14	14
Mo	3	3	1	1	1	3	2	2	1	1
Pb	48	26	22	24	16	40	12	21	34	26
Th	20	31	25	24	27	32	32	32	27	25
U	2	6	10	5	7	4	4	7	7	6
C.I.P.W. NORMS										
Q	24.91	22.89	29.16	22.99	22.67	19.26	22.52	22.40	22.41	24.67
Or	32.26	27.77	29.48	27.06	27.00	36.16	26.53	24.99	26.23	26.70
Ab	28.76	30.45	26.64	30.45	29.18	26.39	29.35	30.45	31.97	29.35
An	3.89	5.77	6.04	10.02	7.77	7.64	11.55	12.04	10.58	9.09
C	2.79	2.38	1.59	1.53	0.85	1.02	———	0.36	———	0.57
Di:Wo	0.00	0.00	0.00	0.00	0.00	0.00	0.05	0.00	0.30	0.00
En	0.00	0.00	0.00	0.00	0.00	0.00	0.03	0.00	0.21	0.00
Fs	0.00	0.00	0.00	0.00	0.00	0.00	0.01	0.00	0.07	0.00
Hy:En	2.94	4.03	2.34	3.71	5.35	3.86	4.57	4.73	4.38	3.86
Fs	0.00	0.00	1.36	1.30	1.51	0.40	1.71	1.44	1.45	1.88
Mt	1.99	2.01	0.94	1.58	1.93	2.58	1.64	1.70	1.91	1.46
He	0.04	0.71	———	———	———	———	0.00	———	———	———
Il	0.87	1.39	0.66	0.93	1.33	1.23	1.08	1.50	1.14	0.91
Ru	———	———	———	———	———	———	———	———	———	———
Ap	0.50	0.50	0.47	0.52	0.55	0.52	0.57	0.55	0.55	0.50

SAMPLE NUMBERS	PROPYLITIC ALTERATION (P)							
	A6	E117	D102	E138	A17	E126B	E126A	E127
SiO2	68.70	68.60	63.00	66.50	65.50	71.03	67.96	68.40
TiO2	0.53	0.76	0.88	0.55	0.86	0.55	0.74	0.70
Al2O3	14.30	14.78	15.46	15.77	15.30	14.12	14.20	14.88
Fe2O3	4.90	2.88	2.08	1.90	2.26	1.21	1.20	1.83
FeO	1.40	1.17	1.94	1.40	2.32	1.61	2.04	1.66
MnO	0.02	0.02	0.07	0.04	0.09	0.05	0.05	0.05
MGO	2.60	1.67	2.96	1.15	2.86	1.91	2.11	2.51
CaO	0.70	0.68	3.46	1.31	3.00	1.31	1.65	1.08
Na2O	2.80	3.90	5.22	4.51	3.94	3.86	3.84	4.15
K2O	0.14	2.89	3.28	4.51	3.34	3.86	4.26	2.45
P2O5	0.16	0.25	0.27	0.24	0.24	0.23	0.25	0.27
H2O	1.10	1.36	0.82	1.69	1.67	1.36	1.67	1.68
TOTAL	97.4	99.0	99.4	99.6	101.5	101.1	100.0	99.7
Li	22	34	36	58	60	66	82	61
V	71	63	89	56	86	80	79	90
Cr	35	37	58	36	79	62	63	65
Co	33	67	35	26	20	44	26	61
Ni	37	24	27	19	39	29	36	39
Cu	4	11	14	16	14	18	20	6
Zn	39	41	39	62	119	61	66	72
Rb	6	151	156	224	159	202	211	127
Sr	305	392	455	334	436	205	219	224
Y	6	16	18	19	16	18	18	16
Zr	128	219	262	221	244	232	231	242
Nb	12	17	16	14	14	15	14	15
Mo	2	1	3	2	2	1		2
Pb	7	18	13	20	48	5	10	7
Th	12	30	19	22	30	32	32	28
U	2	7	4	2	8	7	9	6
C.I.P.W. NORMS								
Q	46.97	31.63	10.17	19.11	19.39	28.30	22.63	29.39
Or	0.83	17.07	19.38	26.65	19.73	22.81	25.17	14.47
Ab	23.68	32.98	44.15	38.14	33.32	32.65	32.48	35.10
An	2.43	1.74	9.08	4.93	13.31	5.00	6.55	3.59
C	8.65	4.60	———	1.67	0.33	1.76	0.87	4.09
Di:Wo	0.00	0.00	2.64	0.00	0.00	0.00	0.00	0.00
En	0.00	0.00	2.17	0.00	0.00	0.00	0.00	0.00
Fs	0.00	0.00	0.15	0.00	0.00	0.00	0.00	0.00
Hy:En	6.47	4.16	5.20	2.86	7.12	4.76	5.25	6.25
Fs	0.00	0.00	0.37	0.17	1.14	1.14	1.63	0.47
Mt	3.04	1.63	3.02	2.75	3.28	1.75	1.74	2.65
He	2.80	1.75	———	———	———	———	———	———
Il	1.01	1.44	1.67	1.04	1.63	1.04	1.41	1.33
Ru	———	———	———	———	———	———	———	———
Ap	0.38	0.59	0.64	0.57	0.57	0.55	0.59	0.64

	PROPYLITIC ALTERATION (P)									
SAMPLE NUMBERS	E106B	E133	E521A	E357	E185	E148	D115	E395	E108	A7
SiO2	64.80	68.03	63.90	64.90	67.96	66.78	64.80	64.10	66.93	69.70
TiO2	0.82	0.56	0.11	0.85	0.55	0.70	0.85	0.85	0.70	0.86
Al2O3	14.72	15.47	15.48	15.80	15.50	14.80	15.44	15.01	14.39	14.60
Fe2O3	0.92	1.58	1.65	2.51	1.05	1.75	1.81	1.67	2.89	2.20
FeO	3.34	1.45	2.76	1.90	1.85	2.09	1.95	2.52	1.73	1.50
MnO	0.09	0.06	0.07	0.06	0.04	0.10	0.06	0.07	0.06	0.05
MGO	2.81	1.77	2.96	2.71	1.83	2.25	1.99	2.65	2.75	2.50
CaO	2.53	2.17	2.26	1.99	2.03	2.89	3.21	2.87	2.28	1.40
Na2O	3.79	4.06	3.65	3.67	3.87	3.70	4.20	4.57	3.65	4.40
K2O	3.72	4.49	3.93	3.98	4.29	4.17	4.48	3.13	2.99	1.60
P2O5	0.26	0.20	0.31	0.28	0.22	0.26	0.29	0.28	0.26	0.26
H2O	1.72	0.94	2.14	1.68	1.29	0.51	0.63	1.93	0.99	1.43
TOTAL	99.5	100.8	99.2	100.3	100.5	100.0	99.7	99.7	99.6	100.5
Li	59	129	81	83	63	93	114	58	70	47
V	93	61	80	64	74	89	81	75	81	81
Cr	62	48	73	72	43	63	58	63	75	75
Co	44	51	45	50	40	37	47	38	44	35
Ni	32	26	43	42	23	35	38	36	39	51
Cu	11	21	10	19	8	23	12	14	8	13
Zn	67	59	68	78	22	101	64	53	60	64
Rb	157	209	168	178	182	212	195	131	137	66
Sr	388	387	391	405	474	357	347	266	434	237
Y	15	32	20	20	18	17	19	17	18	13
Zr	536	289	285	259	223	286	444	278	235	201
Nb	15	16	17	16	15	16	16	14	16	17
Mo	3	2	3	3	2	2	3	3	1	3
Pb	16	14	33	10	14	21	12	51	12	6
Th	23	36	26	26	29	30	22	23	28	17
U	4	8	6	5	6	4	5	2	6	2
C.I.P.W. NORMS										
Q	17.76	20.28	17.61	20.77	21.82	20.11	14.72	15.61	26.03	31.74
Or	21.98	26.53	23.22	23.51	25.35	24.64	26.47	18.49	17.67	9.45
Ab	32.05	34.34	30.87	31.04	32.73	31.29	35.52	38.65	30.87	37.21
An	10.85	9.46	9.19	8.04	8.63	11.47	10.05	11.21	9.61	5.25
C	0.48	0.47	1.86	2.51	1.33	———	———	———	1.63	3.71
Di:Wo	0.00	0.00	0.00	0.00	0.00	0.49	1.66	0.50	0.00	0.00
En	0.00	0.00	0.00	0.00	0.00	0.35	1.28	0.35	0.00	0.00
Fs	0.00	0.00	0.00	0.00	0.00	0.09	0.20	0.11	0.00	0.00
Hy:En	7.00	4.41	7.37	6.75	4.56	5.25	3.68	6.24	6.85	6.22
Fs	4.19	0.54	3.65	0.12	1.70	1.33	0.59	1.87	0.00	2.51
Mt	1.33	2.29	2.39	3.64	1.52	2.54	2.62	2.42	3.74	0.47
He	———	———	———	———	———	———	———	———	0.31	———
Il	1.56	1.06	0.21	1.61	1.04	1.33	1.61	1.61	1.33	1.63
Ru	———	———	———	———	———	———	———	———	———	———
Ap	0.62	0.47	0.74	0.66	0.52	0.62	0.69	0.66	0.62	0.62

SAMPLE NUMBERS	SLIGHTLY ALTERED GRANODIORITES				FRESH DYKES		
	E125	E337A	E354	E382	E196	E212	E491
SiO2	63.80	67.40	65.60	67.60	65.10	66.79	67.10
TiO2	0.78	0.66	0.74	0.62	0.76	0.67	0.61
Al2O3	15.09	14.88	14.96	15.05	14.83	15.00	14.49
Fe2O3	1.87	1.67	1.92	2.33	2.05	1.55	0.51
FeO	1.98	1.64	2.08	1.19	1.92	2.16	2.46
MnO	0.08	0.06	0.09	0.06	0.07	0.07	0.05
MGO	2.51	1.91	2.17	2.01	2.49	2.52	1.78
CaO	2.87	2.57	3.15	2.21	2.47	2.62	2.76
Na2O	3.30	3.49	3.51	3.55	3.26	3.70	3.40
K2O	3.85	4.49	3.93	4.37	4.40	4.05	4.46
P2O5	0.30	0.21	0.26	0.21	0.28	0.27	0.16
H2O	3.93	0.78	1.85	1.14	1.44	1.25	1.74
TOTAL	100.4	99.8	100.3	100.3	99.1	100.7	99.5
Li	92	41	47	69	52	52	53
V	89	75	75	58	71	71	56
Cr	73	48	48	53	63	63	40
Co	71	52	40	67	27	27	34
Ni	46	24	32	41	32	32	20
Cu	14	14	11	14	24	24	23
Zn	63	49	100	43	71	71	52
Rb	204	219	144	203	177	177	230
Sr	383	323	371	338	439	439	200
Y	18	19	20	21	18	18	22
Zr	269	270	249	241	296	296	351
Nb	17	16	16	18	16	16	17
Mo	2	5	3	3	1	1	3
Pb	16	16	17	20	14	14	10
Th	32	36	30	36	35	35	60
U	6	7	5	8	11	11	11
C.I.P.W. NORMS							
Q	20.41	21.88	20.48	23.11	20.40	20.40	21.04
Or	22.75	26.53	23.22	25.82	23.93	23.93	26.35
Ab	27.91	29.52	29.69	30.02	31.29	31.29	28.76
An	12.28	11.38	13.46	9.59	11.23	11.23	11.11
C	1.00	0.11	———	0.97	0.42	0.42	———
Di:Wo	0.00	0.00	0.19	0.00	0.00	0.00	0.64
En	0.00	0.00	0.14	0.00	0.00	0.00	0.36
Fs	0.00	0.00	0.03	0.00	0.00	0.00	0.26
Hy:En	6.25	4.76	5.26	5.00	6.27	6.27	4.07
Fs	0.95	0.65	1.15	0.00	1.71	1.71	2.92
Mt	2.71	2.42	2.78	2.23	2.25	2.25	0.74
He	———	———	———	0.79	———	———	———
Il	1.48	1.25	1.41	1.18	1.27	1.27	1.16
Ru	———	———	———	———	———	———	———
Ap	0.71	0.50	0.62	0.50	0.64	0.64	0.38

SAMPLE NUMBERS	HORNFELSES				IGNEOUS VEINS		
	E161	E172	E165	E548	B6	A15	D110
SiO2	61.80	64.50	64.70	60.40	73.50	73.00	72.33
TiO2	0.92	1.02	1.07	1.05	0.27	0.55	0.38
Al2O3	16.13	15.60	15.11	16.20	14.50	14.00	13.09
Fe2O3	0.61	1.80	1.41	2.78	0.76	1.11	0.80
FeO	3.89	3.02	2.59	2.99	0.70	0.95	1.15
MnO	0.08	0.09	0.09	0.11	0.03	0.03	0.04
MGO	3.13	3.05	2.36	3.16	0.74	0.88	0.86
CaO	4.21	4.86	4.49	5.02	0.96	1.16	1.28
Na2O	3.97	3.13	3.60	3.90	4.16	3.40	3.44
K2O	3.11	3.43	3.33	3.30	4.78	5.30	5.01
P2O5	0.40	0.39	0.37	0.46	0.09	0.14	0.13
H2O	0.63	0.30	0.98	0.66	0.58	0.49	0.36
TOTAL	98.9	101.2	100.1	100.0	101.1	101.0	98.9
Li	48	30	32	64	26	36	120
V	119	125	145	15	34	46	31
Cr	99	56	74	4	19	35	24
Co	40	39	30	36	27	28	69
Ni	66	40	39	3	3	11	15
Cu	83	20	4	5	7	26	15
Zn	52	73	61	39	31	37	32
Rb	128	146	108	147	229	276	284
Sr	651	695	656	478	401	216	180
Y	18	20	23	24	12	12	14
Zr	341	322	346	289	159	210	178
Nb	15	15	16	18	13	15	15
Mo	1	1	4	3	1	3	7
Pb	10	9	44	20	50	48	18
Th	24	25	23	20	35	31	49
U	7	6	6	4	9	11	12
C.I.P.W. NORMS							
Q	12.14	18.85	19.03	11.25	28.00	29.56	29.10
Or	18.37	20.26	19.67	19.50	28.24	31.31	29.60
Ab	33.58	26.47	30.45	32.98	35.18	28.76	29.09
An	17.01	18.39	15.24	16.96	4.17	4.84	5.49
C	———	———	———	———	0.96	0.90	———
Di:Wo	0.52	1.32	1.93	2.06	0.00	0.00	0.01
En	0.30	0.91	1.32	1.54	0.00	0.00	0.00
Fs	0.20	0.30	0.45	0.32	0.00	0.00	0.00
Hy:En	7.49	6.68	4.54	6.33	1.84	2.19	2.14
Fs	5.07	2.24	1.54	1.34	0.00	0.00	0.90
Mt	0.88	2.61	2.04	4.03	0.27	1.57	1.16
He	———	———	———	———	1.10	0.03	———
Il	1.75	1.94	2.03	1.99	0.51	1.04	0.72
Ru	———	———	———	———	———	———	———
Ap	0.95	0.92	0.88	1.09	0.21	0.33	0.31

Appendix E

REFERENCES

BIBLOGRAPHY

1. ABBEY, S., LEE, N.J., and BOUVIER, J.L. (1974). Analysis of rocks and minerals using an atomic absorption spectrophotometer. Can. Geol. Survey Paper, 74-19, 26pp.
2. ALDERTON, D.H.M., (1979). Luxullianite insitu within the St. Austell granite, Cornwall. Min. Mag., 43, No. 327, pp 441-442.
3. ALDERTON, D.H.M., PEARCE, J.A. and POTTS, P.J. (1980). Rare earth element mobility during granite alteration: Evidence from southwest England. Earth Planet. Sci. Lett., 49, pp 149-165.
4. AMBLER, E.P., (1979). Alteration and mineralization associated with a vesicular Dike near Yeoval in New South Wales. Econ. Geol., 74, pp 67-76.
5. ANDERSON, C.A., (1950). Alteration and metallization in the Bagdad porphyry copper deposit, Arizona. Econ. Geol., 45, pp 609-628.
6. ARMBRUST, G.A., OYARZUN, J. and ARIAS, J. (1977). Rubidium as a guide to ore in Chilean porphyry copper deposits. Econ. Geol., 72 (6), pp 1086-1100.
7. BAILEY, D.G., and HODGSON, C.J. (1979). Transported wall rock in Laharic Breccias at the Cariboo-Bell Cu-Au porphyry deposit, British Columbia. Econ. Geol., 74, pp 125-128.
8. BEANE, R.E., (1981). Hydrothermal alteration in silicate rocks, in TITLEY, S.R., ed., Advances in geology of the porphyry copper deposits of southwestern North America: Tucson, Univ. Arizona Press, pp 117-137.
9. BERNAS, B., (1968). A new method for decomposition and comprehensive analysis of silicates by atomic absorption spectrometry. Anal. Chem., 40, pp 1682-1690.
10. BOTT, M.H.P, (1967). Geophysical investigations of the Northern Pennine basement rocks. Proc. Yorks. geol. Soc., 36, pp 139-168.
11. BRAMMALL, A., and HARWOOD, H.F. (1925). Tourmalinization in the Dartmoor granite. Min. Mag., 20, pp 319-330.
12. BRIMHALL, W.H., (1969). Concentration changes of Th, U and other metals in hydrothermally altered Conway granite, New Hampshire. Geochim. Cosmochim. Acta, 33, pp 1308-1311.
13. BROWN G.C., (1979). Geochemical and geophysical constraints on the origin and evolution of Caledonian granites. in HARRIS, A.L., HOLLAND, C.H. and LEAKE, B.E. (eds.). The Caledonides of the British Isles reviewed. Spec. Publ. geol. Soc. London, 8, pp 645-651.
14. BROWN, G.C., and LOCKE, C.A. (1979). Space-time variations in British Caledonian granites: some geophysical correlations. Earth Planet. Sci. Lett., 45, pp 69-79.

15. BURNHAM, C.W., (1962). Facies and types of hydrothermal alteration. Econ. Geol., 57, pp 768-784.
16. BUTTLER, B.S., and VANDERWILT, J.W. (1933). The climax molybdenum deposit, Colorado. U.S. Geol. Survey, Bull. 846-C.
17. CANN, J.R., (1970). Upward movement of granitic magma. Geol. Mag., 107, pp 335-40.
18. CANN, J.R., (1970). Rb, Sr, Y, Zr and Nb in some ocean floor basaltic rocks. Earth Planet. Sci. Lett., 10, pp 7-11
19. CANN, J.R., (1981). Basalts from the ocean floor, in EMILIANI, C. (ed.). Sea, vol. 7, The oceanic lithosphere, Chapter 10.
20. CARRUTHERS, R.G., BURNETT, G.A., ANDERSON, W. and THOMAS, H.H. (1932). The Geology of the Cheviot Hills. Mem. geol. Survey. U.K.
21. CHARLES F. PARK, JR., MACDIARMID ROY A. (1970). Ore deposits. Second Edition, W.H. Freeman and Company, San Francisco.
22. CHAROY, B., (1981). Tourmalinization in Cornwall. J. Geol. Soc. London, 138, pp 212-213.
23. CHAROY, B., (1982). Tourmalinization in Cornwall, England: Metallization Ass. with mag., 6, pp 63-70.
24. CHENEY, E.S., and TRAMMELL, J.W. (1975). Batholithic ore deposits [Labs.]: Econ. Geol., 70, pp 1318-1319.
25. CHIVAS, A.R., (1978). Porphyry copper mineralization at the Koloula igneous complex, Guadalcanal, Solomon Islands. Econ. Geol., 73, pp 645-677.
26. CLOUGH, C.T., (1882). Notes on the geology of the Cheviot Hills. [Abstract], Proc. Geol. Soc., and Geol. Mag., Dec. 2, ix, 187.
27. ClOUGH, C.T. , (1888). The Geology of the Cheviot Hills (English Side). Mem. geol. Surv. U.K.
28. CONDIE, K.C. , (1978). Geochemistry of proterozoic granitic plutons from New Mexico. USA. Chem. Geol., 21, pp 131-149.
29. CONDIE, K.C., and HARRISON, N.M. (1976). Geochemistry of the Archean Bulawayan Group, Midlands greenstone belt, Rhodesia. Precambrian Res., 3, pp 252-271.
30. CONDIE, K.C., and HUNTER, D.R. (1976). Trace element geochemistry of archean granitic rocks from Barberton region, South Africa. Earth Planet. Sci. Lett., 29, pp 389-400.
31. CREASEY, S.C., (1959). Some phase relations in the hydrothermal altered rocks of porphyry coppper deposits. Econ. Geol., 54, pp 351-373
32. CREASEY, S.C., (1966). Hydrothermal alteration, in TITLEY, S.R. and HICKS, C.L., eds., Geology of the porphyry copper deposits, southwestern North America: Tucson, Univ. Arizona Press, pp 51-75.
33. DEER, W.A., HOWIE, R.A. and ZUSSMAN, J. (1962). Rock-forming minerals, volume 1 (Ortho-and Ring Silicates). Longmans, London.

34. DEER, W.A., HOWIE, R.A. and ZUSSMAN, J. (1963). Rock-forming minerals, volume 2 (Chain Silicates). Longmans, London.
35. DEER, W.A., HOWIE, R.A. and ZUSSMAN, J. (1962). Rock-forming minerals, volume 3 (Sheet Silicates). Longmans, London.
36. DEER, W.A., HOWIE, R.A. and ZUSSMAN, J. (1963). Rock-forming minerals, volume 4 (Framework Silicates). Longmans, London.
37. DEER, W.A., HOWIE, R.A. and ZUSSMAN, J. (1966). An Introduction to the rock-forming minerals. Longmans, London.
38. DEWEY, J.F., (1969). Evolution of the Appalachian/Caledonian orogen. Nature, London, 222, pp 124-9.
39. DEWEY, J.F., and SHACKLETON, R.M. (1984). A model for the evolution of the Grampian tract in the early Caledonides and Appalachians. Nature, London, 312, pp 115-121.
40. DICKINSON, W.R., and HATHERTON, T. (1967). Andesite volcanism and seismicity around the Pacific. Science, 157, pp 801-3.
41. DICKINSON, W.R., (1975). Potash-Depth (K-H) relations in Continental Margin and intra-Oceanic Magmatic Arcs. Geology, 3, No. 2, pp 53-56.
42. DICKINSON, W.R., (1973). Widths of modern arc-trench gaps proportional to past duration of igneous activity in associated magmatic arcs. J. Geophys. Res., 78, pp 3376-89.
43. DUNHAM, K.C., DUNHAM, A.C., HODGE, B.L. and JOHNSON, G.A.L. (1965). Granite beneath Vis'ean sediments with mineralization at Rookhope, northern Pennines. Quart. J. geol. Soc. London, 121, pp 383-417.
44. EINAUDI, M.T., (1981). Skarns associated with porphyry plutons. I. Description of deposits, southwestern North America, II. General features and origin, in TITLEY, S.R., ed., Advances in geology of the porphyry copper deposits of southwestern North America: Tucson, Univ. Arizona Press, pp 139-183.
45. EMMONS, W.J., (1927). Relations of the disseminated copper ores in porphyry to igneous intrusives. Am. Inst. Mining Metall. Engrs. Trans., 75, pp 797-815.
46. EXLEY, C.S., (1957). Magmatic differentiation and alteration in the ST. Austell granite. Q. J. G. S., v. CXIV, Part 2., pp 197-230.
47. EXLEY, C.S., and STONE, M. (1964). The Granitic rocks of south-west England. Roy. Geol. Soc. Cornwall, pp 131-184.
48. FIEREMANS M., (1982). Genesis of tourmalinites from Belgium, Petrographical and chemical evidence. Min. Mag., 46, pp 95-102.
49. FLETCHER, C.J.N., (1977). The Geology, Mineralization, and Alteration of Ilkwang Mine, Republic of Korea. A Cu-W Bearing Tourmaline Breccia Pipe. Econ. Geol., 72, pp 753-768.

50. GARDINER, C.I., and REYNOLDS, S.H. (1932). The Loch Doon "granite" area, Galloway. QJ. Geol. Soc., London, 83, 1-34.
51. GARSON, M.S., and MITCHELL, A.H.G. (1977). Mineralization at destructive plate boundaries - a brief review, in volcanic process in ore genesis: Geol. Soc. London Spec. Pub., pp 81-97.
52. GILL, J.B. (1982). Mountain building and volcanism. In Hsu, K.J. (ed.). Mountain building processes. Academic Press, 13-17.
53. GOLES, G.G., (1968). Rare earth geochemistry of Precambrian Plutonic rocks. XXIII Int. Geol. Cong., 8, pp 237-249.
54. GRANTHAM, D.R., (1928). The petrology of the Shap Granite. Proceedings of the Geologists Association, 39, pp 299-331.
55. GRAYBEAL, F.T., (1981). Geology of the El Tiro ore deposit, Silver Bell mining district, Arizona, in TITLEY, S.R., ed., Advances in geology of the porphyry copper deposits of southwestern North America: Tucson, Univ. Arizona Press.
56. GUILBERT, J.M., and LOWELL, J.D. (1974). Variations in zoning patterns in porphyry ore deposits: Canadian Inst. Mining Metallurgy Trans., 77, pp 105-115.
57. GUSTAFSON, L.B., and HUNT, J.P. (1975). The porphyry copper deposit at El Salvador, Chile: Econ. Geol., 70, pp 857-912.
58. GUSTAFSON, L.B., (1978). Some major factors of porphyry copper genesis: Econ. Geol., 73, pp 600-607.
59. HALLIDAY, A.N., AFTALION, M., VAN BREEMEN, O., and JOCELYN, J. (1979). Petrogenetic significance of Rb-Sr and U-Pb isotope systems in the 400 Ma old British Isles granitoids and their hosts, in HARRIS, A.L., HOLLAND, C.H. and LEAKE, B.E. (eds.). The Caledonides of the British Isles reviewed. Spec. Publ. geol. Soc. London, 8, pp 653-662.
60. HALLIDAY, A.N., STEPHENS, W.E. and HARMON, R.S. (1980). Rb-Sr and O isotopic relationships in 3 zoned Caledonian granitic plutons, Southern Uplands: evidence for varied sources and hybridization of magmas. J. geol. Soc., London, 137, pp 329-48.
61. HARLAND, W.B., COX, A.V., LLEWELLYN, P.G., PICKTON, C.A.G., SMITH, A.G. and WALTERS, R. (1982). A Geologic Time Scale, Cambridge University Press. Published by The British Petroleum Company p.I.c. by arrangement with Cambridge University Press, Second Edition.
62. HASKIN, L.A., FREY, F.A., SCHMITT, R.A. and SMITH, R.H. (1966). Meteoritic, solar and terrestrial rare-earth distributions. Phys. Chem. Earth, 7, pp 167-321.
63. HASLAM, H.W., (1975). Geochemical survey of stream waters and stream sediments from the Cheviot area. Rep. Inst. Geol. Sci., No. 75/6. 29 pp.

64. HASLAM, H.W, (1968). The crystallization of Intermediate and Acid Magmas at Ben Nevis, Scotland. Journ. Petrology, 2, pp 84-104.
65. HATHERTON, T., and DICKINSON, W.R. (1969). The relationship between andesitic volcanism and seismicity in Indonesia, the lesser Antilles and other island arcs. J. Geophys. Res., 74, pp 5301-5310.
66. HEATWOLE, D.A., (1973). Occurrence and distribution of tourmaline in the El Salvador ore body, El Salvador, Chile: Unpub. Company rept., The Anaconda Company.
67. HEY, MAX H., (1954). A new review of the chlorites. Mineral. Mag., vol. 30, pp 277-292.
68. HITCHEN, C.S., (1934). The Skiddaw granite and its residual products. Quart. J. geol. Soc. London, 90, pp 158-200.
69. HOLLAND, J.G. (1967). Rapid analysis of the Weardale grainte. Proc. Yorks. geol. Soc. 36, 91-113.
70. HOLLAND, J.G., and LAMBERT, R.St.J. (1970). Weardale granite. In geology of Durham (JOHNSON, G.A. and HICKLING, G., eds.) Trans. Nat. Hist. Soc. Northumberland and Durham, 41, pp 103-118.
71. HOLLISTER, V.F., (1978). Geology of the porphyry copper deposits of the Western Hemisphere: New York, Soc. Mining Engineers AIME, 219 p.
72. HOLLISTER, V.F., POTTER, R.R. and BARKER, A.L. (1974). Porphyry-type deposits of the Appalachian Orogen Econ. Geol., 69, pp 618-630.
73. HORTON, D.J., (1978). Porphyry-type copper-molybdenum mineralization Belts in eastern Queensland, Australia. Econ. Geol., 73, pp 904-921.
74. HUTCHISON, C.S., (1976). Indonesian active volcanic arc: K, Sr and Rb variation with depth to the Benioff zone. Geology, 4, pp 407-408.
75. JACOBS, D.C., (1979). Geochemistry of Biotite in the Santa Rita porphyry copper deposits, New Mexico. Econ. Geol., 74, pp 860-887.
76. JHINGRAN, A.G., (1942). The Cheviot granite. Q. JL geol. Soc. London, 98, 241.
77. K'OSAKA, H., and WAKITA, K. (1978). Some geologic features of the Mamut porphyry copper deposit, Sabah, Malaysia. Econ. Geol., 73, pp 618-627.
78. KARIG, D.E., LAWRENCE, M.B., MOOR, G.F. and CURRAY, J.R. (1980). Structural framework of the fore-arc basin, NW Sumatra. J. geol. Soc., London, 137, pp 77-91.
79. KINGSLEY, M., (1945). A contribution to the study of Luxullianite. Min. Mag. 27, pp 186-94.
80. KNOPF, A., (1923). The Candelaria Silver district Nevada: U.S. Geol. Survey, Bull. 762A.

81. KNOPF, A., (1924). Geology and ore deposits of the Rochester district, Nevada: U.S. Geol. Survey, Bull. 762.
82. KYNASTON, H., (1899). Contributions to the Petrology of the Cheviot Hills. Trans. geol. Soc. Edin., 7, 390.
83. LANGTON, J.M., (1973). Ore genesis in the Morenci-Metcalf district: Soc. Mining Engineers AIME Trans., 254, pp 247-257.
84. LANIER, G., JHON, E.C., SWENSEN, A.J., REID, J., BARD, C.E., CADDEY, S.W. and WILSON, J.C. (1978). General geology of the Bingham Mine, Bingham Canyon, Utah. Econ. Geol., 73, pp 1228-1241.
85. LEAKE, B.E., (1971). On aluminous and edenitic hornblendes Min. Mag., 38, pp 389-407
86. LEAKE, B.E., (1978). Nomenclature of Amphiboles. Min. Mag., 42, pp 533-563.
87. LEAKE, R.C., and HASLAM, H.W. (1978). A geochemical survey of the Cheviot area in Northumberland and Roxburghshire. using panned mineral concentrates. Rep. Inst. Geol. Sci., No. 78/4, 37 pp.
88. LEAKE, R.C., and BROWN, M.J. (1979). Porphyry style copper mineralization at Black Stockarton Moor, Southwest Scotland. Trans. Instn. Min. Metall. (Sec. B: Appl. earth sci.), 88, B177-81.
89. LEGGETT, J.K., McKERROW, W.S. and EALES, M.N. (1979) The Southern Uplands of Scotland: a lower Palaeozoic accretionary prism. J. geol. Soc., London, 136, pp 755-70.
90. LISTER, C.J., (1978a). Luxullianite insitu within the St. Austell granite, Cornwall: Min. Mag., 42, pp 295-7.
91. LISTER, C.J., (1978b). Some tourmalinized rocks from Cornwall and Devon: Ussher Soc., Proc., 4, part 2, pp 211-214
92. LISTER, C.J., (1979). Quartz-cored tourmalines from Cape Cornwall and other localities. Ussher Soc., Proc., 4, part 7, pp 402-418.
93. LOVERING T.S., (1949). Rock alteration as a guide to ore-East Tintic district, Utah: Econ. Geol. Monograph No.1, 64 pages.
94. LOWELL, J.D., and GUILBERT, J.M. (1970). Lateral and vertical alteration-mineralization zoning in porphyry ore deposits. Econ. Geol., 65, pp 373-408.
95. MACGREGOR, M., (1937). The western part of the Criffell Dalbeattie igneous complex. Q. J. geol. Soc. London, 93, pp 457-486.
96. MANNING, D.A.C., (1982). Chemical and morphological variation in tourmalines from the Hub Kapong batholith of peninsular Thailand. Min. Mag., 45, pp 139-47.
97. McKERROW, W.S., LEGGETT, J.K. and EALES, M.H. (1977). Imbricate thrust model of the southern Uplands of Scotland. Nature, London, 267, pp 237-239.

98. McKINSTRY, H.E., NOBLE, J.A. (1932). The veins of Casapala Peru. Econ. Geol., 27, pp 768-784.
99. MEIGHAN, I.G., and NEESON, J.C. (1979). The Newry Igneous complex, County Down, in HARRIS, A.L., HOLLAND, C.H. and LEAKE, B.E. (eds.). The Caledonides of the British Isles reviewed. Spec. Publ. geol. Soc. London, 8, pp 717-722.
100. MEYER, C., (1965). An early potassic type of wall-rock alteration at Butte, Montana. Am. Mineralogist, 50, pp 1717-1722.
101. MEYER, C., and HEMLEY, J.J. (1967). Wall rock alteration, in BARNES, H.L., ed., Geochemistry of hydrothermal ore deposits: New York, Holt, Rinehart, and Winston, pp 166-235.
102. MEYER, C., SHEA, E.P., GODDARD, C.C.,JR., and Staff, (1968). Ore deposit at Butte, Montana, in RIDGE, J.D., ed., Ore deposits of the united states, 1933-1967 (Graton-Sales vol.): New York, Am. Inst. Mining Metall. Petroleum Engineers, pp 1373-1417.
103. MITCHELL, A.H.G., and GARSON, M.S. (1972). Relationship of porphyry copper and circum-pacific tin deposits to palaeo-Benioff zones: Inst. Mining Metallurgy Trans., 81, sec.B, pp 10-25.
104. MITCHELL, J.G., (1972). Potassium-argon ages from the Cheviot Hills, Northern England. Geol. Mag., 109, pp 421-426.
105. NAKAMURA, N., (1974). Determination of REE, Ba, Fe, Mg, Na and K in carbonaceous and ordinary meteories. Geochim. Cosmochim. Acta, 38, pp 757-775.
106. NIELSON, D.R., and STOIBER, R.E. (1973). Relationship of potassium content in Andesitic Lava and Depth to the seismic zone. J. Geophys. Res., 78, pp 6887-6892.
107. NOCKOLDS, S.R., and MITCHELL, R.L. (1948). The geochemistry of some Caledonian Plutonic Rocks: a study in the relationship between the major and trace elements of igneous rocks and their minerals. Trans. Roy. Soc. Edinb., 61, pp 533-575.
108. NOCKOLDS, S.R., and ALLEN, R. (1953). The geochemistry of some igneous rock series. Geochim. Cosmochim. Acta. 4, pp. 105-142.
109. OHMOTO, H., and RYE, R.O. (1979). Isotopes of sulfur and Carbon in BARNES, H.L., Geochemistry of hydrothermal ore deposits-2nd edition. A Wiley- Interscience Publication John Wiley and Sons.
110. OLADE, M.A., (1977). Nature of volatile element anomalies at porphyry copper deposits, Highland Valley, B.L., Canada. Chem. Geol., 20, pp 235-252.
111. PANKHURST, R.J., (1979). Isotope and trace element evidence for the origin and evolution of Caledonian granites in the Scottish Highlands. in ATHERTON, M.P. and TARNEY, J.: Origin of Granite Batholiths-Geochemical Evidence.

112. PARSLOW, G.R., (1964). The Cairnsmore of Fleet Granite and its aureole. Unpublished Ph.D., University of Newcastle upon Tyne.
113. PEACH, B.N., and HORNE, J. (1899). The Silurian Rocks of Britain 1: Scotland, Mem. geol. Surv. G.B., pp 1-749.
114. PEARCE, J.A., (1976). Statistical analysis of major element pattern in Basalt. J. Petrol., 17, pp 15-43.
115. PEARCE, J.A., and CANN, J.R. (1973). Tectonic setting of Basic volcanic rocks determined using trace element analysis. Earth. Planet. Sci. Lett., 19, pp 290-300.
116. PEARCE, J.A., HARRIS, N.B.W. and TINDLE, A.G. (in press). Trace element discrimination diagrams for the tectonic interpretation of granitic rocks. J. Petrol., 25.
117. PEARCE, J.A., (1973). Some relationships between the geochemistry and tectonic setting of basic volcanic rocks. Unpublished Ph.D. thesis, East Anglia University.
118. PEARCE, J.A., and NORRY, M.J. (1979). Petrogenetic implications of Ti, Zr, Y, and Nb variations in volcanic rocks. Contrib. Mineral. Petrol., 69, pp 33-47.
119. PHILLIPS, C.H., GAMBELL, N.A., and FOUNTAIN, D.S. (1974). Hydrothermal alteration, mineralization, and zoning in the Ray Deposit. Econ. Geol., 69, pp 1237-1250.
120. PHILLIPS, W.E.A., STILLMAN, C.J. and MURPHY, T. (1976). A Caledonian Plate Tectonic model. J. geol. Soc. London, 132, pp 579-609.
121. PHILLIPS, W.J., (1956). The Criffell-Dalbeattie granodiorite complex. Q. Jl. geol. Soc., London, 12, pp 221-240.
122. PHILPOTTS, J.A., and SCHNETZLER, C.C. (1970). Phenocryst matrix partition coefficients for K, Rb, Sr and Ba with applications to anorthosite and basalt genesis. Geochim. Cosmochim. Acta, 34, pp 307-322.
123. Power G.M., (1968). Chemical variation in tourmalines from SW England: Min. Mag., 36, No. 284, pp 1078-1089.
124. RAYLEIGH, J.W.S., (1896). Theoritical considerations respecting the separation of gases by diffusion and similar processes. Philos. Mag., 42, pp 77-107.
125. READ, H.H., (1961). Aspects of Caledonian magmatism in Britian. Liverpool. Manchester-geol., J. 2, pp 653-83.
126. RICE, R., and SHARP, G. (1976). Copper mineralization in the forest of Coed-Y-Brenin, North Wales. Trans. Inst. Min. Metall., 85, B1-B14
127. ROBERTS, J.L., (1974). The evolution of the Glencoe Cauldron. Scott. J. Geol., 10, No. 4, pp 269-282.
128. ROBSON, D.A., (1976). A guide to the geology of the Cheviot Hills. Nat. Hist. Soc. Northumb., 43, pp 1-23.
129. ROBSON, D.A., (1977). The Structural history of the Cheviot and adjacent regions. Scott. J. Geol., 14, pp 255-262.

130. ROBSON, D.A., and GREEN A.G. (1980). A magnetic survey of the aureole around the Cheviot granite. Scott. J. Geol., 16, pp 11-27.
131. ROSE, A.W., (1970). Zonal relations of wall rock alteration and sulfide distribution at porphyry copper deposits. Econ. Geol., 65, pp 920-936.
132. SALES, R.H., and MEYER, C. (1948). Wall rock alteration at Butte, Montana Am. Inst. Min. Eng. Trans., 178, pp 9-35
133. SALES, R.H., and MEYER, C. (1950). Interpretation of wall rock alteration at Butte, Montana: Colo. Sch. Mines Quart., 45(1B), pp 261-274.
134. SCHMITT, R.A., SMITH, R.H. and OLEHY, D.A. (1964). Rare-earth, Yttrium and Scandium abundances in meteoritic and terrestrial matter. Geochim. Cosmochim. Acta, 28, 67.
135. SCHWARTZ G.M., (1955). Hydrothermal alteration as a guide to ore. Econ. Geol. 50th Anniversary volume, pp 300-323.
136. SCHWARTZ G.M., (1947). Hydrothermal alteration in the porphyry copper deposits. Econ. Geol., 42, pp 319-352.
137. SCOTT, K.M., (1978). Geochemical aspects of the alteration-mineralization at Copper Hill, New South Wales, Australia. Econ. Geol., 73, pp 966-976.
138. SEELY, D.R., VAIL, P.R. and WALTON, G.G. (1974). Trench Slope Model. in BURK, C.A. and DRAKE, C.L., (eds). The geology of the Continental Margins. Springer-Verlag, New York, pp 249-260.
139. SEN GUPTA, J.G., (1976). Determination of Lanthanides and Yttrium in rocks and minerals by atomic-absorption and flame-emission spectrometry. Talanta, 23, pp 343-348.
140. SEN GUPTA, J.G., (1977). Determination of traces of rare-earth elements, yttrium and thorium in several international geologic reference samples and comparison with other published data. Geostandards Newsletter, 1, pp 149-156.
141. SEN GUPTA, J.G., (1981). Determination of Y and rare earth elements in rocks by flameless AAS. Talanta, 28, pp 31-36.
142. SHEPHERD, T.J., BECKINSALE, R.D., RUNDLE, C.C. and DURHAM, J. (1976). Genesis of Carrock Fell tungsten deposits, Cumbria: Fluid inclusion and isotopic study. Trans. Inst. Min. Metall. B85, pp 63-74.
143. SILLITOE, R.H., (1973). The tops and bottoms of porphyry copper deposits: Econ. Geol., 68, pp 799-815.
144. SILLITOE, R.H., (1976). Andean mineralization: A model for the metallogeny of convergent plate margins, in STRONG, D.F., ed. Metallogeny and plate tectonics: Geol. Assoc. Canada Spec. Paper 14, pp 59-100.
145. SILLITOE, R.H., (1972). A plate tectonic model for the origin of porphyry copper deposits: Econ. Geol., 67, pp 184-197.
146. STEPHENS, W.E., and HALLIDAY, A.N. (1979). Compositional variation in the Galloway plutons. in ATHERTON M.P. and TARNEY J. (eds.) origin of Granite Batholiths: Geochemical Evidence, Shiva Publishing, Orpington, pp 9-17.

147. STONE, M., (1963). Lithium in the Tregonning-Godolphin granite. Ussher Soc., Proc., 1, part 2, pp 50-53.
148. STONE, M., (1975). Structure and petrology of the Tregonning-Godolphin granite, Cornwall. Proc. Geol. Ass., 86, pp 155-170.
149. STRINGHAM B., (1953). Granitization and hydrothermal alteration at Bingham, Utah. Geol. Soc. America Bull., 64, pp 945-992.
150. TATE, G., (1867). The Cheviots, their geographical range, physical features, mineral characteristics, relation to stratified rocks, origin, age, botanical peculiarities. Proc. Berwicksh. Nat. Field Club, 5, pp 359-370.
151. TAYLOR, R.P., (1981). Isotope Geology of the Bakircay porphyry copper prospect, Northern Turkey. Mineral Deposita, 16, pp 375-390.
152. TAYLOR, R.P., and FRYER, B.J. (1980). Multiple stage hydrothermal alteration in porphyry copper systems in northern Turkey: The temporal interplay of potassic, propylitic, and phyllic fluids. Can. J. Earth Sc., 17, pp 901-927.
153. TAYLOR, S.R., (1965). The application of trace element data to problems in petrology. Phys. Chem. Earth, 6, pp 133-214.
154. TEALL, J.J.H.(1885). On some Quartz-Felsites and Augite-Granites from the Cheviot District. Geol. Mag., Dec III, v. II, 106.
155. THIRLWALL, M.F., (1981). Implications for Caledonian plate tectonic models of chemical data from volcanic rocks of the British Old Red Sandstone. J. geol. Soc. London, 138, pp 123-138.
156. THORNING, L., (1974). Palaeomagnetic results from the Lower Devonian rocks of the Cheviot Hills, northern England. Geophys. J. R. astr. Soc.
157. THORNTON, C.P., and TUTTLE, O.F. (1960). Chemistry of Igneous Rocks: Pt.1, Differentiation Index. Am. Journ. Sci., 258, pp 664-684.
158. TINDLE, A.G., and PEARCE, J.A. (1981). Petrogenetic modelling of insitu Fractional crystallization in the zoned Loch Doon Pluton, Scotland. Contrib. Mineral. Petrol., 78, 196-206.
159. TITLEY, S.R., (1975). Geological characteristics and environment of some porphyry copper occurrences in the southwestern Pacific: Econ. Geol., 70, pp 499-514.
160. TITLEY, S.R., and HEIDRICK, T.L. (1978). Intrusion and fracture styles of some mineralized porphyry systems of the southwestern Pacific and their relationship to plate interactions: Econ. Geol., 73, pp 891-903.
161. TOMKEIEFF, S.I., (1965). Cheviot Hills. Geologists Assoc. Guides, No. 37.

162. TOWELL, D.G., WINCHESTER, J.W. and SPRIN, R.V. (1965). Rare-earth distribution in some rocks associated minerals of the batholith of southern California. J. Geophys. Res., 70, pp 3485-3496.
163. TURNER, F.J., and VERHOOGEN, J. (1960). Igneous and Metamorphic petrology, 2nd edition (McGraw-Hill Book Company).
164. TUTTLE, O.F., and BOWEN, N.L. (1958). Origin of granite in the light of experimental studies in the system NaAlSi3O8-KAlSi3O8-SiO2-H2O. Geol. Soc. Am. Mem., 74.
165. WADGE, A.J., GALE, N.H., BECKINSALE, R.D., and RUNDLE, C.C. (1978). A Rb-Sr isochron of the Shap Granite. Proc. Yorks. geol. Soc., 42, pp 297-305.
166. WATMUFF, G., (1978). Geology and alteration-mineralization zoning in the central portion of the Yandera porphyry copper prospect, Papua New Guinea. Econ. Geol., 73, pp 829-856.
167. WATSON, J., (1984). The ending of the Caledonian orogeny in Scotland. J. geol. Soc., London, 141, pp 193-214.
168. WILSON, I.R., (1972). Wall rock alteration at Geevor Tin Mine, Cornwall and Ashanti Mine, Ghana. Unpublished Ph.D. Thesis, Leeds University
169. WINCH, N.J., (1817). Observations on the geology of Northumberland and Durham. Trans. geol. Soc. London, 4, 1.
170. WOLFE, J.A., MANUZON, M.S. and DIVIS, A.F. (1978). The Taysan porphyry copper deposit, southern Luzon Island, Philippines. Econ. Geol., 73, pp 608-617..

Plate 1. THE GEOLOGICAL MAP OF THE CHEVIOT GRANITES.
Scale 1 : 25000

- FINE GRAINED EVOLVED WOOLHOPE GRANITE
- FINE GRAINED PORPHYRITIC HEDGEHOPE GRANODIORITE
- COARSE BROWN LINHOPE GRANODIORITE
- COARSE GREY GRANULAR STANDROP GRANODIORITE
- PINK PORPHYRITIC DUNMOOR GRANODIORITE
- GREY MEDIUM GRAINED MARGINAL GRANODIORITE
- PYROCLAST, HORNFELS AND ANDESITE
- DYKES : Mp : MICA PORPHYRITE
  pp : PYROXENE PORPHYRITE
  Qp : QUARTZ PORPHRY
  F : FELSITE
  p : PORPHYRITE
- FAULT

Cross section (see fig 2.2)

Harthope Fault

Breamish Fault